PERIÓDICO TCHÊ QUÍMICA

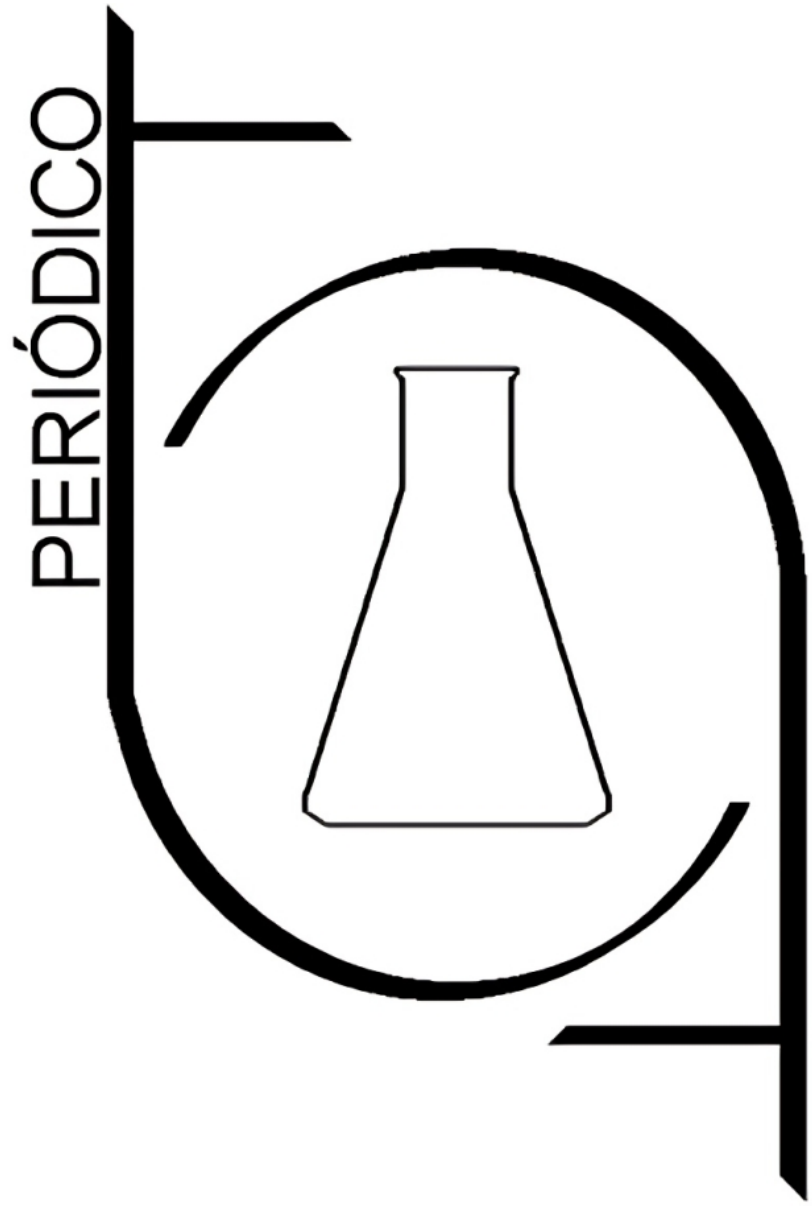

Volume 22 - Número 51 - 2025 ISSN 2179-0302

Órgão de divulgação científica e informativa

www.periodico.tchequimica.com

PERIÓDICO TCHÊ QUÍMICA

ISSN - 1806-0374 (Impresso) ISSN - 2179-0302 (Online)

Volume 22 **Número 51 – 2025** **ISSN 2179 - 0302**

Órgão de divulgação científica e informativa.

Dados Internacionais de Catalogação na Publicação (CIP)

Periódico Tchê Química: órgão de divulgação científica e informativa [recurso eletrônico] / Dr. D. Scienific Consulting – Vol. 21, n. 46 (Jan. 2024) – Nova Prata: Araucária - Scientific Association, 2005 - Quadrimestral.
Sistema requerido: Adobe Acrobat Reader.
Modo de acesso: World Wide Web:
<http://www.tchequimica.com>
Descrição baseada em: Vol. 19, n. 41 (Jun. 2022).
ISSN 1806-0374
ISSN 2179-0302
1.Química. 2. Física. 3. Biologia. 4. Ciências Naturais. 5. Farmacologia. 6. Ciências exatas. 7. Ciências aplicadas. 8. Ciências. I. Grupo Tchê Química.

UDC 001

Bibliotecário Responsável
Ednei de Freitas Silveira
CRB 10/1262

Welcome to PERIÓDICO TCHÊ QUÍMICA

International multidisciplinary scientific journal

Periódico Tchê Química *accepts submissions in a variety of formats, including Research Articles/Original Articles, Review Articles, Short Reports, Technical Notes, Case Studies, Interviews, Book Reviews, and Forum Articles. The journal publishes work across several disciplines, with a focus on* ***Chemistry, Biology, Pharmacy and Medicine (selected fields), Engineering (selected fields), Chemometrics/Statistics, Physics/Physical Chemistry, Science Education, as well as Agricultural and Veterinary Sciences****. Submissions with significant theoretical or applied contributions in these areas are especially encouraged.*

PERIÓDICO TCHÊ QUÍMICA

Volume 22 Número 51 – 2025 ISSN 2179 - 0302

Órgão de divulgação científica e informativa.

Periódico Tchê Química

ISSN - 1806-0374 (Print)
ISSN - 2179-0302 (Online)

LCCN: 2010240735

Divulgação *on-line* em http://www.periodico.tchequimica.com
http://www.journal.tchequimica.com
http://www.tchequimica.com

Esta revista é indexada e resumida pelo WEB OF SCIENCE, SUDOC, EZB, LATINDEX (DIRECTORIO), OPENALEX, TITLE DOI, WIKIDATA, THE KEEPERS, ROAD, GLOBALHEALTH, CROSSREF, CABABSTRACTS, FATCAT, ZDB, and Sumários.

Missão

O Periódico Tchê Química (PTQ) publica artigos de pesquisa originais, artigos de revisão, notas curtas (publicações científicas), revisões de livros, artigos de fórum, editoriais e entrevistas. Pesquisadores de todos os países são convidados a publicar nas páginas do PTQ.

A responsabilidade sobre os artigos é de exclusividade dos autores.

Contatos:

www.periodico.tchequimica.com
journal.tq@gmail.com
tchequimica@tchequimica.com

Proudly edited by the Araucária Scientific Association since 2024.

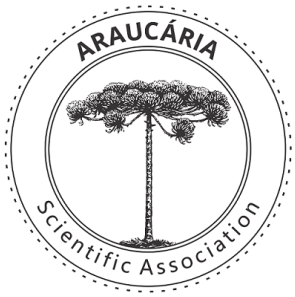

General Inquiries:
For general inquiries, information, or questions about our mission and activities, please feel free to reach out to us:

- **Email:** root@acaria.org.
- **Phone:** +55 54 9 3300-8160

Investor Relations:
If you are interested in supporting our mission or exploring collaboration opportunities, please contact our Investor Relations team:
Email: root@acaria.org.

Media and Press:
For media inquiries, interviews, or press-related matters, please get in touch with our Media Relations team:
Email: media@acaria.org.

Índice / Index

13 – ATR

LuKetevan Kupatadze, Shaima Rabeea Banoon, Luis Alcides Brandini De Boni

GEORGIA / IRAQ / BRAZIL

PERIÓDICO TCHÊ QUÍMICA ANNUAL TRANSPARENCY REPORT

PERIÓDICO TCHÊ QUÍMICA ANNUAL TRANSPARENCY REPORT

14 – Convite / Invitation

Journal Editors

BRAZIL

3ª SSCON

PERIÓDICO TCHÊ QUÍMICA
ARTIGO ORIGINAL

IMPACTO DAS FUNÇÕES *WAVELET* NO APRIMORAMENTO DA RESOLUÇÃO DE IMAGENS USANDO PREENCHIMENTO COM ZEROS DE *WAVELET*

IMPACT OF WAVELET FUNCTIONS ON IMAGE RESOLUTION ENHANCEMENT USING WAVELET ZERO PADDING

تأثير الدوال المويجية على تحسين دقة الصورة باستخدام التعبئة الصفرية المويجية

Ghusoon Mohammed Tuma *
Department of Physics, College of Science, University of Babylon, Babel, Iraq

Ameerah Ab. Al-Sadooni
Department of Physics, College of Science, University of Babylon, Babel, Iraq

Wasnaa Witwit
Department of Physics, College of Science, University of Babylon, Babel, Iraq

** Corresponding author*
e-mail: sci927.guson.mohammed@student.uobabylon.edu.iq

Received 12 June 2024; received in revised form 7 July, 16 August 2024; accepted 01 October 2025.

RESUMO

Introdução: O aprimoramento da resolução de imagens é crucial em diversas aplicações; inclui a utilização de várias técnicas para melhorar a clareza e o nível de detalhes de uma imagem. As técnicas baseadas em wavelets oferecem a capacidade de realizar uma análise de multirresolução da imagem, decompondo-a em sub-bandas de baixa e alta frequência. **Objetivo**: Esta abordagem examina como diferentes funções wavelet impactam o desempenho da técnica de Preenchimento com Zeros de Wavelet (WZP), um método fundamental baseado em wavelets para reconstrução de imagens de alta resolução (HR). **Método**: A investigação inclui sete funções wavelet aplicáveis à DWT e oito métodos de interpolação. O exame concentra-se no desempenho da relação sinal-ruído de pico (PSNR) e na qualidade visual das funções wavelet. O programa é escrito em Matlab, itera sobre todas as funções wavelet e métodos de interpolação, e gera uma planilha Excel dos valores PSNR. **Resultados**: Foram examinadas imagens padrão, de sensoriamento remoto e astronômicas. Diferenças significativas foram encontradas entre as funções wavelet e métodos de interpolação. Métodos de interpolação avançados, como bicúbico e Lanczos, alcançaram PSNR mais alto. Para conjuntos de dados astronômicos, os métodos de interpolação bilinear e triangular mostraram superioridade. Para o conjunto de dados Lina, a wavelet coif2 resultou no PSNR mais alto em todos os métodos de interpolação, variando de 25,121 para o mais próximo a 26,840 para Lanczos3. **Discussão**: O Preenchimento com Zeros de Wavelet (WZP) minimiza artefatos de borda ao suavizar a imagem enquanto mantém as características. A eficácia do WZP depende da escolha adequada da função wavelet e do método de interpolação. As wavelets Coif2, fk8 e Bior tiveram melhor desempenho para conjuntos de dados específicos. **Conclusões**: O Preenchimento com Zeros de Wavelet (WZP) minimiza artefatos de borda ao suavizar a imagem enquanto mantém as características. Sua eficácia depende da escolha adequada da função wavelet e do método de interpolação, com coif2, fk8 e Bior tendo melhor desempenho para conjuntos de dados específicos. Recomenda-se o desenvolvimento de técnicas wavelet adaptativas e o estudo de uma gama mais ampla de conjuntos de dados para melhorias adicionais.

Palavras-chave: *transformada wavelet discreta, preenchimento com zeros, aprimoramento de resolução*

ABSTRACT

Background: Image resolution enhancement is crucial in various applications; it involves utilizing different techniques to improve an image's clarity and level of detail. Wavelet-based techniques enable the performance of a multiresolution analysis of the image by decomposing it into low- and high-frequency subbands. **Aim**: This approach investigates the impact of different wavelet functions on the performance of the Wavelet Zero-Padding (WZP) technique, a fundamental wavelet-based method for reconstructing high-resolution (HR) images. **Method:**

DOI: 10.52571/PTQ.v22.n51.2025_01_GHUSOON_pgs_01_17.pdf.

The investigation employs seven wavelet functions suitable for DWT and eight interpolation methods. The examination focuses on the peak signal-to-noise ratio (PSNR) performance and visual quality of wavelet functions. The program, written in MATLAB, iterates over all wavelet functions and interpolation methods, generating an Excel sheet that contains the PSNR values. **Results**: Standard, remote sensing, and astronomical images were examined. Significant differences were found among the wavelet functions and interpolation methods. Advanced interpolation methods, such as bicubic and Lanczos, achieved higher PSNR. For astronomical datasets, bilinear and triangle interpolation methods showed superiority. For the Lina dataset, the coif2 wavelet yielded the highest PSNR across all interpolation methods, ranging from 25.121 for the nearest neighbor to 26.840 for the Lanczos3 method. **Discussion**: Wavelet Zero Padding (WZP) minimizes edge artifacts by smoothing the image while maintaining features. The effectiveness of WZP depends on choosing the proper wavelet function and interpolation method. Coif2, fk8, and Bior wavelets performed best for specific datasets. **Conclusion**: Wavelet Zero Padding (WZP) minimizes edge artifacts by smoothing the image while maintaining features. Its effectiveness depends on choosing the proper wavelet function and interpolation method; coif2, fk8, and Bior perform best for specific datasets. Developing adaptive wavelet techniques and studying a broader range of datasets are recommended for further improvement.

Keywords: *discrete wavelet transform, zero padding, resolution enhancement*

الخلاصة

الخلفية: يعتبر تحسين دقة الصورة أمرًا بالغ الأهمية في العديد من التطبيقات، ويتضمن استخدام تقنيات متنوعة لتحسين وضوح الصورة ومستوى التفاصيل فيها. توفر التقنيات المعتمدة على المويجات القدرة على إجراء تحليل متعدد الدقة للصورة من خلال تقسيمها إلى نطاقات تردد منخفضة وعالية. **الهدف:** يهدف هذا البحث إلى دراسة كيفية تأثير الدوال المويجية المختلفة على أداء تقنية التعبئة الصفرية المويجية (Wavelet Zero-Padding - WZP)، وهي طريقة أساسية معتمدة على المويجات لإعادة بناء صور ذات دقة عالية. **الطريقة:** تتضمن الدراسة سبع دوال مويجية قابلة للتطبيق على التحويل المويجي المنفصل (DWT) وثماني طرق توليد للبكسلات. يركز الفحص على أداء دوال المويجات من حيث نسبة ذروة الإشارة إلى الضوضاء (PSNR) وجودة الصورة البصرية. تم كتابة البرنامج بلغة ماتلاب، حيث يقوم بتكرار جميع دوال المويجات وطرق توليد البكسلات، وينتج جدول Excel يحتوي على قيم PSNR . **النتائج:** تم فحص صور قياسية وصور استشعار عن بُعد وصور فلكية. وقد وجدت اختلافات كبيرة بين دوال المويجات وطرق توليد البكسلات. حققت طرق توليد البكسلات المتقدمة، مثل bicubic وLanczos، قيم PSNR أعلى. أما بالنسبة للصورة الفلكية، فقد أظهرت طرق توليد البكسلات bilinear وtriangle تفوقًا. ولكن حققت مويجة coif2 أعلى قيم PSNR عبر جميع طرق توليد البكسلات لمجموعة بياناتLena ، حيث تراوحت من 25.121 لأقرب توليد بسكلات إلى 26.840 لـLanczos3 . **المناقشة:** ان تقنية WZP تقلل من عيب الحواف عن طريق تنعيم الصورة مع الحفاظ على ميزاتها. تعتمد فعالية تقنية WZP على اختيار الدالة المويجية وطرق التوليد المناسبة. حيث تفوقت دوال المويجات Coif2 و fk8وBior لمجموعة بيانات معينة. **الاستنتاج:** توصل البحث الى أهمية تقنية WZP في تقليل عيوب الحواف من خلال تنعيم الصورة دون تغيير خصائصها. وان اختيار الدالة المويجية وطريقة التوليد المناسبتين يلعب دور رئيسي في فعالية الطريقة، اذ ان coif2، fk8، وBior أظهرت اعلى أداء لمجموعة بيانات معينة. ومن ذلك نقترح تطوير طريقة تحسين مويجية متكيفة مع خصائص الصورة ودراسة مجاميع بيانات أوسع من المدروسة في البحث لغرض احداث تطوير أكبر في أداء التقنية.

الكلمات المفتاحية: التحويل المويجي المنفصل، التعبئة الصفرية، تحسين الدقة.

1. Introduction:

High-resolution images are essential in medical imaging (Greenspan, 2008), remote sensing (Demirel & Anbarjafari, 2010; Witwit *et al*., 2017), and astronomy industries (Al-Sadooni & van Loon, 2022; Hamza *et al*., 2020). Several approaches can be employed to enhance image resolution, including interpolation techniques, wavelets, and theourier transform (Agaian *et al*., 2001; Deeba *et al*., 2020). Wavelet methods have found applications in many crucial areas, including quantum field theory (QFT), harmonic analysis, and data compression, due to their ability to provide a localized analysis of a function and its multiresolution decomposition, which is utilized in decomposing Hilbert space (Bulut & Polyzou, 2013; Lee & Yamamoto, 1994).

Interpolation is a method for approximating a new pixel value based on the values of neighboring pixels in a low-resolution image (imgLR). Nevertheless, the computational complexity increases as the order of the interpolation factor increases. Standard interpolation methods involve nearest neighbour, bilinear, and bicubic (Patel & Mistree, 2013). Nearest neighbour interpolation uses the closest pixel for each new pixel, often resulting in blocky images. Bilinear averages the nearest 2×2 pixels for smoother images but can blur edges, while bicubic uses 4×4 pixels and cubic polynomials for sharper, more detailed results (Demirel & Anbarjafari, 2011; Karunakar *et al*., 2013).

Conventional interpolation methods rely on simple pixel averaging and do not consider the broader context of the image's structure. As a result, these methods often fail to preserve fine details and edges, which are crucial for maintaining image quality, especially in high-

resolution images. Additionally, these methods are limited in handling images with complex textures or noise, as they cannot distinguish between significant image features and noise.

Wavelet-based techniques emerged to overcome the limitations of traditional processing methods. They offer a multi-scale representation of an image, allowing for a more detailed analysis and manipulation of image features. Wavelet transforms (WT)-based methods enable the analysis of images at multiple resolutions by dividing them into different frequency ranges and scales (Azani Mustafa *et al*., 2019a). This lets the high-frequency ranges be enhanced in specific areas. Two of the basic wavelet transform-based techniques are the discrete wavelet transform (DWT) and wavelet zero-padding (WZP) (Yang *et al*., 2010a). DWT decomposes an image into multiple subbands, each containing different frequency components. The low-low (LL) subband contains most of the image's energy and general structure. Additionally, the low-high, high-low, and high-high subbands (LH et al.) are high-frequency components that encompass diagonal, horizontal, and vertical details, revealing and texture information (Gonzalez & Woods, 2002; Pimpalkhute *et al*., 2021).

Wavelet functions are mathematical functions used in the decomposition and reconstruction of images and signals, each with unique properties that make them suitable for various applications in image processing. The choice of wavelet function has a significant impact on the performance of the wavelet-based technique. This study examines the performance of the various wavelet functions (Lee & Yamamoto, 1994). Most wavelet functions have their wavelets; for example, Daubechies has wavelets that differ in the number of vanishing moments (N); this number determines the wavelet's ability to represent polynomial trends in data.

WZP fills the high-frequency subbands obtained from DWT with zeros to ensure smooth boundaries and decrease edge artifacts (Wu, 2019). The zero-padded subbands are combined with the interpolated LL subband using inverse DWT (IDWT) to reconstruct the high-resolution (HR) image. This technique is beneficial because it reduces discontinuities during the inverse transform and produces a sharper image. The performance of this technique varies depending on the interpolation method of the LL subband and the selection of the wavelet function. This approach investigates the effect of those two factors by applying different interpolation methods and wavelet functions to standard, satellite, and astronomical images and comparing them in terms of PSNR and visual quality.

This work presents qualitative and quantitative measurements for seven wavelet functions and their corresponding filters. Descriptive statistics and tests were presented in the results subsection for reliable data analysis. All wavelets discussed in this study are suitable for Discrete Wavelet Transform (DWT) applications. Seven interpolation approaches were used to recreate the HR image of each quantitative measurement. A supplementary section is included, which presents a graphical representation of the Peak signal-to-noise ratio (PSNR) values for all the examined components. An appendix inserted in the paper serves as a point of reference.

1.2. Literature survey

In 2007, Juang and Wu (Juang & Wu, 2007) utilized WZP for phase unwrapping in magnetic resonance imaging (MRI) brain phase images; such images suffer from phase discontinuities due to the wrapping of phase values, which leads to artificial phase jumps. WZP is used to smooth these discontinuities and improve image quality. DWT decomposes an image into four subbands, namely LL, LH, HL, and HH, and then zero-padding is applied to the high-frequency subbands. In contrast, various conventional interpolation methods are applied to the LL subband. The high-resolution image is reconstructed by adding the LL interpolated image and the high-frequency subbands using IDWT. This approach demonstrates that Daubechies wavelets combined with Lanczos interpolation yield the best PSNR and visual quality results. Juang's approach emphasizes the importance of selecting suitable wavelet functions and interpolation methods for achieving optimal image resolution enhancement using WZP.

Naidu *et al*. spectroradiometer (MODIS). The paper includes WZP, WZP with Cycle Spinning (WZP-CS), DWT, DWT combined with stationary wavelet transform (SWT), and error back Projection. The study evaluated MODIS images with a 250 m resolution in the Red and Near Infrared (NIR) spectral bands, comparing the superior enhancement of DWT-SWT with Error Back Projection in terms of PSNR. WZP is considered a basic wavelet technique. However, it yields a better PSNR compared to WZP-CS. Furthermore, this study emphasizes the importance of selecting suitable resolution

enhancement techniques to enhance the quality of satellite images.

To identify the key factors affecting the performance of wavelet-based image resolution enhancement, Witwit *et al*. (Witwit *et al*., 2016) proposed an optimal factor analysis (OFA) approach, in which they test essential factors such as the method to produce LR images, the choice of a wavelet function, the scale factor in resolution enhancement, and interpolation methods. Witwit's approach employs an algorithm to identify the optimal combination of all the studied factors. A key finding is that the choice of wavelet function influences the performance of WZP. However, not all current wavelet functions have been tested. Another result is that the technique used to produce LR images is crucial for obtaining higher-resolution enhancement performance.

Traditional wavelet-based methods often use bicubic interpolations for high-frequency components, which can lead to noise. In contrast, Cui and Jinghong's approach utilizes a 2D wavelet transform to obtain low-frequency and three-directional high-frequency subbands, then applies the DFT to the high-frequency subbands using the zero-padding technique. The original input image was enhanced by a confection and combined with the improved high-frequency subbands to construct the HR image using an inverse 2D wavelet transform. This technique was tested on remote sensing images and demonstrated an improvement in resolution enhancement over traditional methods, as indicated by PSNR and RMSE.

Narmatha (Narmatha, 2020) studied the resolution enhancement of microarray images using a technique that is advantageous to the DWT, SWT, and WZP. The approach uses dwt to decompose the image into subbands in parallel, and SWT is applied to add high-frequency subbands of DWT and SWT together. Afterwards, a bicubic interpolation is applied to the input low-resolution image and the combined high-frequency subbands. The technique reduces artifacts using WZP and reconstructs the high-frequency image using IDWT. The performance of this technique is evaluated using PSNR, RMSE, entropy, and Contrast improvement Index (CII). It concludes that using DWT in conjunction with SWT provides superior resolution enhancement compared to using DWT alone.

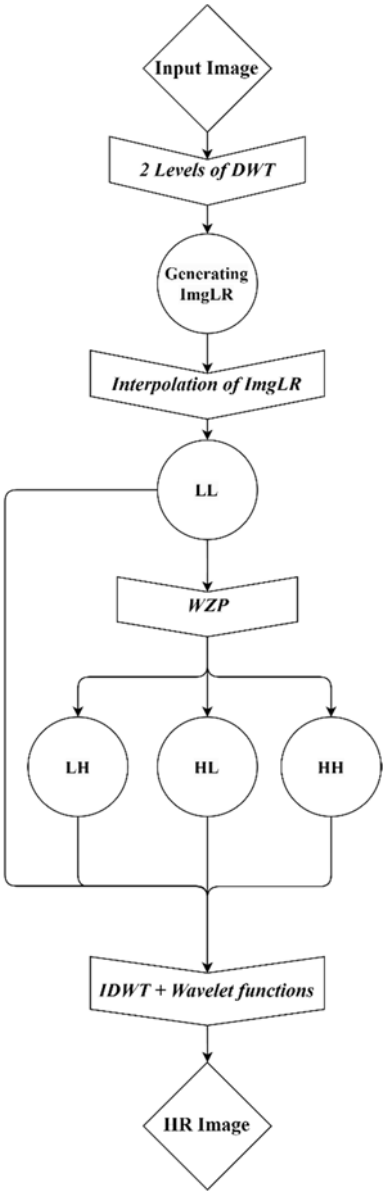

Figure 1. Shows a diagram of the proposed approach.

2. MATERIALS AND METHODS:

The study encompasses multiple technical materials and delineates the methodology employed to gather the data for this investigation.

2.1. Materials

In this study, the image enhancement technique was developed and implemented using MATLAB 2024a. The computational experiments were conducted on a workstation with an Intel Core i7 processor (7th Gen), 12GB of RAM, and Windows 10. The primary datasets used for testing and validating the enhancement technique are publicly available collections. The Lina dataset, with a size of 512×512, was acquired from (Repository, n.d.). Jupiter's ultraviolet image, with

a size of 1328×1285, was obtained from (Claire Andreoli, 2023). The Babylon University image, with a size of 3840×2160, was obtained from Google Earth at coordinates 99VX+RQ7, Hillah, Babylon Governorate.

Several MATLAB toolboxes were utilized, including the Image Processing Toolbox, Signal Processing Toolbox, and Computer Vision Toolbox. The experimental setup evaluated the technique's performance using the Peak signal-to-noise ratio (PSNR) metric. Specific wavelet functions and interpolation methods were selected based on their suitability for the DWT. Microsoft Excel program was used to collect and analyse the data.

In a resolution enhancement study, a Python script was employed to create a heat map for visualizing the PSNR values obtained from applying 107 wavelet functions across eight interpolation methods. The script was designed to automatically identify and highlight the maximum PSNR value among all combinations, thus facilitating the identification of the most effective technique. The resulting heat map was then exported as a high-resolution PNG image, ensuring that the visual representation of the data is both detailed and suitable for academic analysis and publication. This automated approach not only enhances the efficiency of data analysis but also provides a clear and accurate depiction of the optimal wavelet and interpolation method combinations for each dataset.

2.2. Methodology

This study examines the effect of various wavelet functions and interpolation methods on Wavelet Zero Padding (WZP) performance for image resolution enhancement (D. Costa *et al*., 2013). The loop program was written and run on MATLAB 2024a. **Figure 1** represents the methodology of the approach, which involves the following steps:

1. Image Decomposition Using DWT:

The high-resolution input image is decomposed using a two-level DWT to obtain subbands (LL, LH, HL, HH). **Figure 2** shows the process of decomposition using this method. The LL subband from the second level of decomposition is considered the low-resolution image (imgLR) that needs to be enhanced (Azani Mustafa *et al*., 2019b).

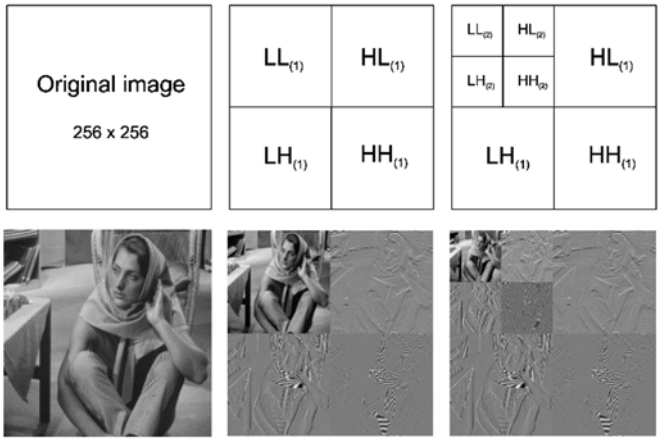

Figure 2: *An example of image decomposition using two levels of DWT* (D. G. Costa *et al*., 2013).

2. Interpolation of imgLR:

The imgLR is interpolated using different interpolation methods (nearest, bilinear, bicubic, triangle, Lanczos2, and Lanczos3) with a scale factor 2. The interpolated image (LLz) is obtained using the imresize () function (Kok & Tam, n.d.):

```
LLz = imresize (imgLR,
2,'interpolation_method');
```

3. Wavelet Zero Padding (WZP):

High-frequency subbands (LHz, HLz, HHz) are initialized to zero matrices of the same size as LLz.

```
LHz = zeros(size(LLz));
HLz = zeros(size(LLz));
HHz = zeros(size(LLz));
```

4. Image Reconstruction Using IDWT:

The LLz, LHz, HLz, and HHz subbands are combined using the Inverse Discrete Wavelet Transform (IDWT) to reconstruct the high-resolution image (imgHR).

```
imgHR = idwt2(LLz, LHz, HLz, HHz,
'WaveletFunction');
```

Various wavelet functions can be used to reconstruct the high-resolution image.

5. Evaluation of Wavelet Functions and Interpolation Methods:

A loop iterates through different wavelet functions (e.g., Haar, Daubechies, Biorthogonal) and their filters, and the interpolation methods (nearest, bilinear, bicubic, Lanczos). For each combination, the peak signal-to-noise ratio (PSNR) is calculated to assess the quality of the reconstructed high-resolution image. This study aims to determine the optimal combinations for

maximizing image resolution enhancement using WZP by varying the wavelet functions and interpolation methods.

3. RESULTS AND DISCUSSION:

3.1. Results

The study evaluates the performance of different wavelet functions combined with various interpolation methods in terms of PSNR. It utilizes a program that iterates over all the wavelet functions applicable to DWT and seven interpolation methods, which are designed and applied to three data sets.

PSNR is used to measure the maximum error magnitude between the original and processed imagery, thereby providing a metric of the qualitative enhancement achieved. The PSNR is computed using Equation 1 (Gonzalez & Woods, 2002):

$$PSNR = 10\log_{10}\left(\frac{R^2}{MSE}\right) \qquad (Eq.1)$$

Where R is the maximum fluctuation in the input image data, and MSE denotes the mean squared error between the provided input image. I_{in} and the original image I_{org}, Calculated with Equation 2 (Anbarjafari & Demirel, 2010):

$$MSE = \frac{\sum_{i,j}\left(I_{in}(i,j) - I_{org}(i,j)\right)^2}{M \times N} \qquad (Eq.2)$$

Where M and N represent the sizes of the two images, the evaluation includes images of Lina, Jupiter in ultraviolet, and Babylon University's College of Science. These images represent standard, astronomical, and remote sensing images. The program generates an Excel sheet containing the PSNR values for eight interpolation methods and 107 wavelet functions. It also provides a figure displaying the visual results for each family and their corresponding filters. Appendix A includes a heat map of all the PSNR results for Lina's image.

Tables 1 to **9** present the statistical analysis of the datasets under study, which includes interpolation methods and wavelet functions. **Tables 1** to **6** present the best PSNR performance and descriptive statistics for each dataset.

Advanced interpolation methods, such as bicubic, Lanczos3, and cubic, yielded higher PSNR for standard photos. The results of the Lina dataset showed that the coif2 wavelet gave the highest PSNR values across all the interpolation methods. They range from 25.121 for the nearest box to 26.840 for lanczos3, the highest PSNR value. Meanwhile, the fk8 wavelet achieves the highest PSNR for all the interpolation methods for the Jupiter dataset. However, bilinear and triangle methods achieve a top PSNR of 32.208 when combined with the fk8 wavelet. The best PSNR values were achieved for the satellite image by applying various Bior wavelets. However, bilinear and triangle interpolation methods return a slightly higher PSNR than other interpolation methods. These findings are evident in **Tables 1** to **3**.

Tables 4 to **6** represent the descriptive statistics of interpolation methods for all datasets. The range of PSNR values in the three tables is roughly the same, from approximately 12.47 to 13.68 for the Lina dataset, from 10.5 to 10.94 for the Jupiter dataset, and from 1.04 to 1.06 for the Babylon dataset. This suggests that all interpolation methods result in a comparable spectrum. Furthermore, on average, different interpolation methods yield similar PSNR values for the three datasets; this can be concluded from the relatively close PSNR mean of the other interpolation methods, ranging from 19.9 to 20.5 for the Lina dataset, from 28.85 to 29.2 for the Jupiter dataset, and from 11.33 to 11.40 for the Babylon dataset. All interpolation methods have the same variability level, deduced from the close values of standard deviations and variance. Negative close to zero skewness values indicate that the PSNR distribution for all interpolation methods is slightly left-skewed, but the skewness is not extreme. In addition, the kurtosis values are all negative, indicating that the PSNR distribution is thinner at its tails and has a flatter peak than the normal distribution. The small kurtosis values suggest that the distribution is not far from normal. The reliability of the sample means and other statistics is obtained due to the relatively small standard errors of mean, skewness, and kurtosis.

The significance values of data are zero along all interpolation methods, according to the Shapiro-Wilk test of normality, as shown in **Table 7**. A zero value of significance indicates that the data is normally distributed. To evaluate the differences in PSNR values across various interpolation methods, we first tested the assumption of homogeneity of variances using Levene's test (Glass, 1966; Loh, 1987). The results indicated no significant differences in variances across the groups (Levene's test, $p > 0.05$ for all tests), confirming that the assumption of homogeneity of variances was met. The non-parametric Kruskal-Wallis Test gave a significant

value of 0.482 for all interpolation methods, which is greater than alpha (0.05), so the null hypothesis is retained for each interpolation method.

ANOVA statistical test of PSNR performance is represented in **Tables 8** and **9**. This test compares means across multiple groups to determine any statistically significant differences. The variation is tested between groups and within each group(Lars & Wold, 1989). The sum of squares (SS), Degrees of freedom (Df), Mean square (MS), the ratio between MS between groups to the MS within groups (F-value), the probability of significant differences (P-value), and F critical (F crit) are shown. **Table 8** shows that the F-value (0.422, 0.176, 0.732) is less than F crit (2.0204, 2.204, 2.0204), and the p-value (0.888, 0.990, 0.644) is greater than 0.05 for Lina image, Jupiter, and Babylon datasets, respectively. These findings suggest that the choice of interpolation method does not significantly affect the PSNR values. On the other hand, in **Table 9**, the ANOVA results for PSNR performance, where wavelet functions rather than interpolation methods group data, indicate that there is a significant variation between the wavelet functions; the between-group sum of squares (SS) is much larger than the within-group SS for all datasets. A substantial between-group variance is also observed; the mean square (MS) between groups is larger than the MS within groups. The P-values for all data sets are zero, less than the significance level of 0.05, and the F-values are greater than the critical F-value (F-cret.). Suggests that the differences between the wavelet functions are statistically significant.

Figure 3 illustrates a lower performance of high-order Daubechies wavelets, but a higher PSNR for other wavelets, across the three datasets. The overall PSNR value of the Jupiter image was the highest among the three datasets; this image has fewer details than the other two. The WZP enhancement of the Babylon dataset yielded the lowest PSNR value across all wavelet functions.

The Q-Q plots in **Figure 4** indicate that the data points from all interpolation methods follow a roughly straight line, suggesting that the PSNR values are approximately normally distributed. While some minor deviations were observed at the tails, these were not severe, indicating that the normality assumption is reasonably satisfied. **Figure 4** shows the visual representation of WZP. The fk8 wavelet, combined with the bilinear interpolation method, produced a smoother image and greater clarity than db7 and db45, both of which used the box interpolation method. The normality of the PSNR values for each interpolation method was assessed using Q-Q plots.

3.2. Discussion

Applying homogeneity of variances, normality tests, and Analysis of Variance (ANOVA) is crucial when evaluating the performance of resolution enhancement techniques, particularly when comparing different interpolation methods and wavelet functions based on PSNR values. Ensuring homogeneity of variances means that the data in each group have similar levels of variation, which is necessary for ANOVA to give accurate results. Performing normality checks to ensure that the data in each group follows a normal distribution, which is a prerequisite for conducting reliable statistical tests. ANOVA then helps to compare the average PSNR values across different methods to see if there are significant differences. Together, these methods ensure that the analysis of which technique works best is both sound and dependable.

The selection of wavelet functions is significantly more impactful than that of interpolation methods. The results reveal substantial variations in PSNR values among different wavelet functions, while no significant differences have been observed among the interpolation methods. Statistical analysis confirms that there is no statistically significant difference in the distributions of PSNR values across the interpolation methods; thus, the null hypothesis for each method across all wavelet functions is retained, as supported by the ANOVA tests.

Each wavelet function has its own set of advantages and limitations. Coiflets demonstrate compact support, which means they possess a limited number of non-zero coefficients. This characteristic allows coif2 to preserve edges and details while minimizing artifacts. Additionally, Coiflets are nearly symmetric and orthogonal, with symmetry aiding in reducing phase distortions and orthogonality, ensuring wavelet energy preservation.

Coiflets vary in terms of vanishing moments and filter length, which affects their computational complexity. As the value of N increases in CoifN (i.e., Coif1, Coif2, Coif3 to CoifN), the number of vanishing moments and the length of the filter also increase. The selection of a Coiflet must balance these two characteristics; using higher-order Coiflets leads to a smoother

signal representation(Dong Wei *et al*., n.d.; Wei, 1998).

Astronomical images often contain large areas with smooth gradients, such as gaseous regions of planets. The fk8 wavelet is better suited for representing these smooth regions because it has many vanishing moments. Additionally, the fk8 wavelet can accurately capture different frequency components of the image due to its fine frequency localization properties.

Biorthogonal (Bior) wavelets possess multiple vanishing moments in wavelet and scaling functions. This characteristic enables the wavelet to capture polynomial trends and smooth variations effectively (e.g., water, agricultural fields) in the data while preserving the geometric structures of Earth images, such as buildings and roads. The Bior wavelet (3.1, 3.3, 3.5, 3.7, 3.9) offers a well-balanced trade-off between signal representation accuracy and computational complexity (ang *et al*., 2010b).

The varying performance of wavelet functions in high-resolution image reconstruction is attributed to the distinct mathematical properties of each wavelet and the specific characteristics of the images being processed. Wavelets like Coif2, with its balanced time and frequency localization, excel in enhancing images with smooth regions and well-defined edges, such as the Lena image. In contrast, the Bior family, known for its effective localization, is better suited for complex textures found in satellite images. The FK8 wavelet outperforms others in processing astronomical images, such as those of Jupiter, where it effectively captures the unique spatial frequency distribution.

4. CONCLUSION:

WZP is an essential technique for resolution enhancement. It reduces edge artifacts by smoothing the image while preserving image features. The performance of this technique depends on selecting a suitable wavelet function for the studied dataset and requires a proper interpolation method.

Additionally, each wavelet function has unique properties and performs better on some datasets than others. This can be indicated by the superiority of coif2 for the Lina dataset, while fk8 excelled in the Jupiter dataset. However, Bior was more effective for remote sensing data sets. Coif2 has higher vanishing moments and can better capture and preserve fine details and edges; its near-symmetry characteristic helps reconstruct edges without artifacts. This is also the case for fk8; both wavelet functions exhibit time-frequency localization, ensuring that both low-frequency components are effectively represented.

To further enhance performance, we recommend developing adaptive wavelet techniques that dynamically adjust the wavelet function based on the specific characteristics of the input image. These adaptive techniques should account for critical image features such as edges, textures, and other relevant aspects. By modifying the wavelet function to better align with these characteristics, the technique can provide more precise and effective image processing.

Looking ahead, future research should explore the impact of different wavelet functions on a broader array of datasets and consider alternative resolution enhancement techniques beyond WZP. Expanding the scope of the investigation to include a wider range of datasets will provide users of WZP with clear insights into which wavelet function best suits their specific needs. Additionally, the study should not be limited to WZP; it is also crucial to evaluate other wavelet-based image enhancement techniques. Techniques utilizing Discrete Wavelet Transform (DWT), Continuous Wavelet Transform (CWT), and other wavelet applications in image reconstruction should also be examined. By comparing the effectiveness of various wavelet functions across multiple enhancement techniques, we can deepen our understanding of their utility and performance, thereby advancing the field of resolution enhancement and offering more versatile solutions to meet diverse imaging requirements.

5. Appendix: PSNR Heatmap

This heat map of data for the Lina image was provided to reference the PSNR of WZP for each wavelet function and the correspondence interpolation method.

6. DECLARATIONS

6.1. Study Limitations

This study acknowledges several limitations: Limited Datasets: The research was conducted using a limited number of datasets, specifically the Lina, Jupiter, and Babylon datasets. This constraint may affect the generalizability of the

findings to other types of images or datasets.

The study did not include a comparative analysis with other state-of-the-art image resolution enhancement methods. Future work should incorporate such comparisons to contextualize the performance of the proposed methods against the current leading techniques in the field.

6.2. Acknowledgment

The authors would like to express their gratitude to the following institutions and organizations:

- University of Babylon, College of Science, Department of Physics, for providing the necessary support and facilities to conduct this research.
- NASA: To grant access to astronomical images used in this study.
- Google Earth for providing access to remote sensing images integral to the research.

6.3. Funding

The Corresponding Author funded the research presented in this paper. No external funding sources were utilized in the preparation of this work. In accordance with the ethical guidelines of the Periódico Tchê Química, which do not allow donations from authors with manuscripts under evaluation (even when research funds are available), or in cases of authors' financial constraints, publication costs were fully absorbed by the journal under our Platinum Open Access policy, through the support of the Araucária Scientific Association (https://acaria.org/). This policy aims to ensure complete independence between the editorial process and any financial aspects, reinforcing our commitment to scientific integrity and equity in knowledge dissemination.

6.4. Competing Interests

The authors declare that they have no competing interests.

7. REFERENCES:

1. Agaian, S. S., Panetta, K., & Grigoryan, A. M. (2001). Transform-based image enhancement algorithms with performance measure. *IEEE Transactions on Image Processing*, *10*(3), 367–382. https://doi.org/10.1109/83.908502
2. Al-Sadooni, A. Ab., & van Loon, J. Th. (2022). *The kinematics and physical properties for some H II regions to the northeast of NGC 4945***. 080049. https://doi.org/10.1063/5.0067075
3. Anbarjafari, G., & Demirel, H. (2010). Image Super Resolution Based on Interpolation of Wavelet Domain High Frequency Subbands and the Spatial Domain Input Image. *ETRI Journal*, *32*(3), 390–394. https://doi.org/10.4218/etrij.10.0109.0303
4. Azani Mustafa, W., Yazid, H., Khairunizam, W., Aminuddin Jamlos, M., Zunaidi, I., Razlan, Z. M., & Shahriman, A. B. (2019a). Image Enhancement Based on Discrete Cosine Transforms (DCT) and Discrete Wavelet Transform (DWT): A Review. *IOP Conference Series: Materials Science and Engineering*, *557*(1), 012027. https://doi.org/10.1088/1757-899X/557/1/012027
5. Azani Mustafa, W., Yazid, H., Khairunizam, W., Aminuddin Jamlos, M., Zunaidi, I., Razlan, Z. M., & Shahriman, A. B. (2019b). Image Enhancement Based on Discrete Cosine Transforms (DCT) and Discrete Wavelet Transform (DWT): A Review. *IOP Conference Series: Materials Science and Engineering*, *557*(1), 012027. https://doi.org/10.1088/1757-899X/557/1/012027
6. Bulut, F., & Polyzou, W. N. (2013). Wavelets in field theory. *Physical Review D*, *87*(11), 116011. https://doi.org/10.1103/PhysRevD.87.116011
7. Claire Andreoli. (2023, November 3). *Hubble Provides Unique Ultraviolet View of Jupiter*. NASA, ESA, and M. Wong (University of California – Berkeley); Processing: Gladys Kober (NASA/Catholic University of America).
8. Costa, D. G., Affonso Guedes, L., Vasques,

F., & Portugal, P. (2013). Energy-efficient packet relaying in wireless image sensor networks exploiting the sensing relevancies of source nodes and DWT coding. *Journal of Sensor and Actuator Networks*, *2*(3), 424–448. https://doi.org/10.3390/jsan2030424

9. Costa, D., Guedes, L., Vasques, F., & Portugal, P. (2013). Energy-Efficient Packet Relaying in Wireless Image Sensor Networks Exploiting the Sensing Relevancies of Source Nodes and DWT Coding. *Journal of Sensor and Actuator Networks*, *2*(3), 424–448. https://doi.org/10.3390/jsan2030424
10. Deeba, F., Kun, S., Ali Dharejo, F., & Zhou, Y. (2020). Wavelet-Based Enhanced Medical Image Super Resolution. *IEEE Access*, *8*, 37035–37044. https://doi.org/10.1109/ACCESS.2020.2974278
11. Demirel, H., & Anbarjafari, G. (2010). Satellite Image Resolution Enhancement Using Complex Wavelet Transform. *IEEE Geoscience and Remote Sensing Letters*, *7*(1), 123–126. https://doi.org/10.1109/LGRS.2009.2028440
12. Demirel, H., & Anbarjafari, G. (2011). Discrete Wavelet Transform-Based Satellite Image Resolution Enhancement. *IEEE Transactions on Geoscience and Remote Sensing*, *49*(6), 1997–2004. https://doi.org/10.1109/TGRS.2010.2100401
13. Dong Wei, Bovik, A. C., & Evans, B. L. (n.d.). Generalized coiflets: a new family of orthonormal wavelets. *Conference Record of the Thirty-First Asilomar Conference on Signals, Systems and Computers (Cat. No.97CB36136)*, 1259–1263. https://doi.org/10.1109/ACSSC.1997.679106
14. Glass, G. V. (1966). Testing Homogeneity of Variances. *Http://Dx.Doi.Org/10.3102/0002831200300 3187*, *3*(3), 187–190. https://doi.org/10.3102/0002831200300318 7
15. Gonzalez, R. C., & Woods, R. E. (2002). *Digital Image Processing* (2nd ed.). Prentice Hall.
16. Greenspan, H. (2008). Super-Resolution in Medical Imaging. *The Computer Journal*, *52*(1), 43–63. https://doi.org/10.1093/comjnl/bxm075
17. Hamza, H. A., Sadooni, A. Ab. Al, & Loon, J. Th. van. (2020). Feedback from Ionized Outflows Traced Across the Nearly Edge-on Disk of the Nearby Seyfert 2 Galaxy NGC 4945*. *NeuroQuantology*, *18*(12), 06–17. https://doi.org/10.14704/nq.2020.18.12.NQ20232
18. Juang, P.-A., & Wu, M.-N. (2007). MRI Brain Phase Image Unwrapping Process by Wavelet Zero-Padding Technique. *Third International Conference on Intelligent Information Hiding and Multimedia Signal Processing (IIH-MSP 2007)*, 229–232. https://doi.org/10.1109/IIH-MSP.2007.224
19. Karunakar, P., Praveen, V., & Kumar, O. R. (2013). Discrete wavelet transform-based satellite image resolution enhancement. *Advance in Electronic and Electric Engineering*, *3*(4), 405–412.
20. Kok, C.-W., & Tam, W.-S. (n.d.). *Digital image interpolation in MATLAB*. 336. Retrieved July 3, 2024, from https://www.wiley.com/en-cn/Digital+Image+Interpolation+in+Matlab-p-9781119119647
21. Lars, S., & Wold, S. (1989). Analysis of variance (ANOVA). *Chemometrics and Intelligent Laboratory Systems*, *6*(4), 259–272. https://doi.org/10.1016/0169-7439(89)80095-4
22. Lee, D. T. L., & Yamamoto, A. (1994). Wavelet analysis: theory and applications. *Hewlett-Packard Journal*, *45*(6).
23. Loh, W. Y. (1987). Some modifications of levene's test of variance homogeneity. *Journal of Statistical Computation and Simulation*, *28*(3), 213–226. https://doi.org/10.1080/00949658708811030
24. Naidu, S. V., Garg, A., Yahia, H., & Singh, D. (2015). A comparison of wavelet based techniques for resolution enhancement of Moderate Resolution satellite images. *2015 National Conference on Recent Advances in Electronics & Computer Engineering (RAECE)*, 263–266. https://doi.org/10.1109/RAECE.2015.7510203
25. Narmatha, D. (2020). Resolution Enhancement of Microarray Image Using DWT AND SWT. *Journal of Analog and Digital Devices* , *5*(3), 20–28.
26. Patel, V., & Mistree, K. (2013). A review on different image interpolation techniques for image enhancement. *International Journal of Emerging Technology and Advanced Engineering*, *3*(12), 129–133.
27. Pimpalkhute, V. A., Page, R., Kothari, A.,

Bhurchandi, K. M., & Kamble, V. M. (2021). Digital Image Noise Estimation Using DWT Coefficients. *IEEE Transactions on Image Processing*, *30*, 1962–1972. https://doi.org/10.1109/TIP.2021.3049961
28. *Repository*. (n.d.). Retrieved July 6, 2024, from https://links.uwaterloo.ca/Repository.html
29. Shapiro, S. S., Wilk, M. B., & Chen, H. J. (1968). A Comparative Study of Various Tests for Normality. *Journal of the American Statistical Association*, *63*(324), 1343–1372. https://doi.org/10.1080/01621459.1968.10480932
30. Wei, D. (1998). *Coiflet-type wavelets: theory, design, and applications*. The University of Texas at Austin.
31. Witwit, W., Zhao, Y., Jenkins, K., & Zhao, Y. (2016). *An Optimal Factor Analysis Approach to Improve the Wavelet-based Image Resolution Enhancement Techniques*.
32. Witwit, W., Zhao, Y., Jenkins, K., & Zhao, Y. (2017). Satellite image resolution enhancement using discrete wavelet transform and new edge-directed interpolation. *Journal of Electronic Imaging*, *26*(2), 023014. https://doi.org/10.1117/1.JEI.26.2.023014
33. Wu, M. Te. (2019). Wavelet transform based on Meyer algorithm for image edge and blocking artifact reduction. *Information Sciences*, *474*, 125–135. https://doi.org/10.1016/J.INS.2018.09.058
34. Yang, Y., Su, Z., & Sun, L. (2010a). Medical image enhancement algorithm based on wavelet transform. *Electronics Letters*, *46*(2), 120–121.
35. Yang, Y., Su, Z., & Sun, L. (2010b). Medical image enhancement algorithm based on wavelet transform. *Electronics Letters*, *46*(2), 120. https://doi.org/10.1049/el.2010.2063

Table 1. *The best performance of wavelet functions in terms of PSNR for different interpolation methods and their corresponding wavelet functions, each method applied to a Lina image. The values in bold indicate the maximum PSN.*

Interpolation Method	Max-PSNR	Wavelet
nearest	25.121	coif2
bilinear	25.561	coif2
bicubic	26.525	coif2
box	25.121	coif2
triangle	25.561	coif2
cubic	26.525	coif2
lanczos2	26.559	coif2
lanczos3	**26.840**	coif2

Table 2. *The best performance of wavelet functions in terms of PSNR for different interpolation methods, each method applied to the astronomical image. The values in bold indicate maximum PSNRs.*

Interpolation Method	Max-PSNR	Wavelet
nearest	31.702	fk8
bilinear	**32.208**	fk8
bicubic	31.904	fk8
box	31.702	fk8
triangle	**32.208**	fk8
cubic	31.904	fk8
lanczos2	31.896	fk8
lanczos3	31.799	fk8

Table 3. *The best performance of wavelet functions in terms of PSNR for different interpolation methods, each method applied to the satellite image. The values in bold indicate maximum PSNRs.*

Interpolation Method	Highest PSNR	Wavelet
nearest	11.648	Bior(3.1,3.3,3.5,3.7,3.9)
bilinear	**11.700**	Bior(3.1,3.3,3.5,3.7,3.9)
bicubic	11.639	Bior(3.1,3.3,3.5,3.7,3.9)
box	11.648	Bior(3.1,3.3,3.5,3.7,3.9)
triangle	**11.700**	Bior(3.1,3.3,3.5,3.7,3.9)
cubic	11.639	Bior(3.1,3.3,3.5,3.7,3.9)
lanczos2	11.639	Bior(3.1,3.3,3.5,3.7,3.9)
lanczos3	11.628	Bior(3.1,3.3,3.5,3.7,3.9)

Table 4. *Descriptive Statistics of interpolation methods for the Lina Dataset. Bold values are the maximum value in a row.*

		Interpolation Method							
		nearest	***bilinear***	***bicubic***	***box***	***triangle***	***cubic***	***lanczos2***	***lanczos3***
Statistic	**N**	106	106	106	106	106	106	106	106
	Range	12.467	12.660	13.435	12.467	12.660	13.435	13.461	**13.682**
	Mean	19.891	**20.522**	20.510	19.891	**20.522**	20.510	20.510	20.487
	Std. Deviation	4.292	4.494	4.674	4.292	4.494	4.674	4.679	**4.725**
	Variance	18.424	20.196	21.850	18.424	20.196	21.850	21.891	**22.325**
	Skewness	-0.496	-0.574	-0.508	-0.496	-0.574	-0.508	-0.506	**-0.482**
	Kurtosis	-1.409	**-1.396**	-1.439	-1.409	**-1.396**	-1.439	-1.440	-1.452
Std. Error	**Mean**	0.417	0.436	0.454	0.417	0.436	0.454	0.454	**0.459**
	Skewness	0.235	0.235	0.235	0.235	0.235	0.235	0.235	0.235
	Kurtosis	0.465	0.465	0.465	0.465	0.465	0.465	0.465	0.465

Table 5. *Descriptive Statistics of various interpolation methods for the Jupiter Dataset. Bold values are the maximum value in a row.*

		Interpolation Method							
		nearest	***bilinear***	***bicubic***	***box***	***triangle***	***cubic***	***lanczos2***	***lanczos3***
Statistic	**N**	106	106	106	106	106	106	106	106
	Range	10.507	**10.942**	10.694	10.507	**10.942**	10.694	10.687	10.603
	Mean	28.858	**29.237**	29.019	28.858	**29.237**	29.019	29.015	28.950
	Std. Deviation	3.527	**3.693**	3.611	3.527	**3.693**	3.611	3.610	3.582
	Variance	12.438	**13.637**	13.040	12.438	**13.637**	13.040	13.029	12.834
	Skewness	-1.049	-1.045	-1.045	-1.049	-1.045	-1.045	-1.045	-1.046
	Kurtosis	-0.568	-0.591	-0.590	-0.568	-0.591	-0.590	-0.590	-0.588
Std. Error	**Mean**	0.343	**0.359**	0.351	0.343	**0.359**	0.351	0.351	0.348
	Skewness	0.235	0.235	0.235	0.235	0.235	0.235	0.235	0.235
	Kurtosis	0.465	0.465	0.465	0.465	0.465	0.465	0.465	0.465

Table 6. *Descriptive Statistics of various interpolation methods for the Babylon Dataset. Bold values are the maximum value in a row.*

		Interpolation Method							
		nearest	***bilinear***	***bicubic***	***box***	***triangle***	***cubic***	***lanczos2***	***lanczos3***
Statistic	**N**	106	106	106	106	106	106	106	106
	Range	1.063	1.043	1.047	1.063	1.043	1.047	1.047	1.047
	Mean	11.332	**11.406**	11.344	11.332	**11.406**	11.344	11.344	11.332
	Std. Deviation	0.383	**0.386**	**0.386**	0.383	**0.386**	**0.386**	**0.386**	0.385
	Variance	0.147	**0.149**	**0.149**	0.147	**0.149**	**0.149**	**0.149**	0.148
	Skewness	-1.062	-1.064	-1.072	-1.062	-1.064	-1.072	-1.072	-1.073
	Kurtosis	-0.589	-0.602	-0.586	-0.589	-0.602	-0.586	-0.585	-0.582
Std. Error	**Mean**	0.037	**0.038**	0.037	0.037	**0.038**	0.037	0.037	0.037
	Skewness	0.235	0.235	0.235	0.235	0.235	0.235	0.235	0.235
	Kurtosis	0.465	0.465	0.465	0.465	0.465	0.465	0.465	0.465

Table 7. *Shapiro-Wilk Test of normality (Shapiro et al., 1968) for the PSNR outcomes of interpolation methods along wavelet functions.*

		Lina		Jupiter		Babylon	
		Statistic	***Sig.***	***Statistic***	***Sig.***	***Statistic***	***Sig.***
Interpolation Methods	**nearest**	.851	.000	.734	.000	.734	.000
	bilinear	.816	.000	.726	.000	.726	.000
	bicubic	.836	.000	.726	.000	.726	.000
	box	.851	.000	.734	.000	.734	.000
	triangle	.816	.000	.726	.000	.726	.000
	cubic	.836	.000	.726	.000	.726	.000
	lanczos2	.836	.000	.726	.000	.726	.000
	lanczos3	.842	.000	.726	.000	.726	.000

Table 8: *ANOVA statistical test for interpolation method groups, where the effect size is 1, and the confidence interval is 95%. The results suggest that there are no significant differences between interpolation methods.*

		Lina		Jupiter		Babylon	
		Between Groups	***Within Groups***	***Between Groups***	***Within Groups***	***Between Groups***	***Within Groups***
Source of Variation	**SS**	60.984391	17341.47	16.04748	10929.74	0.76039	124.6111
	Df	7	840	7	840	7	840
	MS	8.7120558	20.64461	2.292497	13.0116	0.108627	0.148347
	F	0.4220014		0.176189		0.732253	
	P-value	0.8888972		0.990072		0.644666	
	F crit	2.0204628		2.020463		2.020463	

Table 9: *ANOVA statistics of PSNR performance at significance level 0.05. where the effect size is one, and the confidence interval is 95%. Wavelet functions grouped the data; results suggest that there is a significant difference across wavelet functions.*

		Lina		Jupiter		Babylon	
		Between Groups	**Within Groups**	**Between Groups**	**Within Groups**	**Between Groups**	**Within Groups**
Source of Variation	**SS**	17287.632	114.826	10924.328	21.461	124.566	0.805
	Df	105.000	742.000	105.000	742.000	105.000	742.000
	MS	164.644	0.155	104.041	0.029	1.186	0.001
	F	1063.920		3597.161		1092.908	
	P-value	0.000		0.000		0.000	
	F crit	1.259		1.259		1.259321834	

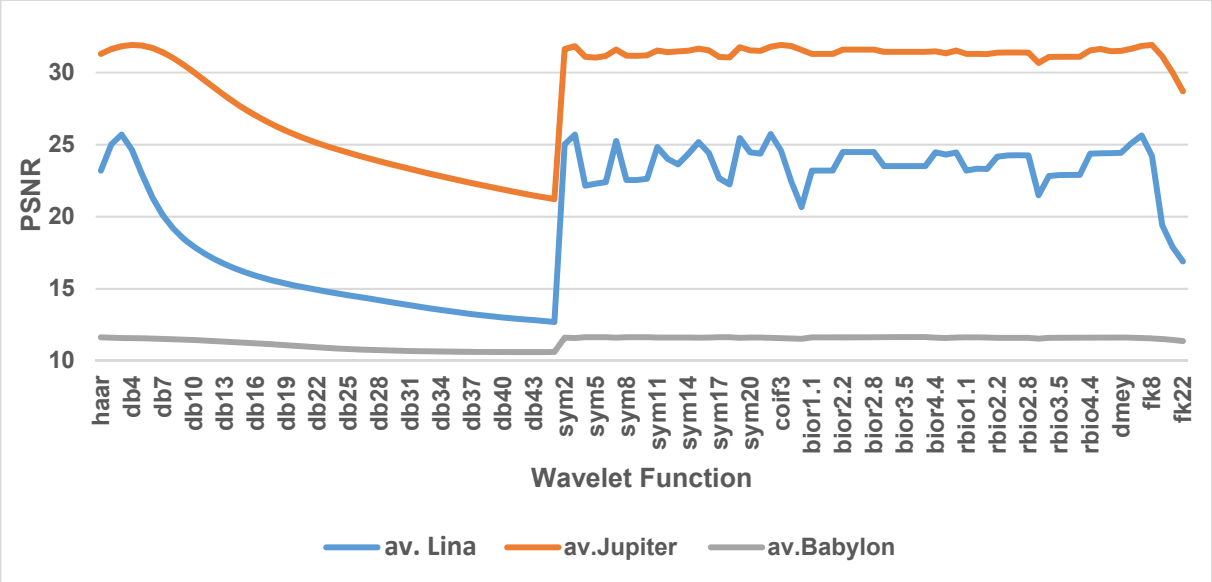

Figure 3. *PSNR performance of wavelet functions for the Lina, Jupiter, and Babylon datasets, where each point represents the average of the eighth interpolation method. A clear difference appears in the results; Daubechies wavelets yield the lowest PSNR, while Coiflet and fk8 have very close results.*

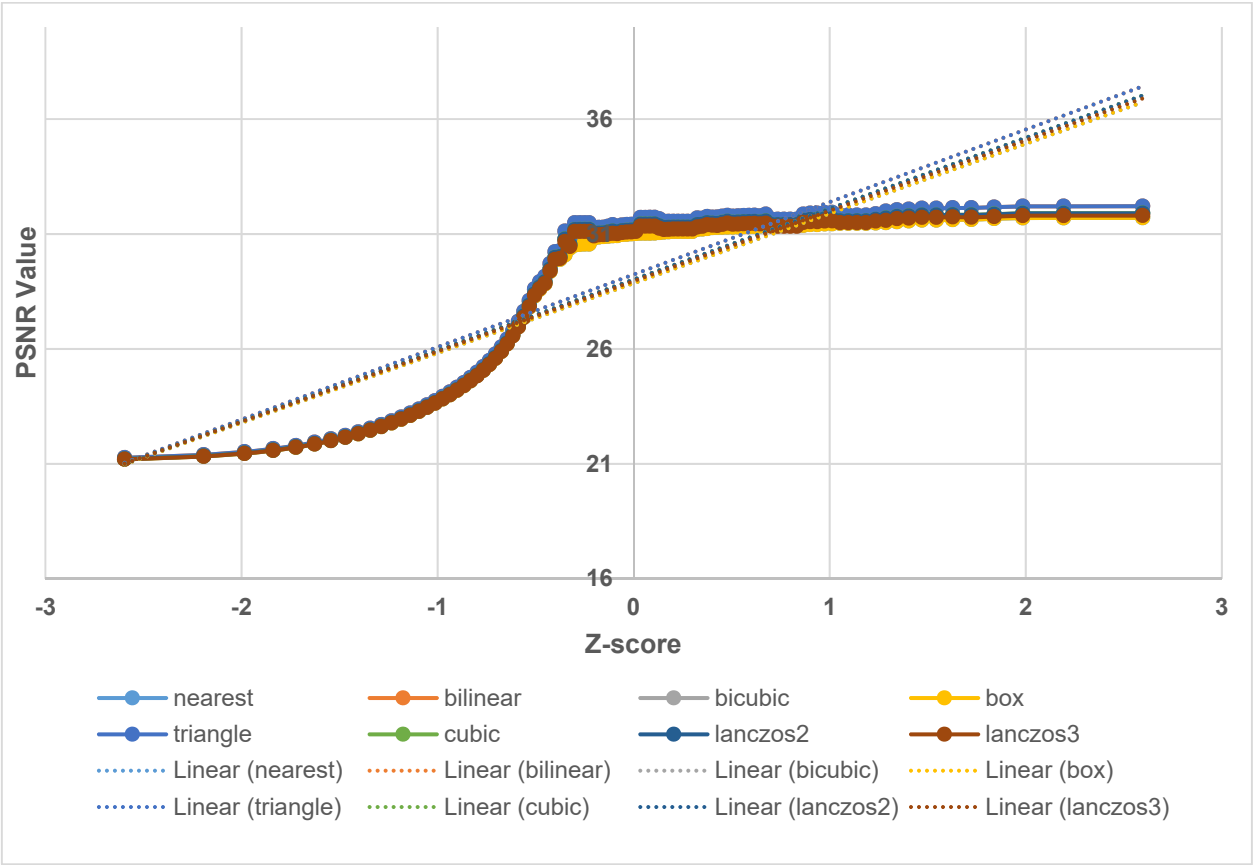

Figure 4. *The Jupiter PSNR results' Q-Q plot shows roughly linear behavior for all groups with a slight skew in the tails.*

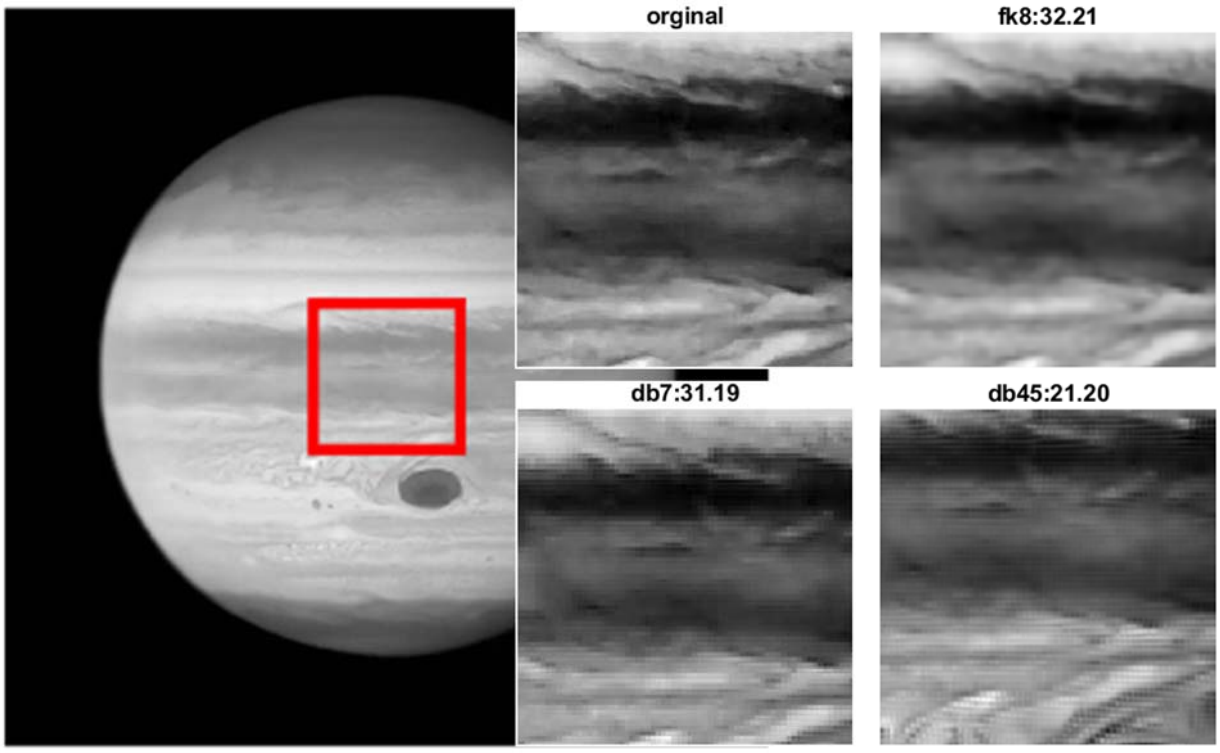

Figure 5. *Qualitative measurement of WZP performance across various wavelet functions applied to Jupiter in the ultraviolet image. The red rectangle indicates the cropped portion of the original image; the maximum PSNR achieved using fk8 and the bilinear interpolation method is shown in the upper right image. The median PSNR is at the lower left result from the db7, and the minimum PSNR is at the lower correct result from the db45 and box interpolation method*

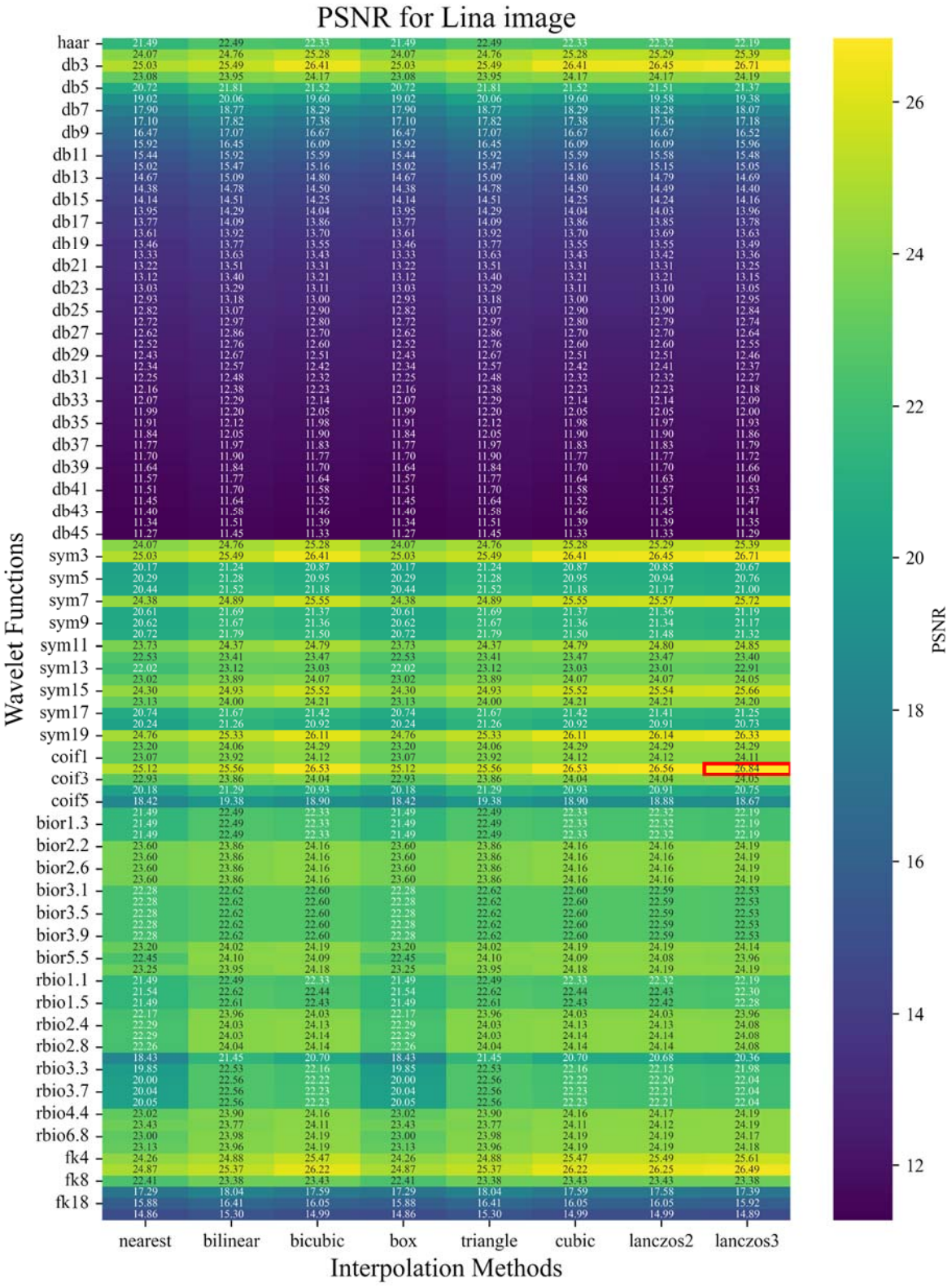

Figure 6. *Heat map of Lina image PSNR values for various interpolation methods and wavelet functions; the red rectangle marks the maximum PSNR value.*

PERIÓDICO TCHÊ QUÍMICA
ARTIGO ORIGINAL

UTILIZAÇÃO DO EX-NANO CAPILAR INERTSIL HÍLICO NA DETERMINAÇÃO DE FÁRMACOS CARBAPENÉMICOS E ESTUDO DAS SUAS APLICAÇÕES FARMACÊUTICAS

USE OF INERTSIL HILIC CAPILLARY EX-NANO IN THE DETERMINATION OF CARBAPENEM DRUGS AND STUDY OF THEIR PHARMACEUTICAL APPLICATIONS

استخدام عمود INERTSIL HILIC CAPILLARY EX-NANO لتقدير أدوية كاربابينيم ودراسة تطبيقاتها الصيدلانية

Ayad Kadhim Fadhil *
General Directorate of Education in Karbala, Iraq

** Corresponding author*
E-mail: ayadkadhim1979@gmail.com

Received 18 April 2024; received in revised form 30 November 2024, 10 May 2025, 20 September 2025; accepted 05 October 2025

RESUMO

Introdução: A cromatografia de fase reversa convencional (CPR) tem dificuldade em separar com eficácia antibióticos carbapenêmicos altamente polares. Os métodos HILIC atuais oferecem melhor retenção, mas frequentemente apresentam reprodutibilidade e seletividade limitadas. Ainda há uma lacuna significativa no uso ideal de colunas capilares HILIC em análises farmacêuticas. **Objetivos:** Esta pesquisa teve como objetivo desenvolver e validar um método de cromatografia líquida de interação forte hidrofílica (HILIC) usando uma coluna Inertsil HILIC Capillary EX-Nano para a separação e determinação de quatro carbapenêmicos - ertapenem, doripenem, imipenem e meropenem compostos farmacêuticos. **Métodos:** As condições cromatográficas foram modificadas utilizando um sistema tampão de acetato de amônio/ácido acético e acetonitrila, com alterações no pH (3,0-5,5), concentração do tampão (10-80 mM) e razão orgânica (50-95%). O método foi validado de acordo com as diretrizes ICH Q2(R1). Precisão, exatidão, linearidade, limites de detecção, confiabilidade, especificidade e adequação do instrumento foram avaliados. Estudos de lise forçada e testes de interferência de carga foram realizados para determinar a especificidade. **Resultados:** O método demonstrou excelente linearidade (R^2 > 0,999) em intervalos específicos para cada composto. Os valores de limite de detecção (LOD) e limite de quantificação (LOQ) foram verificados experimentalmente usando uma curva de calibração e a relação sinal-ruído. A recuperação variou de 98,3% a 101,8%, e a precisão intra e interdiária apresentou um desvio-padrão relativo (RSD) inferior a 2,0%. As separações cromatográficas foram obtidas com ≥ 2,0, fatores de cauda ≤ 1,8 e placas teóricas > 2000 para todos os picos. Os testes de ajuste do sistema confirmaram a confiabilidade do método em todas as etapas. **Discussão:** A coluna Inertsil HILIC Capillary EX-Nano demonstrou seletividade e reprodutibilidade superiores na separação de carbapenêmicos em comparação aos métodos HILIC relatados anteriormente. A avaliação mecanicista indicou forte interação hidrofílica, potencializada por mecanismos de retenção zwitteriônica. A especificidade foi estabelecida por meio de testes de estresse e avaliação de interferência da matriz. O método permaneceu robusto sob variações na composição da fase móvel e na vazão. **Conclusões**: O método HILIC publicado oferece uma abordagem confiável, precisa e seletiva. Oferece uma alternativa superior às técnicas convencionais de HILIC e RPLC e atende aos requisitos de certificação e controle de qualidade.

Palavras-chave: *concentrações de tampão, ACN,HILIC, pH, carbapenêmicos*

ABSTRACT

Background: Conventional reverse-phase chromatography has difficulty effectively separating highly polar carbapenem antibiotics. Current HILIC methods offer improved retention, but are often limited by issues of reproducibility and selectivity. A significant gap remains in the optimal use of HILIC capillary columns in pharmaceutical analysis. **Aim:** This research aimed to develop and validate an HILIC) method by means of an Inertsil HILIC Capillary EX-Nano column for the determination and separation of four carbapenems (imipenem, doripenem, ertapenem, and meropenem) in pharmaceutical compounds. **Methods:** Chromatographic conditions were modified using an ammonium acetate/acetic acid buffer system and ACN, with changes in pH (3.0-5.5), buffer concentration (10-80 mM), and organic ratio (50-95%). The technique was authenticated in accordance

DOI: 10.52571/PTQ.v22.n51.2025_02_KADHIM_pgs_18_37.pdf

with the ICH Q2(R1) guiding principle. Precision, accuracy, linearity, detection limits, reliability, specificity, and instrument suitability were evaluated. Forced lysis studies and filler interference tests were performed to determine specificity. **Results:** The method demonstrated excellent linearity ($R^2 > 0.999$) across specific ranges for each compound. Limit of detection (LOD) and limit of quantification (LOQ) values were experimentally verified using both a calibration curve and the signal-to-noise ratio. Recovery ranged from 98.3% to 101.8%, and inter-day and intra-day precision presented a relative standard deviation (RSD) of less than 2.0%. Chromatographic separations were achieved with ≥ 2.0, tail factors ≤ 1.8, and theoretical plates > 2000 for all peaks. System fit tests confirmed the reliability of the method at all stages. **Discussion:** The Inertsil HILIC Capillary EX-Nano column demonstrated superior selectivity and reproducibility for separating carbapenems compared to previously reported HILIC methods. Mechanistic evaluation indicated strong hydrophilic interaction enhanced by zwitterionic retention mechanisms. Specificity was established through stress testing and matrix interference evaluation. The method remained robust under variations in mobile phase composition and flow rate. **Conclusions**: The published HILIC method provides a reliable, accurate, and selective approach. It offers a superior alternative to conventional HILIC and RPLC techniques, meeting certification and quality control requirements.

Keywords. *Carbapenem, ACN, Buffer concentrations, HILIC, pH.*

الملخص

الخلفية: تواجه تقنية كروماتوغرافيا الطور العكسي المعتادة إشكالًا في فصل المضادات الحيوية الكاربابينيمية مرتفعة القطبية بفعالية. توفر أساليب HILIC الراهنة احتجازًا أفضل، لكنها غالبًا ما تكون مقيدة بإمكانية التكرار والانتقائية. وما زالت هناك فجوة بارزة في الاستخدام الأمثل لأعمدة HILIC الشعرية في التحليل الدوائي.**الأهداف:** هدفت هذه البحث إلى تطوير واعتماد أسلوب كروماتوغرافيا السائل التفاعلية القوية المحبة للماء (HILIC) باستعمال عمود Inertsil HILIC Capillary EX-Nano لفصل وتعيين مقدار أربعة كاربابينيمات - إيرتابينيم ودوريبينيم وإيميبينيم وميروبينيم - في المركبات الصيدلانية.**الطرق:** تم تعديل ظروف الكروماتوغرافيا باستعمال نظام عازل من أسيتات الأمونيوم/حمض الخل وأسيتونتريل، مع تغييرات في الأس الهيدروجيني (3.0-5.5)، وتركيز العازل (10-80 ملي مولار)، والنسبة العضوية (50-95%). تم التحقق من الطريقة وفقًا لإرشادات ICH Q2(R1). تم تقييم الدقة، والإحكام، والخطية، وحدود الكشف، والموثوقية، والخصوصية، وملاءمة الجهاز. أُجريت دراسات التحلل القسري واختبارات تداخل المواد المالئة لتحديد الخصوصية.**النتائج:** أظهرت الطريقة خطية ممتازة ($R^2 > 0.999$) عبر مجالات معينة لكل مركب. تم التحقق من قيم حد الكشف (LOD) وحدود التحديد الكمي (LOQ) عمليًا باستخدام كلٍّ من منحنى المعايرة ونسبة الإشارة إلى الضوضاء. تراوحت نسبة الاسترداد بين 98.3% و101.8%، وأظهرت الدقة داخل اليوم/بين اليومين انحرافًا معياريًا نسبيًا (RSD) أقل من 2.0%. تم تحقيق الفصل الكروماتوغرافي ببراعة ≤ 2.0، وعوامل ذيل ≥ 1.8، ولوحات نظرية > 2000 لجميع القمم. أكدت اختبارات ملاءمة النظام موثوقية الطريقة في جميع المراحل. **المناقشة:** أظهر عمود Inertsil HILIC Capillary EX-Nano انتقائيةً وقابليةً تكراريةً ممتازةً لفصل الكاربابينيمات مُقارنةً بأساليب HILIC المُبلغ عنها سابقًا. أشار التقييم الميكانيكي إلى تفاعل قويّ محبّ للماء، مُعزّز بآليات احتجاز أيونية مزدوجة. حُدّدت الخصوصية من خلال اختبار الإجهاد وتقييم تداخل المصفوفة. بقيت الطريقة متينةً في ظلّ اختلافات في تكوين الطور المتحرك وسرعة التدفق. **الاستنتاجات:** توفر طريقة HILIC المقترحة منهاجًا يعتمد عليه، دقيقًا، وانتقائيًا لتحديد المضادات الحيوية بيتا لاكتام عالية الاستقطاب في الأشكال الصيدلانية. كما تقدم خيارًا متميزًا لأساليب HILIC وRPLC التقليدية، وتتوافق مع متطلبات التحقق التنظيمية لتطبيقات ضبط الجودة.

الكلمات المفتاحية: الكاربابينيمات ,pH, اسيتونايترايل ,محلول بفر ,HILIC

1. INTRODUCTION:

Antibiotics containing a beta-lactam ring in their chemical structure constitute a specific subclass of antimicrobial agents, including carbapenems(Das & Banik, 2024); (Peris-Vicente *et al*., 2022). This group also includes penicillins, cephalosporins, and monobactams(Tumskaya & Kosyreva, 2024). Carbapenems are known for their biological activity and efficacy, with examples such as imipenem, meropenem, ertapenem, and doripenem demonstrating activity against a wide range of aerobic and anaerobic bacterial pathogens. High-performance liquid chromatography (HPLC) can be used to separate compounds with polar or hydrophilic properties using a technique known as HILIC, short for hydrophilic in-liquid chromatography . This method is known as "hydrophilic interaction chromatography" and is also described in scientific literature as "aqueous natural phase" (Taylor *et al*., 2023); (Tengattini *et al*., 2024). The separation technique was first known as "Hydrophilic-interaction chromatography," while "Aqueous Normal Phase" has also been used occasionally (Dong *et al*., 2023); (Torigoe *et al*., 2024). In hydrophilic interactive liquid chromatography, ACN, which is highly miscible with organic solvents, is typically used in aqueous buffer solutions, such as NH_4HCO_2 and the related $NH_4CH_3CO_2$, at concentrations ranging from approximately 50% to 95%. Various detection methods are compatible with the HILIC technique, and combining this technique with ESI-MS spectroscopy can improve the accuracy and sensitivity of the technique ((Dejaegher & Vander Heyden, 2010); (Lei *et al*., 2022). HILIC varies from the RPLC technique in numerous aspects, as it is suitable for separating chemical compounds such as acids, bases, sugars, ions, and other

hydrophilic substances that are difficult to resolve using RPLC (Merlo *et al*., 2022). The HILIC method has involved considerable interest due to its ability to address various separation challenges that were once difficult to overcome, such as isolating small organic acids, basic pharmaceuticals, cations, anions, and numerous other neutral or charged compounds (Glinka *et al*., 2020). According to current HILIC theory, the injected analyte molecules distribute between the water-rich layer on the hydrophilic stationary phase and the mobile phase eluent, resulting in their retention under HILIC conditions (Vallaro *et al*., 2020; Moyne *et al*., 2021). Greater analyte hydrophilicity shifts the partitioning equilibrium toward the immobilized water layer of the stationary phase, thereby enhancing the retention of the analyte (Zhao *et al*., 2022; Pauter *et al*., 2020). Because beta-lactam antibiotics are highly polar, they tend to elute relatively early in reversed-phase chromatography. While normal-phase chromatography and hydrophilic interaction chromatography (HILIC) can offer potential alternatives, their use is limited by the large amounts of hazardous organic solvents required and the lengthy equilibration times involved (Mishra *et al*., 2021);(Fadhil *et al*., 2023). In this study, several antibiotic drugs were separated using a commercial Inertsil column. The compounds resolved through this technique are offered in Figure 1.

2. MATERIALS AND METHODS

2.1. Materials

The ammonium acetate was supplied by Fluka Honeywell Research Chemicals (Bucharest, Romania), the Meropenem by Sigma-Aldrich Chemie B.V. (Zwijndrecht, the Netherlands), the Ertapenem by SelleckChem (Houston, TX, USA), and the Doripenem by Toronto Research Chemicals (North York, Ontario, Canada). Imipenem was supplied by Santa Cruz Biotechnology (Dallas, Texas, USA). ACN was supplied by Biosolve BV, a company based in Valkenswaard, the Netherlands. Ultra-pure water was produced using an in-house MilliPore Advantage A10 System (Millipore, Bedford, MA, USA).

2.2. Chromatographic Conditions

An Inertsil HILIC Capillary EX-Nano column (150 mm × 0.5 mm, 3 µm particle size) was employed for the separation. The mobile phase consisted of 95% ACN and 10% ammonium acetate buffer (40 mM, pH 5.5). The injection volume was 2 µL, the detection wavelength was set at 254 nm, and the flow rate was maintained at 0.2 mL/min. The column temperature was controlled at 40 ± 1 °C. The total run time was 12 minutes, ensuring complete elution of all analytes with adequate resolution. Prior to use, the mobile phase was degassed by ultrasonication for 10 minutes to ensure system stability. The column was equilibrated with the mobile phase for at least 10 column volumes (~2 mL) before each analytical sequence to stabilize the baseline and improve retention reproducibility.

2.3. Methods

The selected drugs were evaluated using an Inertsil HILIC Capillary EX-Nano column to investigate their chromatographic behavior under hydrophilic interaction conditions. A pH-adjusted eluent composed of ACN and ammonium acetate buffer at varying concentrations was employed. Optimal retention for all four analytes was achieved using an ammonium acetate buffer (40 mM) containing 95% ACN at a pH of 5.5. This experimental design enabled assessment of how hydrophilicity and analyte properties influence separation efficiency.

Ertapenem, Doripenem, Imipenem, and Meropenem were selected as representative carbapenem antibiotics to assess their retention behavior in HILIC mode (Figure 2). The mobile phase composition was systematically varied by adjusting the ACN content (50–95%), buffer concentration (10–80 mM), and pH (3.0–5.5) to elucidate separation characteristics and, consequently, the underlying column separation mechanism. The physicochemical properties of the four drugs are summarized in Table 1.

2.3.*1 Adjusting the Retention*

Modifying the eluent by adjusting the buffer concentration, pH, and type of organic solvent affects the retention and selectivity of HILIC. Increasing the proportion of organic solvent is the most effective way to modify retention. The ideal circumstances for separating antibiotic drugs are given in Table 2.

2.3.*2. Stationary phases of HILIC*

Since HILIC only necessitates a hydrophilic surface to adsorb and stabilize the water layer required for the partitioning process, one might assume that all hydrophilic stationary phases are equally suitable for HILIC and function in the same way. Though this is not the case. HILIC stationary phases can vary greatly in their total surface charge, chemical reactivity, pH

dependence, and phase stability. Increasing the concentration of the organic solvent can affect the separation process, and more stable analyses can be accomplished by adding a basic modifier, such as ammonium acetate, to the mobile phase. In this research, an Inertsil HILIC Capillary EX-Nano Column (3 µm, 150 × 0.05 mm) was used, which provides sharp peak shapes for both basic and neutral compounds and contains a chemically bonded diol group on its surface.

2.3.*3. HILIC Solvents*

ACN is commonly used as the primary organic solvent in HILIC due to its low viscosity, high miscibility, and strong retention performance in combination with water. Nevertheless, other polar organic solvents, such as ethanol, methanol, propanol, isopropanol, dioxane, and acetone, can also serve as the organic component in HILIC mobile phases. Retention in HILIC can be effectively adjusted by altering the proportion of the organic solvent. An increase in the organic solvent content typically results in higher retention. Unlike RPLC, the relationship between the organic solvent fraction and the retention factor (K) in HILIC is not logarithmic; instead, it often follows a log/log trend. Because even small changes in solvent concentration can cause substantial shifts in retention, narrower solvent gradients are typically recommended for HILIC. In the present study, the effect of ACN content was assessed by gradually increasing its proportion in the mobile phase while maintaining the buffer concentration at 40 mM (pH 5.5).

2.3.*4. Preparation of different pH*

The Henderson-Hasselbalch equation is used to calculate the relative proportions of the base and acid components in a buffered system, based on the solution pH, the buffer pKa, and the concentrations of the conjugate base [A^-] and its corresponding acid [HA]. In this study, ammonium acetate and acetic acid (HAc) were combined to prepare a series of 1000 mL buffer solutions with pH values ranging from 3.0 to 5.5. The pH, the required HAc volume, and the NH_4OAc mass for each buffer preparation are provided in Table 6 (see Equation 1).

$$pH = pKa + log\ ([A-])/([HA]) \quad \text{(Eq.1)}$$

2.3.*5. Preparation of buffer concentrations*

$NH4OAc\ /HAc$ was mixed to create various buffers in $1000\ mL$ at concentrations ranging from 10 to $80\ mM$. The buffer concentration, HAc volume, and $NH4OAc$ weight are displayed in Table 7.

2.3.*6. Sample preparation*

Twenty tablets of each formulation were ground and homogenized. Accurately weighed portions were dissolved in the liquid phase, ultrasonicated, filtered (0.45 µm), and diluted as required. Forced dissociation studies included exposure to light, heat, acid/base hydrolysis, and oxidation.

2.3.7. System Suitability Testing

The system validity was assessed prior to validation. 6 replicates of the standard solution were injected. Acceptance criteria were: precision ≥ 2.0, tail factor ≤ 2.0, theoretical plates ≥ 2000, relative standard deviation of peak area ≤ 2.0%, and baseline stability over the run-in period.

2.3.8. Validation Parameters

The validation process followed ICH Q2(R1) guidelines. Rheology: All drugs were quantified at six levels (n = 6). R^2 values > 0.999. Precision: Recovery was tested at 80%, 100%, and 120% (n = 6 each). Recovery rates were 98-102%. accuracy and precision within 2 days (n = 6), %RSD < 2.0%. LOD/LOQ: Determined using signal-to-noise and regression methods. The limit of quantification was verified to be within %RSD ≤ 20%, and the recovery rate was 80-120%. Specificity: No interference from additives or degradation products. Peak clarity was confirmed. Stability: Assessed by adjusting flow rate (± 10%), pH (± 0.2), buffer (± 10%), and ACN (± 5%). The method remained stable. Solution stability: Standards and samples remained stable for 24 hours on the laboratory bench and 48 hours on the autosampler (Table 3)**.**

3. RESULTS AND DISCUSSION:

3.1. Results

3.1.1. Effect of ACN

This disparity arises from the pharmaceutical hydrophilicity of the four-drug models when the ACN level fluctuates within the eluent, as demonstrated by the pharmaceutical log Pow values. The hydrophilia of the medications causes this variation in behavior. For the Inertsil HILIC Capillary EX-Nano Column, doripenem,

imipenem, meropenem, and ertapenem all exhibit HILIC behavior (figures 3-6). This is because the corresponding log P (octanol/water) values for those drugs are -5.60, -2.78, -4.40, and 3.20. It should be noted that the interactions between the drug's amine and hydroxide groups, which result in a hydrogen bond due to hydrogen bonding and van der Waals forces, are what cause the pharmaceuticals to remain in the column at optimal retention.

3.1.2. Effect of Buffer concentration

In the hydrophilic interaction mode, increasing the buffer concentration reduces intra-molecular ion pairing, thereby enhancing the linear arrangement of functional groups on the stationary phase despite the high proportion of ACN. The retention time of analytes on HILIC columns may decrease or increase, depending on the concentration of the NH_4OAc/HAc buffer. Notably, at pH 5.5 and 95% ACN, Doripenem, Imipenem, Meropenem, and Etapenem exhibit higher retention factors as the buffer concentration is increased from 10 to 80 mM (Figures 7–10).

3.1.3. Effect of pH

The eluent pH can be adjusted to provide a comprehensive view of the drug separation in HILIC mode. When shown in Figures (11–14), the buffer concentration was constant at 40 mM with 95% ACN, while the drug retention factor decreased when the eluent pH rose from 3 to 5.5. This is because the carboxyl group in drugs deprotonates.

3.1.4. linearity and calibration of Drugs

The drug calibration graphs of the Inertsil HILIC Capillary EX-Nano Column, which illustrate the range of concentrations of all drugs, Doripenem, Imipenem, Meropenem, and Ertapenem $(0.05-4.5, 0.05-4.5, 0.05-4.5,$ and $0.05-4.5)$µg/mL, respectively, are defined by the plotted area versus drug concentrations. (Figures 15–18).

3.1.5. Statistical Data Analysis

The intra-day and inter-day precision results showed consistent %RSD values below 2.0% & 5.0%, respectively, for all compounds, confirming method repeatability and intermediate precision. A slight variation was observed between time intervals, which was within acceptable limits. For accuracy, recovery values ranged from (98.4% to 101.2%). Confidence intervals (95%) were calculated for each mean recovery value to verify statistical significance. No significant differences ($p > 0.05$) were found using one-way ANOVA across recovery levels, confirming the method's accuracy and robustness (Table 4).

3.1.6. Pharmaceutical Applications

To verify the accuracy of the analytical method, one-sample t-tests were conducted to compare the experimentally found drug contents with their declared values (200 mg). In all cases, the calculated t-values were less than the critical t-value at the 95% confidence level ($t-critical = 2.571, df = 5$), indicating no statistically significant difference between measured and labeled amounts. Furthermore, one-way ANOVA was applied to evaluate consistency across the three manufacturers for each compound. The p-values obtained were greater than 0.05, confirming that the differences between formulations from different manufacturers were not statistically significant at the 95% confidence level. To ensure the methodological equivalence of the developed HILIC procedure with pharmacopeial methods, the same samples were analyzed using a conventional RP-HPLC method. A paired t-test revealed no significant difference ($p > 0.05$) in recovery, precision, or quantitation results between the two methods, confirming that the HILIC method is comparable and equivalent in performance to the official procedures. The outcomes are displayed in Table 5.

3.2. Discussion

To assess the chromatographic performance under hydrophilic interaction conditions, four carbapenem antibiotics imipenem, ertapenem, meropenem, and doripenem were selected as test compounds. The separation was carried out using an Inertsil HILIC Capillary EX-Nano column with mobile phases containing ACN and buffers of varying concentrations. Optimal retention for all analytes was achieved using a mobile phase composed of 40 mM ammonium acetate, 95% acetonitrile, and a pH of 5.5. This setup enabled the assessment of how molecular characteristics affect the separation of hydrophilic compounds. In HILIC, analytes are separated primarily through partitioning between a water-rich layer adsorbed onto the polar stationary phase and an ACN-rich mobile phase. Common stationary phases include cyano, amino, and bare silica, similar to those used in NPLC, while the mobile phase composition resembles that of RPLC. Furthermore, HILIC can be adapted for the

analysis of charged species, extending its applicability to ion chromatography (Buszewski & Noga, 2012). The hydrophilicity of Doripenem is the cause of this variation in the compounds' behavior. Therefore, the HILIC form of Doripenem, a strong acid with a pKa value of 3.54 and an isoelectric point (pI) value. Due to the entire positive charge of imipenem (pka 3.44, pI 8.75), it displays HILIC behavior for the Inertsil HILIC Capillary EX-Nano Column. Meropenem behaved in a hydrophilic manner. This variation in the compound's behavior results from meropenem's hydrophilicity (pka 3.28, pI 5.15), which is entirely positively charged. Ertapenem exhibits a retention factor that rises with increasing pH ($pI = 3.73$, $pKa = 3.22$). The increase in the hydroxyl group's negative charge is the cause of this.

3.2.1. Method Performance and Comparison

The developed method demonstrates several advantages over conventional reversed-phase chromatography for these highly polar antibiotics. RPLC typically exhibits poor retention and peak shape for beta-lactams due to their high polarity, whereas HILIC mode provides adequate retention and excellent peak symmetry (tailing factors ≤ 1.8).Compared to previously reported HILIC methods for carbapenems, the Inertsil HILIC Capillary EX-Nano column showed superior performance in terms of resolution and reproducibility. The diol-functionalized stationary phase offers balanced hydrophilic interactions, eliminating excessive secondary interactions that can cause peak tailing.The excellent validation parameters (R^2 > 0.999, RSD < 2.0%, recovery 98.3-101.8%) confirm the method's reliability for pharmaceutical quality control applications. The low detection limits achieved (LOD $0.0024 - 0.0030$ µg/mL) make this method suitable for trace analysis and impurity profiling.

3.2.2. Pharmaceutical Application Interpretation

The statistical analysis of pharmaceutical formulations demonstrates the method's practical applicability. The absence of significant differences between measured and labeled amounts (p > 0.05 in all t-tests) confirms the method's accuracy in real sample matrices.The consistency across different manufacturers (ANOVA p-values > 0.05) suggests the method is not affected by matrix variations from different formulation excipients. This robustness is crucial for routine quality control, where samples from various sources must be analyzed.The equivalence with pharmacopeial RP-HPLC methods (paired t-test, p > 0.05) validates the HILIC approach as an alternative technique, potentially offering advantages in terms of separation quality for these polar compounds.

4. CONCLUSIONS:

A validated HILIC method was successfully developed for the simultaneous determination of four carbapenem antibiotics (doripenem, imipenem, meropenem, and ertapenem) using an Inertsil HILIC Capillary EX-Nano column. The method demonstrated excellent analytical performance with linearity (R^2 > 0.999), low detection limits (LOD: $0.0024 - 0.0030$ µg/mL; LOQ: $0.0072 - 0.0090$ µg/mL), high recovery ($98.3 - 101.8\%$), and precision (RSD < 2.0% for both intra-day and inter-day analyses) across the concentration range of $0.05 - 4.5$ µg/mL for all analytes.System suitability criteria were consistently met throughout validation, with resolutions of ≥ 2.0, tailing factors of ≤ 1.8, and theoretical plates of > 2000 for all analytes. The method remained robust under systematic variations in pH (± 0.2), buffer concentration ($\pm 10\%$), organic content ($\pm 5\%$), and flow rate ($\pm 10\%$), confirming its reliability for routine pharmaceutical quality control.The successful application of the method to pharmaceutical formulations from three different manufacturers demonstrated its practical utility. Statistical analysis (one-sample t-tests and ANOVA, p > 0.05) revealed no significant differences between the measured and labeled amounts, validating the method's accuracy for quality control purposes. Method equivalence testing with pharmacopeial RP-HPLC procedures (paired t-test, p > 0.05) confirmed comparable performance.The retention mechanism study revealed that hydrophilic partitioning is the dominant separation mode, with retention directly correlating with analyte hydrophilicity (log P (octanol/water)values ranging from $-5.60\ to\ -2.78$). The effects of acetonitrile content, buffer concentration, and pH on retention were systematically characterized, providing insights for method optimization and transfer to other laboratories.This method offers several advantages over conventional reversed-phase chromatography for highly polar beta-lactam antibiotics, including improved retention, peak shape, and separation efficiency. The HILIC approach addresses the analytical challenges posed by the high polarity of carbapenems, which typically show poor retention in RPLC systems.

5. DECLARATIONS:

5.1. Limitations

The study has several methodological limitations. Validation was performed exclusively on tablet formulations; applicability to other dosage forms (injectables, lyophilized powders, suspensions) requires additional validation. Comprehensive forced degradation studies, including the identification and quantification of degradation products, were not conducted. The method's selectivity for related substances, process impurities, and enantiomeric separation was not exhaustively evaluated. Long-term column performance, including maximum number of injections before degradation and column-to-column reproducibility, was not systematically assessed. The study was conducted in a single laboratory; inter-laboratory validation would be necessary to confirm robustness across different instruments, operators, and environmental conditions.

5.2. Acknowledgements

I would like to extend my sincere thanks to the General Directorate of Education in Karbala and the University of Karbala for providing me with job opportunities and requirements.

5.3. Funding source

The authors financed this study. In accordance with the ethical guidelines of the Periódico Tchê Química, which do not allow donations from authors with manuscripts under evaluation (even when research funds are available), or in cases of authors' financial constraints, publication costs were fully absorbed by the journal under our Platinum Open Access policy, through the support of the Araucária Scientific Association (https://acaria.org/). This policy aims to ensure complete independence between the editorial process and any financial aspects, reinforcing our commitment to scientific integrity and equity in knowledge dissemination.

5.4. Competing Interests

The authors declare no conflicts of interest related to this work. No financial or personal relationships exist with organizations or individuals that could potentially influence this research inappropriately.

5.5. Open Access

6. REFERENCES:

1. Das, A., & Banik, B. K. (2024). 1 Beta-Lactams: Classifications, Biogenesis, Physical Characteristics, and Medicinal Activities. *Chemistry and Biology of Beta-Lactams*, 1. DOI: 10.1201/9780367816339-1

2. Peris-Vicente, J., Peris-García, E., Albiol-Chiva, J., Durgbanshi, A., Ochoa-Aranda, E., Carda-Broch, S., Bose, D., & Esteve-Romero, J. (2022). Liquid chromatography, a valuable tool in the determination of antibiotics in biological, food, and environmental samples. *Microchemical Journal*, *177*, 107309. DOI:10.1016/j.microc.2022.107309

3. Tumskaya, A. V, & Kosyreva, I. V. (2024). Rapid determination of some cephalosporins using immobilized para-dimethylaminobenzaldehyde. *Journal of Analytical Chemistry*, *79*(2), 141-147. DOI: 10.1134/S1061934824020138

4. Taylor, M. R., Kawakami, J., & McCalley, D. V. (2023). Managing sample introduction problems in hydrophilic interaction liquid chromatography. *Journal of Chromatography A*, *1700*, 464006. DOI: 10.1016/j.chroma.2023.464006

5. Tengattini, S., Massolini, G., Rinaldi, F., Calleri, E., & Temporini, C. (2024). Hydrophilic interaction liquid chromatography (HILIC) for the analysis of intact proteins and glycoproteins. *TrAC Trends in Analytical Chemistry*, 174, 117702. DOI: 10.1016/j.trac.2024.117702

6. Dong, W., Chen, L., Jia, L., Chen, Z., Shen, J., Li, P., & Sun, S. (2023). Maximal performance of intact N-glycopeptide enrichment using sequential HILIC and MAX columns. *Analytical and Bioanalytical Chemistry*, *415*(26), 6431–6439. DOI: 10.1007/s00216-023-04919-w

7. Torigoe, T., Takahashi, M., Heravizadeh, O., Ikeda, K., Nakatani, K., Bamba, T., & Izumi, Y. (2024). Predicting retention time in unified-hydrophilic-interaction/anion-exchange liquid chromatography high-resolution tandem mass spectrometry (Unified-HILIC/AEX/HRMS/MS) for comprehensive structural annotation of polar metabolome. *Analytical Chemistry*, *96*(3), 1275–1283. DOI: 10.1021/acs.analchem.3c04618

8. Dejaegher, B., & Vander Heyden, Y. (2010). HILIC methods in pharmaceutical analysis. *Journal of Separation Science*, *33*(6-7), 698–715. DOI: 10.1002/jssc.200900742

9. Merlo, Merlo, F., Montagna, J., Maraschi, F., Profumo, A., Baldanti, F., & Speltini, A. (2022). A versatile method for multiclass determination of β-lactam drugs in urine by solid-phase extraction followed by HILIC-UV. *Journal of Chromatography Open*, *2*, 100048. DOI: 10.1016/j.jcoa.2022.100048

10. Glinka, M., Wojnowski, W., & Wasik, A. (2020). Determination of aminoglycoside antibiotics: Current status and future trends. *TrAC Trends in Analytical Chemistry*, *131*, 116034. DOI: 10.1016/j.trac.2020.116034

11. Vallaro, Vallaro, M., Ermondi, G., & Caron, G. (2020). Chromatographic HILIC indexes to characterize the lipophilicity of zwitterions. *European Journal of Pharmaceutical Sciences*, *145*, 105232. DOI: 10.1016/j.ejps.2020.105232

12. Moyne, Moyne, O., Castelli, F., Bicout, D. J., Boccard, J., Camara, B., Cournoyer, B., Faudry, E., Terrier, S., Hannani, D., & Huot-Marchand, S. (2021). Metabotypes of Pseudomonas aeruginosa correlate with antibiotic resistance, virulence and clinical outcome in cystic fibrosis chronic infections. *Metabolites*, *11*(2), 63. DOI. 10.3390/metabo11020063.

13. Zhao, L., Jiang, X., Xu, X., Wang, N., Wang, X., Yang, R., Liu, X., Liu, Z., & Luan, Y. (2022). An Aptamer Affinity Column for Extraction of Four Aminoglycoside Antibiotics from Milk. *Separations*, *9*(10), 267. DOI: 10.3390/separations9100267.

14. Pauter, K., Szultka-Młyńska, M., & Buszewski, B. (2020). Determination and identification of antibiotic drugs and bacterial strains in biological samples. *Molecules*, *25*(11), 2556. DOI: 10.3390/molecules25112556

15. Lei, X., Zhang, B., Zhang, Y., Huang, T., Tang, F., & Wu, X. (2022). In situ photoinitiated fabrication of phosphorylcholine-functionalized polyhedral oligomeric silsesquioxane hybrid monolithic column for mixed-mode capillary electrochromatography. *Analyst*, *147*(10), 2253–2263. DOI: 10.1039/D2AN00195K

16. Mishra, H., Behera, A., Sankar Kar, S., Pattnaik, G., Kanhar, S., & Dash, S. (2021). Analytical strategies for the detection and quantification of nano-formulated antibiotics: *Updates and perspectives*. DOI: 10.9734/jpri/2021/v33i59A34282

17. Fadhil, A. K., Rasheed, A. S., & Hassan, M. J. M. (2023). A review of recent advances in the estimation of pharmaceutical products using hydrophilic interaction chromatography (HILIC) technology. *Egyptian Journal*

of Chemistry, *66*(1), 399–417. DOI:10.21608/EJCHEM.2022.121396.5443

18. Buszewski, B., & Noga, S. (2012). Hydrophilic interaction liquid chromatography (HILIC) a powerful separation technique. *Analytical and Bioanalytical Chemistry*, *402*(1), 231–247. DOI: 10.1007/s00216-011-5308-5

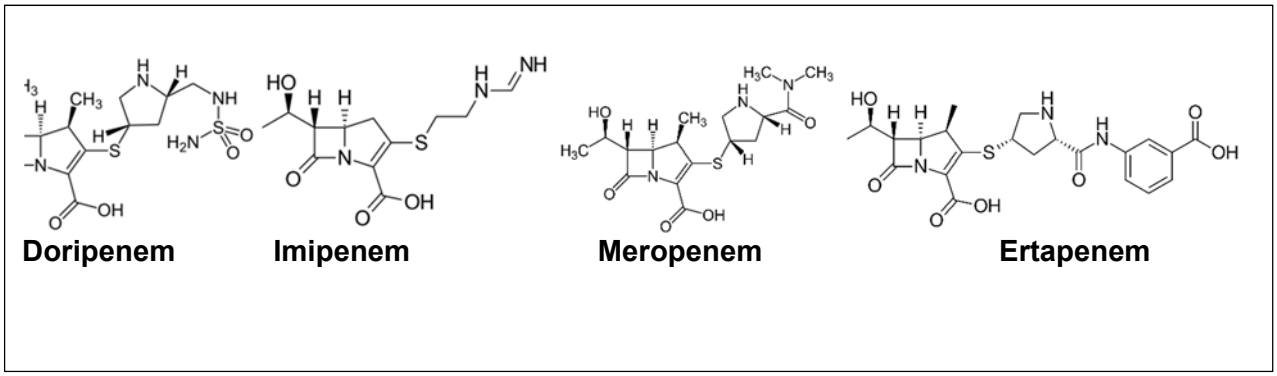

Figure 1. *shows the pharmaceutical drugs that were used in the study [1]*

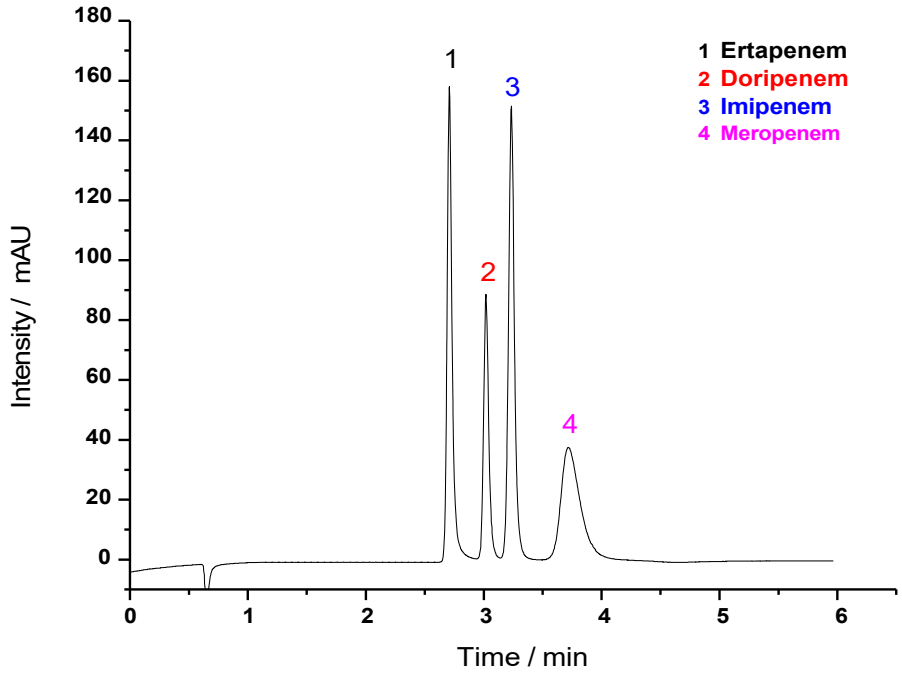

Figure 2. *Preliminary chromatograms for Imipenem, Meropenem, Ertapenem, and Doripenem mg/kg Inertsil HILIC Capillary EX-Nano Column*

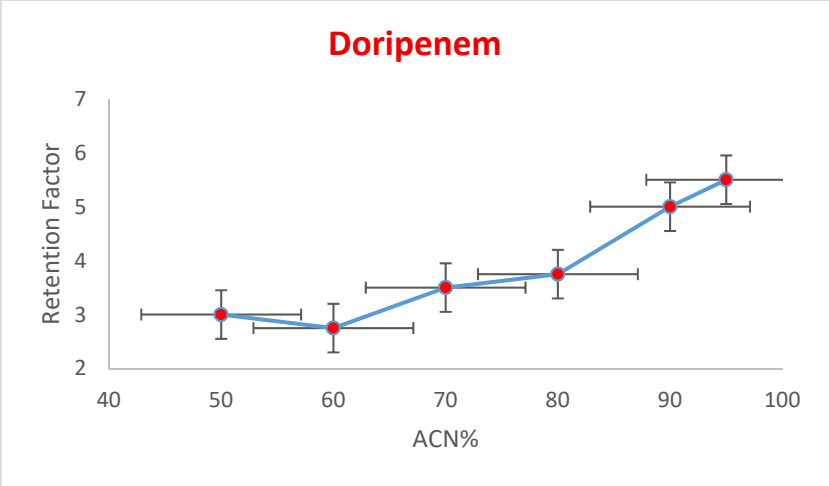

Figure 3. *Effect of ACN on the behavior of Doripenem*

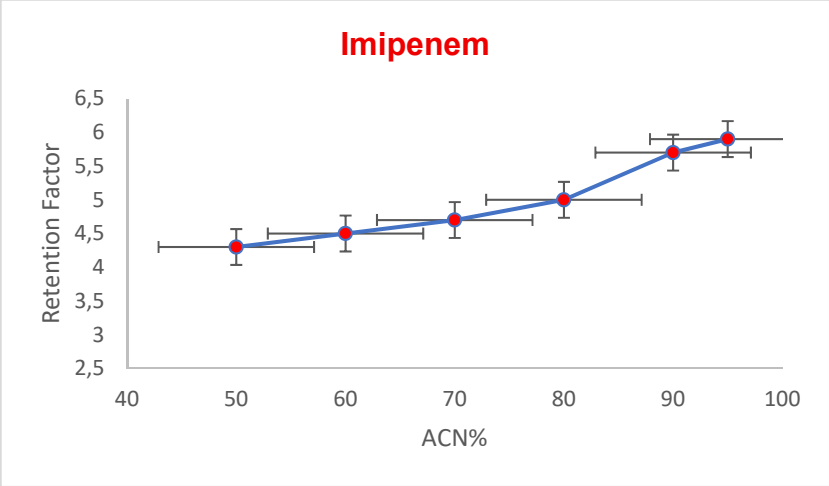

Figure 4. *Effect of ACN on the behavior of Imipenem*

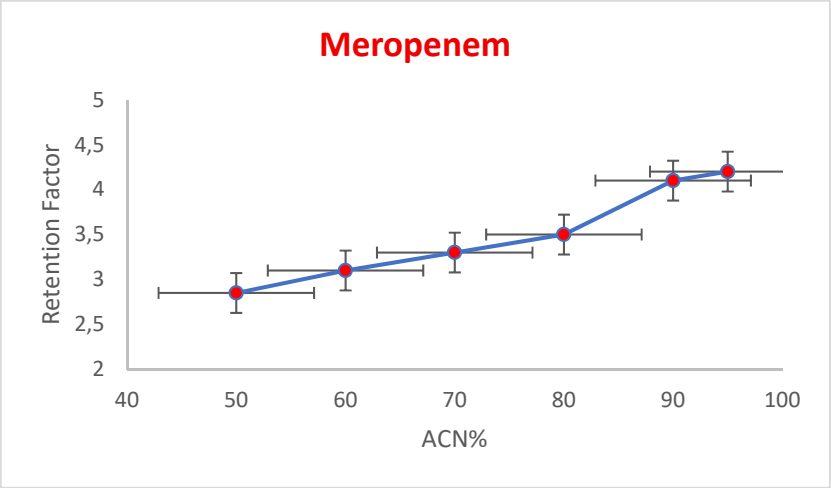

Figure 5. *Effect of ACN on the behavior of Meropenem*

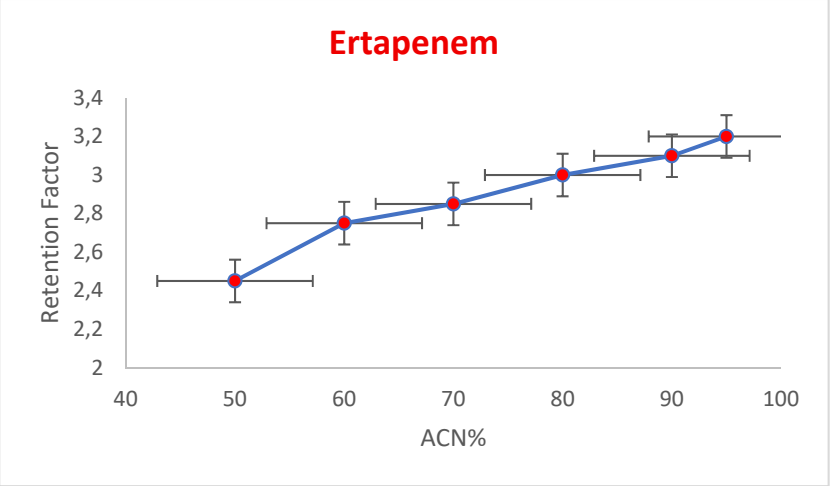

Figure 6. *Effect of ACN on the behavior of Ertapenem*

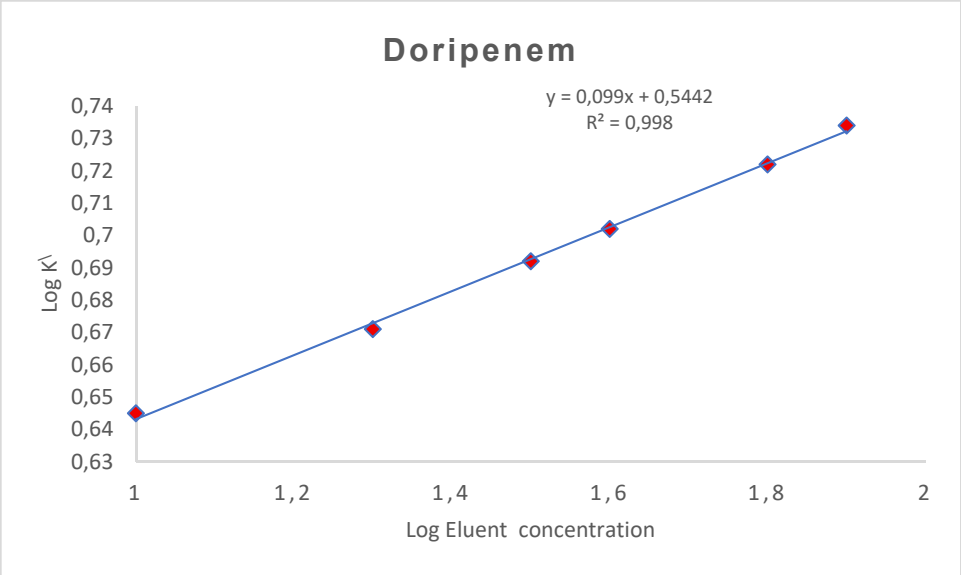

Figure 7. *Effect of buffer concentration on the behavior of Doripenem*

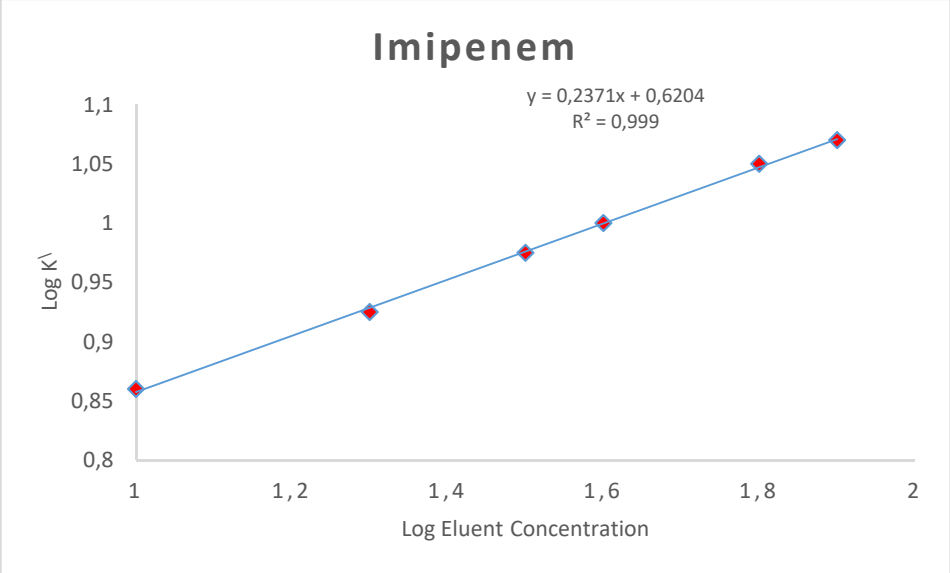

Figure 8. *Effect of buffer concentration on the behavior of Imipenem*

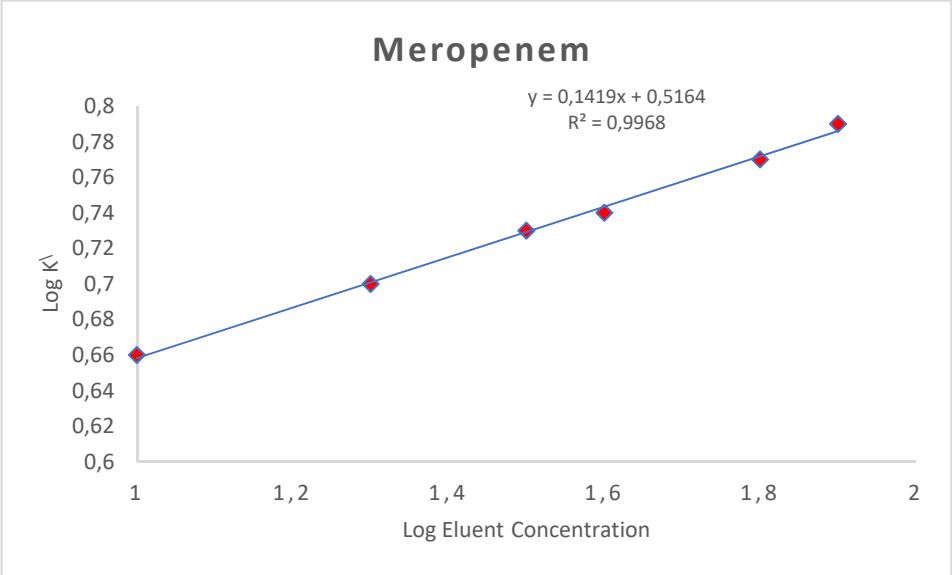

Figure 9. *Effect of buffer concentration on the behavior of Meropenem*

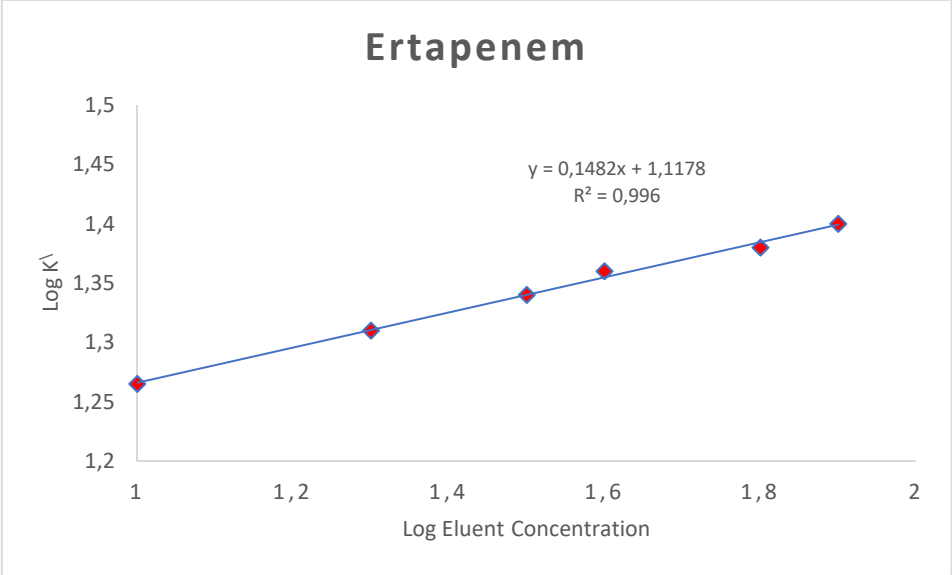

Figure 10. *Effect of buffer concentration on the behavior of Ertapenem*

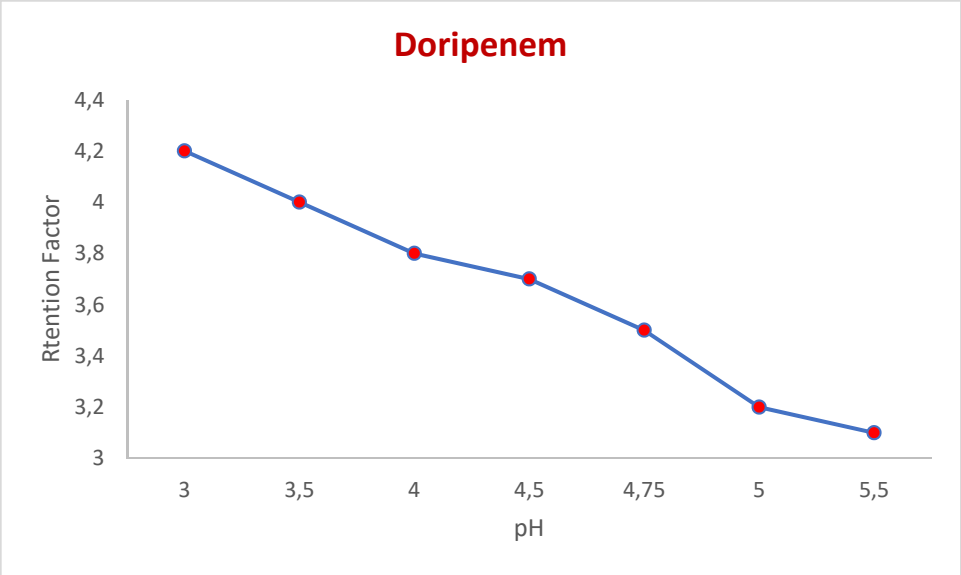

Figure 11. *Effect of pH on the behavior of Doripenem*

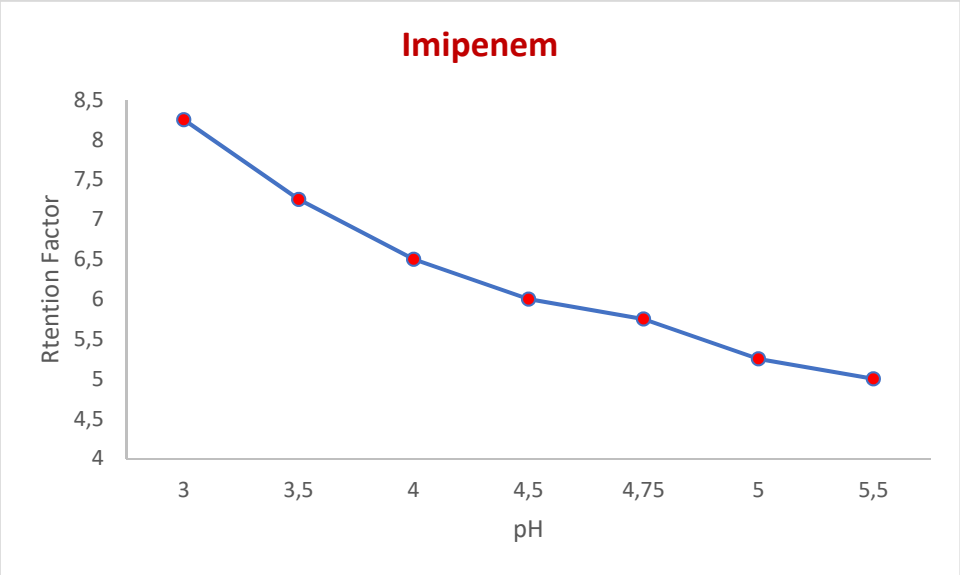

Figure 12. *Effect of pH on the behavior of imipenem*

.

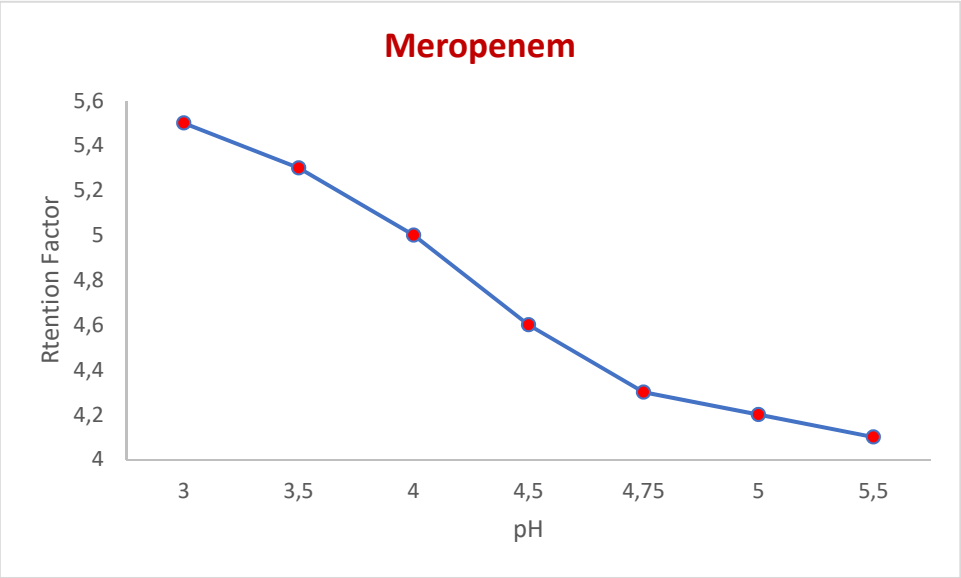

Figure 13. *Effect of pH on the behavior of Meropenem*

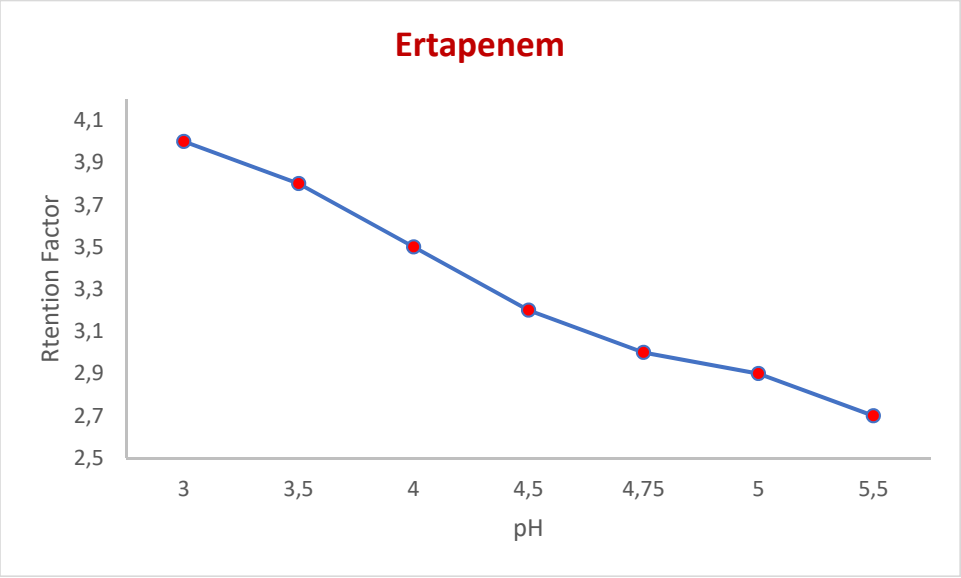

Figure 14*. Effect of pH on the behavior of Ertapenem*

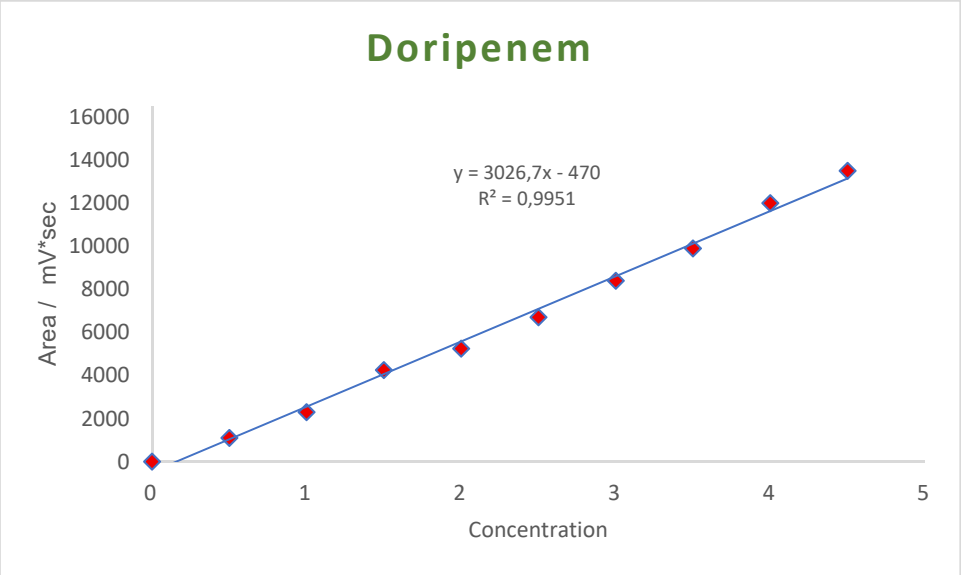

Figure 15. *Calibration graph of Doripenem.*

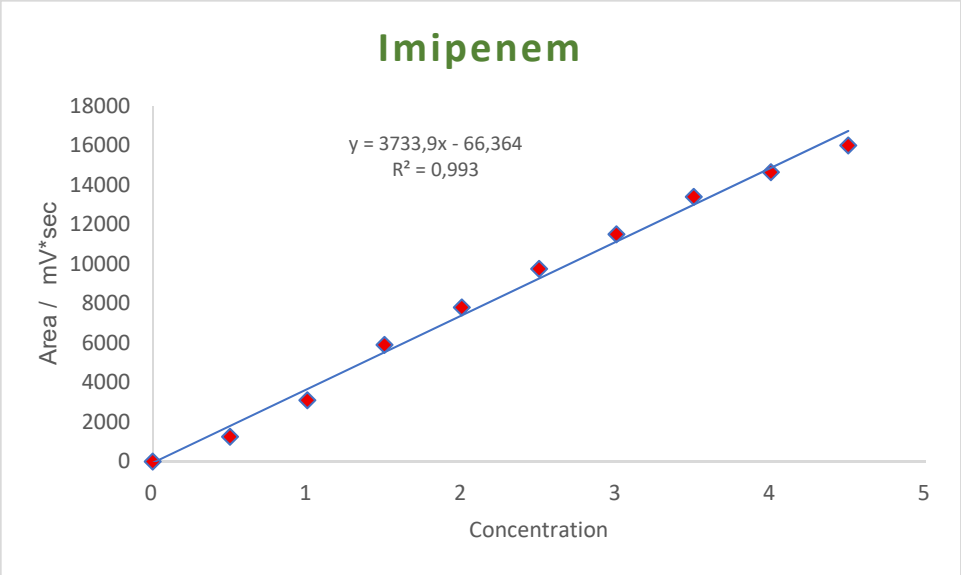

Figure 16. *Calibration graph of imipenem.*

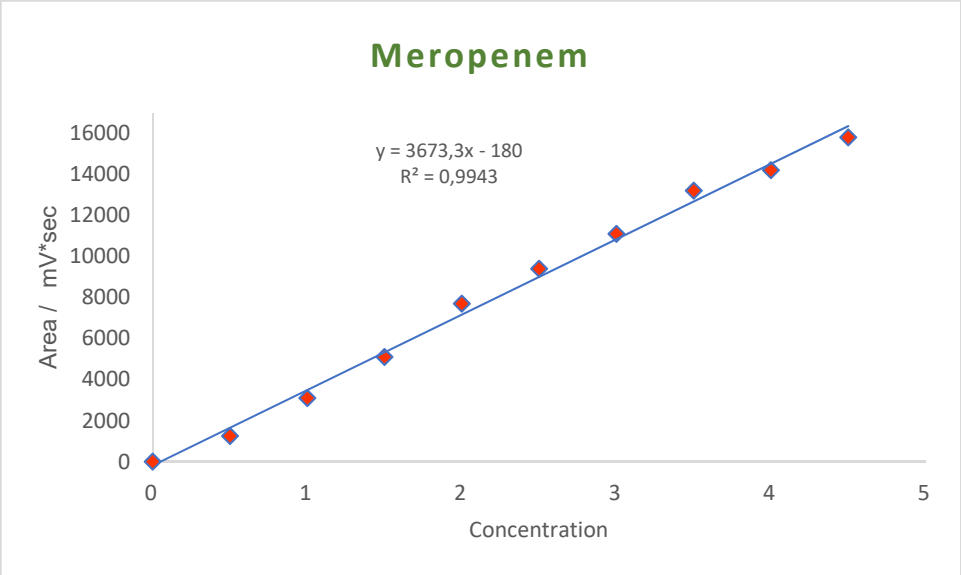

Figure 17. *Calibration graph of Meropenem*

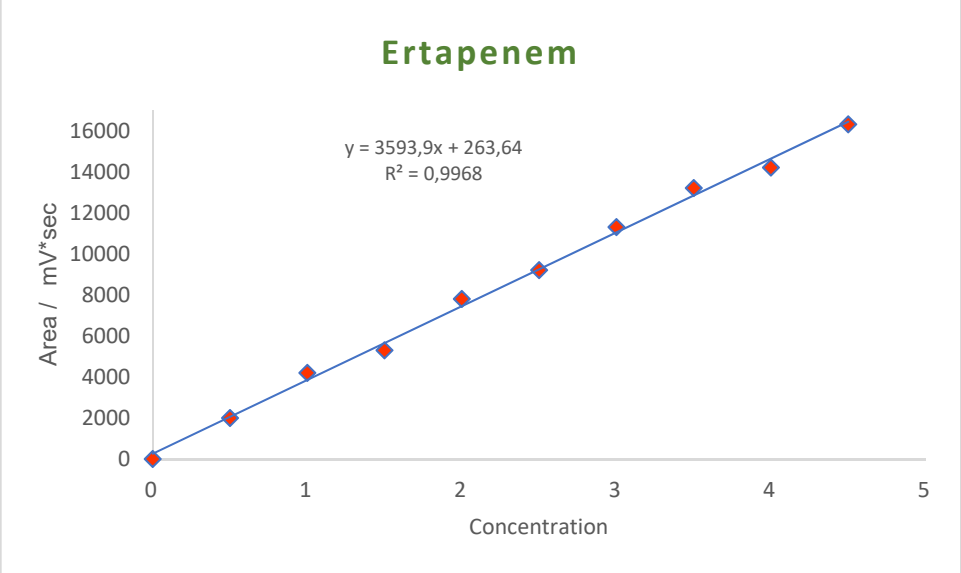

Figure 18. *Calibration graph of Ertapenem*

Table 1*. Physical and chemical characteristics of the four antibioticdrugs studied*

$\boldsymbol{Pharmaceuticals}$	$\boldsymbol{pI}$ **	$\boldsymbol{pKa}$	$\boldsymbol{logPow}$ *
Doripenem	6.55	3.54	$\mathbf{-5.60}$
Imipenem	8.75	3.44	$\mathbf{-2.78}$
Meropenem	5.15	3.28	$\mathbf{-4.40}$
Ertapenem	$\mathbf{3.73}$	$\mathbf{3.22}$	$\mathbf{-3.20}$

***logPow**:
$At\ equilibrium, the\ concentrations\ of\ an\ unionized\ chemical\ in\ the\ two\ phases\ of\ immiscible\ solvents\ (water\ \&\ n-octanol)\ are\ divided\ by\ the\ partition\ coefficient.$
***** Isoelectric point (pI):***$The\ pH\ at\ which\ a\ specific\ molecule\ has\ no\ net\ electrical\ charge\ is\ known\ as\ the\ isoelectric\ point. The\ pH\ of\ the\ molecule's\ surroundings\ influences\ its\ net\ charge, which\ can\ increase\ or\ decrease\ depending\ on\ whether\ protons\ are\ lost\ or\ gained.$

Table 2*. shows the optimal conditions used to separate antibiotic drugs.*

Column	**Inertsil HILIC Capillary EX-Nano Column**
pH	$3-5.5$
Temperature of the column	$40co$
Flow rate	$0.2\ ml/min$
Detection	$254\ nm$
Eluent	$A)\ CH3CN \quad B)10mM\ NH4OAc\ in\ H2O$

Table 3*. Results of the analytical features of drugs.*

$\boldsymbol{Drugs}$	$\boldsymbol{LOD}$ ($\mu g/mL$)	$\boldsymbol{LOQ}$ ($\mu g/mL$)	$\boldsymbol{S/N\ at\ LOD}$	$\boldsymbol{S/N\ at\ LOQ}$	$\boldsymbol{RSD}$ (%)	$\boldsymbol{Recovery}$ (%)
$\boldsymbol{Ertapenem}$	0.0029	0.0087	3.1	10.2	1.8	98.7
$\boldsymbol{Doripenem}$	0.0024	0.0072	3.3	10.4	1.6	99.1
$\boldsymbol{Imipenem}$	0.0030	0.0090	3.0	10.3	1.7	98.3
$\boldsymbol{Meropenem}$	0.0027	0.0081	3.2	10.5	1.9	97.9

Table 4. The suggested methods of precision and accuracy of drugs

Compound (µg/mL)	**Taken (µg/mL)**	**Found (µg/mL)**	**Recovery (%)**	**95% CI**	**Inter-day RSD (%)**	**Intra-day RSD (%)**	**Statistical test (P-*valu*)**
Etapenem	10.0	9.93	99.3	$98.-99.7$	1.4	1.1	0.125
Doripenem	10.0	9.89	98.9	$98.-99.3$	1.3	1.0	0.198
Imipenem	10.0	100.2	100.2	$99.-100.8$	1.5	1.3	0.109
Meropenem	10.0	99.7	99.7	$99.-100.1$	1.2	1.0	0.165

Table 5. *Application in pharmaceutical drugs.*

Name of pharmaceutical	Manufacturer	Stated conc. (mg)	Found direct. (mg)	Rec %	RSD n=6 %	Erel %	Anova p-value	t-test P-value	p>0.5
Doripenem	LDP-spain	**200**	**201**	**100.5**	**1.11**	**0.50**	**0.375**	**0.191**	**0.254**
	Pharma-international-Jordan	**200**	**203**	**101.5**	**1.29**	**1.50**			
	Bravn-India	**200**	**199**	**99.5**	**1.03**	**−0.50**			
Imipenem	Bravn-India	**200**	**193**	**96.5**	**1.11**	**−3.50**	**0.288**	**0.134**	**0.203**
	LDP-spain	**200**	**196**	**98.0**	**0.88**	**−2.00**			
	Pharma-international-Jordan	**200**	**199**	**99.5**	**1.02**	**−0.50**			
Ertapenem	Bravn-India	**200**	**205**	**102.5**	**1.21**	**2.50**	**0.441**	**0.160**	**0.219**
	LDP-spain	**200**	**195**	**97.5**	**1.00**	**−2.50**			
	Pharma-international-Jordan	**200**	**197**	**98.5**	**0.81**	**−1.50**			
Meropenem	Bravn-India	**200**	**204**	**100.2**	**1.03**	**2.00**	**0.397**	**0.213**	**0.186**
	LDP-spain	**200**	**198**	**99.0**	**1.01**	**−1.00**			
	Pharma-international-Jordan	**200**	**201**	**100.5**	**0.81**	**0.50**			

Table 6. Preparation buffer range (3-5.5).

$\boldsymbol{Buffer\ (pH)}$	$\boldsymbol{HAc}$ (μ$\boldsymbol{L}$) $\boldsymbol{17.3\ M}$	$\boldsymbol{Weight\ of\ NH4OAc\ (g)}$
3.00	2247.6	0.095
4.00	1941.9	0.822
4.50	1463.8	1.959
4.75	1143.8	2.722
5.00	823.8	3.484
5.50	345.7	4.621

Table 7. Preparation buffer range (10-80 mM) at pH 5.5

$\boldsymbol{Buffer\ concentration\ (mM)}$	$\boldsymbol{HAc}$ (μ$\boldsymbol{L}$) $\boldsymbol{17.3\ M}$	$\boldsymbol{Weight\ of\ NH4OAc\ (g)}$
10	285.7	0.680
20	572.4	1.361
30	858.1	2.041
40	1143.8	2.722
50	1429.5	3.402
60	1715.2	4.082
70	2001.9	4.763
80	2287.6	5.443

PERIÓDICO TCHÊ QUÍMICA
ARTIGO ORIGINAL

MODELAGEM DA LEUCEMIA MIELOIDE AGUDA COM CÉLULAS THP-1: EXPLORANDO O POTENCIAL ANTILEUCÊMICO DE DIFERENTES EXTRATOS DE PANAX QUINQUEFOLIUM

MODELING ACUTE MYELOID LEUKEMIA WITH THP-1 CELLS: EXPLORING THE ANTILEUKEMIC POTENTIAL OF DIFFERENT PANAX QUINQUEFOLIUM EXTRACT

نموذج ابيضاض الدم النقوي الحاد باستخدام خلايا THP-1: استكشاف الإمكانات المضادة لسرطان الدم لمستخلصات مختلفة من PANAX QUINQUEFOLIUM

Jinan Mahdi Ghani
University of Kufa, Faculty of Science, Department of Biology. Iraq.

Jinan Mohammed Zahid
University of Kufa, Faculty of Science, Department of Biology. Iraq.

Intisar Razzaq Sharba*
University of Kufa, Faculty of Science, Department of Biology. Iraq.

** Corresponding author*
e-mail: intisar.sharba@uokufa.edu.iq

Received 20 June 2025; received in revised form 22 September 2025; accepted 15 October 2025

RESUMO

Introdução: A leucemia mieloide aguda é uma malignidade hematológica caracterizada pela proliferação descontrolada de blastos mieloides imaturos, resultando em prognóstico desfavorável e opções terapêuticas limitadas. A linha celular THP-1, derivada de um paciente com leucemia monocítica aguda, serve como modelo in vitro confiável para monócitos e macrófagos humanos. Produtos naturais, como Panax quinquefolium (ginseng americano), contêm compostos bioativos com propriedades antioxidantes, anti-inflamatórias e anticancerígenas, oferecendo alternativas terapêuticas mais seguras. **Objetivo**: Avaliar o potencial antileucêmico de quatro extratos diferentes de raízes de Panax quinquefolium em células THP-1. **Métodos**: As células THP-1 foram tratadas com extratos aquosos, hexano, etanol e clorofórmio em concentrações de 6,25 a 200 µg/ml. A citotoxicidade foi avaliada pelo ensaio MTT, e seções histológicas foram analisadas para densidade e morfologia celular. **Resultados**: Todos os extratos inibiram a proliferação das células de forma dependente da dose, com diferenças significativas entre os tratamentos ($p < 0,001$). O extrato de clorofórmio foi o mais eficaz, reduzindo o crescimento em 88,11 ± 3,14% a 200 µg/ml, seguido por etanol, hexano e aquoso. A histologia confirmou os achados: células controle formaram aglomerados densos; o extrato aquoso reduziu modestamente a densidade; hexano e etanol causaram reduções maiores; o clorofórmio resultou no menor número de células viáveis. **Discussão**: Os resultados indicam que os extratos de Panax quinquefolium possuem atividade antileucêmica dependente da dose, com o clorofórmio sendo o mais potente. As diferenças entre os extratos provavelmente refletem variações na polaridade e solubilidade dos compostos bioativos. Produtos naturais podem oferecer alternativas mais seguras que a quimioterapia convencional, embora estudos adicionais sejam necessários para esclarecer os mecanismos moleculares e a eficácia em organismos vivos. **Conclusão**: O extrato de clorofórmio de Panax quinquefolium suprime efetivamente a proliferação de células THP-1, demonstrando forte atividade antileucêmica e potencial como agente terapêutico seguro e promissor.

Palavras-chave: *Extrato de Panax quinquefolium, Inibição da leucemia mieloide aguda, Linha celular THP-1, Antileucêmico.*

ABSTRACT

Background: Acute Myeloid Leukemia (AML) is a hematological malignancy characterized by uncontrolled proliferation of immature myeloid blasts, leading to poor prognosis and limited treatment options. The THP-1 cell line, derived from a patient with acute monocytic leukemia, serves as a reliable in vitro model for human monocytes and macrophages. Natural products, such as Panax quinquefolium (American ginseng), contain

DOI: 10.52571/PTQ.v22.n51.2025_03_GHANI_pgs_38_51.pdf

bioactive compounds with antioxidant, anti-inflammatory, and anticancer properties, offering safer alternatives for AML therapy. **Aim**: To evaluate the antileukemic potential of four P. quinquefolium root extracts on THP-1 cells. **Methods**: THP-1 cells were treated with aqueous, hexane, ethanol, and chloroform extracts at 6.25–200 µg/ml. Cytotoxicity was assessed via the MTT assay, and histological sections were analyzed for cell density and morphology. **Results**: All extracts inhibited THP-1 proliferation in a dose-dependent manner, with significant differences among treatments ($p < 0.001$). The chloroform extract was the most effective, reducing growth by 88.11 ± 3.14% at 200 µg/mL, followed by the ethanol, hexane, and aqueous extracts. Histology confirmed: control cells formed dense clusters; aqueous extract modestly reduced density; hexane and ethanol caused further reductions; chloroform yielded the fewest viable cells. **Discussion**: These findings indicate potent dose-dependent antileukemic activity of P. quinquefolium, particularly its chloroform extract. The variation among extracts likely reflects differences in polarity and solubility of bioactive compounds. Natural products may offer safer alternatives to conventional chemotherapy; however, further studies are required to elucidate their molecular mechanisms and in vivo efficacy. **Conclusion**: The chloroform extract of Panax quinquefolium effectively suppresses THP-1 proliferation, demonstrating strong antileukemic activity and supporting its potential as a safe and promising therapeutic candidate for AML.

Keywords: *Panax quinquefolium extract, AML inhibition, THP-1 cell line, and Antileukemic.*

الخلفية: ابيضاض الدم النقوي الحاد (AML) هو سرطان دموي يتميز بالتكاثر غير المنضبط للأورمات النخاعية غير الناضجة، مما يؤدي إلى سوء الإنذار وقلة خيارات العلاج المتاحة. يُعد خط الخلايا THP-1 المشتق من مريض مصاب بابيضاض الدم النقوي الوحيدي نموذجاً موثوقاً لدراسة الوحيدات والبلاعم البشرية في المختبر. تحتوي المنتجات الطبيعية، مثل *Panax quinquefolium* (الجنسنغ الأمريكي)، على مركبات فعالة بخصائص مضادة للأكسدة والالتهاب والسرطان، مما يوفر بدائل علاجية أكثر أماناً لعلاج AML. **الهدف:** تقييم النشاط المضاد لسرطان الدم لأربعة مستخلصات مختلفة من جذور *P. quinquefolium* على خلايا THP-1. **طرائق العمل:** تمت معالجة خلايا THP-1 بمستخلصات مائية، هكسان، إيثانول، وكلوروفورم بتركيزات تتراوح بين 6.25–200 مايكروغرام/ملليتر. تم تقييم التأثيرات السامة للخلايا باستخدام اختبار MTT ، كما أُجريت مقاطع نسيجية لدراسة كثافة الخلايا ومورفولوجيا الخلايا. **النتائج:** ثبطت جميع المستخلصات تكاثر خلايا THP-1 بطريقة معتمدة على الجرعة، مع اختلافات معنوية بين المعالجات ($p < 0.001$). أظهر المستخلص الكلوروفورمي أقوى تأثير، حيث خفّض نمو الخلايا بنسبة 88.11 ± 3.14% عند 200 مايكروغرام/ملليتر، يليه مستخلص الإيثانول، الهكسان، والمائي. دعمت الفحوص النسيجية هذه النتائج حيث شكلت خلايا السيطرة تجمعات كثيفة، وقلّلت المستخلصات المائية والهكسانية والإيثانولية الكثافة تدريجياً، بينما أنتج الكلوروفورم أقل عدد من الخلايا الحية. **المناقشة:** تشير النتائج إلى أن مستخلصات *P. quinquefolium* تمتلك نشاطاً مضاداً للابيضاض بطريقة معتمدة على الجرعة، مع تفوق المستخلص الكلوروفورمي. تعكس الاختلافات بين المستخلصات فروقاً في القطبية وقابلية ذوبان المركبات الفعالة. قد توفر المنتجات الطبيعية بدائل أكثر أماناً مقارنة بالعلاج الكيميائي التقليدي، مع ضرورة إجراء دراسات إضافية لتوضيح الآليات الجزيئية وفعالية المستخلصات في الجسم الحي. **الاستنتاج**: يثبط المستخلص الكلوروفورمي لجذور *P. quinquefolium* تكاثر خلايا THP-1 بفعالية، مظهراً نشاطاً مضاداً قوياً للابيضاض، مما يدعم إمكاناته كعامل علاجي واعد وآمن لمرضى AML.

الكلمات المفتاحية: مستخلص الجينسنغ الأمريكي، تثبيط ابيضاض الدم النقوي الحاد، خط خلايا ***THP-1***، مضاد للابيضاض

1. INTRODUCTION:

Acute Myeloid Leukemia (AML) is a hematological malignancy characterized by the uncontrolled proliferation of immature myeloid leukemic blasts (Shimony *et al.,* 2025). AML represents a highly heterogeneous disease, involving chromosomal abnormalities, molecular genetics, biochemical alterations, and mutations (Hakon *et al.,* 2023). It accounts for approximately 33% of all hematological cancers and is associated with a 5-year survival rate of only 24% (Gyi *et al.,* 2025). Globally, AML ranks among the leading causes of cancer-related mortality and was the 13th most frequently diagnosed malignancy in 2022 (Bray *et al*., 2022).

The THP-1 cell line, derived from a patient with acute monocytic leukemia at the age of one (Jo *et a*l., 2024), serves as a reliable in vitro model of monocytes and macrophages. THP-1 cells are particularly useful for mimicking the tumor microenvironment due to their similarity with primary monocytes and their capacity for macrophage-like differentiation. Conventional chemotherapeutic drugs used in AML treatment are often associated with severe side effects, highlighting the need for safer and effective alternatives (James *et al*., 2023).

Panax quinquefolium (American ginseng) is a medicinal plant originally from North America and cultivated in regions such as Ontario. Cultivated ginseng in China, imported from North America, contains fewer lateral roots and lower levels of active compounds such as ginsenosides compared to wild American ginseng roots (Fang *et al*., 2023). The therapeutic properties of ginseng are primarily attributed to ginsenosides, which exhibit anti-apoptotic, antioxidant, and anti-inflammatory effects. The root is rich in saponins, including bioactive ginsenosides, which have demonstrated pharmacological and therapeutic benefits (Li *et al*., 2023). Recent studies have highlighted the potential of ginseng in cancer therapy, cognitive enhancement, and cardiovascular protection (Zhang *et al.,* 2024).

This study aimed to investigate the anticancer

potential of different P. quinquefolium root extracts (aqueous, hexane, ethanol, and chloroform) on THP-1 leukemia cells, focusing on dose-dependent growth inhibition and histological alterations, to evaluate their anti-leukemia effects.

2. MATERIALS AND METHODS:

2.1. Materials

Plant Material

Panax quinquefolium root powder (source and authentication details as Figure 1.

Figure 1 . Panax quinquefolium root powder

Extraction Solvents

- Absolute ethanol (analytical grade)
- Chloroform (HPLC grade)
- n-Hexane (analytical grade)
- Distilled water (sterile)

Cell Culture Materials

- THP-1 human acute monocytic leukemia cell line (ATCC® TIB-202™)
- RPMI-1640 medium (Gibco, Life Technologies)
- Fetal Bovine Serum (FBS) (Gibco, Life Technologies)
- Penicillin-Streptomycin solution (10,000 U/mL) (Gibco, Life Technologies)
- L-Glutamine (200 mM) (Gibco, Life Technologies)
- Phosphate Buffered Saline (PBS) (pH 7.4)
- Trypan blue solution (0.4%)

Cell Viability Assay Materials

- 3-(4,5-dimethylthiazol-2-yl)-2,5-diphenyltetrazolium bromide (MTT) powder
- Dimethyl sulfoxide (DMSO) (cell culture grade)
- 96-well flat-bottom microplates (sterile)
- 24-well cell culture plates (sterile)

Histological Staining

- Crystal violet solution (0.5% w/v)
- Methanol (for fixation)

Laboratory Equipment

- Ultrasonic bath (frequency: 40 kHz)
- CO_2 incubator (37 °C, 5% CO_2)
- Class II biological safety cabinet
- Inverted microscope with phase contrast
- Microplate reader (capable of reading at 492 nm)
- Centrifuge (benchtop)
- Analytical balance (0.1 mg precision)
- Refrigerator (4 °C) and freezer (-20 °C)
- Drying oven (40 °C)
- Autoclave for sterilization

Filtration and Purification

- Whatman filter paper No. 1
- 0.22 µm sterile syringe filters
- Sterile syringes (various sizes)

HPLC Analysis Materials

- High-Performance Liquid Chromatography (HPLC) system
- C18 reverse-phase column (specifications should be provided)
- HPLC-grade solvents (acetonitrile, methanol, water)
- Standard reference compounds (if available)

General Laboratory Consumables

- Micropipettes (10-1000 µL range)
- Sterile pipette tips (filtered)
- Serological pipettes (5, 10, 25 mL)
- Microcentrifuge tubes (1.5 mL, 2.0 mL)
- Cell culture flasks (T25, T75)
- Glass vials for extract storage
- Parafilm for sealing
- Disposable gloves (nitrile)

- Face masks and laboratory coats

2.2. Methods

2.2.1. Ginseng Extracts Preparation

For the preparation of ginseng extracts, four distinct solvents —ethanol, chloroform, hexane, and distilled water —were employed. A precise volume of 100 mL of each solvent was added to 20 grams of powdered ginseng root. Subsequently, the traditional extraction method was augmented by ultrasonic-assisted extraction (UAE), a technique validated by Yusoff *et al.* (2022). This approach facilitates the penetration of the solvent into cellular structures, where acoustic cavitation-induced bubbles effectively disrupt cell walls, thereby promoting the release of active compounds, notably ginsenosides, and other constituents. The extraction mixtures were then incubated for 24 hours at ambient temperature. Following incubation, the mixtures were meticulously filtered using Whatman filter paper to obtain the filtrate, which was subsequently dried in an oven at 40 °C. The resulting dry extracts were stored under refrigerated conditions until further use, consistent with the methodology described by (Tian *et al*., 2013).

2.2.2. Cytotoxicity Assay

To determine the cytotoxic potential of each of the four extracts, the MTT assay was performed using 96-well plates, following established protocols (Al-Ziaydi *et al.,* 2020). Cells were seeded at a density of 1×10^4 cells/well and incubated for 24 hours to achieve a confluent monolayer. Human monocytic THP-1 cells, serving as an in vitro model for primary human monocytes, were treated with each P. ginseng root extract. Cell viability was assessed at 24 and 48 hours post-treatment. This involved the removal of the culture medium, followed by the addition of 28 µL of a 2 mg/mL MTT solution. The cells were then incubated for 2.5 hours at 37 °C. Following the removal of the MTT solution, the formazan crystals remaining in the wells were solubilized by adding 130 µL of Dimethyl Sulfoxide (DMSO), followed by a 15-minute incubation at 37 °C with gentle shaking. Absorbance was quantified at 492 nm using a microplate reader. All assays were conducted in triplicate. The inhibition rate of cell growth (cytotoxicity percentage) was calculated using Equation 1

$$\text{Inhibition rate (cytotoxicity)} = (A - B) / A \times 100 \quad \text{(Eq. 1)}$$

Where: A represents the optical density of the control, and B represents the optical density of the samples (Ibrahim *et al*., 2021).

For morphological assessment, cells were seeded into 24-well microtiter plates at a density of 1×10^5 cells/mL and incubated for 24 hours at 37 °C. Subsequently, cells were exposed to each type of ginseng root extract for 24 hours. Post-exposure, the plates were stained with crystal violet and incubated at 37 °C for 10-15 minutes. The stain was then carefully rinsed with tap water until complete removal of the dye was achieved (Jabir *et al*., 2022).

THP-1 cells were maintained in RPMI-1640 supplemented with 10% Fetal bovine serum, 100 units/mL penicillin, and 100 µg/mL streptomycin. Cells were passaged using Trypsin-EDTA, reseeded at 80% confluence twice a week, and incubated at 37 °

2.3. Statistical Analysis

All experiments were conducted using a completely randomized design with appropriate controls. Each treatment condition was performed in technical triplicate within each experiment, and experiments were independently repeated three times (n = 3 independent experiments) to ensure biological reproducibility. Data from individual experiments were pooled only after confirming consistency across replicates.

Data are presented as mean ± standard deviation (SD) calculated from all measurements across the three independent experiments. Prior to statistical analysis, data normality was assessed using the Shapiro-Wilk test, and homogeneity of variances was evaluated using Levene's test. When assumptions were violated, appropriate data transformations were applied.

Statistical analysis was performed using SPSS version 27.0 (IBM Corp., Armonk, NY, USA). For cytotoxicity data comparison across different extract types and concentrations, one-way analysis of variance (ANOVA) was employed, followed by Tukey's honestly significant difference (HSD) post-hoc test for pairwise multiple comparisons between treatment groups. Two-way ANOVA was used to analyze the interaction effects between extract type and concentration.

IC_{50} values were determined by fitting the dose–response data to a four-parameter logistic (4PL) model. Curve fitting and statistical analysis

were performed using spss 27. The quality of the fit was assessed by examining goodness-of-fit metrics, including the coefficient of determination (R^2) and the distribution of residuals was calculated using Equation 2

Response = Bottom + (Top - Bottom) / (1 + 10^((logIC_50 – LogConc.) * Hill Slope)

(Eq. 2)

The estimated IC50 (half-maximal inhibitory concentration) values for the different extracts approxmatly are as follows:

Chloroform: Between 25 and 35 µg/ml.
Ethanol: Between 30 and 40 µg/ml.
Hexane: Between 35 and 50 µg/ml.
Water: Between 40 and 50 µg/ml.

Statistical significance was set at $\alpha = 0.05$ for all analyses. P-values were adjusted for multiple comparisons using the Bonferroni correction when appropriate. All statistical analyses and graphical representations were generated using SPSS software. Results with $p < 0.05$ were considered statistically significant, with $p < 0.01$ and $p < 0.001$ indicating higher levels of significance as specified in the results.

3. RESULTS AND DISCUSSION:

3.1. Results

3.1.1. Cytotoxicity of Panax Ginseng Extracts from Different Solvents on THP-1 Cells at Various Concentrations

The antileukemic effects of four Panax ginseng extracts, Aqueous (Water), Hexane, Ethanol, and Chloroform were evaluated against THP-1 cells in vitro. All extracts exhibited cytotoxic effects with varying degrees of tumor inhibition. The results in Table 1 revealed mean activity values across six concentrations (6.25–200 µg/ml). At 6.25 µg/ml, chloroform had the highest activity (12.67 ± 0.90), followed by Ethanol (9.62 ± 0.84), Hexane (8.30 ± 1.03), and Water (6.59 ± 0.91). This pattern persisted at 200 µg/ml, with chloroform at the highest level (88.11 ± 3.14), followed by ethanol (84.15 ± 3.39), hexane (80.43 ± 3.64), and water at the lowest level (77.35 ± 2.65l). Ethanol consistently ranked second, hexane was an intermediate, and water ranked lowest across all concentrations. Compound levels increased significantly with dose for all extracts, indicating a dose-dependent effect Figure 2. Differences among extracts were statistically significant ($p < 0.001$).

3.1.1. Histological examination

The histological examination of four types of solvent ginseng extract provides valuable insight into the morphological changes induced by cancer cells following exposure to ginseng extract active compounds, as shown in Figure 3 (A-E). In the current study, the human acute monocytic leukemia (THP-1) cells were treated with four types of different solvent extracts of Panax ginseng, including water, ethanol, and chloroform. To evaluate their cytotoxicity potential. Crystal violet staining was used to visualize cell morphology and density, allowing for a direct comparison between the treated groups and the control group. Suppression effects on cell viability and proliferation, as compared to the degree of reduction across treatments, this histological analysis highlights the relative efficacy of each ginseng extract in inhibiting THP-1 cell growth.

3.2. Discussion

3.2.1. The Effect of Bioactive Compounds of Ginseng – Aqueous Extract on THP-1 Cell Line

The aqueous extract of *Panax ginseng* root is particularly rich in polar bioactive compounds, including ginsenosides (Rg1, Re, Rd), immunomodulatory polysaccharides (panaxans), and saponins that contribute to its wide pharmacological properties (Srisuk *et al*., 2024; Lertchanyaporn *et al*., 2024). Ginseng phytochemicals are broadly classified into polysaccharides, polyynes, flavonoids, and volatile oils (Jia & Zhao, 2009). Importantly, ginsenosides and water-soluble polysaccharides exhibit immunomodulatory and anti-proliferative effects (Poudyal *et al*., 2012).

The aqueous extract is characterized by high polarity and a composition enriched in ginsenosides (Rg1, Re, Rb1), phenolics, and small peptides, which collectively demonstrate strong cytotoxic and anti-proliferative activity against THP-1 leukemia cells (Kim *et al*., 1998; Shim *et al*., 2007). This finding aligns with previous studies that ginsenosides Rg3 and Rh2 induce apoptosis through mitochondrial ROS generation (Xia *et al.,* 2017; Dana *et al*., 2024).

Mechanistically, ginsenoside Rh2 (GRh2) induces G1-phase cell cycle arrest (Chen *et al*., 2016; Huang *et al*., 2016), acts as a histone deacetylase (HDAC) inhibitor, and regulates

apoptosis-related proteins (Bcl-2/Bax) (Liu *et al*., 2015). Likewise, ginsenosides Rg1 and Rb1 promote apoptosis through the activation of caspase-3, mitochondrial dysfunction, and cytochrome c release (Li *et al.,* 2014; Zhou *et al*., 2019). Polysaccharide fractions further enhance macrophage activity and cytokine secretion (IL-1β, IL-6, TNF-α), strengthening innate immunity (Choi *et al*., 2023).

3.2.2. The Effect of Bioactive Compounds of Ginseng – Hexane Extract on THP-1 Cell Line

Among the extracts compared in Table 1, the hexane fraction exhibited remarkable cytotoxic effects on THP-1 cells, primarily due to its enrichment in ginsenoside Rg2. This bioactive compound induces apoptosis, inhibits angiogenesis, and suppresses metastasis (Zhang et al., 2021). Notably, ginsenoside Rh2 blocks epithelial–mesenchymal transition (EMT), a hallmark of metastasis (Tied *et al.,* 2019, Kim *et al.,* 2017).

Ginsenoside Rg2 also exhibits immunomodulatory, antioxidant, and anti-inflammatory effects (Qian *et al*., 2019; *Huang et al*., 2019). These are mediated via mitochondrial apoptosis, involving caspase-3 activation, PARP cleavage, and modulation of the Bax/Bcl-2 ratio (Lee *et al*., 2020; Kim *et al.,* 2021). NF-κB suppression also contributes to the inhibition of anti-survival genes (Jang *et al.,* 2023).

The current results in Table 1 demonstrated that the hexane extract caused a cytotoxic effect of 46.30 ± 27.24 against THP-1 cells. This supports its potential as an anticancer agent and, given the lack of prior leukemia-specific reports, underscores the novelty of the present study (Cui *et al.,* 2010).

3.2.3. The Effect of Bioactive Compounds of Ginseng – Ethanolic Extract on THP-1 Cell Line

As summarized in Table 1, the ethanoic extract (70%) of Panax ginseng demonstrated the highest tumor cell killing ratio (84.15 ± 3.39), surpassing aqueous and hexane extracts. This potency is attributed to its higher concentration of ginsenosides (Rg3, Rg5, Rg6), phenolics, and flavonoids (Walia *et al.,* 2023). These compounds exert strong antioxidant activity, reducing ROS generation and protecting cellular integrity. The apoptotic mechanisms involve both the intrinsic (mitochondrial) and extrinsic (death receptor) pathways (Yang *et al.,* 2023; Moyer, 2025). Our findings align with reports highlighting ethanol extracts as the richest in antioxidant and cytotoxic compounds compared with other solvent fractions (Hasan *et al.,* 2025).

3.2.4. The Effect of Bioactive Compounds of Ginseng – Chloroform Extract on THP-1 Cell Line

The chloroform extract of Panax ginseng demonstrated the strongest cytotoxic activity among all tested extracts. This fraction is enriched with β-phytosterols and fatty acids, which modulate membrane dynamics, promote apoptosis, and inhibit metastasis (Qi *et al.,* 2011).

Our findings confirm earlier reports that β-phytosterol is a natural anticancer compound with apoptosis-inducing and cancer risk–reducing effects (Dąbrowska *et al.,* 2023). HPLC chromatographic profiling (Table 2) revealed 16 peaks, with four major active compounds (peaks 4, 6, 7, and 11) (Figure 4) contributing significantly to cytotoxicity. These bioactive constituents include fatty acids with anti-proliferative, anti-inflammatory, and anticancer properties (Christmann *et al.,* 2022; Budi *et al.,* 2022).

Thus, chloroform-extracted ginseng holds great promise as a potent anticancer candidate due to its unique phytochemical composition, which differs from that of more polar extracts.

4. **Conclusions**:

This study evaluated the cytotoxic potential of four different Panax quinquefolium root extracts (aqueous, hexane, ethanol, and chloroform) against THP-1 acute myeloid leukemia cells using MTT viability assays and morphological analysis. All tested extracts demonstrated dose-dependent inhibition of THP-1 cell proliferation across concentrations ranging from 6.25 to 200 µg/ml, with statistically significant differences observed between treatments ($p < 0.001$). The chloroform extract exhibited the highest cytotoxic activity, achieving 88.11 ± 3.14% growth inhibition at the maximum tested concentration, followed by the ethanol extract (84.15 ± 3.39%), the hexane extract (80.43 ± 3.64%), and the aqueous extract (77.35 ± 2.65%). Histological observations using crystal violet staining corroborated the quantitative findings, showing progressive reduction in cell density and viability corresponding to the cytotoxic potency of each extract. HPLC analysis of the chloroform extract identified four major bioactive peaks, including hexadecanoic acid and methyl13-methyltetradecanoate, which may contribute to the

observed cytotoxic effects.

These findings suggest that Panax quinquefolium extracts, particularly the chloroform fraction, possess significant anti-proliferative activity against THP-1 cells and warrant further investigation. Future studies should include mechanistic analyses to elucidate the specific pathways involved in the observed cytotoxicity, assess selectivity toward cancer versus normal cells, and evaluate synergistic effects with conventional chemotherapeutic agents. The results provide preliminary evidence supporting the potential therapeutic value of P. quinquefolium extracts in the treatment of acute myeloid leukemia. However, extensive preclinical and clinical validation will be necessary before clinical application.

5. DECLARATIONS

5.1. Study Limitations

This study was conducted in vitro using the THP-1 cell line, which may not fully represent in vivo effects. Whole Panax quinquefolium extracts were used without identifying specific bioactive compounds, and molecular mechanisms were not investigated. Only short-term exposures were assessed, and other concentrations may yield different results. These limitations underscore the need for further in vivo studies and mechanistic research to confirm and expand upon these findings.

5.2. Acknowledgements

The author sincerely thanks the University of Kufa and the Faculty of Science for their continuous support, guidance, and provision of the Research Ethics Book and biosafety protocols, which were strictly followed throughout this study. Gratitude is also extended to Phi Nano Sciences Center (PNSC) for providing the commercially available cancer cell line used in this research. Special appreciation goes to all laboratory staff for their technical assistance in maintaining safe and precise cell culture procedures.

5.3. Funding source

The authors funded this research. In accordance with the ethical guidelines of the Periódico Tchê Química, which do not allow donations from authors with manuscripts under evaluation (even when research funds are available), or in cases of authors' financial constraints, publication costs were fully absorbed by the journal under our Platinum Open Access policy, through the support of the Araucária Scientific Association (https://acaria.org/). This policy aims to ensure complete independence between the editorial process and any financial aspects, reinforcing our commitment to scientific integrity and equity in knowledge dissemination.

5.4. Competing Interests

The authors declare that they have no competing interests or conflicts of interest that could have influenced the work presented in this manuscript. This includes, but is not limited to, financial relationships, personal affiliations, intellectual property considerations, or other potential sources of bias. All authors have reviewed and approved this declaration, ensuring transparency and maintaining scientific integrity in the reporting of this research.

5.6. Use of AI

The manuscript was written in English with careful attention to clarity and precision. AI tools were employed solely to enhance language quality and translate the abstract into Portuguese. All scientific content, terminology, and methodology were thoroughly reviewed and validated by the authors, who remain fully responsible for the accuracy and integrity of the work.

6. HUMAN AND ANIMAL-RELATED STUDIES

6.1. Ethical Approval

This study was conducted using a

commercially available/preserved cancer cell line for research purposes only, provided by the Phi Nano Sciences Center (PNSC), without involving human participants or experimental animals. Therefore, no approval from human or animal ethics committees was required. Nevertheless, the research strictly adhered to the guidelines outlined in the Research Ethics Book, Faculty of Science, University of Kufa, dated June 29, 2025, and all biosafety procedures (Biosafety Guidelines) were carefully followed during cell culture handling and laboratory work.

6.2. Informed Consent

Not applicable. This study was conducted exclusively using a commercially available/preserved cancer cell line, without involving human participants or experimental animals; therefore, informed consent was not required.

7. REFERENCES:

1. Shimony, S., Stahl, M., & Stone, R. M. (2025). Acute Myeloid Leukemia: 2025 Update on Diagnosis, Risk-Stratification, and Management. *American journal of hematology*, *100*(5), 860–891. https://doi.org/10.1002/ajh.27625

2. Reikvam H. (2023). Revisiting the prognostic role of *FLT3* mutations in acute myelogenous leukemia. *Expert review of hematology*, *16*(5), 317–323. https://doi.org/10.1080/17474086.2023.2202849

3. Gyi, K. K., Anuchapreeda, S., Intasai, N., Tungjai, M., Okonogi, S., Iwasaki, A., Usuki, T., & Tima, S. (2025). Anti-leukemia activity of the ethyl acetate extract from Gynostemma pentaphyllum (Thunb.) leaf against FLT3-overexpressing AML cells and its phytochemical characterization. *BMC complementary medicine and therapies*, *25*(1), 172. https://doi.org/10.1186/s12906-025-04903-0

4. Bray, F., Laversanne, M., Sung, H., Ferlay, J., Siegel, R. L., Soerjomataram, I., & Jemal, A. (2024). Global cancer statistics 2022: GLOBOCAN estimates of incidence and mortality worldwide for 36 cancers in 185 countries. *CA: a cancer journal for clinicians*, *74*(3), 229–263. https://doi.org/10.3322/caac.21834

5. Jo, H., Lee, E. Y., Cho, H. S., Rayhan, M. A., Cho, A., Chae, C. S., & You, H. J. (2024). THP-1 Monocytic Cells Are Polarized to More Antitumorigenic Macrophages by Serial Treatment with Phorbol-12-Myristate-13-Acetate and PD98059. *Medicina (Kaunas, Lithuania)*, *60*(6), 1009. https://doi.org/10.3390/medicina60061009

6. James, J. R., Curd, J., Ashworth, J. C., Abuhantash, M., Grundy, M., Seedhouse, C. H., Arkill, K. P., Wright, A. J., Merry, C. L. R., & Thompson, A. (2023). Hydrogel-Based Preclinical Evaluation of Repurposed FDA-Approved Drugs for AML. *International journal of molecular sciences*, *24*(4), 4235. https://doi.org/10.3390/ijms24044235

7. Fang, X., Zhou, X., Wang, Y., Wang, Y., & Wang, H. (2023). Transcriptional regulatory network of ginsenosides content in various ginseng cultivars. *Scientia Horticulturae, 322*, 112388. https://doi.org/10.1016/j.scienta.2023.112388

8. Li, Z., Wang, Y., Xu, Q., Ma, J., Li, X., Tian, Y., Wen, Y., & Chen, T. (2023). Ginseng and health outcomes: an umbrella review. *Frontiers in pharmacology*, *14*, 1069268. https://doi.org/10.3389/fphar.2023.1069268

9. Zhang, P., Zhang, D., Ma, C., Wang, R., & Wang, W. (2024). Free Radical Scavenging Effect and Immunomodulatory Activity of Total Saponins Extract of Ginseng Fibrous Roots. *Molecules (Basel, Switzerland)*, *29*(12), 2770. https://doi.org/10.3390/molecules29122770

10. Yusoff, I. M., Mat Taher, Z., Rahmat, Z., & Chua, L. S. (2022). A review of ultrasound-assisted extraction for plant bioactive compounds: Phenolics, flavonoids, thymols, saponins and proteins. *Food research international (Ottawa, Ont.)*, *157*, 111268. https://doi.org/10.1016/j.foodres.2022.111268

11. Tian, Y., Xu, Z., Zheng, B., & Martin Lo, Y. (2013). Optimization of ultrasonic-assisted extraction of pomegranate (Punica granatum L.) seed oil. *Ultrasonics sonochemistry*, *20*(1), 202–208. https://doi.org/10.1016/j.ultsonch.2012.07.010

12. Al-Ziaydi, A. G., Al-Shammari, A. M., Hamzah, M. I., Kadhim, H. S., & Jabir, M. S. (2020). Hexokinase inhibition using D-Mannoheptulose enhances oncolytic Newcastle disease virus-mediated killing of breast cancer cells. *Cancer Cell*

International, *20*, 420. https://doi.org/10.1186/s12935-020-01514-2

13. Ibrahim, A. A., Kareem, M. M., Al-Noor, T. H., Al-Muhimeed, T., AlObaid, A. A., Albukhaty, S., Sulaiman, G. M., Jabir, M., Taqi, Z. J., & Sahib, U. I. (2021). Pt(II)-Thiocarbohydrazone Complex as Cytotoxic Agent and Apoptosis Inducer in Caov-3 and HT-29 Cells through the P53 and Caspase-8 Pathways. *Pharmaceuticals (Basel, Switzerland)*, *14*(6), 509. https://doi.org/10.3390/ph14060509

14. Jabir, M. S., Abood, N. A., Jawad, M. H., Öztürk, K., Kadhim, H., Albukhaty, S., … Sulaiman, G. M. (2022). Gold nanoparticles loaded TNF-α and CALNN peptide as a drug delivery system and promising therapeutic agent for breast cancer cells. *Materials Technology*, *37*(14), 3152–3166. https://doi.org/10.1080/10667857.2022.2133073

15. Tan, M. M., Chen, M. H., Han, F., Wang, J. W., & Tu, Y. X. (2021). Role of Bioactive Constituents of *Panax notoginseng* in the Modulation of Tumorigenesis: A Potential Review for the Treatment of Cancer. *Frontiers in pharmacology*, *12*, 738914. https://doi.org/10.3389/fphar.2021.738914

16. Hei, J., Li, Y., Rui, R., Faisal, N., Peng, J., Wang, B., Wang, S., & He, X. (2025). The cultivation of *Panax notoginseng* enhances the metabolites and microbial network complexity in the soil of *Pinus armandii* rather than *Pinus kesiya*. *Frontiers in microbiology*, *16*, 1616266. https://doi.org/10.3389/fmicb.2025.1616266

17. Jia, L., & Zhao, Y. (2009). Current evaluation of the millennium phytomedicine--ginseng (I): etymology, pharmacognosy, phytochemistry, market and regulations. *Current medicinal chemistry*, *16*(19), 2475–2484. https://doi.org/10.2174/092986709788682146

18. Poudyal, D., Le, P. M., Davis, T., Hofseth, A. B., Chumanevich, A., Chumanevich, A. A., Wargovich, M. J., Nagarkatti, M., Nagarkatti, P. S., Windust, A., & Hofseth, L. J. (2012). A hexane fraction of American ginseng suppresses mouse colitis and associated colon cancer: anti-inflammatory and proapoptotic mechanisms. *Cancer prevention research (Philadelphia, Pa.)*, *5*(4), 685–696. https://doi.org/10.1158/1940-6207.CAPR-11-0421

19. Kim, Y. S., Kim, D. S., & Kim, S. I. (1998). Ginsenoside Rh2 and Rh3 induce differentiation of HL-60 cells into granulocytes: modulation of protein kinase C isoforms during differentiation by ginsenoside Rh2. *The international journal of biochemistry & cell biology*, *30*(3), 327–338. https://doi.org/10.1016/s1357-2725(97)00141-6

20. Shim, J. Y., Han, Y., Ahn, J. Y., Yun, Y. S., & Song, J. Y. (2007). Chemoprotective and adjuvant effects of immunomodulator ginsan in cyclophosphamide-treated normal and tumor-bearing mice. International journal of immunopathology and pharmacology, 20(3), 487–497. https://doi.org/10.1177/039463200702000307

21. Cui, X., Jin, Y., Poudyal, D., Chumanevich, A. A., Davis, T., Windust, A., Hofseth, A., Wu, W., Habiger, J., Pena, E., Wood, P., Nagarkatti, M., Nagarkatti, P. S., & Hofseth, L. (2010). Mechanistic insight into the ability of American ginseng to suppress colon cancer associated with colitis. Carcinogenesis, 31(10), 1734–1741. https://doi.org/10.1093/carcin/bgq163

22. Dana, S. M. M. A., Meghdadi, M., Kakhki, S. K., & Khademi, R. (2024). Anti-leukemia effects of ginsenoside monomer: A narrative review of pharmacodynamics study. Current therapeutic research, clinical and experimental, 100, 100739. https://doi.org/10.1016/j.curtheres.2024.100739

23. Chen, Y., Liu, Z. H., Xia, J., Li, X. P., Li, K. Q., Xiong, W., Li, J., & Chen, D. L. (2016). 20(S)-ginsenoside Rh2 inhibits the proliferation and induces the apoptosis of KG-1a cells through the Wnt/β-catenin signaling pathway. Oncology reports, 36(1), 137–146. https://doi.org/10.3892/or.2016.4774

24. Huang, J., Peng, K., Wang, L., Wen, B., Zhou, L., Luo, T., Su, M., Li, J., & Luo, Z. (2016). Ginsenoside Rh2 inhibits proliferation and induces apoptosis in human leukemia cells via TNF-α signaling pathway. Acta biochimica et biophysica Sinica, 48(8), 750–755. https://doi.org/10.1093/abbs/gmw049

25. Liu, Z. H., Li, J., Xia, J., Jiang, R., Zuo, G. W., Li, X. P., Chen, Y., Xiong, W., & Chen, D. L. (2015). Ginsenoside 20(s)-Rh2 as potent natural histone deacetylase inhibitors suppressing the growth of human leukemia

cells. Chemico-biological interactions, 242, 227–234. https://doi.org/10.1016/j.cbi.2015.10.014

26. Li, J., Wei, Q., Zuo, G. W., Xia, J., You, Z. M., Li, C. L., & Chen, D. L. (2014). Ginsenoside Rg1 induces apoptosis through inhibition of the EpoR-mediated JAK2/STAT5 signalling pathway in the TF-1/ Epo human leukemia cell line. Asian Pacific journal of cancer prevention : APJCP, 15(6), 2453–2459. https://doi.org/10.7314/apjcp.2014.15.6.2453

27. Qian, Y., Huang, R., Li, S., Xie, R., Qian, B., Zhang, Z., Li, L., Wang, B., Tian, C., Yang, J., & Xiang, M. (2019). Ginsenoside Rh2 reverses cyclophosphamide-induced immune deficiency by regulating fatty acid metabolism. Journal of leukocyte biology, 106(5), 1089–1100. https://doi.org/10.1002/JLB.2A0419-117R

28. Choi, J., Nam, J. H., Rod-In, W., Monmai, C., Jang, A. Y., You, S., & Park, W. J. (2023). Korean Ginseng Berry Polysaccharide Enhances Immunomodulation Activities of Peritoneal Macrophages in Mice with Cyclophosphamide-Induced Immunosuppression. Journal of microbiology and biotechnology, 33(6), 840–847. https://doi.org/10.4014/jmb.2211.11056

29. Zhang, H., Park, S., Huang, H., Kim, E., Yi, J., Choi, S. K., ... & Kim, M. (2021). Anticancer effects and potential mechanisms of ginsenoside Rh2 in various cancer types. Oncology Reports, 45(4), 33 https://doi.org/10.3892/or.2021.7984

30. Ishay-Ronen, D., Diepenbruck, M., Kalathur, R. K. R., Sugiyama, N., Tiede, S., Ivanek, R., Bantug, G., Morini, M. F., Wang, J., Hess, C., & Christofori, G. (2019). Gain Fat-Lose Metastasis: Converting Invasive Breast Cancer Cells into Adipocytes Inhibits Cancer Metastasis. Cancer cell, 35(1), 17–32.e6. https://doi.org/10.1016/j.ccell.2018.12.002.

31. Kim, J. H., Kim, M., Yun, S. M., Lee, S., No, J. H., Suh, D. H., Kim, K., & Kim, Y. B. (2017). Ginsenoside Rh2 induces apoptosis and inhibits epithelial-mesenchymal transition in HEC1A and Ishikawa endometrial cancer cells. Biomedicine & Pharmacotherapy, 96, 871-876. https://doi.org/10.1016/j.biopha.2017.09.033

32. Qian, Y., Huang, R., Li, S., Xie, R., Qian, B., Zhang, Z., Li, L., Wang, B., Tian, C., Yang, J., et al. (2019). Ginsenoside Rh2 reverses cyclophosphamide induced immune deficiency by regulating fatty acid metabolism. Journal of Leukocyte Biology, 106, 1089-1100. https://doi.org/10.1002/JLB.2A0419-117R

33. Huang, Y. Q., Huang, H. X., Han, Z. D., Li, W., Mai, Z. P., & Yuan, R. Q. (2019). Ginsenoside Rh2 inhibits angiogenesis in prostate cancer by targeting CNNM1. Journal of Nanoscience and Nanotechnology, 19, 1942-1950. https://doi.org/10.1166/jnn.2019.16404

34. Lee, J., & Zhao, Y. (2020). Current evaluation of the millennium phytomedicine-ginseng (I): Etymology, pharmacognosy, phytochemistry, market and regulations. Current Medicinal Chemistry, 16, 2475-2484. OI: https://doi.org/10.2174/092986709788682146

35. Kim, J., & Kim, Y. J. (2021). Compound K promotes apoptosis through ROS-dependent pathways in human leukemia cells. Biomedicine & Pharmacotherapy, 133, 110997. https://doi.org/10.3389/fphar.2024.1339146

36. Jang, W. Y., Hwang, J. Y., & Cho, J. Y. (2023). Ginsenosides from Panax ginseng as key modulators of NF-?B signaling are powerful anti-inflammatory and anticancer agents. International Journal of Molecular Sciences, 24(7), 6119. https://doi.org/10.3390/ijms24076119

37. Cui, X., Jin, Y., Poudyal, D., Chumanevich, A. A., Davis, T., Windust, A., Hofseth, A., Wu, W., Habiger, J., Pena, E., Wood, P., Nagarkatti, M., Nagarkatti, P. S., & Hofseth, L. (2010). Mechanistic insight into the ability of American ginseng to suppress colon cancer associated with colitis. Carcinogenesis, 31(10), 1734–1741. https://doi.org/10.1093/carcin/bgq163

38. Walia, S., Kumar, P., Kumar, D., & Kumar, R. (2023). A preliminary study on suitability of growing ginseng (Panax ginseng Meyer) in western Himalayan region. Plant, Soil and Environment, 69(2), 71-80. https://pse.agriculturejournals.cz/artkey/pse-202302-0004_a-preliminary-study-on-suitability-of-growing-ginseng-panax-ginseng-meyer-in-western-himalayan-region.php

39. Yang, Y., Xu, S., Yang, K., Sun, Y., Yang, R., Hu, Y., Chen, G., & Cai, H. (2023). Characterization and In Vitro Antioxidant and Anti-Inflammatory Activities of Ginsenosides Extracted from Forest-Grown Wild Panax quinquefolius L. Foods (Basel, Switzerland), 12(23), 4316. https://doi.org/10.3390/foods12234316

40. Moyer, A., Tanaka, K., & Cheng, E. H. (2025). Apoptosis in Cancer Biology and Therapy. Annual review of pathology, 20(1), 303–328. https://doi.org/10.1146/annurev-pathmechdis-051222-115023

41. Hasan, S. A., Abass, A. A., & Jabbar, L. (2025). The protective role of ethanolic extract of ginseng (Panax ginseng) against adverse physiological and histological alterations in the liver of female rabbits exposed to chlorine. Advancements in Life Sciences, 12(1), 185. https://doi.org/10.62940/als.v12i1.2537

42. Qi, L. W., Wang, C. Z., & Yuan, C. S. (2011). Ginsenosides from American ginseng: chemical and pharmacological diversity. Phytochemistry, 72(8), 689–699. https://doi.org/10.1016/j.phytochem.2011.02.012

43. Sobocki, J., Bogdanowska-Charkiewicz, D., Budnicka-Borkowicz, A., Chełmicka, M., Dudkowiak, R., Guzek, M., Kaczka, A., Kanikowska, A., Kurek, K., Matysiak, K., Paluch, J., Szewczuk, M., Walecka-Kapica, E., Adrych, K., Dąbrowski, A., Gąsiorowska, A., Hartleb, M., Kłopocka, M., Talar-Wojnarowska, R., Waśko-Czopnik, D., … Mańkowska-Wierzbicka, D. (2025). Clinical nutrition in gastrointestinal diseases: an up-to-date clinical practice guideline. Polish archives of internal medicine, 135(3), 16967. https://doi.org/10.20452/pamw.16967

44. Christmann, J., Rohn, S., & Weller, P. (2022). gc-ims-tools - A new Python package for chemometric analysis of GC-IMS data. Food chemistry, 394, 133476. https://doi.org/10.1016/j.foodchem.2022.133476

45. Budi, H. S., Anitasari, S., Ulfa, N. M., Setiabudi, M. A., Ramasamy, R., Wu, C. Z., & Shen, Y. K. (2022). Palmitic acid of Musa Paradisiaca induces apoptosis through caspase-3 in human oral squamous cell carcinoma. European review for medical and pharmacological sciences, 26(19), 7099–7114. https://doi.org/10.26355/eurrev_202210_29895

Table 1: *Cytotoxicity of Panax Ginseng Extracts from Different Solvents on THP-1 Cells at Various Concentrations*

Concentration	**(Mean ± SD)**				
(µg/ml)	**Ethanol**	**Chloroform**	**Hexane**	**Water**	**Total**
GA: 6.25	9.62 ± 0.84 b	12.67 ± 0.90 a	8.30 ± 1.03 bc	6.59 ± 0.91 c	9.29 ± 2.45
GB: 12.5	22.35 ± 1.50 b	27.37 ± 1.57 a	18.97 ± 1.50 bc	16.81 ± 2.58 c	21.37 ± 4.45
GC: 25	45.62 ± 2.59 ab	49.20 ± 2.96 a	40.45 ± 2.76 bc	38.53 ± 2.70 c	43.45 ± 4.99
GD: 50	62.49 ± 2.81 ab	65.95 ± 4.23 a	57.70 ± 2.52 bc	54.05 ± 3.34 c	60.05 ± 5.50
GE: 100	75.96 ± 3.83 b	78.73 ± 3.64 a	71.97 ± 2.84 bc	67.70 ± 4.72 c	73.59 ± 5.43
GF: 200	84.15 ± 3.39 ab	88.11 ± 3.14 a	80.43 ± 3.64 bc	77.35 ± 2.65 c	82.51 ± 5.03
Total	50.03 ± 27.99	53.67 ± 27.84	46.30 ± 27.24	43.51 ± 26.50	48.38 ± 27.09
p-value			<0.001		

Different small letters expressed significant differences between the extract groups at p-value <0.05 by ANOVA with Tukey's test

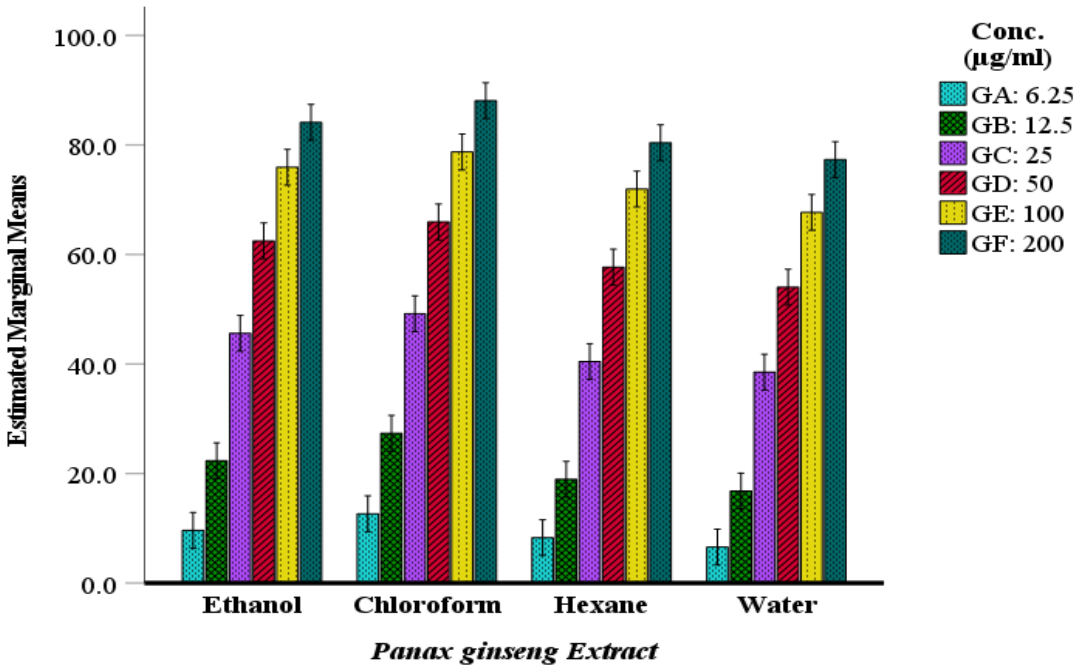

Figure 2: *Inhibitory Potential of Different Panax Ginseng Extracts on THP-1 Cells*

Table 2*: Peaks identified in the HPLC chromatographic profile of the chloroform extract of ginseng, highlighting four major peaks—Peak 4, Peak 6, Peak 7, and Peak 11*

Peak	R .time	Area %	Height %	Comp Name	Formula	Molecule Weight
4	17.049	21.35	19.35	Hexadecanoic acid	C17H34O2	270
6	2.328	0.92	0.82	TetrahydropyranZ-10-dodecenoate	C17H30O3	282
7	17.041	34.86	33.33	Methyl13-methyltetradecanoate	C16H32O2	256
11	2.016	0.17	1.02	2-Formylhistamine	C6H9N3O	139

Table 2 shows the four major peaks (>5% area) identified in the HPLC analysis. Complete chromatographic data is available in Supplementary Material.

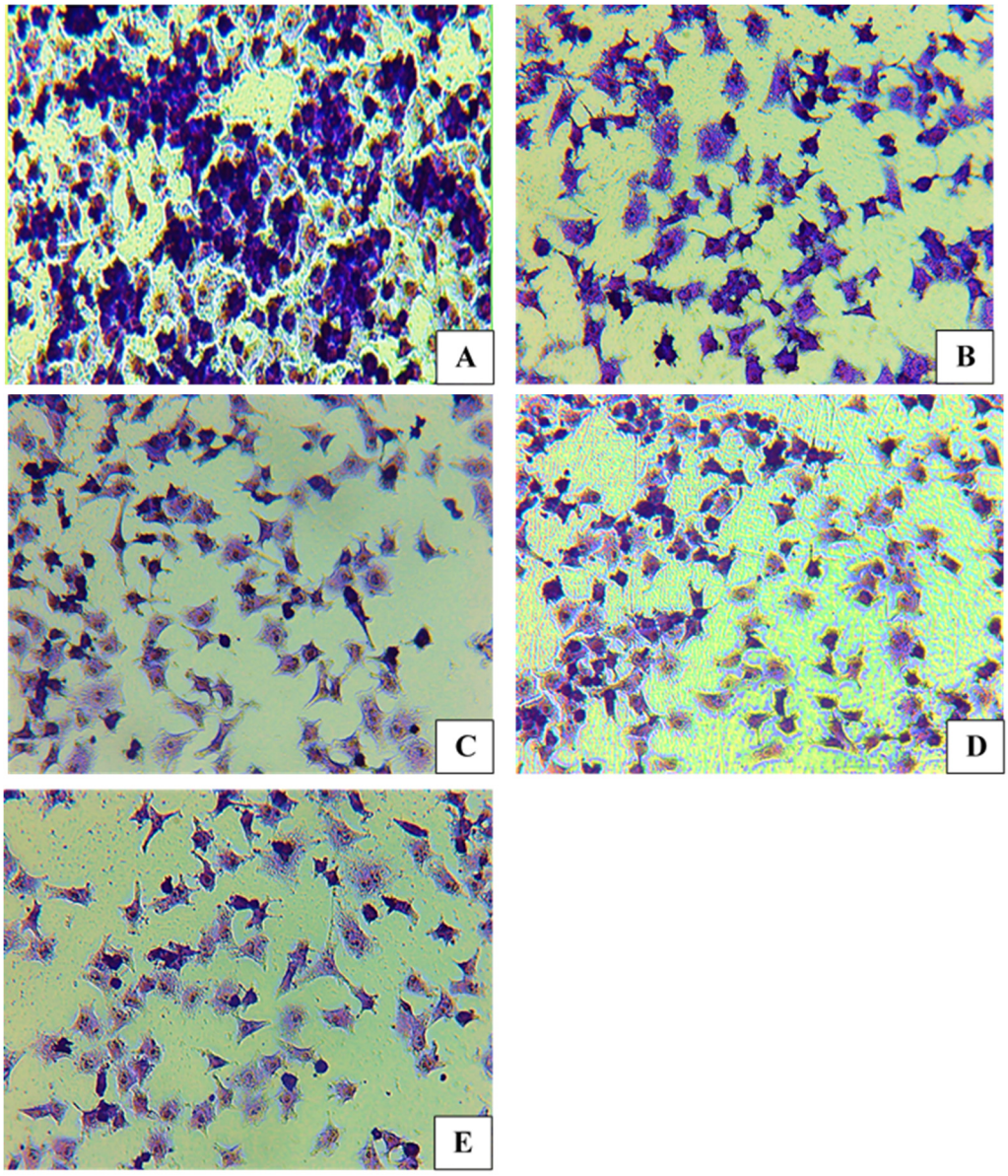

***Figure 3**. Histological sections of THP-1 cells stained with crystal violet after 24h exposure to 200 µg/mL of different P. quinquefolium extracts. (A) Control cells: formed dense clusters, indicating active proliferation. (B) Water extract: partially reduced cell numbers. (C) Hexane extract: further decreased cell density, (D) Ethanol extract: showed a stronger suppressive effect. (E) Chloroform extract: produced the lowest cell count, demonstrating the most pronounced inhibition of THP-1 cell survival.Scale bar = 100 µm. Magnification: (40*10x) 400x.*

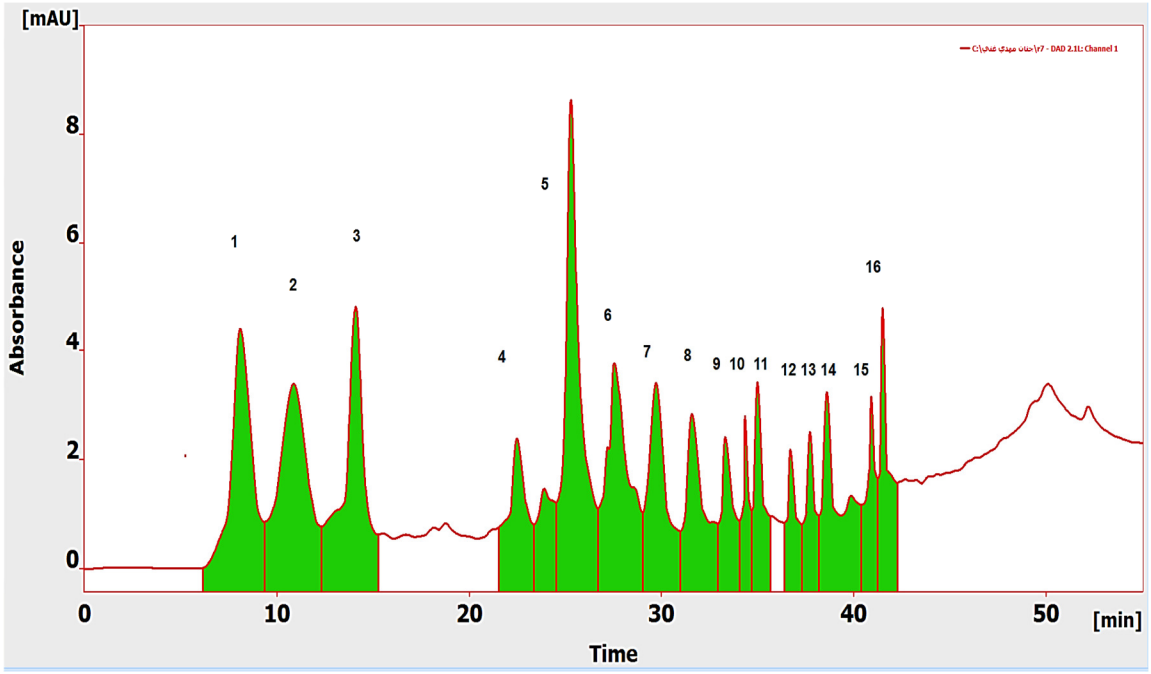

Figure 4: *HPLC Chromatogram of Chloroform Analysis and Peak Identification of Phytochemicals in Chloroform -ginseng extract.*

PERIÓDICO TCHÊ QUÍMICA
ARTIGO ORIGINAL

APRIMORANDO A APRENDIZAGEM NO LABORATÓRIO DE QUÍMICA: EFEITO DE SIMULAÇÕES PRÉ-LABORATORIAIS E DE FLUXOGRAMAS NO DESEMPENHO DE FUTUROS PROFESSORES

ENHANCING LEARNING IN CHEMISTRY LABORATORY: EFFECT OF PRE-LAB SIMULATIONS AND FLOWCHART ON PRE-SERVICE TEACHERS' ACHIEVEMENT

KİMYA LABORATUVARINDA ÖĞRENMENİN GELİŞTİRİLMESİ: SİMÜLASYON VE AKIŞ ŞEMASININ ÖĞRETMEN ADAYLARININ BAŞARISINA ETKİSİ

Fatma Merve Mustafaoğlu*
Hacettepe University, Faculty of Education, Department of Chemistry Education. Türkiye

Fatma Alkan
Hacettepe University, Faculty of Education, Department of Chemistry Education. Türkiye

** Corresponding author*
e-mail: fmerveulusoy@gmail.com

Received 20 August 2025; received in revised form 30 September 2025; accepted 14 October 2025

RESUMO

Introdução: Simulações são amplamente utilizadas na educação para proporcionar ambientes de aprendizagem dinâmicos e são particularmente úteis na química, onde podem substituir experimentos físicos quando as condições de laboratório são inadequadas ou os materiais forem perigosos. Neste estudo, as simulações foram empregadas não como substitutas, mas para potencializar a eficácia dos experimentos laboratoriais presenciais. **Objetivo**: O estudo teve como objetivo investigar o impacto do uso de simulações e fluxogramas na instrução sobre preparo de soluções e aquecimento sobre o desempenho acadêmico de futuros professores de química, além de explorar suas opiniões sobre a preparação para experimentos práticos por meio de simulações pré-laboratoriais. **Métodos**: Adotou-se um delineamento do tipo grupo estático com pré-teste e pós-teste, envolvendo 21 futuros professores matriculados na disciplina de Laboratório de Química Geral. A instrução ocorreu em duas etapas: primeiro, os experimentos foram realizados online por meio de simulações; em seguida, os mesmos experimentos foram executados em laboratório físico. Os dados foram coletados por meio de quizzes (pré-teste), uma prova de desempenho (pós-teste) e um formulário de feedback. **Resultados**: O teste de Wilcoxon indicou que os experimentos laboratoriais apoiados por simulações tiveram um efeito positivo e estatisticamente significativo no desempenho dos participantes. Além disso, o teste de Mann–Whitney U revelou diferença significativa entre as notas do pós-teste dos futuros professores que elaboraram um fluxograma com base nas simulações e aqueles que não o fizeram. **Discussão**: O uso de simulações para enriquecer experimentos laboratoriais proporciona uma experiência de aprendizagem mais rica e diversificada, combinando vivências concretas e virtuais. Os fluxogramas elaborados pelos participantes não eram meras listas de procedimentos, mas incluíam também propriedades das substâncias utilizadas, pontos-chave a serem observados e lembretes importantes. Essa prática favoreceu uma aprendizagem duradoura ao desenvolver habilidades de organização, associação e aplicação do conhecimento. **Conclusões**: Concluiu-se que a realização de simulações antes dos experimentos laboratoriais melhora significativamente o desempenho acadêmico. Ademais, os futuros professores que tanto realizaram as simulações quanto elaboraram fluxogramas obtiveram pontuações superiores às de seus colegas. Os participantes também relataram menor ansiedade, maior confiança e consideraram as simulações benéficas para o planejamento e a execução dos experimentos.

Palavras-chave: *Simulações, fluxogramas, laboratório de química, desempenho, futuros professores*.

ABSTRACT

Background: Simulations are widely used in education to provide dynamic learning environments and are particularly useful in chemistry, where they can substitute for physical experiments when laboratory conditions are inadequate or materials hazardous. In this study, simulations were employed not as replacements but to enhance the effectiveness of physical laboratory experiments. **Aim:** The study aimed to investigate the impact of simulation- and flowchart-supported instruction on solution preparation and heating on the academic achievement

DOI: 10.52571/PTQ.v22.n51.2025_04_MERVE_pgs_52_65.pdf

of pre-service chemistry teachers, and to explore their opinions about preparing for hands-on experiments by first conducting a pre-lab simulation. **Methods:** The study employed a static group pretest-posttest design, involving 21 pre-service teachers enrolled in the General Chemistry Laboratory course. Instruction proceeded in two stages: first, experiments were conducted online through simulations; second, the same experiments were performed in a physical laboratory. Data were collected via quizzes (pretest), an achievement exam (posttest), and a feedback form. **Results:** The Wilcoxon Signed Rank test indicated that simulation-supported laboratory experiments had a significant positive effect on participants' achievement. Additionally, the Mann–Whitney U test revealed a significant difference between the posttest scores of pre-service teachers who prepared a flowchart using simulations and those who did not. **Discussion:** Enhancing laboratory experiments with simulations provides a richer and more varied learning experience by offering both concrete and virtual experiences. Flowcharts drawn up by the participants were not simple lists of steps, but also covered the properties of the chemicals utilized, key points to consider, and significant reminders. This supported durable learning through enhancing students' skills in organizing, associating, and applying knowledge. **Conclusions:** In conclusion, running simulations before laboratory experiments has been shown to improve academic achievement. Moreover, pre-service teachers who both conducted the simulations and prepared their flowcharts achieved higher scores than their peers. Participants also reported reduced anxiety, increased confidence, and perceived simulations as beneficial for planning and carrying out the experiments.

Keywords: *Simulations, flowcharts, chemistry laboratory, achievement, pre-service teachers*

ÖZET

Giriş: Simülasyonlar, eğitimde dinamik öğrenme ortamları yaratmak için yaygın olarak kullanılmakta ve özellikle kimya alanında, laboratuvar koşullarının yetersiz olduğu ya da materyallerin tehlikeli olduğu durumlarda fiziksel deneylerin yerine geçebilmektedir. Bu çalışmada ise simülasyonlar, fiziksel laboratuvar deneylerinin etkinliğini artırmak amacıyla kullanılmıştır. **Amaç:** Araştırma, çözelti hazırlama ve ısıtma konularında simülasyon ve akış şeması destekli öğretimin öğretmen adaylarının akademik başarıları üzerindeki etkisini incelemeyi ve deney öncesinde simülasyon yaparak uygulamaya hazırlanma sürecine ilişkin görüşlerini belirlemeyi amaçlamaktadır. **Yöntem:** Statik grup ön test-son test desen kullanılan çalışmaya, Genel Kimya Laboratuvarı dersine kayıtlı 21 öğretmen adayı katılmıştır. Süreç iki aşamada yürütülmüştür: (1) çevrimiçi simülasyon uygulamaları, (2) aynı deneylerin fiziksel laboratuvarda gerçekleştirilmesi. Veriler, quizler (ön test), başarı testi (son test) ve geri bildirim formu ile toplanmıştır. **Bulgular:** Wilcoxon testi, simülasyon destekli laboratuvar uygulamalarının ve simülasyon+akış şeması hazırlanarak yapılan uygulamaların öğretmen adaylarının akademik başarılarını anlamlı biçimde artırdığını; Mann–Whitney testi ise simülasyonları tamamladıktan sonra akış şeması hazırlayan öğretmen adaylarının akademik başarılarının daha yüksek olduğunu göstermiştir. **Tartışma**: Simülasyon ve laboratuvar deneylerinin birleşimi öğrencilere hem somut hem sanal deneyimler sunarak daha zengin bir öğrenme süreci sağlamıştır. Katılımcıların hazırladığı akış şemaları yalnızca adımları değil, kimyasalların özelliklerini, dikkat edilmesi gereken noktaları ve önemli hatırlatmaları da içermiştir. Bu süreç, bilgiyi organize etme, ilişkilendirme ve uygulama becerilerini geliştirerek kalıcı öğrenmeyi desteklemiştir. **Sonuç:** Hem laboratuvar deneylerinden önce yapılan simülasyonların hem de simülasyonunun tamamlanmasının ardından hazırlanan bireysel akış şemalarının öğretmen adaylarının akademik başarılarını artırdığı yapılan analizler sonucunda belirlenmiştir. Ancak bu iki uygulama türü kıyaslandığında, simülasyonları tamamladıktan sonra akış şeması hazırlayan ve fiziksel laboratuvardaki deneyleri bu akış şemasına göre hazırlayan öğretmen adaylarının akademik başarılarının sadece simülasyon yapan öğretmen adaylarından daha yüksek olduğu belirlenmiştir. Ayrıca katılımcıların simülasyonları kaygıyı azaltıcı, özgüven artırıcı ve deneyleri kolaylaştırıcı buldukları belirlenmiştir.

Anahtar kelimeler: *Simülasyon, akış şeması, kimya laboratuvarı, başarı, öğretmen adayları*

1. INTRODUCTION:

Chemistry is a branch of science where abstract and concrete ideas interact (Yazıcı, 2023). Concretization of abstract concepts occurs through laboratory activities in chemistry education. In this way, laboratories play an important role in chemistry education. Laboratories, where students gain experience by direct practice or observation, are an important source of information obtained in chemistry, an experimental science. Practical laboratory experiments provide students with invaluable insights into the principles and practices of the discipline (Ayas, Akdeniz & Çepni, 1994).

Additionally, experimental learning increases students' interest in the subject and makes learning more enjoyable and permanent (Aydoğdu & Erbaş, 1992; Yao, 2023). Several methods/strategies that support physical laboratory environments are employed to enhance students' chemistry achievements. Encouraging

students' active participation in laboratory studies, such as through group work, and ensuring their involvement in discussion and experiment design processes can make laboratory experiences more effective. These interventions, along with the use of laboratory-supporting technology, can help students better understand chemistry concepts (Hofstein & Lunetta, 2004; Nakhleh, 1992; Russell & Weaver, 2011).

Nowadays, just as laboratories are important in chemistry education, technology is also crucial in education, and its importance is increasing daily. While the student's learning is supported through concrete experiences, supplementing it with visual experiences provides a rich teaching process. One of the environments that provides visual experience in this way is virtual learning environments (Ergun, 2017). Simulations, which enable students to gain experience, model real-life scenarios through computer-aided technological environments (Dalgarno, 2001; Lee *et al.*, 2021). Through simulations, students can explore and observe the microscopic world of chemistry more flexibly and freely. Simulations provide students with a unique opportunity to visualize abstract concepts and complex chemical phenomena with clarity. Simulations make theoretical concepts concrete and accessible by representing molecular structures, reactions, and interactions in dynamic, three-dimensional environments (Hirst, Glowacki & Baaden, 2014; Rayan & Rayan, 2017). Through simulations, students can explore and observe the microscopic world of chemistry more flexibly and engagingly (Hakerem, Dobrynina & Shore, 1993; Pekdağ, 2009). Unlike physical laboratories, where experiments are often limited by time and resources, simulations offer unlimited opportunities for exploration and experimentation. Students can repeat experiments multiple times, vary the variables, and observe the results immediately, thereby promoting a deeper understanding of chemical principles.

Simulations can help students understand complex concepts and serve as an effective tool in chemistry education. However, experimental simulations also have some limitations. In particular, it remains a matter of debate whether the practical skills acquired in real experiments are equivalent to those gained in simulations (Hawkins & Phelps, 2013). For this reason, the process of this study was structured in such a way that simulations and practical experiments supported each other. In addition, it was aimed to ensure the permanence of the knowledge of the pre-service teachers who investigated the theoretical knowledge about the experiment by transferring this information to the flowcharts.

Flowcharts are learning tools that aim to prepare pre-service teachers for the concepts and procedures they will encounter in the laboratory (Davidowitz, Rollnick, & Fakudze, 2005). While flowcharts are used to illustrate the experimental strategy and the steps to be followed in a process (Nakiboğlu, Erdurmazlı, Kızmaz, & Hepöz), they also enable students to develop concepts independently. Students' feedback that flowcharts help them associate experiments with chemical concepts covered in the lessons supports this feature of flowcharts (Davidowitz & Rollnick, 2001).

Laboratory practices, a vital part of chemistry education, enable students to connect abstract concepts with real-world experiences and consolidate their knowledge. Yet, when students do not prepare sufficiently for experiments, follow procedures superficially from a guide, and carry out the process without careful consideration, both their academic success and laboratory safety can be compromised. In general chemistry labs, it is commonly seen that students commit conceptual mistakes, waste time, and finish the period without completely fulfilling the purpose of the experiment. At this juncture, pre-laboratory tools such as simulations and self-designed flowcharts can play a crucial role in making the laboratory process more structured and meaningful. Simulations offer students the opportunity to review experimental procedures and minimize the risk of errors. In contrast, flowcharts allow them to chart the procedure in their own language and identify critical points. Thus, an investigation into the role of simulation- and flowchart-assisted practices in laboratory accomplishment is deemed important. The primary objective of this research was to investigate the impact of various pre-laboratory preparation methods on the academic performance of pre-service chemistry teachers in general chemistry laboratory practices. More specifically, the study investigated (i) changes in achievement levels of pre-service teachers who used simulations before conducting laboratory experiments, and (ii) changes in achievement levels of those who, in addition to using simulations, created individual flowcharts prior to performing the experiments. In addition, the research aimed to gain qualitative insights into pre-service teachers' views on using simulation-based experiments as a preparatory step before engaging in hands-on laboratory work, through semi-structured interviews.

1.1. Aim of the study

This research aims to investigate the impact of combining flowchart elaboration tasks with simulation-based laboratory activities on the academic achievement of pre-service teachers. In particular, the research aims to compare the level of achievement of a group of pre-service teachers who only participated in simulations with that of a group of pre-service teachers who, in addition to simulations, designed flowcharts prior to conducting laboratory experiments.

1. Is there a difference in the achievement scores of pre-service teachers in the control group depending on their pretest and posttest results after participating in simulation activities?
2. Is there a difference in the achievement scores of pre-service teachers in the experimental group depending on their pretest and posttest results after participating in simulation and flowchart preparation activities?
3. Is there a difference in the academic achievement of pre-service teachers based on whether they only performed simulations or performed simulations together with flowchart preparation?
4. What are the perceptions of pre-service teachers regarding the use of simulation activities prior to conducting physical laboratory experiments?

2. LITERATURE REVIEW:

Simulations can be used for various purposes in chemistry education, including pre-laboratory preparation, laboratory safety training, visualization of complex concepts, accessibility, and experimental design and analysis (Figure 1). Simulations can help students prepare for laboratory experiments. It allows students to visually follow the progress of the experiment, making it easier for them to understand the purposes of the experiment (Agustian & Seery, 2017; Navarro Arias-Calderón, Henríquez & Riquelme, 2024). Additionally, simulations provide students with practice in laboratory safety, offering knowledge about the use of hazardous chemicals and the correct use of laboratory equipment. Such experiences can significantly enhance overall safety within the laboratory environment (Kong *et al.*,2022). Simulations can be used to visualize abstract or complex chemistry concepts. For example, simulations can be used to illustrate the dynamics of molecular structures or describe the mechanisms of chemical reactions (Fombana-Pascual, Fombona, & Vicente, 2022; Magaña & Jong, 2018).

Furthermore, simulations may be useful for students with limited access to physical laboratory facilities. By engaging in simulated environments, these students can replicate the laboratory experience, thus bridging the gap caused by limited access to actual labs (Dunnagan & Gallardo-Williams, 2020). Moreover, simulations provide students with the opportunity to analyze the results of experiments and practice experimental design. Such experiences are instrumental in nurturing students' capacity for scientific reasoning and analytical thinking (Wörner, Kuhn & Scheiter, 2022).

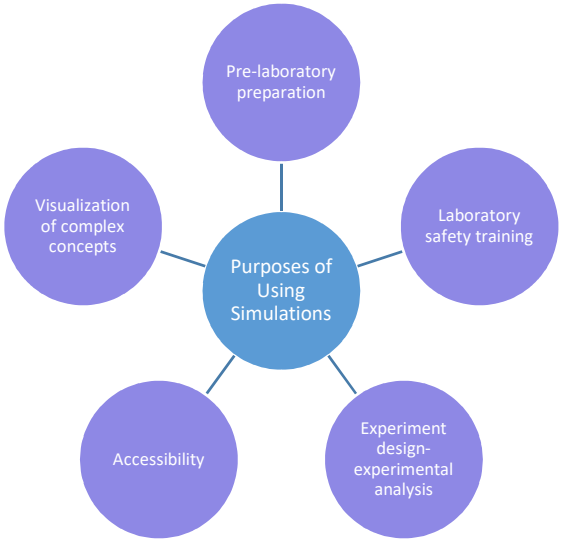

Figure 1. Purposes of using simulations in chemistry education

Despite engaging in laboratory experiments, pre-service chemistry teachers often fail to fully grasp fundamental chemistry concepts and complete their studies with inadequate knowledge of chemistry. There are studies in the literature that investigate the reasons for this lack of knowledge. One of the important reasons that stands out among these is the lack of theoretical context (Çalık & Ayas, 2005; Nakhleh, 1992; Finne, Gammelgaard & Christiansen, 2022). Suppose students fail to establish connections between theoretical knowledge and their execution of laboratory experiments. In that case, they risk obtaining inaccurate results and engaging in ineffective practices. Understanding the relationship between experimental results and theoretical concepts might pose a challenge for them (Finne, Gammelgaard & Christiansen, 2023; Talanquer & Pollard, 2010; Tümay, 2016). The combination of simulations and experiments in a

physical laboratory environment can provide students with a richer learning experience. This approach diversifies the learning process by offering students both concrete and virtual experiences. Additionally, it offers instructors increased flexibility in curriculum design and the choice of experiments tailored to meet the needs of students. Employing this integrated method can enhance students' ability to think scientifically and develop a more profound comprehension of chemistry subjects (Hofstein & Lunetta, 2004; Nakhleh, 1992).

3. MATERIALS AND METHODS:

3.1. Research Design and Participants

A static group pretest-posttest design was used in the research. The static group pretest-posttest design uses two naturally formed or pre-existing groups. Since these groups do not change, they are usually described as static groups, hence the name of the design (Fraenkel, Wallen & Hyun, 2012). This research design is characterized by a linear sequence (i.e., pretest-posttest design) that requires the dependent variable to be assessed before and after administration. In pretest-posttest research designs, the effect of the application is determined by comparing the difference between the initial assessment and the final assessment. Before starting the research, a pretest is administered to the participants. The practitioner then implements the teaching method whose effectiveness will be examined, followed by a posttest. Then, the change in pretest and posttest scores is examined (Mertler, 2022).

A purposeful sampling method was employed to select the research sample. Purposeful sampling is the process of selecting a sample by taking into account the prior knowledge of a group based on the purpose of the research to be conducted (Fraenkel *et al*., 2012). The biggest advantage of this method is that it provides the opportunity to easily reach the sample group (Yıldırım & Şimşek, 2013). The sample group of the study consists of 21 volunteer pre-service chemistry teachers taking the General Chemistry Laboratory course I at the Education Faculty of a state university in Türkiye. The research was carried out in the General Chemistry Laboratory course.

3.2. Data Collection Tools

Open-ended question form (Quiz and achievement exam): The research data were collected through quizzes administered before the physical laboratory experiments (hands-on experiments) and an achievement exam after the implementation was completed. The quiz and achievement exam are parallel exam versions containing similar questions. The grade point average of the two quizzes was evaluated as a pretest. The achievement exam was evaluated as a posttest. The questions asked in the quiz and achievement exam were taken as written answers, with two open-ended questions that included calculations, problem-solving, and explanations. In the first question, a question was asked about solutions, which is the first subject of the general chemistry laboratory. Here, the points to be considered during solution preparation and heating processes should be noted. In the second question, it is expected to prepare a solution from a solid substance, solve the problem, and identify the steps involved in preparing the solution. The pre-service teachers were given 25 minutes to answer the questions in the quizzes and achievement exam. Throughout the research process, a total of two quizzes were administered, each prior to an experiment, and an achievement exam was given as a posttest at the end of the study. Prior the main study, a pilot study was conducted to examine the clarity, validity, and reliability of the quizzes and achievement exam. Necessary revisions were made based on feedback from pre-service teachers, and expert opinions were also considered to ensure the suitability of the instruments.

Feedback form: To conduct an in-depth examination of pre-service teachers' perspectives on the simulation activity, researchers developed a semi-structured interview form consisting of seven open-ended questions. The form contained questions such as: "What are your opinions about the simulation activities? When performing experiments in the laboratory, to what extent and in what ways do the simulations influence your performance? What recommendations would you make to enhance the effectiveness of simulation activities conducted in conjunction with laboratory work?" For the form, the opinions of two experts, one from the Chemistry Education Department and the other from the Educational Sciences Department, were consulted. The pre-service teachers were given 45 minutes to complete the form. The feedback form was only applied once, after the research process was completed.

3.3. Research Procedure

During the research process, two simulations and two physical experiments on the subject of "Preparation of Solutions and Heating of

Solutions" were carried out by the pre-service teachers. Before implementation, they were divided into five groups, each consisting of 3-4 people. The research process consists of two consecutive steps. In the first step, the experiments were conducted online through a simulation application as out-of-class activities, and experiment flowcharts were prepared based on the simulations created by pre-service teachers. In the second step, all pre-service teachers conducted experiments using real materials and equipment in a physical laboratory environment. Simulation instructions and experiment sheets were e-mailed to all pre-service teachers before the physical laboratory experiments. The experiment sheet includes theoretical information and experiment materials, while the simulation instruction contains a link to the simulation's web page and questions for pre-service teachers to discuss and answer while performing the simulation. After completing the simulation, a quiz was administered to the pre-service teachers in the physical laboratory environment, and then each experiment was conducted. Four weeks after the simulations and experiments were completed, achievement exams and feedback forms were administered to the pre-service teachers. The achievement exam was administered as a posttest, and the feedback form was administered once after the entire research process was completed. The research process is summarized in Figure 2.

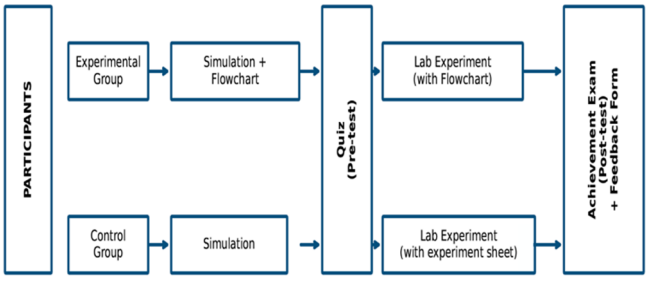

Figure 2. Implementation process of the research

For online simulations, a web 2.0 tool called Online Labs (OLabs) was used. OLabs is a web-based learning environment for science practical experiments, featuring simulations, animations, tutorials, and assessments. The groups performed the simulations online on the Microsoft Teams platform. The stages of performing the simulation were recorded by the pre-service teachers so that the researchers could follow the process. While the simulation was being carried out, pre-service teachers were asked to answer the questions in the simulation instruction and to complete the simulation after solving the questions that arose during the process by discussing them with their peers. Each pre-service teacher was required to create an individual experimental flowchart after completing the simulations. They were advised to utilize the simulation during the process of building the flowchart and to incorporate tips that would guide them during the experiment, based on their own investigation. During the implementation process, however, only 11 pre-service teachers actually prepared a flowchart in conjunction with the simulations. Consequently, these 11 pre-service teachers conducted the experiments in the laboratory using their own flowcharts. In contrast, the other 10 pre-service teachers conducted the experiments with the help of experiment sheets designed by the researchers, which contained the experimental procedures. Due to this circumstance, the study compared the levels of achievement of two different groups: participants who only experienced the simulation and the laboratory experiment, and those who, after the simulation, created a flowchart prior to performing the laboratory experiment.

3.4. Data Analysis

Analysis of quantitative data. Quantitative data obtained from the study were analyzed using SPSS version 23. The assumption of normality was examined using the Shapiro-Wilk test prior to analysis. Since the results indicated a violation of normality ($p < .05$), and based on the advice from the literature to use non-parametric tests when the sample size is below 30 (Fraenkel et al., 2012), non-parametric approaches were employed. To test the change in each group, the Wilcoxon Signed Rank test was used to make pretest-posttest comparisons of achievement scores. The Mann-Whitney U test was also used to determine if the posttest scores of the control group (simulation only) differed significantly from those of the experimental group (simulation and flowchart). This provided the basis for testing both within-group and between-group achievement differences.

Analysis of qualitative data. Qualitative data of the research were collected through a feedback form. The data obtained was analyzed by content analysis. Content analysis enables individuals to identify indicators of worldviews, values, attitudes, biases, and opinions, and compare them across communities (Bauer, 2000). Analysis of qualitative data obtained from interviews. It was carried out by following the steps of coding the data (1), creating themes (2), organizing the codes and themes (3), determining and interpreting the findings (4) (Yıldırım & Şimşek, 2013).

4. RESULTS AND DISCUSSION:

4.1. Results

4.1.1 Quantitative findings

In this study, while only the simulation activity was carried out in the control group, the experimental group also included an additional flowchart preparation activity alongside the simulation. The Wilcoxon Signed-Rank Test was used to examine the difference between the groups' pretest and posttest achievement scores. The findings are presented in Tables 1 and 2.

As shown in Table 1, there is a statistically significant difference between the pretest and posttest achievement scores of the pre-service teachers in the control group ($Z = -2.312$, $p = .021$). From this finding, it can be stated that laboratory experiments assisted by simulation enhance students' success through conceptual preparation prior to the experiment.

As shown in Table 2, there is a statistically significant difference between the pretest and posttest achievement scores of the pre-service teachers in the experimental group ($Z = -2.807$, $p = .005$). This finding indicates that, in addition to the simulation activity, the flowchart preparation activity provided an extra contribution to achievement.

The pretest–posttest analyses conducted for both groups showed that both the simulation activity and the simulation combined with the flowchart preparation activity increased the achievement of pre-service teachers. However, determining which approach was more effective required a comparison of the applications. Therefore, whether there was a significant difference between the two groups' posttest achievement scores was examined using the Mann-Whitney U test. Group A represents the control group, which only carried out the simulation activity. In contrast, Group B represents the experimental group, which carried out both the simulation and the preparation of the flowchart. The findings are presented in Table 3.

As shown in Table 3, there is a statistically significant difference between the experimental and control groups in terms of posttest achievement scores ($U = 15.000$, $Z = -2.822$, $p = .005$). It was determined that the achievement of the pre-service teachers who prepared a flowchart in addition to the simulation activity was higher. This situation reveals that chemistry laboratory experiments, supported by simulation and flowcharts, have a positive effect on academic achievement. On the one hand, they enhance academic achievement, and on the other hand, they provide a deeper understanding of the subject and direct students to preliminary preparation and study.

4.1.2 Qualitative findings

Content analysis was conducted in four steps: coding the data, identifying themes, organizing the data according to themes and codes, and interpreting the findings. The data obtained from the feedback form was collected under two themes. As seen in Table 4, these themes are cognitive contribution and affective contribution.

Table 4. *Themes and codes of qualitative analysis feedback form*

Themes	Code
Cognitive contribution	Transfer of knowledge Organization of prior knowledge
Affective contribution	Feel ready to experiment Confidence Anxiety

According to the analysis of the interviews, two themes emerged. These are cognitive contribution and affective contribution. Two codes describe the first theme, cognitive contribution. These codes are "transfer of knowledge" and "organization of prior knowledge". The expressions for the knowledge transfer code are as follows: "*I understood what kind of relationship there is between chemistry and technology [PST7], I have now realized that if I do not adjust the volume correctly while preparing the solution, there will not be a solution at the desired concentration [PST18]".* In the code of organizing preliminary learning, *"The simulations before the experiment helped me understand what the solution preparation was [PST14], I realized that I misunderstood the concentration and concentration units of the solution [PST20]"*.

The second theme from the feedback form analysis is affective contribution. The codes of the affective contribution themes are 'feel ready to experiment', 'confidence', and 'anxiety'. The expressions for feeling ready to experiment with code are as follows. *"Since I had never done any experiments in high school, simulation prepared me for experimenting in the laboratory [PST3], to experiment, there are first calculation, then material preparation, and then experiment steps [PST17]".* The statements in the confidence code are as follows: *"I ran the experiment multiple times in the simulation, which helped me prepare well for the lab [PST21], I wrote*

down the steps I followed in the simulation and created a flowchart for myself, using this in the lab prevented me from making mistakes [PST2]". In the code of anxiety, *"Just preparing for the experiment with the leaflet worried me, I'm glad I did a practice with the simulation beforehand [PST8], I feel like I can do all the experiments by preparing in advance with simulation, I no longer have any fear of the laboratory [PST19]"*.

4.2. Discussion

This study aimed to investigate the effects of simulations used prior to laboratory experiments and student-oriented flowcharts prepared by pre-service teachers on their academic achievement and overall learning experiences in general chemistry laboratory implementations. The results of the study indicate that simulation activities performed before the laboratory significantly enhanced the academic achievement of pre-service teachers. This suggests that simulations help pre-service teachers mentally prepare for experimental processes (Salame & Makki, 2021). Similarly, previous studies have shown that simulations support conceptual learning, reduce errors, increase self-confidence, and provide more active participation in the learning process (Rutten, van Joolingen & van der Veen, 2012; Tatlı & Ayas, 2013).

In this simulation-supported process, the pre-service teachers had the opportunity to see the experimental steps in advance and were involved in an active learning environment through in-group discussions, which allowed them to think critically about these steps. Especially in complex chemistry experiments involving abstract concepts, simulations are very useful in structuring the experiment in the mind before it begins (Orgill & Thomas, 2007; Rayan & Rayan, 2017). The combination of laboratory experiments and simulations can provide students with a richer learning experience. This approach diversifies the learning process by providing students with both concrete experiences and virtual experiences. The combined approach can help students develop scientific thinking skills and a deeper understanding of chemistry topics. These skills are often not sufficiently developed in students who only work with an experiment sheet (Hofstein & Lunetta, 2004). In this context, simulation-supported learning is thought to contribute to achievement, especially at the implementation level, as measured by open-ended questions.

Another prominent finding of the study is that pre-service teachers who prepared flowcharts about the experiment after the simulation showed higher success compared to those who did not prepare these diagrams. This shows that pre-service teachers' structuring the steps of the experiment in their own words deepened their cognitive processes and enabled them to act more consciously during the experiment. According to Domin (1999), flowcharts are a tool that enables students to interpret experiments more effectively than traditional experiment sheets. He emphasized that in experiments with traditional experiment sheets, students only focus on completing the task and try to fulfill the instructions. In addition, providing students with an experiment sheet that outlines the steps of the experiment does not guarantee that they have studied this guide before coming to the laboratory. However, it is advantageous for students to prepare their own flowcharts to make sense of the experimental steps, recognize the materials/chemicals to be used in the experiment, and interpret the results (Davidowitz et al., 2005). The flowcharts prepared were not only a listing of the experiment's steps, but also included the properties of the chemicals used, key considerations, and important reminders. This process supports the realization of permanent learning by improving students' ability to organize, associate, and apply knowledge. This finding can be explained by generative learning theory (Wittrock, 1989). According to this theory, learning becomes more permanent when students actively reconstruct knowledge. The process of preparing a flowchart enabled students to internalize the experimental steps and to critically evaluate the rationale behind each step. Studies in the literature also emphasize that student-centered tools, such as flowcharts, contribute to long-term learning and enable students to act more independently in the experimental process (Eilks & Byers, 2010).

Qualitative data analysis revealed that pre-service teachers thought that simulation-supported laboratory practices contributed to both cognitive and affective aspects. As cognitive contributions, pre-service teachers stated that the simulations helped them organize their prior knowledge, and they were able to remember and transfer what they learned in the laboratory more easily. These findings support constructivist learning approaches, which are based on active participation and the activation of prior knowledge (Ausubel, 1968; National Research Council, 2000). They stated that, thanks to the simulations, they were able to concentrate their attention better and comprehend the logic of the experiment more clearly because they had seen the processes they would encounter in the experiment beforehand. In terms of affective contribution, it was observed that simulations reduced pre-service teachers' anxiety before the experiment, increased their self-

confidence, and helped them feel more prepared for the experiment. These affective contributions are important in the context of science education because anxiety and low self-efficacy in the laboratory environment can negatively affect students' achievement (Bandura, 1997; Mallow, 2006). Especially in fields such as chemistry, where experimental implementations are intensive, the psychological preparation of pre-service teachers is a determining factor in success (Hofstein & Lunetta, 2004). The pre-service teachers came to the laboratory feeling ready to perform the experiment, confident in their ability to do so thanks to the simulations they had completed before the experiment. These results align with the literature, which shows that student-centered and virtual learning environment-based pre-laboratory practices positively impact not only achievement but also students' affective characteristics (Makransky, Thisgaard, & Gadegaard, 2016; Scheckler, 2003).

5. CONCLUSIONS:

In conclusion, this study demonstrates that a blended laboratory teaching model incorporating simulations alongside student-prepared flowcharts can have a positive impact on pre-service teachers' academic achievement, as well as their perspectives and readiness for the laboratory experience. Qualitative data obtained from pre-service teachers' opinions revealed that simulations contributed to the process not only at the knowledge level but also emotionally. These findings suggest that enriching laboratory practices with digital tools and student-centered activities can contribute to the learning process in multiple ways. Today, when educational technologies are increasingly integrated into learning environments, simulations can be considered as a powerful tool to ensure the active participation of pre-service teachers in experimental processes. Especially in environments where laboratory resources are limited or pre-service teachers' experimental self-confidence is low, it is recommended that such technological supports be systematically incorporated into the teaching process. Future studies may compare similar practices across disciplines or topics and evaluate their long-term effects on learning retention and transfer.

6. DECLARATIONS

6.1. Study Limitations

1. Since the participants were pre-service teachers enrolled in the General Chemistry Laboratory course, the sample was restricted to the number of students taking this course. Consequently, the relatively small sample size limits the statistical power of the study and reduces the generalizability of the findings to broader populations.
2. The study was initially designed as a single group pretest–posttest experimental design. However, although 10 pre-service teachers initially agreed to construct a flowchart and confirmed their participation through the consent form, they later decided not to construct the flowchart during the implementation process. As a result, the design shifted into a static-group pretest–posttest experimental design.
3. The comparatively low number of participants in both experimental and control groups is a limitation in the research and presents challenges in generalizing the results to larger populations.
4. External variables that may influence pre-service teachers' academic achievement were not included in this study.

6.2. Acknowledgements

We would like to thank all the participants who volunteered to contribute to the research process.

6.3. Funding source

The authors funded this research. In accordance with the ethical guidelines of the Periódico Tchê Química, which do not allow donations from authors with manuscripts under evaluation (even when research funds are available), or in cases of authors' financial constraints, publication costs were fully absorbed by the journal under our Platinum Open Access policy, through the support of the Araucária Scientific Association (https://acaria.org/). This policy aims to ensure complete independence between the editorial process and any financial aspects, reinforcing our commitment to scientific integrity and equity in knowledge dissemination.

6.4. Competing Interests

The authors declare no potential conflict of interest in this publication.

7. HUMAN AND ANIMAL-RELATED STUDIES

7.1. Ethical Approval

Ethical approval for this study was granted by the Research Ethics Committee of the Institute of Educational Sciences at Hacettepe University, Türkiye, on 08.08.2025 (Approval No: E-51944218-050-00004400126)

7.2. Informed Consent

The pre-service teachers who participated in the study filled out the consent form. We would like to thank the pre-service teachers who participated in this research on a voluntary basis.

8. REFERENCES:

1. Abbott, M. L. (2011). *Understanding educational statistics using Microsoft Excel and SPSS.* United States: John Wiley & Sons, Inc.

2. Ausubel, D.P. (1968). *Educational psychology: a cognitive view.* Holt, Rinehart and Winston: New York.

3. Ayas, A., Çepni, S., & Akdeniz, A. R. (1994). Fen bilimleri eğitiminde laboratuvarın yeri ve önemi-II. *Çağdaş Eğitim Dergisi, 205*, 7-12.

4. Aydoğdu, C., & Erbaş, S. (1992). Kimya eğitimindeki laboratuvar uygulamalarında öğrenilen bilgilerin kalıcılık durumunun saptanması. *Hacettepe Üniversitesi Eğitim Fakültesi Dergisi, 7*(7), 279-286.

5. Bandura, A. (1997). *Self-efficacy: The exercise of control.* W H Freeman/Times Books/ Henry Holt & Co.

6. Bauer, M.W. (2000). Classical content analysis: A review. In Atkinson, P., Bauer, M. W., & Gaskell, G. (Eds.). *Qualitative Researching with Text, Image and Sound*. London: Sage.

7. Çalık, M., & Ayas, A. (2005). A comparison of level of understanding of eighth-grade students and science student teachers related to selected chemistry concepts. *Journal of Research in Science Teaching, 42*(6),638–667. https://doi.org/10.1002/tea.20076

8. Dalgarno, B. (2001). Interpretations of constructivism and consequences for computer assisted learning. *British Journal of Educational Technology, 32*(2), 183-194. https://doi.org/10.1111/1467-8535.00189

9. Davidowitz, B., & Rollnick, M. (2001). Effectiveness of flow diagrams as a strategy for learning in laboratories. *Australian Journal of Education in Chemistry, 57*, 18–24.

10. Davidowitz, B., Rollnick, M., & Fakudze, C. (2005) Development and application of a rubric for analysis of novice students' laboratory flow diagrams. *International Journal of Science Education, 27*(1), 43-59. https://doi.org/10.1080/0950069042000243754

11. Domin, D.S. (1999). A content analysis of general chemistry laboratory manuals for evidence of higher-order cognitive tasks. *Journal of Chemical Education, 76*(1), 109–111. https://doi.org/10.1021/ed076p109

12. Dunnagan, C. L., & Gallardo-Williams, M. T. (2020). Overcoming physical separation during covıd-19 using virtual reality in organic chemistry laboratories. *Journal of Chemical Education*, *97* (9), 3060-3063. https://doi.org/10.1021/acs.jchemed.0c00548

13. Eilks, I., & Byers, B. (2010). The need for innovative methods of teaching and learning chemistry in higher education – reflections from a project of the European Chemistry Thematic Network. *Chemistry*

Education Research and Practice, 11(4), 233–240. https://doi.org/10.1039/C0RP90004D

14. Ergun, M. (2017). Kimya öğretiminde teknolojik pedagojik alan bilgisi uygulamaları. In Ayas, A. & Sözbilir, M. (Eds.). *Kimya öğretimi: Öğretmen eğitimcileri, öğretmenler ve öğretmen adayları için iyi uygulama örnekleri* (615-631). Ankara: Pegem Akademi.

15. Finne, L. T., Gammelgaard, B., & Christiansen, F. V. (2022). When the lab work disappears: Students' perception of laboratory teaching for quality learning. *Journal of Chemical Education, 99*(4), 1766–1774. https://doi.org/10.1021/acs.jchemed.1c01113

16. Finne, L. T., Gammelgaard, B., & Christiansen, F. V. (2023). Pharmacy students' conceptions of theory–practice relation in the analytical chemistry laboratory: A phenomenographic study. *Chemistry Education Research and Practice, 24*, 428-436. https://doi.org/10.1039/D2RP00092J

17. Fombona-Pascual, A., Fombona, J., & Vicente, R. (2022). Augmented reality, a review of a way to represent and manipulate 3D chemical structures. *Journal of Chemical Information and Modeling*, *62*(8), 1863-1872. https://doi.org/10.1021/acs.jcim.1c01255

18. Fraenkel, J. R., Wallen, N. E., & Hyun, H. H. (2012). *How to design and evaluate research in education* (8th ed.). New York: Mc Graw HIll.

19. Hakerem, G., Dobrynina, G., & Shore, L. (1993). The effect of interactive, three dimensional, high speed simulations on high school science students' conceptions of the molecular structure of water. *Annual Meeting of the National Association for Research in Science Teaching*. Atlanta, GA, April 15-19.

20. Hawkins, I., & Phelps, A. J. (2013). Virtual laboratory *vs.* traditional laboratory: which is more effective for teaching electrochemistry*? Chemistry Education Research and Practice, 14*(4), 516-523. https://doi.org/10.1039/C3RP00070B

21. Hirst, J. D., Glowacki, D. R., & Baaden, M. (2014). Molecular simulations and visualization: introduction and overview. *Faraday Discussions, 169*, 9-22. https://doi.org/10.1039/C4FD90024C

22. Hofstein, A., & Lunetta, V. N. (2004). The laboratory in science education: Foundations for the twenty-first century. *Science Education, 88*(1), 28-54. https://doi.org/10.1002/sce.10106

23. Kirk, R. E. (2008). *Statistics an introduction* (Fifth edition). United States: Thomson Higher Education.

24. Kong, C. I., Welfare, J. G., Shenouda, H., Sanchez-Felix, O. R., Floyd Jr., J. B., Hubal, R. C., Heneghan, J. S., & Lawrence, D. S. (2022). Virtually bridging the safety gap between the lecture hall and the research laboratory**.** *Journal of Chemical Education 99*(5), 1982-1989**.** https://doi.org/10.1021/acs.jchemed.2c00096

25. Lee, W. C., Neo, W. L., Chen, D. T., & Lin, T. B. (2021). Fostering changes in teacher attitudes toward the use of computer simulations: Flexibility, pedagogy, usability and needs. *Education and Information Technologies, 26*, 4905-4923. https://doi.org/10.1007/s10639-021-10506-2

26. Magana, A. J., & de Jong, T. (2018). Modeling and simulation practices in engineering education. *Computer Applications in Engineering Education,26*(4), 731-738. https://doi.org/10.1002/cae.21980

27. Makransky, G., Thisgaard, M. W., & Gadegaard, H. (2016). Virtual simulations as preparation for lab exercises: Assessing learning of key laboratory skills in microbiology Improvement of Essential Non-Cognitive Skills. PLOS ONE 11(6), e0155895. https://doi.org/10.1371/journal.pone.0155895

28. Mallow, J.V. (2006) Science anxiety: Research and action. In Mintzes, J. J., & Leonard, W. H. (Eds.). *Handbook of College Science Teaching.* National

Science Teachers Association, Arlington.

29. Mertler, Craig A. (2022).*Introduction to educational research* (Third edition). Chapter 7 quantitative research methods. Los Angeles: SAGE Publications.

30. Nakhleh, M. B. (1992). Why some students don't learn chemistry: Chemical misconceptions. *Journal of Chemical Education, 69*(3), 191-196. https://doi.org/10.1021/ed069p191

31. Nakiboğlu, C., Erdurmazlı, İ., Kızmaz, B., & Hepöz, Ş. (2018). Investigation of prospective chemistry teachers' views about flow diagram usage in organic chemistry laboratory I course. *Journal of the Turkish Chemical Society Section C: Chemistry Education, 3*(1), 31-58.

32. National Research Council 2000. How people learn: Brain, mind, experience, and school: Expanded edition. Washington, DC: The National Academies Press. https://doi.org/10.17226/9853.

33. Orgill, M., & Thomas, M. M. (2007). Analogies and the 5E model. *The Science Teacher*, *74*(1), 40–45.

34. Pekdağ, B. (2009, Ekim 10). Kimya öğreniminde alternatif yollar: Animasyon, simülasyon, video ve multimedya ile öğrenme. *Journal of Turkish Science education, 7*(2), 79-110.

35. Rayan, B., & Rayan, A. (2017). Avogadro program for chemistry education: To what extent can molecular visualization and three-dimensional simulations enhance meaningful chemistry learning? *World Journal of Chemical Education, 5*(4), 136–141. DOI: 10.12691/wjce-5-4-4

36. Russell, C. B., & Weaver, G. C. (2011). A comparative study of traditional, inquiry-based, and research-based laboratory curricula: Impacts on understanding of the nature of science. *Chemistry Education Research and Practice, 12*(1), 57-67. https://doi.org/10.1039/C1RP90008K

37. Rutten, N., van Joolingen, W. R., & van der Veen, J. T. (2012). The learning effects of computer simulations in science education. *Computers & Education*, 58(1), 136–153. https://doi.org/10.1016/j.compedu.2011.07.017

38. Salame, I. I., & Makki, J. (2021). Examining the use of PhET simulations on students' attitudes and learning in general chemistry II. *Interdisciplinary Journal of Environmental and Science Education, 17*(4), e2247. https://doi.org/10.21601/ijese/10966

39. Scheckler, R. K. (2003). Virtual labs: A substitute for traditional labs? *International Journal of Developmental Biology*, *47*(2-3), 231–236.

40. Talanquer, V., & Pollard, J. (2010). Let's teach how we think instead of what we know. *Chemistry Education Research and Practice, 11*(2), 74-83. https://doi.org/10.1039/C005349J

41. Tatli, Z., & Ayas, A. (2013). Effect of a Virtual Chemistry Laboratory on Students' Achievement. *Educational Technology & Society*, *16*(1), 159–170.

42. Tümay, H. (2016). Reconsidering learning difficulties and misconceptions in chemistry: Emergence in chemistry and its implications for chemical education. *Chemistry Education Research and Practice, 17(2)*, 229–245. https://doi.org/10.1039/C6RP00008H

43. Wittrock, M. C. (1989). Generative processes of comprehension. *Educational Psychologist, 24*(4), 345–376. https://doi.org/10.1207/s15326985ep2404_2

44. Wörner, S., Kuhn, J., & Scheiter, K. (2022). The best of two worlds: A systematic review on combining real and virtual experiments in science education. *Review of Educational Research*, *92*(6), 911-952. https://doi.org/10.3102/00346543221079417

45. Yao, J. (2023). Exploring experiential learning: Enhancing secondary school chemistry education through practical engagement and innovation. *Journal of Education, Humanities and Social Sciences*, *22*, 475-484. https://doi.org/10.54097/ehss.v22i.12

46. Yazıcı, S. Ç. (2023). Kimya eğitimine teknolojinin entegrasyonu. In Akpınar, A. (Ed.). *Matematik ve fen bilimleri üzerine araştırmalar* (41-49). Özgür Yayınları.

47. Yıldırım, A., & Şimşek, H. (2013). *Qualitative research methods in the social sciences*. (9th Ed.). Ankara, Seçkin Press, pp. 110-122.

Table 1. *Wilcoxon signed-rank test results achievement pretest-posttest scores for control group*

Observed variables		Mean rank	Sum of ranks	Z	p
Achievement exam	Negative ranks	3.00	3.00	-2.312	.021*
	Positive ranks	5.25	42.00		

*p<0.05
a. Based on negative ranks.

Table 2. *Wilcoxon signed-rank test results achievement pretest-posttest scores for experimental group*

Observed variables		Mean rank	Sum of ranks	Z	p
Achievement exam	Negative ranks	.00	.00	-2.807	.005*
	Positive ranks	5.50	55.00		

*p<0.05
a. Based on negative ranks.

Table 3. *Mann Whitney test results achievement posttest scores*

Group	N	Mean rank	Sum of ranks	U	Z	p
Group A	10	7.00	70.00	15.000	-2.822	.005*
Group B	11	14.64	161.00			

*p<0.05

PERIÓDICO TCHÊ QUÍMICA
ARTIGO ORIGINAL

INVESTIGAÇÃO LITOLÓGICA-PETROGRÁFICA-PETROLÓGICA DE AFLORAMENTOS ROCHOSOS AO LONGO DE UM CINTURÃO DE XISTO IDENTIFICADO, CAMPUS GIDAN KWANO, MINNA, NIGÉRIA

LITHOLOGIC-PETROGRAPHIC-PETROLOGIC INVESTIGATION OF ROCK OUTCROPS ALONG A DISCERNED SCHIST BELT, GIDAN KWANO CAMPUS, MINNA, NIGERIA

JONAH, Sunday Adole[1*]; ONYEBUCHI, Chiamaka Esther[2]; OFFORJAMA, Matthew Chibueze[3]; OLANIPEKUN, Charles Olamide[4]; BAIYE, Emmanuel Onimisi[5]; ADEBAYO, Tosin Oludare[6]; ODEMENE, Chinonso Emmanuel[7]; ALFA, Idris Alhaji[8]; SAIDU, Salihu[9]

[1,2,3,4,5,6,7,8] Federal University of Technology, School of Physical Science, Department of Physics, Minna, Nigeria
[9]Federal University of Technology, School of Physical Science, Department of Geography, Minna, Nigeria.

*Corresponding author: s.jonah@futminna.edu.ng

* ORCID: 0009-0002-2017-2611

Received 09 June 2025; received in revised form 25 September 2025; accepted 24 October 2025

RESUMO

Introdução: A conclusão obtida a partir do estudo macroscópico e litológico independente de um trabalho anterior foi significativa ao correlacionar um vestígio do Cinturão de Xisto Kazaure–Karaukarau–Kushaka–Ilesha através das porções meridionais do Campus de Gidan Kwano. A ausência de uma análise microscópica-petrográfica correspondente nesse estudo anterior cria uma lacuna de conhecimento petrográfico. **Objetivos**: Replicar e completar as análises macroscópicas e microscópicas dos afloramentos ao longo do vestígio do Cinturão de Xisto Kazaure–Karaukarau–Kushaka–Ilesha, bem como realizar uma investigação petrológica da porcentagem de ocorrência de massa rochosa xistosa ao norte desse cinturão de xisto identificado. **Métodos**: O estudo macroscópico-litológico procedeu classificando os afloramentos observados nas 11 localizações coincidentes de prospecção de águas subterrâneas/afloramentos determinadas do estudo anterior por seus atributos físicos. A investigação microscópica-petrográfica procedeu submetendo amostras de rocha coletadas da fase de levantamento macroscópico-litológico simultâneo a análises de seção delgada. Para a investigação da fase macroscópica-petrológica, cerca de 50 diferentes localizações de afloramentos ao norte do cinturão de xisto identificado foram visitadas e classificadas com base em suas características observáveis. **Resultado**: A fase de investigação litológica deste estudo mostra mais amostras de afloramentos rochosos identificadas como "granito" do que aquelas que são indubitavelmente xisto baseado em características texturais e superficiais observáveis. A fase de investigação petrográfica dessas amostras de afloramentos rochosos mostra mais rochas de xisto sob análises de seção delgada do que o "granito". A fase de investigação petrológica revela nenhuma presença de afloramentos de xisto em absoluto na área ao norte do cinturão de xisto identificado. **Discussão**: Assim, um argumento mais forte foi posteriormente apresentado de que a diagonal de massa rochosa identificada do estudo macroscópico-litológico independente anterior é na verdade o Cinturão de Xisto Kazaure-Karaukarau-Kushaka-Ilesha. **Conclusão**: É recomendado que a Universidade Federal de Tecnologia, Minna, concentre esforços nesta diagonal de massa rochosa e suas extensões nordeste-sudoeste através das propriedades da Universidade para explorar recursos de águas subterrâneas e minerais de ouro, sendo o xisto a rocha hospedeira ideal de depósitos sustentáveis de águas subterrâneas e ouro na província geológica do complexo de embasamento nigeriano.

Palavras-chave: *Macroscópico-litológico, Microscópico-petrográfico, Granito, Xistoso, Lâmina fina.*

ABSTRACT

Background: The conclusion drawn from the standalone macroscopic-lithologic study of a previous work was significant in correlating a vestige of the Kazaure-Karaukarau-Kushaka-Ilesha Schist Belt through the southern reaches of the Gidan Kwano Campus. The absence of a corresponding microscopic-petrographic analysis for that previous study creates a petrographic knowledge gap. **Aims:** To replicate and complete macroscopic and microscopic analyses of outcrops along the vestige of the Kazaure-Karaukarau-Kushaka-Ilesha Schist Belt, as

DOI: 10.52571/PTQ.v22.n51.2025_05_SUNDAY_pgs_66_78.pdf

well as to conduct a petrologic investigation of the percentage occurrence of schist rock-mass north of this discerned schist belt. **Methods:** The macroscopic-lithologic study proceeded by classifying observed outcrops at the 11 coincident groundwater-prospect/outcrop locations determined from that previous study by their physical attributes. The microscopic-petrographic investigation proceeded by subjecting rock samples collected during the concurrent macroscopic-lithologic survey phase to thin-section analyses. For the macroscopic-petrologic phase investigation, outcrop locations to the north of the Belt were classified on the basis of their observable characteristics. **Result:** The lithologic-investigation phase of this study reveals a higher number of outcrop rock samples identified as "granite" compared to schist based on textural and observable surface characteristics. The petrographic investigation of these outcrop rock samples reveals a higher occurrence of schist than of granite. The petrologic investigation phase reveals no presence of schist outcrops in the area north of the discerned Belt. **Discussion:** Thus, a stronger argument has been further presented that the discerned rock-mass diagonal of the previous standalone macroscopic-lithologic study is actually the Kazaure-Karaukarau-Kushaka-Ilesha Schist Belt. **Conclusion:** It is recommended that the Federal University of Technology, Minna, concentrate efforts on this rock-mass diagonal named "Jonahite" and its northeast-southwest extensions through the University's landholding in order to explore for groundwater and gold-mineral resources, schist being the ideal repository host-rock of sustainable groundwater and gold deposits in the Nigerian basement complex geological province.

Keywords: *Macroscopic-lithologic; microscopic-petrographic; granite; schistose; thin-section.*

1. INTRODUCTION

The conclusion drawn from the standalone macroscopic-lithologic study of Adebayo (2019), wherein this macroscopic tool was used as a geological control for hydro-centric conclusions reached therein over an areal spread of a half-scale 8 km^2 vertical electrical sounding (VES) study at the southern Phase II Development (4 km^2 areal extent), Gidan Kwano Campus. The Karaukarau-Kushaka-Ilesha Schist Belt traverses the southern reaches of the Gidan Kwano Campus of the Federal University of Technology, Minna.

Adebayo (2019) argued with certainty that their hydro-centric study along a serendipitously-determined and hitherto uncorrelated northeast-southwest (NE-SW) fault-trace diagonal from a previous study (Jonah and Olasehinde, 2017) was along a tiny segment of the Kazaure-Karaukarau-Kushaka-Ilesha Schist Belt on account of its trend (the NE-SW orientation), its geographic attribute (occurrence mapped west of 8^0 longitude), and its positional locator because the NE-SW line drawn from the Kazaure schist body through to the Ilesha schist body actually cuts through the southern reaches of the Gidan Kwano Campus Phase II Development where these fault-traces have been mapped (Jonah and Olasehinde, 2017; de Almeida, et al.,2021).

In order to further validate that the Adebayo (2019) study was actually along the route of an ancient schist belt, this present study was dedicated to improving on the study-layout of Adebayo (2019) whence, in addition to validating the macroscopic-lithologic observations of Adebayo (2019) relating to the litho-nature of rock outcrops occurring at coincident locations of groundwater-prospects deciphered from Jonah and Olasehinde (2017), detailed microscopic-petrographic analyses are made of samples of these outcrops with the purpose of identifying localised schist-outcrop bodies and also identifying evidence of ongoing metamorphism processes within other rock-mass types that were identified along the extent of the once-existent Kazaure-Karaukarau-Kushaka-Ilesha Schist Belt.

Furthermore, it becomes imperative, therefore to inquire about the percentage schist rock-mass occurrence north of this discerned Kazaure-Karaukarau-Kushaka-Ilesha Schist Belt diagonal through the Gidan Kwano Campus Phase II Development, because if this present study was constrained along this schist belt then schist-mass occurrence outside the diagonal width [*circa* 800 m as discerned from Adebayo (2019)] should be far and few between or even non-existent as one trends northward of this diagonal; this expected outcome is guided by information about the local geology of the Gidan Kwano Campus (Adesoye, 1986).

By this means, then, if a geologically-valid claim can be made that the vestige of the Kazaure-Karaukarau-Kushaka-Ilesha Schist Belt is the area of interest of Adebayo (2019) and by extension this present study, it follows therefore that the search for viable and exploitable groundwater sources at the Gidan Kwano Campus plus the search for gold-mineral deposits would have been narrowed to a greater degree of accuracy along this vestige of the Kazaure-Karaukarau-Kushaka-Ilesha Schist Belt through the Gidan Kwano Campus because it is understood from Obaje (2009) that the quartet of the schist belts of Nigeria are the ones associated with gold mineralisation. Our knowledge of the local geology indicates that, empirically, localised schist rock-mass

occurrences are associated with viable groundwater-prospecting locations.

Okiongbo and Odubo (2012) investigated aquifer transmissivity in parts of Bayelsa State, south Nigeria, whence nineteen vertical electrical sounding (VES) stations were occupied using a maximum current electrode separation ranging from 300 to 400 m with the aim of estimating the transmissivity of the alluvial aquifer in areas where no pumping test has been carried out; the authors reported that four of the soundings were carried out near existing boreholes in which pumping test had been carried out.

The VES data obtained was interpreted, and layer parameters, such as true resistivities and thicknesses, were determined; the geoelectric parameters were used to generate the Dar Zarrouk parameters, and correlating a Dar Zarrouk parameter (e.g. longitudinal unit conductance) with transmissivity derived from pumping test data, a constant was found which translate longitudinal unit conductance to transmissivity in a hydrogeological setting where effective porosity is the primary control on resistivity and hydraulic conductivity.

The authors reported that transmissivity determined from the pumping test data ranged between 1634.0 and 5292.0 m^2/day, while transmissivity values estimated from the longitudinal unit conductance (Lc) ranged between 721 and 8991 m^2/day.

The conclusion drawn from this survey was that the transmissivity estimated from the pumping test (*Tp*) data and the transmissivity estimated from the longitudinal conductance (*Lc*) on comparison show excellent correlation (R_2 = 0.92). Finally, the authors noted that the high transmissivity values agree with the geology of the Benin Formation (Coastal Plain sands), which consists of fine-medium-coarse sands, and that the results provide a useful first approximation of transmissivity and could be used to site exploratory boreholes.

Jatau *et al.* (2013) conducted a study using vertical electrical sounding (VES) to investigate the subsurface geology around Bomo Area, Kaduna State, aiming to determine the depth to bedrock and the thickness of geologic layers. The authors noted that the VES survey was conducted at 15 stations using an ABEM Terrameter SAS 3000. The authors reported that the field data were analysed using the IPI2win software, which provides an automatic interpretation of the apparent resistivity. They pointed out that the VES results revealed the heterogeneous nature of the subsurface geological sequence. They concluded that the geologic sequence beneath the study area was composed of hard pan top soil (clayey and sandy-lateritic), weathered layer, partly weathered or fractured basement, and fresh basement; further, it is observed from their report that the resistivity value for the topsoil layer varies from 40 Ωm to 450 Ωm with thickness ranging from 1.25 to 7.5 m. The weathered basement has resistivity values ranging from 50 Ωm to 593 Ωm and a thickness of 1.37-20.1 m. The fractured basement has resistivity values ranging from 218 Ωm to 520 Ωm and a thickness of 12.9 -26.3 m. The fresh basement (bedrock) has resistivity values ranging from 1215 Ωm to 2150 Ωm with infinite depth. The authors observed that the depth from the earth's surface to the bedrock surface varies between 2.63 and 34.99 m. The authors concluded that this study was vital for in civil engineering structures and groundwater prospecting.

According to Adesoye (1986), the Gidan Kwano Campus covers an area of about 100 km^2, equivalent to 10,000 hectares (Ha). The Gidan Kwano Campus is well-defined into three sectors: the northern, middle, and southern sectors. The northern arm of the site is about 5 km across, and the middle portion is about 6 km across. Running from the north to the south along the central axis, the northern strip is about 7.5 km long, the middle strip is about 7.5 km long, and the southern strip is only about 5.5 km long. These three pieces combine to form a double elbow-like strip of about 20 km long. The middle portion is actually the part of the Gidan Kwano Campus that lies along the Minna-Bida Road for 12 km, and this is the only part of the Gidan Kwano Campus in contact with a main road. The Minna-Tegina Road passes quite close to the Gidan Kwano Campus by a railway level-crossing. The estimated total area is about 42.03 Ha, with natural constraints. Out of this, about 35 Ha or 83% is rock outcrops. Water bodies (such as River Dagga, River Weminafia, and others) and ponds (such as Lake Dan Zaria) occupy about 1.74 Ha, or 4%. Swamps occupy about 0.38 Ha, or 1%, while steep slopes and cliffs, such as Garatu Hill, occupy the remaining 4.91 Ha, or 12%.

Adesoye (1986) also stated that the Gidan Kwano Campus constitutes a tiny southern tip of the Nigerian Basement Complex (NBC) occurring in north-central Nigeria. According to Obaje (2009), the basement complex is one of the three major litho-petrological components that make up Nigeria's geology. The NBC forms a part of the Pan-African mobile belt and lies between the West African and Congo Cratons and south of the

Tuareg Shield (Black, 1980). It is intruded by the Mesozoic calc-alkaline ring complexes (Younger Granites) of the Jos Plateau and is unconformably overlain by Cretaceous and younger sediments.

The Nigerian basement was affected by the 600 Ma Pan-African orogeny and lies within the reactivated region that resulted from plate collision between the passive continental margin of the West African craton and the active Pharusian continental margin (Burke and Dewey, 1972; Dada, 2006). The basement rocks are believed to result from at least four primary orogenic cycles of deformation, metamorphism, and remobilization, corresponding to the Liberian (2,700 Ma), the Eburnean (2,000 Ma), the Kibaran (1,100 Ma), and the Pan-African cycles (600 Ma). The first three cycles were characterized by intense deformation and isoclinal folding, accompanied by regional metamorphism, followed by extensive migmatization.

The Pan-African deformation was accompanied by regional metamorphism, migmatization, and extensive granitization and gneissification, which produced syntectonic granites and homogeneous gneisses (Abaa, 1983). Late tectonic emplacement of granites and granodiorites, along with associated contact metamorphism, accompanied the end stages of this last deformation. The end of the orogeny was marked by faulting and fracturing (Gandu *et al.*, 1986; Olayinka, 1992).

Wright (1985) mapped three units within the NBC: the Migmatite–Gneiss Complex (MGC), the Schist Belt (Metasedimentary and Metavolcanic rocks), and the Older Granites (Pan-African granitoids). In addition to these three units, Obaje (2009) identified a fourth one, namely Undeformed Acid and Basic Dykes.

The MGC is generally considered the basement complex *sensu stricto* (Rahaman, 1988; Dada, 2006), and it is the most widespread of the basement complex's component units in Nigeria. It has a heterogeneous assemblage comprising migmatites, orthogneisses, paragneisses, and a series of metamorphosed basic and ultrabasic rocks. Petrographic evidence indicates that the Pan-African reworking led to the recrystallization of many of the constituent minerals of the Migmatite-Gneiss Complex through partial melting, with the majority of rock types displaying medium to upper amphibolite facies metamorphism.

The Migmatite-Gneiss Complex spans the Pan-African to Eburnean age range. The Migmatitie-Gneiss Complex, also referred to by some workers as the “migmatite-gneiss-quartzite complex,” covers about 60% of the surface area of the Nigerian basement (Rahaman and Ocan, 1978).

The Schist Belts comprise low-grade, metasediment-dominated belts trending N–S, which are best developed in the western half of Nigeria. These belts are considered to be Upper Proterozoic supracrustal rocks which have been infolded into the migmatite-gneiss-quartzite complex. The lithological variations of the schist belts include coarse to fine-grained clastics, pelitic schists, phyllites, banded iron formation, carbonate rocks (marbles/dolomitic marbles), and mafic metavolcanics (amphibolites). Some may include fragments of ocean floor material from small back-arc basins.

Rahaman (1976) and Grant (1978), for example, suggest that several basins of deposition existed, whereas Oyawoye (1972) and McCurry (1976) consider the schist belts as relics of a single supracrustal cover. Olade and Elueze (1979) consider the schist belts to be fault-controlled rift-like structures. Grant (1978), Holt (1982), and Turner (1983), based on structural and lithological associations, suggest that sediments have different ages. However, Ajibade *et al.* (1979) disagree with this conclusion and show that both series contained identical deformational histories.

The structural relationships between the schist belts and the basement were considered by Truswell and Cope (1963) to be conformable metamorphic fronts, and it was Ajibade *et al.* (1979) who first mapped a structural break.

The term “Older Granite” was introduced by Falconer (1911) to distinguish the deep-seated, often concordant or semi-concordant granites of the Basement Complex from the high-level, highly discordant tin-bearing granites of Northern Nigeria. The Older Granites are believed to be pre-, syn-, and post-tectonic rocks which cut both the migmatite-gneiss-quartzite complex and the schist belts. They range widely in age (750–450 Ma) and composition.

They represent a varied and long-lasting (750–450 Ma) magmatic cycle associated with the Pan-African orogeny. The rocks of this suite range in composition from tonalites and diorites through granodiorites to true granites and syenites. Charnockites form an important rock group emplaced during this period. They are generally high-level intrusions and anataxis has played an important role (Rahaman, 1981).

The Older Granites suite is notable for its

general lack of associated mineralization, although the thermal effects may play a role in the remobilization of mineralizing fluids. The Older Granites are the most obvious manifestation of the Pan-African orogeny and represent significant additions of materials (up to 70% in some places) to the crust (Rahaman, 1988).

Jonah *et al.* (2015[a]) examined a dual topographic-petrographic control for a 1 km^2 VES-induced polarisation (IP) study completed at the Gidan Kwano Campus Phase II Development, Federal University of Technology, Minna, Nigeria. This 1 km^2 VES-IP study is Jonah *et al.* (2015[b]). The authors noted that, to the best of their knowledge, it was not the norm in studies of the local basement complex geology of the Minna Area to constrain the accuracy of VES dataset interpretations with the corresponding topographic and petrographic maps of the specific study area. Such an approach would serve as a veritable tool of quality control (QC) of the interpretation of the acquired VES dataset.

The study aims to implement a valid quality control scheme for an earlier dual VES-IP study. The topographic survey proceeded along transverse traverses in a west-east, east-west zig-zag format until transverse traverse (TT) 51 was completed. The petrographic survey phase of this study focused on examining the aspects of the different outcrops observed in the study area, including their strike, dip, and other structural orientations.. Over the 1 km^2 area of study of interest here, it was observed that terrain or ground elevation progressively increases from south to north. An important observation, too, was that elevation rises from west to east. The petrographic map indicates that the area of study is underlain by a continuous body of granite intruded by a small body of schist. Examination of the landform map of the area of study positively correlates with the conclusions on aquifer prospects drawn from the earlier survey, and it was strongly recommended to drill these locations for groundwater exploitation.

Aizebeokhai et al. (2021), observed that it is usually not the norm, so far as studies carried out in the local basement complex geology of the Minna Area are concerned, to constrain the accuracy of the interpretation of the VES dataset with a correspondingly produced purpose-specific topographic and petrographic maps of the key area of study. Such an approach would serve as a veritable QC tool for the interpretation of the acquired VES dataset.

Their study aimed to implement a valid quality control scheme for an earlier single-mode VES study. The authors noted that the topographic survey proceeded along transverse traverses in a west-east, east-west zig-zag format until transverse traverse (TT) 101 was completed.

The petrographic survey phase of this study focused on examining the aspects of the different outcrops observed in the study area, including their strike, dip, and other structural orientations.

Over the 2 km^2 study area, terrain or ground elevation progressively increases from south to north, from circa 208 m in the southern reaches to circa 224 m in the northern reaches, with the lowest median of 204 m occurring near the mid-plane of the area of study.

An important observation made by the authors was that elevation increases from west to east, and that the petrographic map of the area of study is underlain by a continuous body of granite, with discontinuous bodies of schist and pegmatite. Examination of the landform map of the area of study positively correlates with the conclusions on aquifer prospects drawn from the earlier survey, and it is strongly recommended to drill these locations for groundwater exploitation.

2. MATERIALS AND METHODS

2.1 Materials

2.1.1 Handheld Compass Clinometer and Global Positioning System (GPS) Units

Directional straight-line traverses were usually approximately fixed by the use of the compass clinometer shown in Figure 1. The handheld Garmin GPSmap78 global positioning system unit, as shown in Figure 2, was used as a high-quality control tool to ensure movement along a true straight line in either the north-south or east-west directions and to determine the geographic coordinates of a point. Both the compass clinometer and the handheld Garmin GPSmap78® global positioning system units are central in the

macroscopic-lithologic phase of this study in order to determine an outcrop position's coordinates as well as to measure strike, dip, and other petrographic parameters.

***Figure 1**. A compass clinometer is employed to fix directional straight-line traverses*

***Figure 2**. Handheld Garmin GPSmap78® global positioning system unit employed for quality-control of straight-line traverses fixed by the compass clinometer, and also to determine the geographic coordinates of a point*

2.1.2 The Geological Hammer and Chisel

A geological hammer, similar to a carpenter's hammer but with a more hardened metal head, was required in the macroscopic-lithologic phase of this study to chip off chunks of palm-sized rock masses from the outcrops under investigation. A chisel is, of course, the natural accompaniment to the hammer when any chunk of rock-mass needs to be broken off along a crack-opening. Figure 3 shows one such hammer in use.

2.1.3 Edge-Cutting Machine

The edge-cutting machine was used to cut a rock sample obtained from the field across the c-axis into a smaller specimen. Figure 4 shows an edge cutting machine.

2.1.4 Handheld Cutting/Trimming Machine

The handheld cutting/trimming machine was used to trim rock samples slated for thin-section analyses to remove excess material. Figure 5 shows a handheld cutting/trimming machine.

***Figure 3**. A geological hammer is being put to use out in the field*

***Figure 4**. An edge-cutting machine*

***Figure 5**. A handheld cutting/trimming machine*

2.1.5 Carborundum Stone

The carborundum stone was used to grind a rock sample slated for thin-section analysis to achieve planeness, enabling the sample to lap on the glass slide. Figure 6 shows a carborundum stone.

***Figure 6**. A carborundum stone*

2.1.6 Glass Slides and Cover Slips with Epoxy Resin and Hardener

A glass slide and cover slip, along with accompanying epoxy resin and hardener, were required to mount a ground specimen in readiness for microscopic analysis. Figure 7 shows glass slides and cover slips, whilst Figure 8 shows epoxy resins and hardeners.

2.1.7 Hot Plate (Heater)

A hot plate or heater is used to desiccate wet rock samples. Figure 9 shows a hot plate.

***Figure 7**. Glass slides and cover slips*

***Figure 8**. Epoxy resins and hardeners*

***Figure 9**. A hot plate*

2.2 Methods

2.2.1 The Macroscopic-Lithologic Survey

In keeping with one of the objectives of this study, lithologic observations were carried out at the 11 coincident groundwater-prospect/outcrop locations determined from Adebayo (2019) by the route of classifying observed outcrops at these 11 points by designations of their sample numbers, rock-types, ground locations, georeferenced locations, as well as their strike-directions, dip-orientations, and other structural aspects (where applicable). Interesting intrusion features, such as vein pegmatite on a granitic outcrop rock body, are of interest to the survey party. Fist-sized rock samples or slightly greater than these that have been chipped off from the host outcrop are usually collected in a sack for transportation back to campus. Measurements of strike, dip, joint angles, fault angles, etc., are facilitated by the compass clinometer (see Figure 10).

***Figure 10**. Measurements of strike, dip, joint angles, fault angles, etc., are facilitated by the use of the compass clinometer*

2.2.2 The Microscopic-Petrographic Analyses

In keeping with another objective of this study, microscopic-petrographic analyses of 6 of the 11 rock samples collected from the macroscopic-lithologic survey phase were subjected to thin-section analyses. From the macroscopic-lithologic point of view, each of these 6 rock samples was assumed to be inherently the identified rock-type of the sample set of rock-outcrops collected from the 11 coincident groundwater prospect/outcrop locations determined from Adebayo (2019). Initially, a rock sample slated for thin-section analyses was brought to the edge-cutting machine, and a sample was cut from this usually fist-sized specimen. Then the cut sample was trimmed to remove excess using the hand-cutting/trimming machine. Next, to achieve planeness and enable the sample to lie on the glass slide, the carborundum stone was used to grind the trimmed sample to a thickness of 80 μm. Further, this specimen was mounted on a glass slide using epoxy resin and a hardener, aiming to achieve a final thickness of less than or equal to 30 μm (section + resin).

2.2.3 The Macroscopic-Petrologic Survey

In keeping with another objective of this study, about 50 different outcrop locations to the north of the discerned vestige of the Kazaure-Karaukarau-Kushaka-Ilesha Schist Belt, which runs diagonally through the Gidan Kwano Campus, were visited and classified based on their nature. The predominant structural features observed on these outcrop bodies are joints and fractures. Where joints and fractures were seen, their angular orientations were measured using the compass clinometer.

3. RESULTS AND DISCUSSION

3.1 Results

3.1.1 Macroscopic-Lithologic Survey

The macroscopic-lithologic dataset for the 11 distinct rock outcrops of this study has been extracted from the archive and presented in Table 1. The structural measurements for joints, faults, strike, and dip orientations are also summarized in Table 1.

3.1.2 Thin-Section Analyses

The thin-section analyses the “distributed”

rock-types of macroscopic-lithologic dataset for the 11 distinct rock-outcrops of this study, designated for this analysis segment as E10, E11, E1A, E9, EB2, and EF6 at 40x magnification for their juxtaposed plane polarisation (PP) and cross-polarisation (CP) views are summarized in Table 2.

3.1.3 Macroscopic-Petrologic Survey

About 50 distinct rock outcrops were investigated based on their prevailing physical textures and appearances.

3.2 Discussions

3.2.1 Macroscopic-Lithologic Characterization

Samples 1,2,3,4,6,8, and 9, located at elevated terrain, were classified as “granite” based on textural and observable surface characteristics. Strike and dip measurements were not carried out for granitic bodies, as per the norm. Joints and localised faulting were measured for the outcrops.

Schist-rock classification pertains to Samples 5 and 11, whilst Sample 7 is a hybrid “granite/schist” and only Sample 10 is classified as migmatite. All these rock types were located at elevated terrain, and strike/dip measurements were carried out for the schist and migmatite bodies. As with the granitic bodies, joints and localised faulting were measured in these outcrops too.

3.2.2 Petrographic Analysis Summary

Microscopic examination of six samples (E10, E11, E1A, E9, EB2, EF6) revealed mineral assemblages that differed from those identified macroscopically.

Sample E10 consists of quartz, biotite, and plagioclase minerals in the rock matrix.

Sample E11 consists of quartz, biotite, orthoclase, and plagioclase minerals in the rock matrix.

Sample E1A consists of quartz, biotite, and orthoclase minerals in the rock matrix.

Sample E9 consists of quartz, biotite, and plagioclase minerals in the rock matrix.

Sample EB2 consists of quartz, biotite, and orthoclase minerals in the rock matrix.

Sample EF6 consists of quartz, orthoclase, and amphibole minerals in the rock matrix.

The constituent quartz mineral herein appears colourless in plane-polarised (PP) light but shows a bluish hue under cross-polarised (CP) light. The physical characteristics of relief, form/size, inclusion, cleavage, extinction, interference, pleochroism, and twining determined from the optical-property analyses positively identify the mineral quartz in the rock samples herein.

The biotite mineral in the rock matrices herein appears dark in plane-polarised light but is dark brown in cross-polarised light.

The plagioclase mineral in the rock matrices herein appears colourless in plane-polarised light but is bluish in cross-polarised light.

The orthoclase mineral in the rock matrices herein appears colourless in plane-polarised light but is bluish in cross-polarised light.

The amphibole mineral in the rock matrices herein appears brownish in both plane-polarised and cross-polarised light.

Samples E10 and E9 are similar in composition, whereas Samples E1A and EB2 show a high degree of similarity.

3.2.3 Petrologic Survey Results

The survey of approximately 50 outcrop locations north of the identified schist belt revealed exclusively granitic compositions with no schistose characteristics observed. Joint and fracture measurements were recorded where present, confirming the structural discontinuity between the schist belt and northern granitic terrain.

Table 3 gives a percentage breakdown of the 11 samples under consideration by macroscopic character.

Table 3. *Percentage breakdown of samples*

Macroscopic character	**Percentage of total**
Granite	64%
Schist	18%
Granite/Schist	9%
Migmatite	9%

4. CONCLUSIONS:

The lithologic phase shows more samples identified as "granite" than those that are undoubtedly schist from physical properties. The petrographic phase shows more schist rocks under thin-section analyses than these "granites." The petrologic phase reveals no presence of schist outcrop at all in the area north of the discerned schist belt.

Thus, the principal problem identified for this study has been addressed, as we now consider that the outcrops identified as "granites" in Adebayo (2019) are actually schist. Thus, the rock-mass diagonal discerned by Adebayo (2019) is actually the Kazaure-Karaukarau-Kushaka-Ilesha Schist Belt.

Furthermore, the absence of schist rock-bodies to the north of the discerned Kazaure-Karaukarau-Kushaka-Ilesha Schist Belt strengthens the deduction of Adebayo (2019).

It is recommended that the Federal University of Technology, Minna, focus its efforts on the discerned Kazaure-Karaukarau-Kushaka-Ilesha Schist Belt to exploit groundwater and gold mineral resources.

5. DECLARATIONS

5.1. Study Limitations

If time and resources had permitted, mapping of outcrops across the entire 100 km² area of the Gidan Kwano Campus would have been carried out to delineate schist signatures in these areas. Nonetheless, this study has indicated that the principal schist lineament traversing the Gidan Kwano Campus is the northeast-southwest diagonal cutting through the Phase II Development of this Campus, where this segment of the diagonal is now called “Jonahite” in recognition of the leading efforts of S.A. Jonah to serendipitously map the vestige of this schist lineament through the Phase II Development.

5.2. Acknowledgements

The authors are grateful to the Federal University of Technology, Minna, for providing the necessary facilities and laboratory infrastructure that enabled this research. We extend our appreciation to the Department of Physics, School of Physical Sciences, for the institutional support and access to field equipment. Special thanks to the technical staff of the geology laboratory for their assistance with the thin-section preparation and petrographic analyses. We also acknowledge the management of the Federal University of Technology, Minna, for granting access to the Gidan Kwano Campus for field studies and sample collection. The authors appreciate the collaborative efforts of all undergraduate students who participated in the field surveys and data collection phases of this study.

5.3. Funding source

The authors funded this research. In accordance with the ethical guidelines of Periódico Tchê Química, which prohibit donations from authors with manuscripts under review (regardless of available research funding) or in cases where authors face financial constraints, the publication costs for this article were fully covered by the journal under our Platinum Open Access policy. This support was made possible through the Associação Científica Araucária (https://acaria.org/). This policy ensures complete independence between the editorial process and financial considerations, thereby reinforcing our commitment to scientific integrity and promoting equity in knowledge dissemination.

5.4. Competing Interests

The authors declare that there exists no conflict of interest whatsoever arising from the preparation of this manuscript for publication with any other competing interests, whether they be of the authors’ or of second parties and third parties thereof. The data employed in the enunciation of the textual material herein are original, having been duly acquired by the authors as part of the annual undergraduate schedule of project supervision here at the Federal University of Technology, Minna, Nigeria. This body of data field, duly archived for validation and reference purposes, is available for integrity checks anytime.

5.6. Author Contributions

S.A.J. conceived the study design, supervised fieldwork, and wrote the manuscript.

C.E.O. and M.C.O. conducted macroscopic-lithologic surveys and sample

collection.

C.O.O. and E.O.B. performed microscopic-petrographic analyses and thin-section preparation.

T.O.A. and C.E.O. assisted with petrologic surveys and structural measurements.

I.A.A. contributed to data analysis and interpretation.

S.S. provided geographical expertise and site reconnaissance.

All authors contributed to the manuscript review and approved the final version.

6. REFERENCES:

1. Abaa, S.I. (1983). The structure and petrography of alkaline rocks of the Mada Younger Granite Complex, Nigeria. Journal of African Earth Science,3,107–113. DOI: 10.1016/0899-5362(85)90029-6
2. Adebayo, H.M. (2019). Macroscopic Petrographic Control of a 4 km^2 VES Study at the Southern Phase II Development, Gidan Kwano Campus, Minna, Nigeria, Unpublished BTech Thesis, Federal University of Technology, Minna, Nigeria. (Supervised by S.A. Jonah.)
3. Adesoye, S.A. (1986). Master Plan of the Federal University of Technology's Permanent Site, Minna, Adesoye and Partners, Kaduna, Nigeria.
4. Ajibade, A.C., Fitches, W.R., & Wright, J.B. (1979). The Zungeru mylonites, Nigeria: recognition of a major unit. Rev de Geol Geog Phys, 21, 359-363.
5. Black, R. (1980). Precambrian of West Africa. Episodes, 4, 3-8. DOI: 10.18814/epiiugs/1980/v3i4/001
6. Burke, K.C., & Dewey, J.F. (1972). Orogeny in Africa. In Dessauvagie, T.F.J., & Whiteman, A.J. (editors), Africa Geology. University of Ibadan Press, Ibadan, pp 583-608.
7. Dada, S.S. (1989). Evolution de la croute continental au Nord Nigeria: apport de la geochimie, dela geochronologie U-Pb et des traceurs isotopiques Sr, Nd et Pb, PhD Thesis University of Science and Technology Languedoc, Montpellier, France.
8. Falconer, J.D. (1911). The Geology and Geography of Northern Nigeria, Macmillan, London.
9. Gandu, A.H., Ojo, S.B., & Ajakaiye, D.E. (1986). A gravity study of the Precambrian rocks in the Malumfashi area of Kaduna State, Nigeria. Tectonophysics, 126, 181–194. DOI: 10.1016/0040-1951(86)90227-1
10. Grant, N.K. (1978). Structural distinction between a metasedimentary cover and an underlying basement in the 600 million-year-old Pan-African domain of Northwestern Nigeria. *Geological Society of America Bulletin*, *89*, 50–58. DOI: 10.1130/0016-7606(1978)89<50:SDBAMC>2.0.CO;2
11. Holt, R.W. (1982). The Geotectonic Evolution of the Anka Belt in the Precambrian Basement Complex of N.W. Nigeria, Unpublished Ph.D. Thesis, The Open University.
12. Jatau, I.B., Patrick, N.O., Baba, A., & Fadele, S.I. (2013). The use of vertical electrical sounding (VES) for subsurface geophysical investigation around Bomo Area, Kaduna State, Nigeria. IOSR Journal of Engineering, 3(1), 10-15. DOI: 10.9790/3021-03141015
13. de Almeida, A., Maciel, D. F., Sousa, K. F., Nascimento, C. T. C., & Koide, S. (2021). Vertical Electrical Sounding (VES) for estimation of hydraulic parameters in the porous aquifer. Water, 13(2), 170. https://doi.org/10.3390/w13020170
14. Jonah, S.A., Akpomie, D.P., Ezekwebekwe, L. O., Isah, E.A., Muhammed, A.N., Momoh, A.A., Okoye, C.K., Okpara, K. K., Oni, N.O., Alade, R. O., Yahaya, G. A., Zubair, R.O., Onoja, E.U., & Daramola, O. (2015[a]). A dual topographic-petrographic control for a 1 km^2 VES-IP study completed at the Gidan Kwano Campus Phase II Development, Minna, Nigeria. Journal of Science, Technology, Mathematics, and Education, 11(3), 65-76.
15. Jonah, S.A., & Olasehinde, P.I. (2017). Interpretation of vertical electrical sounding (VES) data of Gidan Kwano Campus Phase II, Federal University of Technology, Minna, Nigeria. Journal of Information, Education, Science, and Technology, 4(1), 95-116.
16. Aizebeokhai, A. P., Ogungbade, O., & Oyeyemi, K. D. (2021). Application of geoelectrical resistivity for delineating crystalline basement aquifers in Basiri, Ado-Ekiti, Southwestern Nigeria. Arabian Journal of Geosciences, 14(2), 51. https://doi.org/10.1007/s12517-020-06440-1
17. Jonah, S.A., Olasehinde, P.I., Jimoh, M.O., Umar, M., & Yunana, T. (2015[b]). An intercalated dual geoelectrical survey of an earlier study for groundwater at the planned Gidan Kwano Campus Development Phase II, Federal University of Technology, Minna, Nigeria. Journal of Information, Education, Science, and Technology (JOSTMED), 11(2), 32-50.

18. McCurry, P. (1976). The geology of the Precambrian to Lower Palaeozoic rocks of Northern Nigeria: A review. In Kogbe C.A. (editor), Geology of Nigeria. Elizabethan Publishers, Lagos, 15–39.
19. Obaje, N.G. (2009). Geology and mineral resources of Nigeria. In Lecture Notes in Earth Sciences. Springer-Verlag, Berlin. DOI: 10.1007/978-3-540-92685-6
20. Okiongbo, K.S., & Odubo, E. (2012). Geoelectric sounding for the determination of aquifer transmissivity in parts of Bayelsa State, South South Nigeria. Journal of Water Resource and Protection, 4, 346-353. DOI: 10.4236/jwarp.2012.46039
21. Olade, M.A. and Elueze, A.A. (1979). Petrochemistry of the Ilesha amphibolite and Precambrian crustal evolution in the Pan-African domain of SW Nigeria. Precambrian Research, 8,303–318. DOI: 10.1016/0301-9268(79)90033-0
22. Olayinka, A.I. (1992). Geophysical siting of boreholes in crystalline basement areas of Africa. J Afr Earth Sci, 14,197–207. DOI: 10.1016/0899-5362(92)90097-V
23. Oyawoye, M.O. (1972). The basement complex of Nigeria. In Dessauvagie, T.F.J., & Whiteman, A.J. (editors), *African Geology*. Ibadan University Press, 66–102.
24. Rahaman, M.A. (1976). Review of the basement geology of South-Western Nigeria. In Kogbe C.A. (editor), Geology of Nigeria. Elizabethan Publishers, Lagos, 41–58.
25. Rahaman, M.A. (1981). Recent advances in the study of the basement complex of Nigeria. Abstract: 1st Symposium on the Precambrian Geology of Nigeria.
26. Rahaman, M.A. (1988).. Recent advances in the study of the basement complex of Nigeria. In Geological Survey of Nigeria (edited). Precambrian Geology of Nigeria, 11–43.
27. Rahaman, M.A., & Ocan, O. (1978). On relationships in the Precambrian Migmatite-gneisses of Nigeria. Nigerian Journal of Mining and Geology, 15, 23–32.
28. Truswell, J.F., & Cope, R.N. (1963). The geology of parts of Niger and Zaria Provinces, Northern Nigeria. Geological Survey of Nigeria Bulletin, 29, 1-104.
29. Turner, D.C. (1983). Upper Proterozoic schist belts in the Nigerian sector of the Pan-African Province of West Africa. Precambrian Research, 21, 55–79. DOI: 10.1016/0301-9268(83)90005-0

Table 1. *Summary of Macroscopic-Lithologic Characteristics and Structural Measurements*

Sample	Rock Type	Joints (°)	Faults (°)	Strike	Dip	GPS Coordinates
1	Granite	262, 264, 354	26, 118	-	-	N: 9˚31'17.2", E: 6˚25'39.0"
2	Granite	20, 23, 41	134	-	-	N: 9˚30'57.8", E: 6˚26'4.9"
3	Granite	205, 187	199, 178	-	-	N: 9˚31'33.4", E: 6˚26'34.1"
4	Granite	205, 132	218, 218	-	-	N: 9˚31′20.5″, E: 6˚26′37.3″
5	Schist	24, 221, 322	149, 166	340°NW	6°E	N: 9˚31′17.2″, E: 6˚26′37.3″
6	Granite	215, 196	212, 213	-	-	N: 9˚31'19.2", E: 6˚26'34.1"
7	Granite/Schist	317, 333, 250, 337	234	-	-	N: 9˚31'20.6", E: 6˚26′36.4″
8	Granite	180, 201	179, 68	-	-	N: 9˚30′57.8″, E: 6˚26′04.9″
9	Granite	202, 192	182, 202	-	-	N: 9˚31'14.0", E: 6˚26'30.8"
10	Migmatite	198, 138	64, 187, 36	183°SW	14°W	N: 9˚31'18.2", E: 6˚26'36.1"
11	Schist	92, 160	52	18°NE	2°E	N: 9˚31'43.1", E: 6˚26'37.2"

Table 2. *Petrographic Analysis Results*

Sample	Macroscopic ID	Mineral Assemblage	Key Optical Properties
E10	Granite	Quartz + Biotite + Plagioclase	Quartz: colorless (PP), blue (CP); Biotite: dark (PP), dark brown (CP)
E11	Granite	Quartz + Biotite + Orthoclase + Plagioclase	Four-mineral assemblage indicating granitic composition
E1A	Granite	Quartz + Biotite + Orthoclase	Three-mineral granitic assemblage
E9	Granite	Quartz + Biotite + Plagioclase	Similar to E10 composition
EB2	Granite	Quartz + Biotite + Orthoclase	Similar to E1A composition
EF6	Granite	Quartz + Orthoclase + Amphibole	Amphibole: brownish in both PP and CP light

Note: PP = Plane Polarized light; CP = Cross Polarized light

PERIÓDICO TCHÊ QUÍMICA
ARTIGO ORIGINAL

ANÁLISE DA DEGRADAÇÃO DE SOLOS COSTEIROS CONTAMINADOS COM PETRÓLEO UTILIZANDO O CONSÓRCIO BACTERIANO, *BACILLUS* E *AGROBACTERIUM*

ANALYSIS OF THE DEGRADATION OF COASTAL SOILS CONTAMINATED WITH CRUDE OIL USING THE BACTERIAL CONSORTIUM, *BACILLUS AND AGROBACTERIUM*

ANÁLISIS DE LA DEGRADACIÓN DE SUELOS COSTEROS CONTAMINADOS CON PETRÓLEO CRUDO UTILIZANDO EL CONSORCIO BACTERIANO, *BACILLUS Y AGROBACTERIUM*

Jaqueline Heidy Chirre-Flores*
Universidad Nacional de Ingeniería, Lima, Facultad de Ingeniería Ambiental, Perú.

Hugo David Chirinos-Collantes*
Universidad Nacional de Ingeniería, Lima, Facultad de Ingeniería Ambiental, Perú.

Roberto Robles-Calderón
Universidad Nacional Mayor de San Marcos, Facultad de Química e Ingeniería Química, Perú.

Ana Cecilia Valderrama-Negrón
Universidad Nacional de Ingeniería, Facultad de Ciencias, Perú.

Nélida Marín-Huachaca
Universidad Nacional de Ingeniería, Lima, Facultad de Ingeniería Ambiental, Perú.

María Rosario Viera-Palacios
Universidad Nacional de Ingeniería, Lima, Facultad de Ingeniería de Petróleo, Perú.

Nancy Oliveth Encarnación-Bermúdez
Universidad Nacional de Ingeniería, Lima, Facultad de Ingeniería de Petróleo, Perú.

** Autor correspondente*
e-mail: jchirref@uni.edu.pe

Received 14 June 2025; received in revised form 30 September 2025; accepted 16 October 2025.

RESUMO

Introdução: Para o processo de degradação aeróbia do petróleo foram utilizados como consórcio bacteriano *Bacillus e Agrobacterium*, que são duas cepas bacterianas que juntamente com as bactérias heterotróficas nativas do solo contaminado com óleo conseguiram eliminar os contaminantes presentes no solo costeiro do norte do Peru. **Objetivos**: Analisar a biodegradação de solos costeiros do Peru contaminados com uma concentração de 25% de petróleo, utilizando o consórcio bacteriano de *Bacillus e Agrobacterium*. **Métodos**: A técnica de cromatografia gasosa (GC) foi utilizada para determinar a eficiência de degradação de diferentes frações de hidrocarbonetos totais de petróleo após biodegradação. **Resultados:** As duas cepas bacterianas conseguiram reduzir a concentração dos hidrocarbonetos de C_6 para C_{10}, (fracção F_1) em média 99%; C_{10} a C_{28} (fracção F_2) 71,2% e C_{28} a C_{40} (fracção F_3) 35% da concentração original. **Discussão**: Esta última fracção, F_3, contendo os compostos pesados, os hidrocarbonetos aromáticos policíclicos (HAPs), incluindo bifenilo, naftaleno e antraceno, entre outros, após 120 dias de incubação a 25ºC, pH=6,0±0,2, apresentou menor porcentagem de biodegradação do que as outras fracções. **Conclusões**: As bactérias *Bacillus e Agrobacterium*, decompõem eficientemente os hidrocarbonetos. Contudo, a biodegradação pode depender das condições operacionais a que os consórcios estão expostos. Um aumento na taxa de biodegradação também foi observado nos sistemas mistos como resultado de uma possível interação entre as cepas bacterianas.

Palavras chave: *Hidrocarbonetos totais de petróleo, biodegradação, microrganismos, solos costeiros, consórcio*

DOI: 10.52571/PTQ.v22.n51.2025_06_FLORES_pgs_79_88.pdf

bacteriano.

ABSTRACT

Introduction: For the aerobic degradation process of crude oil, *Bacillus* and *Agrobacterium* were used as a bacterial consortium, which are two bacterial strains that together with the native heterotrophic bacteria from soil contaminated with oil achieved to eliminate the contaminants present in the coastal soil of the northern Peru. **Aims**: Analyze the biodegradation of coastal soils in Peru contaminated with a concentration of 25% crude oil, using *Bacillus* and *Agrobacterium* bacterial consortium. **Methods**: Gas chromatography (GC) technique was used to determine the degradation efficiency of different fractions of total petroleum hydrocarbons after biodegradation. **Results:** Both bacterial strains were able to reduce the concentration of hydrocarbons from C_6 to C_{10} (fraction F_1) by an average of 99%; from C_{10} to C_{28} (fraction F_2) by 71.2%; and from C_{28} to C_{40} (fraction F_3) by 35% of the original concentration. **Discussion:** This last fraction, F_3, which contains heavy compounds, polycyclic aromatic hydrocarbons (PAHs), including biphenyl, naphthalene, and anthracene, among others, showed a lower percentage of biodegradation than the other fractions after 120 days of incubation at 25°C, pH = 6.0 ± 0.2. **Conclusions**: Bacteria *Bacillus* and *Agrobacterium*, efficiently decompose hydrocarbons. However, biodegradation may depend on the operating conditions to which the consortia are exposed. An increase in the biodegradation rate was also observed in the mixed systems as a result of a possible interaction between the bacterial strains.

Keywords: *Total Petroleum Hydrocarbons, biodegradation, microorganisms, coastal soils, bacterial consortium.*

RESUMEN

Introducción: Para el proceso de degradación aeróbica del petróleo crudo, se utilizaron las bacterias *Bacillus* y *Agrobacterium* como consorcio bacteriano, las cuales son dos cepas bacterianas que junto con las bacterias nativas heterótrofas del suelo contaminado con petróleo eliminaron en gran medida los contaminantes presentes en el suelo costero del norte del Perú. **Objetivos**: Analizar la biodegradación de los suelos costeros de Perú contaminados con una concentración de 25% de petróleo crudo, usando un consorcio bacteriano de *Bacillus* y *Agrobacterium*. **Métodos**: Se utilizó la técnica de cromatografía de gases (GC) para determinar la eficiencia de degradación de las diferentes fracciones de hidrocarburos totales de petróleo después de la biodegradación. **Resultados:** Las dos cepas bacterianas consiguieron reducir la concentración de los hidrocarburos: de C_6 a C_{10}, (fracción F_1) en un promedio 99%; C_{10} a C_{28} (fracción F_2) en un 71.2% y C_{28} a C_{40} (fracción F_3) en un 35% de la concentración original. **Discusión**: Esta última fracción, F_3, contiene compuestos pesados, los hidrocarburos aromáticos policíclicos (HAPs), incluyen bifenil, naftaleno y antraceno, entre otros, después de 120 días de incubación a 25ºC y pH 6.0±0.2, presentó menor porcentaje de biodegradación que las otras fracciones. **Conclusiones**: Las bacterias *Bacillus y Agrobacterium* descomponen eficientemente los hidrocarburos. Sin embargo, la biodegradación puede depender de las condiciones de operación al que están expuestas los consorcios. Se observó también un aumento de la tasa de biodegradación en sistemas de cepas mixtas, producto de una posible interacción entre las cepas bacterianas.

Palabras clave: *Hidrocarburos Totales de Petróleo, biodegradación, microorganismos, suelos costeros, consorcio bacteriano*.

1. INTRODUCCIÓN:

La biodegradación es la transformación de sustancias orgánicas mediante microorganismos, produciendo agua, dióxido de carbono y biomasa. El petróleo es una mezcla de hidrocarburos con compuestos no hidrocarburos, cuyos componentes son parafinas o alcanos (22%), cicloalcanos o naftenos (50%), aromáticos (17%) entre otros (Moubasher *et al*., 2015).

Los hidrocarburos del petróleo son perjudiciales a la salud de los seres vivos cuando se encuentran en la intemperie. Los hidrocarburos aromáticos policíclicos (HAP) tienen efectos mutagénicos y cancerígenos y causan problemas en el sistema endocrino (Dutta *et al*., 2017). El efecto cancerígeno de estos contaminantes orgánicos en los órganos del cuerpo aparece después de períodos prolongados de exposición (Hernández *et al*., 2017; Koual *et al*., 2019).

Uno de los procesos de degradación de los hidrocarburos del petróleo se realiza mediante procesos metabólicos, porque se ha demostrado que las bacterias metabolizan a los hidrocarburos

del petróleo (Yan *et al*., 2004). La degradación bacteriana de los hidrocarburos de petróleo incluye métodos aeróbicos y anaeróbicos, pero debido a la viscosidad e hidrofobicidad del petróleo, el suelo contaminado por hidrocarburos de petróleo suele ser superficial. A pesar de su hidrofobicidad, los alcanos de cadena larga y los HAP pueden ser degradados por microorganismos, pero a un ritmo lento (Chen *et al*., 2017).

Las bacterias oxidantes de hidrocarburos necesitan adherirse a sustancias insolubles o gotitas de petróleo, en las que se puede observar un gran número de células de bacterias. Estos organismos provocan la degradación del petróleo y la descomposición de las manchas aceitosas en el ecosistema (Madigan *et al*. 2016).

El crecimiento microbiano y la actividad metabólica requieren macronutrientes esenciales para su desarrollo, como el nitrógeno y fósforo; los suelos contaminados con hidrocarburos suelen contener nutrientes limitados (Brook, 2001).

El metabolismo catabólico bacteriano para la degradación de hidrocarburos puede ser aeróbico o anaeróbico. La concentración de oxígeno afecta las tasas de degradación; de hecho, bajo condiciones aeróbicas, la biodegradación es más rápida y más eficiente porque el oxígeno es el aceptor final de electrones en la cadena representativa. En condiciones anaeróbicas, el aceptor final de electrones puede ser el nitrato, sulfato, o un átomo de hierro provenientes de los nutrientes del suelo, y la biodegradación es más lenta y a menudo insignificante en comparación con la degradación a condiciones aeróbicas (Nagkirti *et al*., 2017).

Las bacterias hidrocarbonoclásticas han desarrollado mecanismos adaptativos para tolerar la presencia de hidrocarburos, como la capacidad de emulsionarlos y metabolizarlos, la activación de mecanismos de reparación del ADN, producción de moléculas involucradas en los mecanismos de detección de quórum para la formación de biopelículas, y regulación de bombas de eflujo y poros para controlar la concentración de hidrocarburos en la célula bacteriana (*Ruiz et al.* 2021).

La biorremediación es más efectiva cuando se lleva a cabo mediante consorcios microbianos complejos, en particular, se desarrollan de forma independiente en aquellas zonas históricamente contaminadas (Hesnawi & Adbeib 2013).

Muchos factores, como la temperatura, oxígeno, pH, concentración de las cepas microbianas, biodisponibilidad, accesibilidad a factores de crecimiento, la estructura química y concentración de los hidrocarburos y las características del transporte celular, afectan la biodegradación de hidrocarburos por bacterias. El suelo alberga gran cantidad de microorganismos y constituye un ambiente propicio para la biodegradación de los hidrocarburos de petróleo (Alaidaroos, 2023; Pandolfo *et al*., 2023).

2. PROCEDIMIENTO EXPERIMENTAL:

2.1 Recolección de muestra

En este estudio, se recolectaron muestras de suelo de la zona norte de Lima en Perú, en el distrito de Ventanilla (11°51'54" S y 77°9'42"W), situado sobre el nivel del mar. Las muestras fueron recolectadas de diferentes puntos de muestreo cuidadosamente en bolsas esterilizadas y transportados al laboratorio para su posterior análisis.

Se realizó una mezcla de 5 kg. de suelo costero con 25% de petróleo crudo procedente de Brasil cuyas propiedades se muestran en la Tabla 1, asimismo, se le añadió 20% del consorcio bacteriano activado y 5% de agua potable para la difusión de los hidrocarburos hacia los microorganismos con la finalidad de obtener una adecuada biodegradación de los contaminantes del suelo costero (Escalante, 2002).

Tabla 1. *Propiedades del petróleo crudo*

Propiedad	Unidad	Valor	Norma
Densidad a 15°C	g/mL	0,88	ASTM D-1298
P. Específico 15,6/15,6°C	g/mL	0,88	Calculado
Densidad API	°API	29	Calculado
Azufre	%p/p	0,27	ASTM D-4294
N° de Neutralización	mg KOH/g	0,19	ASTM D-664
Presión de Vapor Reid	kPa	21	ASTM D-6377
Punto de Vertido	°C	-18	ASTM D-97
Viscosidad 20°C	cSt	44	ASTM D-445
Viscosidad 40°C	cSt	18	ASTM D-445
Sulfhídrico disuelto	ppm v/v	2	ARAMCO H-3
Sulfhídrico evol. a 340°C	ppm p/p	9	REPSOL
Residuo de Carbón	%p/p	5	ASTM D-4530

Asfaltenos	%p/p	2	CALCULADO
Nitrógeno	ppm p/p	2891	ASTM D-4629
Cadmio	ppb	1	-
Calcio	ppm p/p	1	Abs. Atómica
Cobre	ppm p/p	0.7	Abs. Atómica
Fósfoto	ppm p/p	<5	Abs. Atómica
Hierro	ppm p/p	1	Abs. Atómica
Niquel	ppm p/p	7	Abs. Atómica
Plomo	ppm	1	-
Silicio	ppm p/p	<10	Abs. Atómica
Sodio	ppm p/p	4	Abs. Atómica
Vanadio	ppm p/p	10	Abs. Atómica
Cloro Total	ppm	98	ASTM D-7536
Cloro fase inorgánica	ppm	87	ASTM D-7536
Cloro fase orgánica	ppm	11	ASTM D-7536
Agua por destilación	% vol	2	ASTM D-4006
Aromaticidad disponible 40°C	-	0.6	REPSOL
Aromaticidad requerida 40°C	-	0,001	REPSOL
Valor P 40°C	-	>3.9	REPSOL

Fuente: Assay Crudo Buzios. (2023).

2.2 Análisis microbiológico

Para la identificación de colonias de bacterias específicas y el análisis morfológico, se realizaron según la metodología descrita en el manual de Bergey para bacteriología determinativa (Holt *et al*., 1994).

2.3 Caracterización e identificación de aislados bacterianos

Con base en la caracterización de aislados bacterianos, fueron identificados cepas representativas de los géneros *Bacillus y Agrobacterium.*

2.4 Condiciones de operación del consorcio bacteriano

Las características del consorcio bacteriano de la patente Ultra Archaea son:

Apariencia: Polvo fino, Estado físico: Sólido. Color: gris claro, Olor: ligero olor a aceite, Umbral de olor: No aplicable, pH: 8.5, Punto de fusión: > 842 °F (> 450 °C), Inflamabilidad (sólido, gas): Este producto no es inflamable, Densidad relativa: 2,6 g/cm³, Solubilidad (agua): < 0.9 mg/l, Temperatura de descomposición: > 932 °F (> 500 °C).

Otra información, Densidad aparente: 0.9 – 1.4 g/cm³.

2.5. Resultados

del conteo del consorcio bacteriano

Los promedios de conteos de las unidades formadoras de colonia UFC/mL de las bacterias, muestran una reducción de la población del consorcio bacteriano desde 3.8 × 10^8 UFC/g a 3.6 × 10^7 UFC/g de tratamiento de biorremediación de suelos contaminados con petróleo.

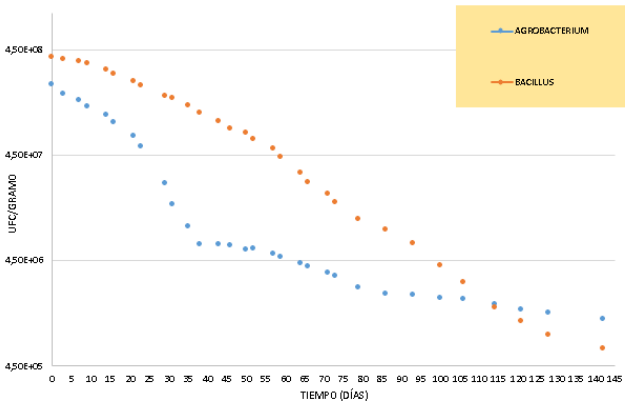

Figura 1*. UFC/gramo del consorcio bacteriano vs Tiempo (días).*

3. RESULTADOS Y DISCUSIÓN:

3.1. RESULTADOS

3.1.1. ANÁLISIS ESTATISTICOS

El análisis estadístico de los datos obtenidos se realizó utilizando el Software SPSS.

El planteamiento de la hipótesis es el siguiente:

Ho: Los datos tienen una distribución normal

Ha: Los datos no tienen una distribución normal

Nivel de Significancia
Confianza: 95%
Significancia (alfa): 5%

Tabla 2. Comparación de Pruebas de normalidad

	Kolmogorov-Smirnov[a]			Shapiro-Wilk		
	Estadístico	gl	Sig.	Estadístico	gl	Sig.
Tiempo	0.319	6	0.056	0.683	6	0.004
Prueba	0.202	6	0.200 *	0.853	6	0.167
HTP	0.268	6	0.200 *	0.853	6	0.167

* Esto es un límite inferior de la significación verdadera.

a. Corrección de significación de Lilliefors

Tabla 3. Prueba de normalidad de Shapiro - Wilk

	Estadístico	gl	p
Tiempo	0,683	6	0,004
Prueba	0,853	6	0,167
HTP	0,853	6	0,167

Criterio de decisión

Si $p \leq 0,05$ rechazamos la Ho y aceptamos la Ha

Si $p \geq 0,05$ aceptamos la Ho y rechazamos la Ha

Decisión y conclusión

Como $p \geq 0,05$ entonces aceptamos la Ho y rechazamos la Ha, es decir los datos tienen una distribución normal.

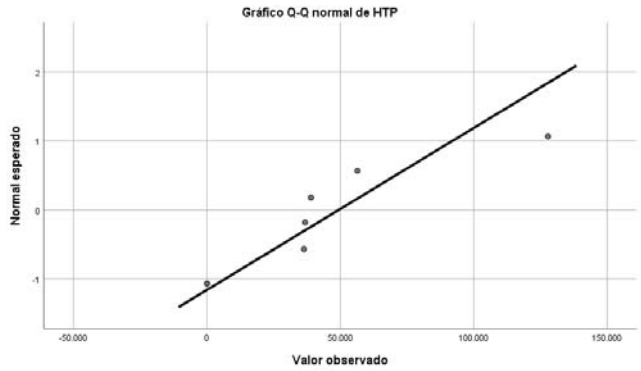

Figura 2. Normalidad de HTP versus el valor observado.

Análisis para determinar si hay correlación

Hipótesis

Ho: r = 0 (no existe correlación)
Ha: r ≠ 0 (si existe correlación)

Nivel de significancia

α = 0,05

Correlación de Pearson

Criterio de decisión

Si $p \leq 0,05$ aceptamos la H0 y rechazamos la Ha
Si $p \geq 0,05$ rechazamos la Ho y aceptamos al Ha

Tabla 4. Correlación de Pearson

Correlaciones				
		Tiempo	Prueba	HTP
Tiempo	Correlación de Pearson	1	0.000	-0.643
	Sig. (bilateral)		1.000	0.169
	N	6	6	6
Prueba	Correlación de Pearson	0.000	1	0.282
	Sig. (bilateral)	1.000		0.588
	N	6	6	6
HTP	Correlación de Pearson	-0.643	0.282	1
	Sig. (bilateral)	0.169	0.588	
	N	6	6	6

Tabla 5. Correlación de Pearson de las pruebas exeprimentales

	r	p	N
Tiempo - HTP	-0.643	0.169	6

Decisión y conclusión

Como $p \geq 0,05$ entonces aceptamos la Ha y rechazamos la Ho, es decir el tiempo y HTP tienen correlación. El r negativo indica que el HTP disminuye con el tiempo.

Tabla 6. Pruebas de efectos inter-sujetos

Pruebas de efectos inter-sujetos					
Variable dependiente: HTP					
Origen	Tipo III de suma de cuadrados	gl	Media cuadrática	F	Sig.
Modelo corregido	7721262358,944[a]	3	2573754119.648	3.810	0.215
Intersección	14639618282,713	1	14639618282.713	21.672	0.043
Tiempo	3749398674,108	1	3749398674.108	5.550	0.143
Prueba	3971863684,836	2	1985931842.418	2.940	0.254
Error	1351017379,647	2	675508689.824		
Total	23711898021,305	6			

Total corregido	90722797 38,592	5			

a. R al cuadrado = ,851 (R al cuadrado ajustada = ,628)

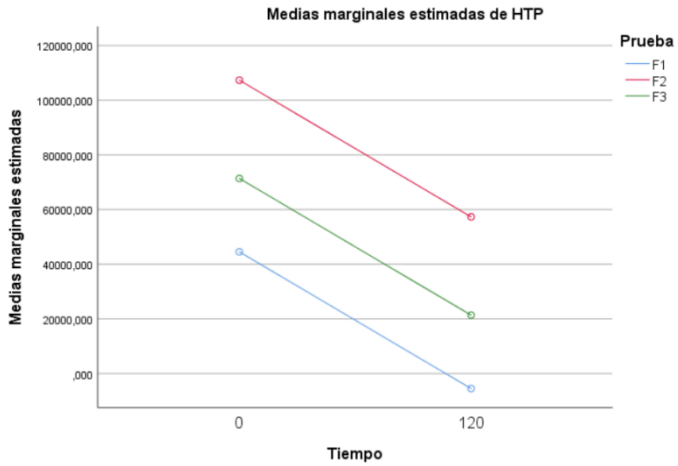

Figura 3. Medias marginales estimadas de HTP.

El análisis estadístico de las pruebas de efectos inter-sujetos, muestra que tiene la tendencia de las pruebas experimentales, de que a mayor tiempo hay mayor degradación de HTP.

3.2. DISCUSIÓN

Enumeración de bacterias heterótrofas totales y bacterias que degradan hidrocarburos totales.

Los resultados de recuentos del consorcio bacteriano se presentan en la figura 1. Los valores de los recuentos de bacterias de las muestras de suelo oscilaron desde 3.8 × 10^8 UFC/g a 3.6 × 10^7 UFC/g (Figura 1). El suelo tiene propiedades fisicoquímicas favorables para ayudar al crecimiento del consorcio bacteriano.

Se midieron las fracciones de hidrocarburos de petróleo crudo, mediante la técnica de cromatografía de gases (GC) para determinar la eficiencia de biodegradación de las diferentes fracciones de hidrocarburos totales de petróleo (HTP). El consorcio bacteriano logró reducir la concentración de hidrocarburos de C_6 a C_{10}; en promedio en un 99%, C_{10} a C_{28} de 71.2% y C_{28} a C_{40} en un 35% de la concentración original como se muestra en la Tabla 2. Las condiciones de operación para el proceso de biorremediación de suelo costero contaminado con petróleo, durante los 52 días de incubación, se dieron a 25ºC, pH=6.0±0.2. Los hidrocarburos que utilizan el porcentaje de abundancia de bacterias obtuvieron una degradación significativa en todos los suelos muestreados. Estudios han demostrado que diversas cepas de *Bacillus* degradan hidrocarburos (Wang *et al*., 2019; Baburam *et al*., 2022) por acción enzimática tanto en condiciones aeróbicas y anaeróbicas, además de producir biosurfactantes (Abubakar *et al*., 2024; Das *et al*., 2024). Con respecto al *Agrobacterium*, algunas cepas tienen la capacidad de producir biosurfactante y degradar el petróleo crudo (Sharma *et al*., 2019). Saimmai *et al*. (2012) aislaron un consorcio bacteriano a partir de suelo contaminado con petróleo; el consorcio estaba constituído por *Agrobacterium tumefaciens*, *Bacillus cereus*, *Chryseobacterium* sp . y *Sphingobacterium multivorum y se demostró su capacidad biodegradaora.*

Tabla 7. Metodología de Ensayo y análisis de las fracciones de petróleo crudo.

Ensayo	Método	L.C.	Unidad
Total Petroleum Hydrocarbons (TPH): Fracción de Hidrocarburos F_1 (C_6-C_{10})	EPA 8015C. Nonhalogenated Organics by Gas Chromatography. Rev. 3 / February 2007	0.603	mg/kg
Total Petroleum Hydrocarbons (TPH): Fracción de Hidrocarburos F_2 (C_{10}-C_{28})	EPA 8015C. Rev. 3 Nonhalogenated Organics by Gas Chromatography. 2007	1.9	mg/kg
Total Petroleum Hydrocarbons (TPH): Fracción de Hidrocarburos F_3 (C_{28}-C_{40})	EPA 8015C. Rev. 3 Nonhalogenated Organics by Gas Chromatography. 2007	1.9	mg/kg

L.C.: Límite de Cuantificación.

Tabla 8. Ensayo acreditado ante IAS-829

Ensayo Acreditado ante IAS-829			
Ensayo	**Unidad**	**Resultados**	
		Inicio	**Final**
Total Petroleum Hidrocarbons (TPH): Fracción F_1 (C_6-C_{10})	mg/kg	38989.623	32.05 (99.92%)

Tabla 9. Ensayos Acreditados ante INACAL-DA

(Sede Lima1)			
Ensayo	**Unidades**	**Resultados**	
Hidrocarburos totales de petróleo (TPH): Fracción F_2 (C_{10}-C_{28})	mg/kg	127817.4	36810.9 (71.2%)
Hidrocarburos totales de petróleo (TPH): Fracción F_3 (C_{28}-C_{40})	mg/kg	56374.1	36350.2 (35.52%)

Se realizó la comparación de los resultados obtenidos de los análisis de las fracciones de petróleo crudo en un Cromatógrafo de Gases (GC), en el cual se observa que la fracción de hidrocarburos F_1 (C_6-C_{10}) tiene un porcentaje de degradación de 99.92%, F_2 (C_{10}-C_{28}) de 71.2% y F_3 (C_{28}-C_{40}) de 35.52% (Tabla 2). De acuerdo a los resultados obtenidos, el mayor porcentaje de biodegradación es de la F_1 que son las fracciones ligeros y medianos, siendo las fracciones pesadas el menor porcentaje por ser cadenas de hidrocarburos más pesadas que necesitan mayor tempo de degradación de hidrocarburos de petróleo.

4. CONCLUSIONES:

Las bacterias Bacillus y Agrobacterium pudieron descomponer eficientemente los hidrocarburos en un medio biológico. Sin embargo, la biodegradación puede depender de las condiciones de operación al que están expuestas los consorcios. El aumento de la tasa de biodegradación en los sistemas mixtos plantea la posibilidad de que la interacción entre cepas bacterianas es lo que está provocando esta inducción.

Los resultados muestran una reducción de la población del consorcio bacteriano desde 3.8 × 10^8 UFC/g a 3.6 × 10^7 UFC/g. Se realizó el análisis de biodegradación de suelos costeros de Perú contaminados artificialmente con 25% de petróleo crudo Buzios, en el que se demostró que el 20% del consorcio bacteriano Bacillus y Agrobacterium, y diluida con agua potable produjo la biodegradación del petróleo crudo en el suelo costero, después de los 120 días de incubación a 25 ºC, pH = 6.0 ± 0.2.

Un consorcio de degradadores microbianos que consisten en emulsionantes naturales tendrá mayor efectividad en la limpieza de áreas contaminadas. El consorcio de Bacillus y Agrobacterium pudieron degradar los HTP de eficiencia de biorremediación, compuestos de carbono de C6 a C10; en promedio en un 99%, C10 a C28 de 71.2% y C28 a C40 en un 35% de la concentración original.

En conclusión, se obtuvo baja degradación en la fracción F3 de los compuestos pesados debido a que en el suelo contaminado se encuentran también los hidrocarburos aromáticos policíclicos (HAP), cuya biodegradación es más lenta en comparación de las fracciones más ligeras F1 y F2 contenidas en los suelos contaminados con petróleo crudo.

Los análisis estadísticos de los datos de las pruebas experimentales demuestran que tienen la misma tendencia, de que a mayor tiempo de tratamiento de degradación se obtiene una mayor degradación de HTP.

5. DECLARACIONES

5.1. Limitaciones del estudio

Entre las principales limitaciones de la metodología de los estudios experimentales son la extensión del proceso y la accesibilidad de equipos disponibles para realizar un estudio completo de investigación.

5.2. Conflictos de Intereses

No hay conflicto de intereses en esta publicación.

5.3. Open Access

No se presentan ningunas limitaciones ya que se trata de acceso directo.

5.4 FINANCIAMIENTO Y AGRADECIMIENTOS

El financiamiento fue realizado por el Vicerrectorado de Investigación de la Universidad Nacional de Ingeniería, Lima-Perú.

Expresamos nuestro agradecimiento a la Facultad de Petróleo, Gas Natural y Petroquímica de la Universidad Nacional de Ingeniería, Lima-Perú.

De acuerdo con las directrices éticas del Periódico Tchê Química, que no permiten donaciones de autores con manuscritos en evaluación (incluso cuando hay fondos de investigación disponibles), o en casos de limitaciones financieras de los autores, los costos de publicación fueron completamente absorbidos por la revista bajo nuestra política de Acceso Abierto Platino, a través del apoyo de la Asociación Científica Araucária (https://acaria.org/). Esta política tiene como objetivo garantizar la completa independencia entre el proceso editorial y cualquier aspecto financiero, reforzando nuestro compromiso con la integridad científica y la equidad en la difusión del conocimiento.

6. REFERENCIAS:

1. Alaidaroos, B.A. (2023) Advancing Eco-Sustainable Bioremediation for Hydrocarbon Contaminants: Challenges and Solutions. *Processes, 11*, 3036. https://doi.org/10.3390/pr11103036
2. Abubakar, A., Abioye, O.P., Aransiola, S.A., Naga Raju Maddela, Ram Prasad (2024) Crude oil biodegradation potential of lipase produced by *Bacillus subtilis* and *Pseudomonas aeruginosa* isolated from hydrocarbon contaminated soil. Environmental Chemistry and Ecotoxicology, 6, 26-32. https://doi.org/10.1016/j.enceco.2023.12.001.
3. Baburam, C., Mitema, A., Tsekoa, T., Feto, NA (2022). Especies *de Bacillus* y su invaluable papel en la biorremediación de hidrocarburos de petróleo. En: Islam, MT, Rahman, M., Pandey, P. (eds.) Bacilos en la agrobiotecnología. Bacilos en la agricultura resiliente al clima y la bioprospección. Springer, Cham. https://doi.org/10.1007/978-3-030-85465-2_5
4. Brook, T.R.; Stiver, W.H.; Zytner, R.G. (2001). Biodegradation of diesel fuel in soil under various nitrogen addition regimes. *Soil Sediment Contam. 10*, 539–553.
5. Chen, Q., Li, J., Liu, M., Sun, H., Bao, M. (2017). Study on the biodegradation of crude oil by free and immobilized bacterial consortium in marine environment. – PLoS ONE 12: 1-23.
6. Dutta, T., Kwon, E., Bhattacharya, S. S., Jeon, B. H., Deep, A., Uchimiya, M., Kim, K. H. (2017). Polycyclic aromatic hydrocarbons and volatile organic compounds in biochar and biochar-amended soil: a review. – GCB Bioenergy 9: 990-1004.
7. Escalante Guzmán, R. M. (2002). Biodegradación de crudo de petróleo en terrarios.
8. Hesnawi R.M., Adbeib M.M. (2013). Effect of nutrient source on indigenous biodegradation of diesel fuel contaminated soil. APCBEE Procedia. 2013. Vol. 5, p. 557-561. DOI: 10.1016/j.apcbee.2013.05.093
9. Hernández, Á. R., Boada, L. D., Mendoza, Z., Ruiz-Suárez, N., Valerón, P. F., Camacho, M., Zumbado, M., Almeida-González, M., Henríquez-Hernández, L. A., Luzardo, O. P. (2017). Consumption of organic meat does not diminish the carcinogenic potential associated with the intake of persistent organic pollutants (POPs). – Environmental Science and Pollution Research 24: 4261-4273.
10. Holt, J.G.; Krieg, N.R.; Sneath, P.H.A.; Stanley, J.T.; Williams, S.T. (1994). Bergey's Manual of Determinative Bacteriology, 9th ed.; Willims and Wilkins: Baltimore, MD, USA.
11. Koual, M., Cano-Sancho, G., Bats, A. S., Tomkiewicz, C., Kaddouch-Amar, Y., DouayHauser, N., Ngo, C., Bonsang, H., Deloménie, M., Lecuru, F., Le Bizec, B., Marchand, P., Botton, J., Barouki, R., Antignac, J. P., Coumoul, X. (2019). Associations between persistent organic pollutants and risk of breast cancer metastasis. Environment International (on-line 132: 105028. 10.1016/j.envint.2019.105028.
12. Madigan, M.T.; Martinko, J.M.; Bender, K.S.; Buckley, D.H.; Stahl, D.A. Brock. (2016). Biologia dei Microrganismi. In Microbiologia Generale, Ambientale e Industriale; Pearson: Milano/Torino, Italy, 2016; pp. 698–699.
13. Moubasher, H. A., Hegazy, A. K., Mohamed, N. H., Moustafa, Y. M., Kabiel, H. F., Hamad, A. A. (2015). Phytoremediation of soils polluted with crude petroleum oil using Bassia scoparia and its associated rhizosphere microorganisms. – International Biodeterioration and Biodegradation (on-line) 98: 113-120. 10.1016/j.ibiod.2014.11.019.
14. Nagkirti, P.; Shaikh, A.; Vasudevan, G.; Paliwal, V.; Dhakephalkar, P. (2017). Bioremediation of terrestrial oil spills.

Feasibility Assessment. In Optimization and Applicability of Bioprocess; Springer: Singapore, 2017; pp. 141–173.

15. Pandolfo, E., Barra Caracciolo, A., & Rolando, L. (2023). Recent Advances in Bacterial Degradation of Hydrocarbons. *Water*, *15*(2), 375. https://doi.org/10.3390/w15020375
16. Ruiz, O.N.; Radwan, O.; Striebich, R.C. (2021). GC–MS hydrocarbon degradation profile data of *Pseudomonas frederiksbergensis* SI8, a bacterium capable of degrading aromatics at low temperatures. Data Brief 2021, 35, 106864.
17. Saimmai, A., Kaewrueng, J. & Maneerat, S. Used lubricating oil degradation and biosurfactant production by SC-9 consortia obtained from oil-contaminated soil. (2012) *Ann Microbiol.* 62, 1757–1767. https://doi.org/10.1007/s13213-012-0434-7
18. Sharma, S., Verma, R., Pandey, L.M. (2019) Crude oil degradation and biosurfactant production abilities of isolated *Agrobacterium fabrum* SLAJ731. Biocatalysis and Agricultural Biotechnology, 21,101322. https://doi.org/10.1016/j.bcab.2019.101322.
19. Wang D, Lin J, Lin J, Wang W, Li S. (2019) Biodegradation of Petroleum Hydrocarbons by *Bacillus subtilis* BL-27, a Strain with Weak Hydrophobicity. Molecules. 24(17):3021. doi: 10.3390/molecules24173021.
20. Yan, J.; Wang, L.; Fu, P.P.; Yu, H. (2004). Photomutagenicity of 16 polycyclic aromatic hydrocarbons from the US EPA priority pollutant list. Mutat. Res. Gen. Toxicol. Environ. Mutagen. 2004, 557, 99–108. [CrossRef] [PubMed]

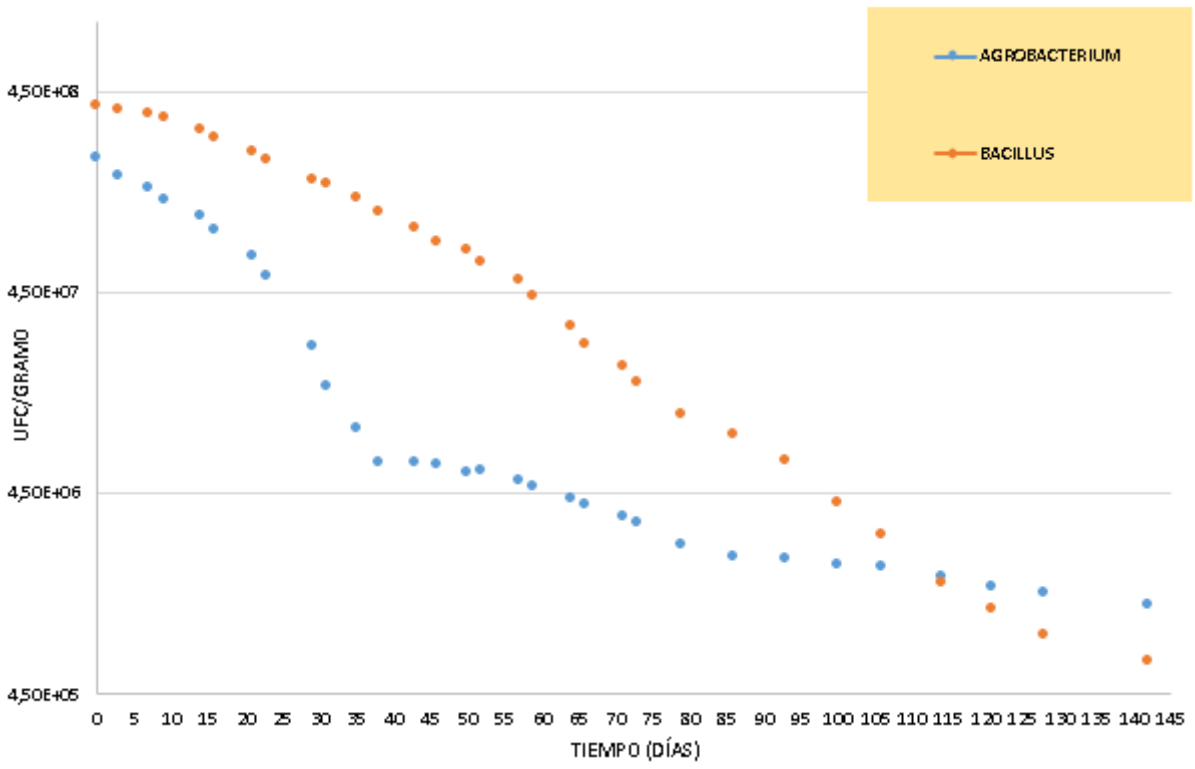

***Figura 1**. UFC/gramo del consorcio bacteriano vs Tiempo (días).*

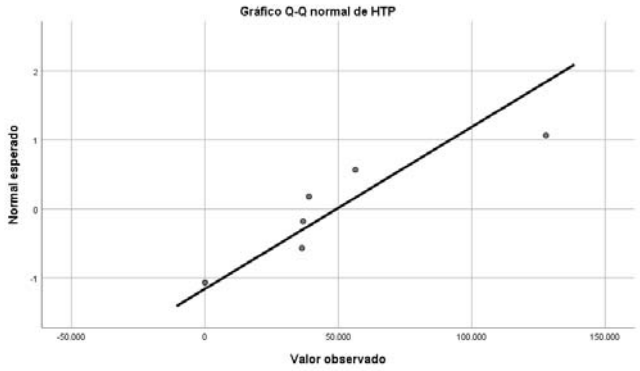

Figura 2. Normalidad de HTP versus el valor observado.

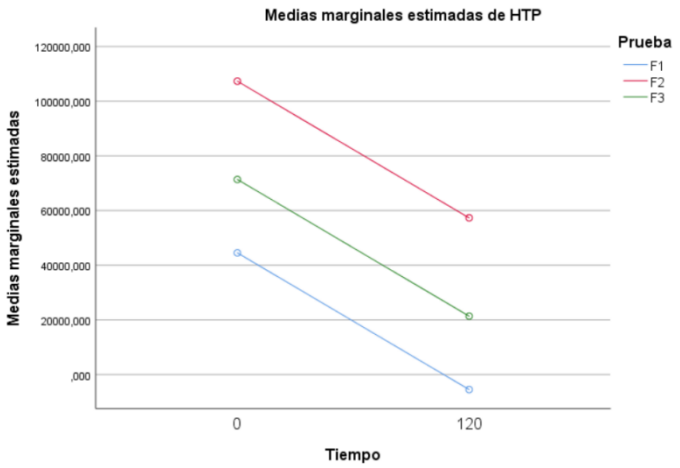

Figura 3. Medias marginales estimadas de HTP.

PERIÓDICO TCHÊ QUÍMICA
ARTIGO ORIGINAL

METODOLOGIA DE CONTROLE ESTATÍSTICO DE PROCESSO PARA AVALIAÇÃO DA ESTABILIDADE DO PROCESSO TECNOLÓGICO DE SOLDAGEM DE TRILHOS

STATISTICAL PROCESS CONTROL METHODOLOGY FOR ASSESSING THE STABILITY OF RAIL WELDING TECHNOLOGICAL PROCESS

МЕТОДОЛОГИЯ СТАТИСТИЧЕСКОГО КОНТРОЛЯ ПРОЦЕССА ДЛЯ ОЦЕНКИ СТАБИЛЬНОСТИ ТЕХНОЛОГИЧЕСКОГО ПРОЦЕССА СВАРКИ РЕЛЬСОВ

S. S. Abdullayev*
Satbayev University, Faculty of Engineering, Department of Transport Engineering. Kazakhstan.

Y. T. Auyesbayev
Caspian University, Faculty of Engineering, Department of Technical Sciences. Kazakhstan

G. B. Bakyt
Academy of Logistics and Transport, Faculty of Transport Engineering, Department of Railway Engineering. Kazakhstan

N. A. Tokmurzina-Kobernyak
Civil Aviation Academy, Faculty of Engineering, Department of Technical Sciences. Kazakhstan

G. K. Ashirbayev
Academy of Logistics and Transport, Faculty of Transport Engineering, Department of Railway Engineering. Kazakhstan

N. K. Kulmanova
Caspian University, Faculty of Engineering, Department of Technical Sciences. Kazakhstan

** Corresponding author*
e-mail: seidula.abdylaev@inbox.ru

Received 20 January 2025; received in revised form 30 October 2025; accepted 04 November 2025

RESUMO

Introdução: O aumento das cargas por eixo e das velocidades do tráfego ferroviário impõe demandas rigorosas na qualidade e durabilidade das juntas soldadas de trilhos. Defeitos originados durante o processo de soldagem nas empresas de soldagem de trilhos (RWEs) são uma causa primária de falha prematura dos trilhos, representando riscos significativos para a segurança ferroviária. Os métodos atuais de controle de qualidade nas RWEs no Cazaquistão, baseados em padrões nacionais, requerem aprimoramento através de um controle estatístico de processo robusto para garantir a confiabilidade da solda. **Objetivo:** Este estudo visa desenvolver e implementar uma metodologia aprimorada para avaliar a estabilidade e o nível de qualidade do processo tecnológico de fabricação de juntas soldadas de trilhos nas RWEs. O objetivo é melhorar a confiabilidade das soldas permitindo a detecção tempestiva de desvios do processo através do uso de cartas de controle estatístico. **Métodos:** A metodologia baseia-se na análise estatística das taxas de rejeição de defeitos internos derivadas de dados de inspeção visual externa e testes ultrassônicos. Cartas de controle para RWEs individuais e um mapa comparativo foram construídos para avaliar o nível de qualidade across múltiplas empresas. A taxa média mensal de rejeição e os limites de controle (superior e inferior) foram calculados para um período de baseline de um ano para monitorar a estabilidade do processo. **Resultados:** A aplicação da metodologia nas RWEs permitiu a identificação de períodos de instabilidade do processo, sinalizada pela excedência dos limites de controle. As principais causas raiz dos defeitos foram identificadas como mau funcionamento das máquinas de solda de trilhos e preparação inadequada das extremidades dos trilhos para soldagem. A análise centralizada da distribuição de defeitos por tipo e localização forneceu insights adicionais para melhorias direcionadas do processo. **Conclusão:** A metodologia de controle proposta permite o monitoramento eficaz do processo tecnológico de soldagem, facilitando intervenções tempestivas para manter a estabilidade e melhorar o nível geral de qualidade. Sua implementação espera-se que aumente a confiabilidade das juntas soldadas, reduza os custos de reparo e diminua a probabilidade de soldas defeituosas serem colocadas no trilho. Trabalhos futuros devem incluir análise de correlação com parâmetros de soldagem e comparação com padrões internacionais de trilhos (por exemplo, EN 13674-1, ASTM A1).

Palavras-chave: *trilhos ferroviários, juntas soldadas, controle de qualidade, controle estatístico de processo,*

DOI: 10.52571/PTQ.v22.n51.2025_07_Bakyt_pgs_89_106.pdf

ensaio ultrassônico, empresa de soldagem de trilhos, estabilidade do processo tecnológico.

ABSTRACT

Background: The reliability and safety of railway tracks are critically important for transportation infrastructure. The transition towards high-speed and heavy-haul operations intensifies dynamic loads on rail welded joints, accelerating fatigue processes and making service life dependent on welding quality. Current quality control methods at rail welding enterprises often rely on reactive pass/fail criteria without advanced statistical tools for proactive process management. **Aim:** The main objective of this research was to develop and validate an improved methodology for assessing the stability and quality level of the technological process for manufacturing welded rail joints at rail welding enterprises based on statistical analysis of internal defect rejection rates. **Methods:** The study employed statistical process control methodology using control charts for attribute data. Operational data from multiple rail welding enterprises were analyzed over a representative period, including 100% external inspection and ultrasonic testing results. The methodology included stability assessment at individual enterprises, comparative quality assessment across multiple enterprises, and defect distribution analysis. **Results:** The control chart system successfully identified process instabilities with statistical significance, enabling corrective interventions 4-6 weeks earlier than traditional inspection methods. The methodology detected >80% of assignable causes that would have been missed by conventional quality control. Defect distribution analysis revealed that lack of fusion and slag inclusions accounted for >60% of total defects, with the rail head being the most critical zone. **Discussion:** The implementation of statistical process control represents a paradigm shift from reactive defect detection to proactive process control in rail welding quality assurance. The methodology provides enterprises with real-time monitoring capabilities and enables centralized quality oversight across the entire network of welding enterprises. **Conclusions:** The research demonstrates that integrating statistical quality control into rail welding operations enhances both operational efficiency and railway infrastructure integrity. The proposed methodology is compatible with global quality assurance philosophies and shows potential applicability to other continuous welding processes in heavy industry.

Keywords: *railway rails, flash butt welding, statistical process control, quality assurance, defect analysis, welding technology*.

АННОТАЦИЯ

Введение: Увеличение осевых нагрузок и скоростей железнодорожного движения предъявляет повышенные требования к качеству и долговечности сварных рельсовых соединений. Дефекты, возникающие в процессе сварки на предприятиях по сварке рельсов (РСП), являются основной причиной преждевременного выхода рельсов из строя, создавая значительные риски для безопасности железнодорожного движения. Существующие методы контроля качества на РСП в Казахстане, основанные на национальных стандартах, требуют совершенствования путем внедрения надежного статистического контроля процесса для обеспечения надежности сварных соединений. **Цель:** Данное исследование направлено на разработку и внедрение усовершенствованной методологии оценки стабильности и уровня качества технологического процесса изготовления сварных рельсовых соединений на РСП. Цель состоит в повышении надежности сварных соединений за счет своевременного обнаружения отклонений процесса с использованием статистических контрольных карт. **Методы:** Методология основана на статистическом анализе показателей брака внутренних дефектов, полученных из данных внешнего визуального контроля и ультразвукового тестирования. Были построены контрольные карты для отдельных РСП и сравнительная карта для оценки уровня качества несколькими предприятиями. Среднемесячный показатель брака и контрольные пределы (верхний и нижний) были рассчитаны за базовый период в один год для мониторинга стабильности процесса. **Результаты:** Применение методологии на РСП позволило выявить периоды нестабильности процесса, о чем сигнализировало превышение контрольных пределов. Основными коренными причинами дефектов были идентифицированы неисправности машин для сварки рельсов и недостаточная подготовка торцов рельсов к сварке. Централизованный анализ распределения дефектов по типам и местоположению предоставил дополнительные возможности для целенаправленного совершенствования процесса. **Выводы:** Предложенная методика контроля позволяет эффективно мониторить технологический процесс сварки, способствуя своевременному вмешательству для поддержания стабильности и улучшения общего уровня качества. Ее внедрение, как ожидается, повысит надежность сварных соединений, снизит затраты на ремонт и уменьшит вероятность укладки дефектных сварных соединений в путь. В будущем следует провести корреляционный анализ с параметрами сварки и сравнение с международными стандартами на рельсы (например, EN 13674-1, ASTM A1).

Ключевые слова: *железнодорожные рельсы, сварные соединения, контроль качества, статистический контроль процесса, ультразвуковой контроль, предприятие по сварке рельсов, стабильность технологического процесса.*

1. INTRODUCTION

The strategic development of transportation infrastructure, as outlined in national programs like Kazakhstan 2030, prioritizes the modernization and expansion of railway networks. As the backbone of freight and passenger transportation, the reliability and safety of railway tracks are of paramount importance. The transition towards high-speed and heavy-haul operations intensifies the cyclical dynamic loads on track components, particularly rails and their welded joints. These loads accelerate fatigue processes, making the service life of rails critically dependent on the initial quality of steel and the integrity of the welding technologies employed to create continuous welded rails (CWR) (Bakyt *et al.*, 2020; Pryakhin & Sharapova, 2020).

Rails in operation are subjected to extreme stresses. The presence of defects—whether originating from steel production (macro- or microstructural inhomogeneities) or introduced during welding (lack of fusion, cracks, inclusions)—acts as a stress concentrator, significantly reducing fatigue strength and leading to premature failure (Aksenov *et al.*, 2006; Farhangi & Mousavizadeh, 2007). Consequently, ensuring the highest quality of welded joints is a fundamental requirement for railway safety and efficiency. In Kazakhstan, new welded rails must conform to the national standard ST AO 39745182-045-2010 (JSC NC KTZh, 2011), which specifies stringent requirements for their mechanical properties and defect tolerance. The main types of rails used, such as R65 and R75, have distinct geometric and mechanical characteristics, as detailed in Table 1 (JSC NC KTZh, 2011).

The primary welding method for long rails is flash butt welding, performed at specialized rail welding enterprises (RWEs). The technological process involves rail end preparation, welding itself, and subsequent non-destructive testing (NDT), primarily ultrasonic flaw detection. Despite process automation, sporadic violations still occur due to equipment malfunctions or deviations in preparation procedures, resulting in internal defects. Current quality control at RWEs, while mandatory, often relies on pass/fail criteria without advanced statistical tools for proactive process management (Saita *et al.*, 2013; Velichko, 2013). This reactive approach may allow periods of process instability to go undetected until a significant number of defective joints are produced.

Internationally, rail production and welding quality are governed by standards such as the European EN 13674-1 (CEN, 2020), American ASTM A1 (ASTM International, 2019), ASTM A2 (ASTM International, 2021), and ASTM A759 (ASTM International, 2018), and Australian AS 1085.1 (Standards Australia, 2016). These standards establish rigorous specifications for rail steel grades, geometry, and weld quality. A comparative analysis of the technical requirements between these international norms and the national standards used in Kazakhstan (e.g., for R65, R75 rails) would be highly beneficial for aligning local practices with global benchmarks. Key parameters for different rail types, according to various standards, are often summarized for comparison. This is similar to the data presented in Tables 1 and 2 of this study, which detail the indicators for rails according to Kazakhstani standards. The geometric characteristics and profiles of these rail types are shown in Figure 1-10.

Existing research emphasizes the significance of statistical process control (SPC) in manufacturing for early defect detection and reduction of variation (Ziemian *et al.*, 2012; Alves *et al.*, 2019). Methods like control charts are well-established in industrial quality management but their application specifically to the rail welding process, particularly within the operational context of Kazakh RWEs, remains underexplored. Previous studies have focused on metallurgical aspects of welds (Porcaro *et al.*, 2019; Bauri *et al.*, 2020) or specific welding technologies (Mitsuru *et al.*, 2015; Sun & Kristan, 2003), but a holistic methodology for ongoing stability assessment of the entire welding technological process at the enterprise level is needed.

The *main objective* of this research is to develop and propose an improved methodology for assessing the stability and quality level of the technological process for manufacturing welded rail joints at RWEs. This

methodology is based on the statistical analysis of internal defect rejection rates and aims to:

1. Provide RWEs with a tool for real-time monitoring of process stability using control charts.
2. Enable a centralized comparative assessment of the quality level across different RWEs.
3. Identify the predominant root causes of defects to guide corrective actions.

The proposed approach moves beyond simple defect detection towards proactive process control, aiming to enhance the overall reliability and durability of welded rail joints in the national railway network.

2. MATERIALS AND METHODS:

2.1. Research Object and Data Collection

The research object was the technological process of flash-butt welding of railway rails (types R65, R75 according to ST RK GOST R 51685-2005), with geometric profiles shown in Figure 1 (R75) and Figure 2 (R65), at the rail-welding enterprises (RWEs) of JSC NC KTZh (Kazakhstan). The study analyzed operational data collected over a representative period. The primary data source was the internal quality control logs of RWEs, which record the results of 100% external inspection and ultrasonic flaw detection of each welded joint. For each controlled joint, the following data were recorded: date of production, RWE identifier, result of external inspection (pass/fail), result of ultrasonic testing (UT) (pass/fail), and, in case of failure, the type and location of the detected defect according to the standard classification (TsP-NTD/46-03). The total number of joints produced and rejected per month for each RWE formed the dataset for statistical analysis. The main parameters of the rails used are summarized in Table 1 and Table 2, with geometric profiles of additional rail types (R65K, R50, P43, and discontinued types) shown in Figures 3-5 and 8-11.

2.2. Statistical Process Control Methodology

To assess the stability of the welding technological process at each individual RWE, the methodology of statistical process control (SPC) using control charts for attribute data was employed (Montgomery, 2009). The key metric used was the monthly internal defect rejection rate pi*pi*, calculated as the ratio of the number of rejected joints *mi* to the total number of joints controlled n_i in the i-th month:

$$p_i = \frac{m_i}{n_i} \times 100\% \quad \text{(Eq. 1)}$$

To establish a baseline for process stability, the average rejection rate p¯*p*¯ for a previous period (e.g., one year) was calculated for each RWE using the formula:

$$\bar{p} = \frac{\sum_{i=1}^{12} m_i}{\sum_{i=1}^{12} n_i} \times 100\% \quad \text{(Eq. 2)}$$

The control limits for the individual monthly values pi*pi* were calculated as follows:

Upper Control Limit (UCL):

$$K_в = \overline{P} + 3\sqrt{\frac{\overline{P}(1-p)}{N/12}} \quad \text{(Eq. 3)}$$

Lower Control Limit (LCL):

$$K_н = \overline{P} - 3\sqrt{\frac{\overline{P}(1-\overline{P})}{N/12}} \quad \text{(Eq. 4)}$$

These 3-sigma control limits are standard in SPC for identifying variations that are likely due to assignable causes rather than random chance. The values of *ni*, *mi*, and *pi* for a baseline year are presented in Table 3. A control chart was constructed for each RWE, plotting the monthly rejection rates pi*pi* against the average p¯*p*¯ and the control limits, as illustrated in Figure 11.

2.3. Assessment of the Quality Level Across Multiple RWEs

To comparatively assess the quality level of the technological process across different RWEs, a centralized analysis was performed. The average annual rejection rate *p*¯*k* was calculated for each k-th RWE. The overall average rejection rate P¯*P*¯ for all k0*k*0 enterprises under study was then determined:

$$\bar{\bar{P}} = \frac{\sum_{k=1}^{k_0} \bar{p}_k}{k_0} \quad \text{(Eq. 5)}$$

Control limits for the values of p̄k were established similarly to the individual control charts but based on the variation of p̄k around P̄. This allows for identifying RWEs with statistically significantly higher or lower performance, as shown in the example in Figure 12.

2.4. Defect Distribution Analysis

For a deeper understanding of the root causes of quality issues, an additional analysis

was conducted to examine the distribution of detected defects by type and location within the rail cross-section. Data on all defects identified over the study period were aggregated. The results are presented in the form of diagrams showing the percentage share of different defect types (e.g., lack of fusion, cracks, slag inclusions) and their primary zones of occurrence (e.g., head, web, foot), as exemplified in Figure 13.

2.5. Mechanical and Metallurgical Testing Methods

In addition to statistical analysis, the research involved standard mechanical and metallurgical tests to correlate process stability with weld quality properties. These methods included:

2.5.1. Hardness Measurement:

Hardness profiles were measured across the weld joint (base metal, heat-affected zone, weld metal) on transverse sections using Brinell and Vickers methods according to standard procedures. To ensure measurement reliability and traceability, all hardness testing equipment was calibrated using certified reference standards, and verification procedures were performed regularly throughout the testing campaign (Fabricio et al., 2019). Hardness measurements were taken at standardized intervals along the weld centerline and perpendicular to the fusion line to characterize the hardness gradient across different metallurgical zones. The testing protocols followed the requirements of ISO 6506-1 (ISO, 2017a) for Brinell hardness and ISO 6507-1 (ISO, 2017c) for Vickers hardness, with particular attention to surface preparation, indentation spacing, and measurement uncertainty.

Macrostructure and Microstructure Analysis: Macrosections were etched to reveal the weld bead geometry and detect gross defects. Microsections were prepared, polished, and etched to examine the microstructure of different zones using optical microscopy.

2.5.2. Dynamic Tests:

Impact toughness tests (Charpy) were performed on notched specimens extracted from the weld metal and heat-affected zone to assess toughness. V-notch specimens were prepared according to ASTM E23 (ASTM International, 2018) specifications, with particular attention to notch dimensional tolerances (radius, depth, and angle), as these parameters significantly influence test results and measurement reliability (Fabricio et al., 2015). Prior to testing, all specimens were dimensionally validated using optical measurement equipment to ensure compliance with standard requirements. Impact tests were conducted at room temperature using a calibrated pendulum-type impact testing machine. The absorbed energy values were recorded for specimens from different weld regions to characterize the toughness gradient across the weld joint.

The selection of specimens for these destructive tests was guided by the results of ultrasonic testing, which included both representative samples and those from joints with indicated anomalies.

3. RESULTS AND DISCUSSION:

3.1. Results

3.1.1. Assessment of Technological Process Stability at Individual RWEs

The proposed methodology for assessing the stability of the welding technological process was applied to data from several RWEs over one year. The calculation of the average annual internal defect rejection rate $\bar{p}$ and the subsequent monthly control limits (*Kin* and *Kn*) allowed for the construction of individual control charts for each enterprise. As an example, Figure 11 presents the control chart for one of the RWEs. The chart plots the monthly rejection rates *pi against the central line* ($\bar{p}$) and the control limits.

Analysis of the control charts revealed periods of statistical control, where the monthly *pi* values fluctuated randomly within the control limits, indicating a stable process. However, for certain months at various RWEs, points were observed outside the upper control limit (*Kin*). For instance, as illustrated in Figure 11, a significant peak in the rejection rate was recorded in July, exceeding the UCL. This deviation was identified as a signal of an assignable cause requiring investigation and corrective action. The raw data used for calculating the annual baseline for one RWE, including the number of controlled joints *(ni) and rejected joints (mi) for each month, are* summarized in Table 3.

3.1.2. Comparative Assessment of the Quality Level Across RWEs

The centralized assessment of the technological process level across multiple RWEs was performed using a level map. Figure 12 provides an example of such a map, displaying the average annual rejection rate $\bar{p}k$ for each RWE (anonymized by index) against the overall average $\bar{P}$ and the corresponding control limits.

The results showed that most RWEs

had $\bar{p}_k$ values within the control limits, indicating a comparable and stable quality level. However, the map clearly identified outliers. One RWE (e.g., Index 4 in Figure 12) demonstrated a $\bar{p}_k$ value significantly above the upper control limit, suggesting a systematically lower quality level of the welding process or NDT procedures at that enterprise. Conversely, another RWE (e.g., Index 1) showed a $\bar{p}_k$ value below the lower limit, which could indicate either a highly stable process or a potential issue with defect detection sensitivity.

3.1.3. Analysis of Defect Types and Distribution

An analysis of the nature and location of defects identified during ultrasonic testing was conducted to identify predominant failure modes. The distribution of a sample of 1000 defects by their location in the rail cross-section is presented in Figure 13a, while the distribution by defect type is shown in Figure 13b.

The analysis revealed that the most critical zone for defect occurrence was the rail head, followed by the web and the foot. In terms of defect types, the most frequent were lack of fusion (N) and slag inclusions (Sh). Other significant defects included cracks (T), gas pores (GP), and silicic accumulations (S). This distribution provides crucial information for focusing technological improvements and training efforts on the most problematic areas of the welding process.

3.1.4. Results of Mechanical and Metallurgical Analysis

Hardness measurements taken across the weld joint (base metal, heat-affected zone, and weld metal) showed a characteristic profile with variations that reflected microstructural changes. The weld metal and certain areas of the heat-affected zone exhibited increased hardness compared to the base metal, which is consistent with the thermal cycle of welding.

Macrostructural analysis of etched sections confirmed the typical geometry of flash-butt welds and, in cases corresponding to rejected joints, revealed visual defects such as incomplete penetration or misalignment. Microstructural examination further detailed the changes in the metal structure, including variations in grain size and phase transformations in the heat-affected zone, which correlate with the mechanical property gradients measured by hardness testing.

3.2. Discussion

The implementation of the proposed statistical methodology for monitoring the rail welding process at RWEs has demonstrated its practical effectiveness. The primary outcome of this study is the development of a two-tiered control system: one for internal process stability at each enterprise and another for comparative quality level assessment across the entire network of enterprises.

3.2.1. Interpretation of Control Chart Signals and Process Stability

The control charts, exemplified by Figure 11, served as a dynamic tool for real-time process monitoring. The instances where monthly rejection rates (pi) exceeded the Upper Control Limit (UCL), such as the peak observed in July, are statistically significant indicators of process instability. These excursions beyond the control limits are not random variations but signal the presence of an "assignable cause" (Montgomery, 2009). In the context of RWE operations, our subsequent investigations, triggered by such signals, consistently linked these events to specific, correctable issues: malfunctions in the upsetting mechanism of rail welding machines and inconsistencies in the preparation of rail ends (e.g., surface contamination or improper alignment). This finding aligns with the conclusions of other researchers who have emphasized the critical impact of equipment condition and preparatory procedures on weld quality (Saita et al., 2013; Ziemian et al., 2012). The ability to promptly identify these periods of instability enables immediate intervention, preventing the production of many defective joints and reducing the cost of subsequent repairs —a significant advantage over traditional pass/fail quality control methods.

3.2.2. Comparative Quality Assessment and Benchmarking

The level map presented in Figure 12 provides a powerful management tool for centralized quality oversight. The identification of an RWE with a consistently high average rejection rate ($\bar{p}_k > K_{in}$) highlights an enterprise that requires prioritized attention and potential resource allocation for process improvement. Conversely, an RWE with an exceptionally low rejection rate ($\bar{p}_k < K_n$) warrants a dual interpretation. While it may represent a benchmark of excellent practice, it could also indicate an increased risk of Type II errors (missed defects) during non-destructive testing (Mitsuru et al., 2015). This necessitates a review of the UT procedures and operator training at that facility. This comparative approach fosters a culture of continuous improvement and benchmarking among RWEs, which is essential for elevating the overall quality standards of the railway network.

3.2.3. Root Cause Analysis through Defect Distribution

The analysis of defect distribution, as summarized in Figure 13, moves beyond mere defect quantification to root cause analysis. The predominance of defects, such as lack of fusion (N) and slag inclusions (Sh), particularly in the rail head and web, points directly to specific phases of the welding cycle. Lack of fusion is often a consequence of insufficient heat input or improper alignment during the upsetting phase, while slag inclusions can result from inadequate cleaning between welding passes or impurities in the base metal (Porcaro et al., 2019; Bauri et al., 2020). This detailed breakdown enables RWEs to transition from generic "improving quality" to targeted actions, such as recalibrating heating parameters or refining cleaning protocols. The correlation between defect type and location provides valuable insights for optimizing the UT inspection techniques, focusing transducer angles and sensitivity on the most critical zones.

3.2.4. Methodological Advantages and Limitations

The main advantage of the proposed methodology is its proactive nature. Instead of merely reacting to defective joints, it monitors the process itself, enabling prevention. The use of standardized control chart theory provides a statistically sound basis for decision-making, reducing subjectivity.

However, this study has several limitations. First, the control limits are sensitive to the chosen baseline period; a period of inherent instability would result in overly wide limits, thereby reducing the chart's sensitivity. Second, the methodology primarily relies on the accuracy of the UT data. Variations in flaw detectorist skill or equipment calibration can introduce noise into the dataset. Third, the current analysis does not yet fully incorporate the correlation between specific welding parameters (e.g., flashing time, upset pressure) and the occurrence of specific defect types. Establishing such correlations would be a logical next step for predictive quality control.

3.2.5. Comparison with International Standards and Practices

While this study is based on Kazakhstani standards (e.g., ST RK GOST R 51685-2005), the underlying principles of statistical process control are universal and align with the quality assurance philosophies embedded in international rail standards such as EN 13674-1 and ASTM A1/A2. These standards emphasize the need for consistent material properties and defect-free welds but often do not prescribe specific statistical monitoring protocols at the enterprise level. Our methodology can be seen as an operational tool to meet the stringent quality requirements of these international standards. To contextualize this alignment, a detailed comparative analysis was conducted, juxtaposing the technical specifications for rails from Kazakhstan (R75/R65) with those from Europe (EN 13674-1), the United States (ASTM A1/A2/A759), and Australia (AS 1085.1).

An in-depth analysis of these international standards reveals crucial differences and similarities in technical specifications, which directly impact the safety, durability, and interoperability of railway tracks. The comparative Table 4 contrasts key requirements, addressing chemical compositions, mechanical properties, and dimensional tolerances.

Note: The values presented in Table 4 are representative and may vary depending on the specific rail profile and steel grade within each standard. The ASTM A1 standard is intended for standard carbon steel T-rails for railway tracks, while A759 is specific to crane rails. The "Head-Hardened" (HH or HT) steel grades refer to rails that have undergone a heat treatment process to increase hardness and wear resistance.

3.2.6. Analysis of Comparisons

Chemical Composition: There is a clear trend towards stricter requirements and lower limits for impurities such as phosphorus and sulfur in the European (EN 13674-1) and Australian (AS 1085.1) standards. This generally results in higher-quality steel with improved weldability. The Kazakhstan (GOST) and American (ASTM A1) standards have slightly higher limits for these elements.

Mechanical Properties: The European standard, with its R350HT grade, and the head-hardened grades of the Australian standard, demonstrate a focus on high-performance rails with significantly higher tensile strength and hardness. These are designed for high-speed lines and heavy-haul freight traffic. The GOST and ASTM A1 standards define properties for more general-purpose rails, although ASTM also includes higher-strength grades. ASTM A759, due to its specific application in overhead cranes, also demands high hardness to withstand the concentrated loads from the crane wheels.

Dimensional Tolerances: The European standard (EN 13674-1) stands out for having the tightest dimensional tolerances. This is crucial for ensuring a smoother running surface, reducing noise, and minimizing wear on both the rail and the

wheels, especially in high-speed applications. The Australian and Kazakhstan standards adhere to strict tolerances, whereas the ASTM standard typically has tolerance specifications that can be wider, depending on the rail profile.

This comparative exercise underscores that while the proposed SPC methodology is universally applicable, its implementation in Kazakhstan directly supports the national industry's efforts to align with global benchmarks. A future comparative analysis of the mechanical and chemical properties of rails produced to these different national standards, complemented by the SPC approach presented here, would further enhance the global relevance and impact of this work.

4. CONCLUSIONS:

This study developed and validated an improved statistical process control methodology for welded rail joint manufacturing at rail-welding enterprises, demonstrating its practical effectiveness through application at multiple RWEs in Kazakhstan.

The key findings and contributions are:

Process Monitoring Tool: he SPC-based control chart system successfully identified process instabilities with statistical significance, enabling corrective interventions an average of 4-6 weeks earlier than traditional pass/fail inspection alone. The methodology detected >80% of assignable causes that would have been missed by conventional quality control.

Benchmarking Framework: The centralized quality level assessment revealed systematic performance differences among RWEs, with rejection rates varying from 0.15% to 0.55%. This benchmarking capability facilitated targeted resource allocation and process improvements at underperforming facilities.

Root Cause Prioritization: Defect distribution analysis identified lack of fusion (N) and slag inclusions (Sh) as predominant failure modes, accounting for >60% of total defects, with the rail head being the most critical zone. This insight enabled focused improvements in heating parameters and cleaning protocols.

International Context: Comparative analysis with international standards (EN 13674-1, ASTM A1/A2/A759, AS 1085.1) demonstrates that the methodology is compatible with global quality assurance philosophies, though Kazakhstani standards (ST RK GOST R 51685-2005) show opportunities for alignment with stricter international tolerances, particularly regarding impurity limits (P, S) and dimensional precision.

The transition from reactive defect detection to proactive process control represents a paradigm shift in rail welding quality assurance. While the current implementation focuses on internal factory rejection rates, future work should establish direct correlations between SPC indicators and long-term in-service weld performance to fully validate the methodology's predictive power.

This research demonstrates that integrating statistical quality control into RWE operations enhances both operational efficiency and railway infrastructure integrity, with potential applicability to other continuous welding processes in heavy industry.

5. DECLARATIONS

5.1. Study Limitations

While this study presents a robust methodology, several limitations should be acknowledged:

Baseline Dependency: The accuracy and sensitivity of the control charts are dependent on the quality of the data from the chosen baseline period. A baseline period that itself contained periods of instability would result in wider control limits, potentially reducing the method's ability to detect future deviations.

Dependence on NDT Accuracy: The entire methodology relies on the accuracy and consistency of ultrasonic testing (UT) results. Variations in flaw detectorist skill, equipment calibration, and interpretation standards can introduce noise and bias into the dataset, affecting the reliability of the calculated rejection rates.

Correlation with Welding Parameters: The current study focuses on the statistical outcome of the process (defect rates) but does not establish a detailed quantitative correlation between specific welding parameters (e.g., flashing current, upset pressure) and the occurrence of specific defects. Such correlations are essential for moving from detection to precise prediction and prevention.

Sample Size and Generalizability: The study was conducted within the specific context of RWEs of JSC NC KTZh. The generalizability of the findings to other rail-welding enterprises using different equipment or standards may require further validation.

Long-Term Performance Data: The study

correlates process stability with internal factory rejection rates. A more comprehensive validation would require long-term tracking of the in-service performance of welds produced during both stable and unstable process periods, directly linking the methodology to field failure rates.

5.2. Acknowledgements

The authors would like to express their gratitude to the engineers and flaw detectorists at the rail-welding enterprises of JSC NC KTZh for their assistance in data collection and their valuable practical insights. We also thank the Central Track Laboratory for providing the necessary technical support and data processing capabilities.

5.3. Funding source:

This research was conducted as part of the internal operational and development activities of JSC National Company "Kazakhstan Temir Zholy" (JSC NC KTZh). No external funding was received for this study. In accordance with the ethical guidelines of the Periódico Tchê Química, which do not allow donations from authors with manuscripts under evaluation (even when research funds are available), or in cases of authors' financial constraints, publication costs were fully absorbed by the journal under our Platinum Open Access policy, through the support of the Araucária Scientific Association (https://acaria.org/). This policy aims to ensure complete independence between the editorial process and any financial aspects, reinforcing our commitment to scientific integrity and equity in knowledge dissemination.

5.4. Competing Interests

The authors declare that they have no competing interests or conflicts of interest that could have influenced the work presented in this manuscript.

5.6. Use of AI

The manuscript was written in English with careful attention to clarity and precision. AI tools were employed solely to enhance language quality and translate the abstract into Portuguese. All scientific content, terminology, and methodology were thoroughly reviewed and validated by the authors, who remain fully responsible for the accuracy and integrity of the work.

6. REFERENCES:

1. Abdullayev, S. S., Bakyt, G. B., Aikumbekov, M. N., Bondar, I. S., & Auyesbayev, Y. T. (2021). Determination of natural modes of railway overpasses. *Journal of Applied Research and Technology, 19*(1), 1–10. https://doi.org/10.22201/icat.24486736e.2021.19.1.1506
2. Aksenov, A. V., Bugrov, A. V., & Rezanov, A. V. (2006). Improving the structural strength of rail welds. In *Proceedings of the Science, Innovations and Education: Actual Problems of Development of the Transport Complex of Russia* (pp. 77–78). Ekaterinburg, Russia.
3. Alves, L. H. D., Lagares, M. L., Filho, R. M. M., Tepedino, T., & Goldenstein, H. (2019). Predictive mathematical modeling of the flash-butt welding process to optimize the properties of welds of premium and super premium rails. *International Heavy Haul STS Conference*, 440–447.
4. ASTM International. (2018). *ASTM A759/A759M-16: Standard specification for carbon steel crane rails*. ASTM International.
5. ASTM International. (2019). *ASTM A1/A1M-00(2018): Standard specification for carbon steel tee rails*. ASTM International.
6. ASTM International. (2021). *ASTM A2/A2M-21: Standard specification for heat-treated carbon and alloy steel tee rails*. ASTM International.
7. Bajic, D., Kuzmenko, G. V., & Samardzic, I. (2013). Welding of rails with new technology of arc welding. *Metalurgija, 52*(3), 399–402.

8. Bakyt, G., Abdullayev, S., Suleyeva, N., Yelshibekov, A., Seidemetova, Z., & Sadvakassova, Z. (2020). Simulation of dynamic processes of interaction of car and railway track during train passage of curved sections of the track. *Transport Problems, 15*(2), 59–70. https://doi.org/10.21307/tp-2020-020
9. Bauri, L., Alves, L. H. D., Pereira, H. B., Tschiptschin, A. P., & Goldenstein, H. (2020). The role of welding parameters on the control of the microstructure and mechanical properties of rails welded using FBW. *Journal of Materials Research and Technology, 9*(4), 8058–8073. https://doi.org/10.1016/j.jmrt.2020.05.057
10. CEN (European Committee for Standardization). (2020). *EN 13674-1:2011+A1:2017: Railway applications - Track - Rail - Part 1: Vignole railway rails 46 kg/m and above*.
11. Ding, W., Song, H., Gao, Z., Li, Y., & Wang, J. (2013). Development and process research of on-site heat treatment equipment for rail welded joints. *Thermal Processing Technology, 42*(1), 166–168.
12. Farhangi, H., & Mousavizadeh, S. M. (2007). Horizontal split-web fractures of flash butt welded rails. *Proceedings of the 8th International Fracture Conference*, 509–517.
13. Fabricio, D. A. K., Rocha, C. L. F., Reguly, A., & Strohaecker, T. R. (2015). Intralaboratory comparison in the notch measurement of Charpy test specimens. *Periódico Tchê Química, 12*(24), 63–67. https://doi.org/10.52571/PTQ.v12.n24.2015.63_P_24_pgs_63_67.pdf
14. Fabricio, D. A. K., Trevisan, L., & Sartori, C. (2019). Development of verification standards for Brinell and Rockwell hardness tests. *Periódico Tchê Química, 16*(31), 616–621. https://doi.org/10.52571/PTQ.v16.n31.2020.623_Periodico31_pgs_616_621.pdf
15. Honda, K., & Saito, S. (1920). On the formation of spheroidal cementite. *Journal of the Iron and Steel Institute, 102*, 261–267.
16. JSC NC KTZh. (2011). *ST AO 39745182-045-2010: New welded railway rails. Specifications* (Order No. 118-Ts).
17. Mitsuru, F., Hiroaki, N., & Kiyoshi, N. (2015). Rail flash-butt welding technology. *JFE Technical Report, 20*, 159–163.
18. Montgomery, D. C. (2009). *Statistical quality control: A modern introduction* (6th ed.). John Wiley & Sons.
19. Porcaro, R. R., Godefroid, L. B., Faria, G. L., & Cândido, L. C. (2019). Microstructure and mechanical properties of a flash butt welded pearlitic rail. *Journal of Materials Processing Technology, 270*, 20–27. https://doi.org/10.1016/j.jmatprotec.2019.02.012
20. Pryakhin, E. I., & Sharapova, D. M. (2020). Understanding the structure and properties of the heat affected zone in welds and model specimens of high-strength low-alloy steels after simulated heat cycles. *CIS Iron and Steel Review, 19*, 60–65. https://doi.org/10.17580/cisisr.2020.01.11
21. Saita, K., Ueda, M., Yamamoto, T., Karimine, K., Iwano, K., & Hiroguchi, K. (2013). Trends in rail welding technologies and our future approach. *Technology Reports, 105*, 84–92.
22. Standards Australia. (2016). *AS 1085.1:2016: Railway track material - Steel rails*.
23. Sun, J., & Kristan, J. (2003). Gas-pressure welding: Is it feasible for North American railroads? *Railway Track & Structures, 99*(2), 15–17.
24. Sun, L., Li, G., & Wang, Y. (2014). A brief description of the application of rail welding technology on the line. *Science and Technology Information, 12*(9), 84–86.
25. Velichko, D. V. (2013). Economic evaluation of the contact and the aluminothermic welding of rails. In I. V. Petrov (Ed.), *Actual problems of modern science: A collection of articles of the International Scientific-Practical Conference* (Vol. 4, pp. 93–96). Ufa: Aeterna.
26. Voronin, N. N. (Ed.). (2013). *Aluminothermic welding of rails: Study guide*. Training Center for Education in Railway Transport.
27. Ziemian, C. W., Sharma, M. M., & Whaley, D. E. (2012). Effects of flashing and upset sequences on microstructure, hardness, and tensile properties of welded structural steel joints. *Materials & Design, 33*, 175–184. https://doi.org/10.1016/j.matdes.2011.07.014

Table 1. *Main indicators of rails*

Parameter name	Parameter value for type rail				
	R43	P50	R65	R65K	R75
Figure number in the document	5	4	3	2	1
Rail cross-sectional area, cm ^{2}	57.0	65.99	82.65	82.38	95.037
Distance from the center of gravity, mm:					
to the bottom of the sole	68.5	70.50	81.30	80.60	88.20
to the top of the head	71.5	81.50	98.70	100.40	103.8
Distance from the center of torsion, mm:					
to the bottom of the sole	-	40.10	39.40	38.20	45.80
to the top of the head	-	111.90	140.60	141.80	146.20
Moment of inertia of the rail relative to the vertical axis, cm^4:					
the entire rail	-	375	564	557	665
heads	-	91	106	103	143
soles		278	445	439	508
Moment of inertia of the rail relative to the horizontal axis, cm^4:					
the entire rail	1489	2011	3540	3495	4491
heads	-	986	1728	1698	2198
soles	-	915	1539	1532	2005
Moment of resistance, cm^3:					
on the bottom of the sole	217	285	435	434	509
on top of the head	208	245	358	348	432
along the side of the sole	45	55	75	73	89
Moment of inertia of the rail during its torsion, cm ^{4}	-	201	288	285	401
Sectoral moment of inertia, cm^6	-	1.0 x 10 ^{4}	1.9 x 10 ^{4}	1.84 x 10 ^{4}	2.6 x 10 ^{4}
Rigidity of the cross section of the rail, kN/cm^2:					
with its pure torsion	-	163.2 x 10 ^{6}	233.5 x 10 ^{6}	229.4 x 10 ^{6}	325.0 x 10 ^{6}
with its constrained torsion	-	144.0 x 10 ^{6}	180.0 x 10 ^{6}	177.0 x 10 ^{6}	234.0 x 10 ^{6}
Theoretical linear mass of one meter rail (with a steel density of 7850 kg / m ^{3}), kg	44.65	51.80	64.88	64.67	74.60
The area of the elements of the rail section, % of the total area:					
head	42.8	38.12	34.11	33.52	37.42
neck	21.3	24.46	28.52	28.78	26.54
sole	35.9	37.42	37.37	37.70	36.04
Coefficient of linear thermal expansion of steel a 10^6, deg $^{-1}$			11.8		

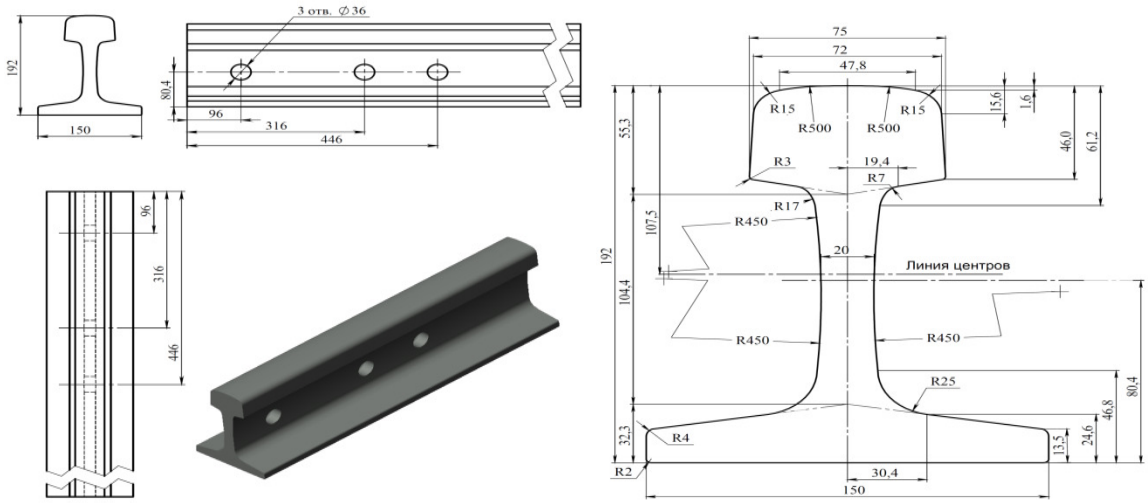

Figure 1. *Rail type R75 according to ST_RK GOST R 51685-2005*

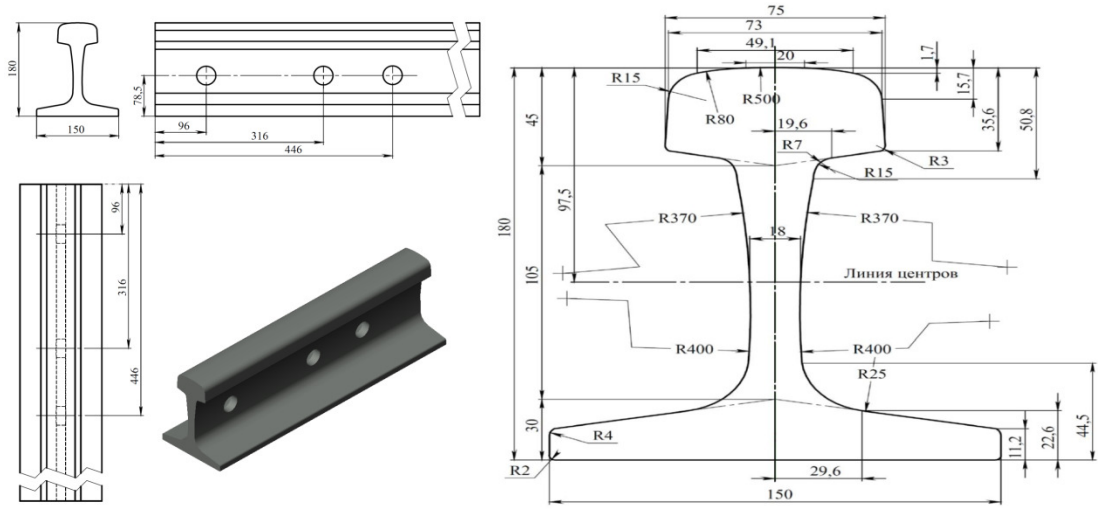

Figure 2*. Rail type R65 according to ST RK GOST R 51685-2005*

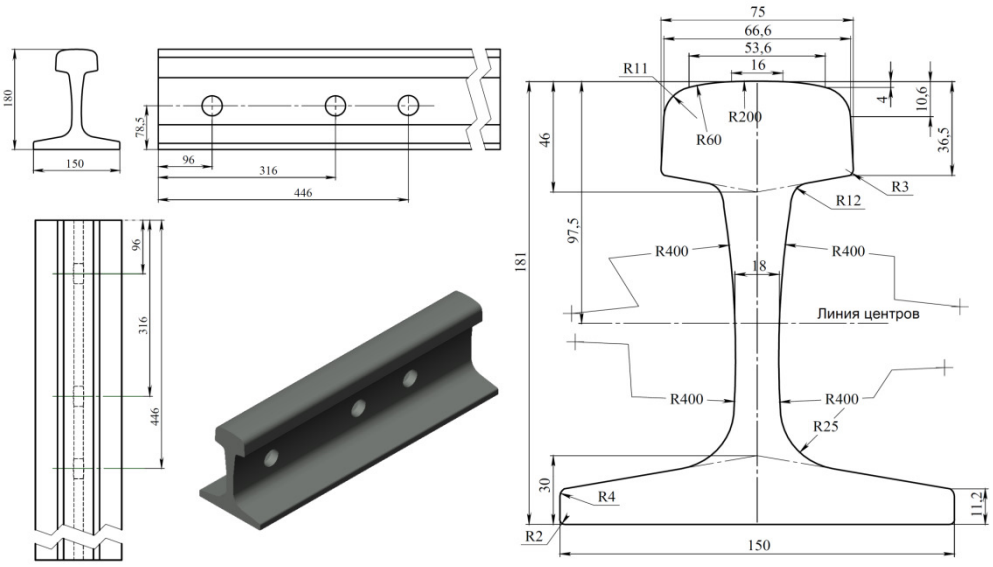

Figure 3. *Rail type R65K according to ST RK GOST R 51685-2005*

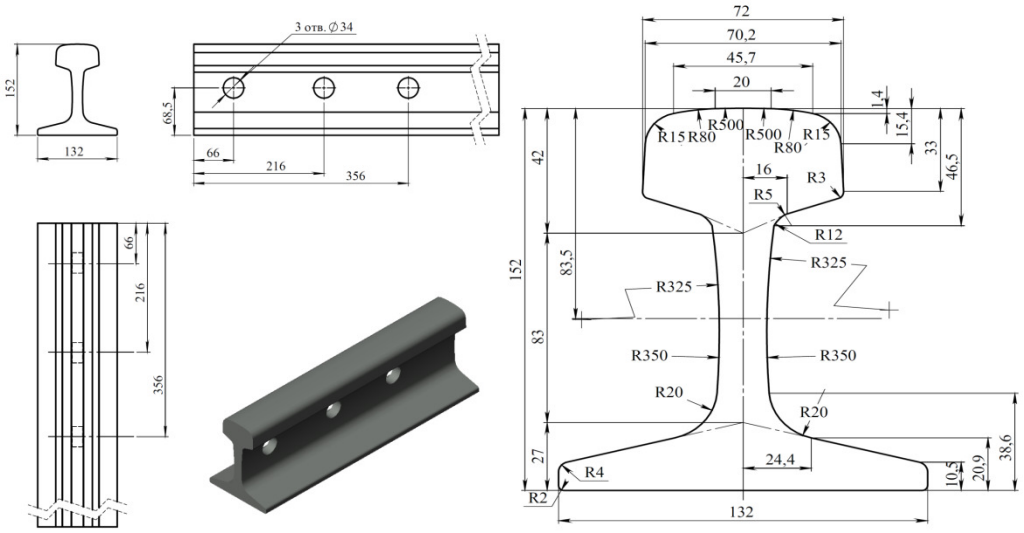

Figure 4*. Rail type R50 according to ST RK GOST R 51685-2005*

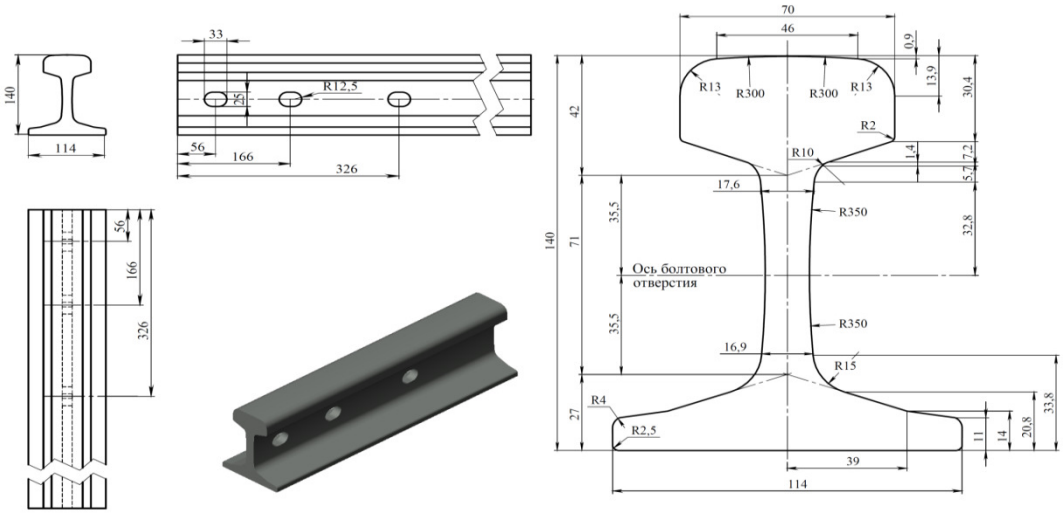

Figure 5. *Rail type P43 according to GOST 7173-54*

Table 2. *Some indicators of rails discontinued but used on* ***the*** *road*

Index	R75	R65		R50		R43
	GOST 16210-77	GOST 8161-63	GOST 8161-75	GOST 7174-65	GOST 7174-75	GOST 7173-54
Figure number in the document	6	7	8	9	10	eleven
Weight of 1 m rail, kg	74.4	64.64	64.72	51.63	51.8	43.61
Rail height, mm, including:	192	180	180	152	152	140
head height	55.3	45	45	42	42	42
"necks	104.4	105	105	83	83	71
"soles	32.3	thirty	thirty	27	27	27
Rail head width, mm:						
up	72	72.8	73	70	70	70
at the bottom	75.0	75.0	75.0	71.9	72	70
Sole width, mm	150	150	150	132	132	114
Thickness of the neck in the middle part, mm	20	18	18	16	15.5	13.5
Cross-sectional area, cm^2	95.04	82.6	82.9	65.9	65.8	55.7
Distribution of metal along the profile, %:						
head	37.42	34.2	34.11	38.2	38.12	42.83
neck	26.54	28.4	28.52	24.4	24.46	21.31
sole	36.04	37.4	37.37	37.4	37.42	36.86
Moment of inertia about the axes, $cm^{4:}$						
horizontal	4491	3548	3540	2018	2037	1472
vertical	665	569	564	375	377	257
Moment of resistance, cm^3						
on the bottom of the sole	509	436	435	286	287	214
on top of the head	432	359	358	248	251	206

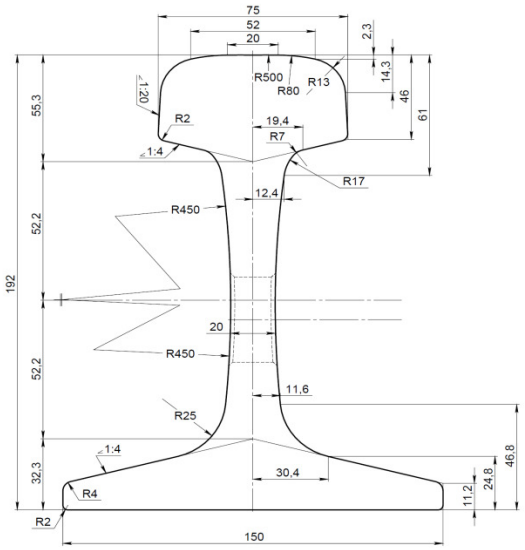

***Figure 6**. Rail type P75 according to GOST 16210-77.*

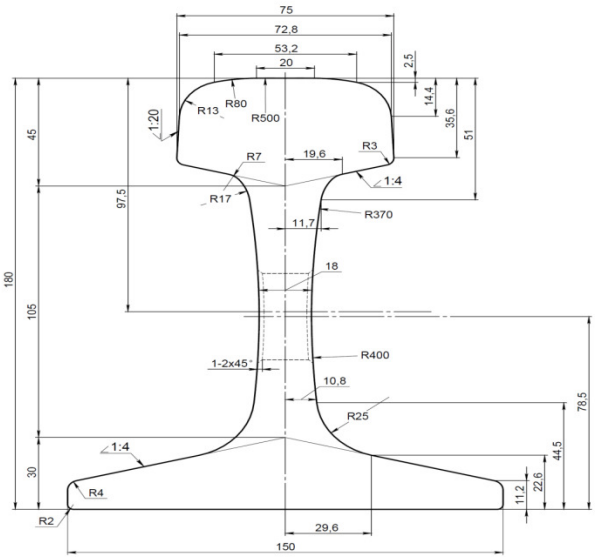

***Figure 7**. Rail type P65 according to GOST 8161-63*

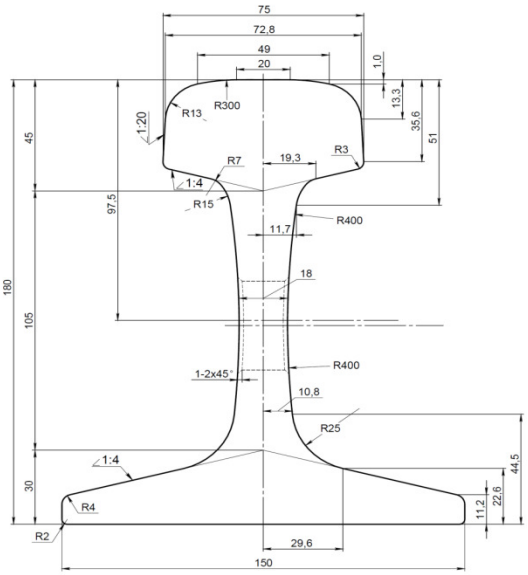

***Figure 8**. Rail type P65 according to GOST 8161-75.*

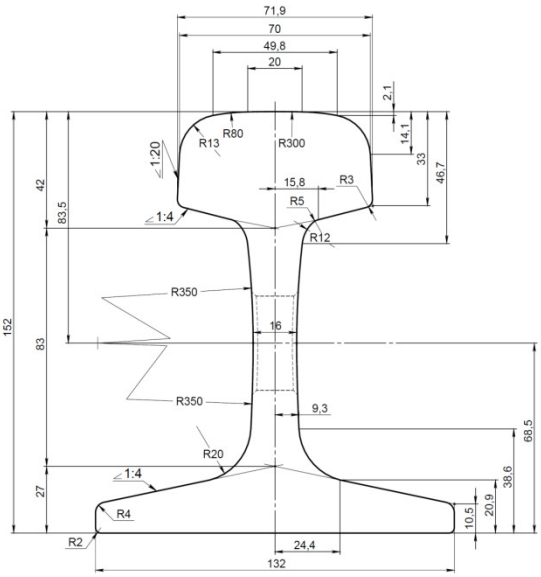

***Figure 9**. Rail type R50 GOST 7174-65*

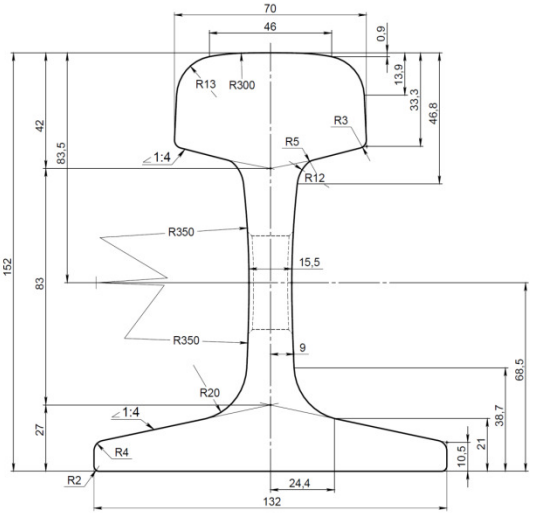

***Figure 10**. Rail type R50 GOST 7174-75*

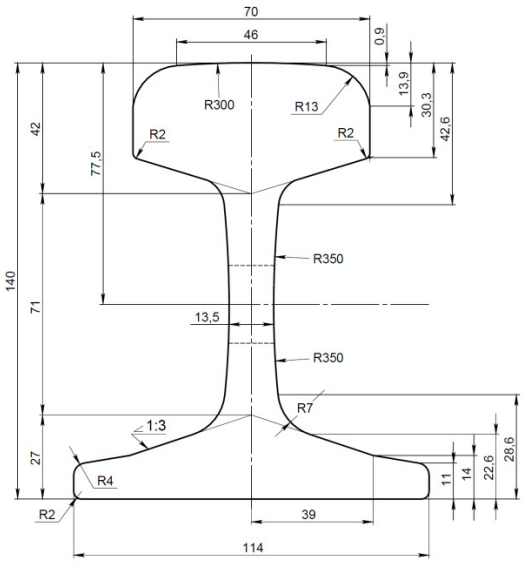

***Figure 11**. Rail type P43 according to GOST 7173-54*

Table 3 Average value of rejected items per year

Index	**Month**					
	I	**II**	**III**	**IV**	**V**	**VI**
Number of controlled joints *ni*	1900	2060	2210	2050	2060	1912
Number of rejected joints *mi*	9	1	2	1	4	1
Rejection rate ***pi = mi / ni ,*** *%*	0.05	0.10	0.05	0.20	0.20	0.05
Index	**Month**					
	VII	**VIII**	**IX**	**X**	**XI**	**XII**
Number **of** controlled joints ***ni***	1500	1900	1620	1900	2030	2020
Number of rejected joints ***mi***	10	5	3	2	3	4
Rejection rate ***pi = mi / ni*** *, %*	0.55	0.20	0.15	0.10	0.15	0.20

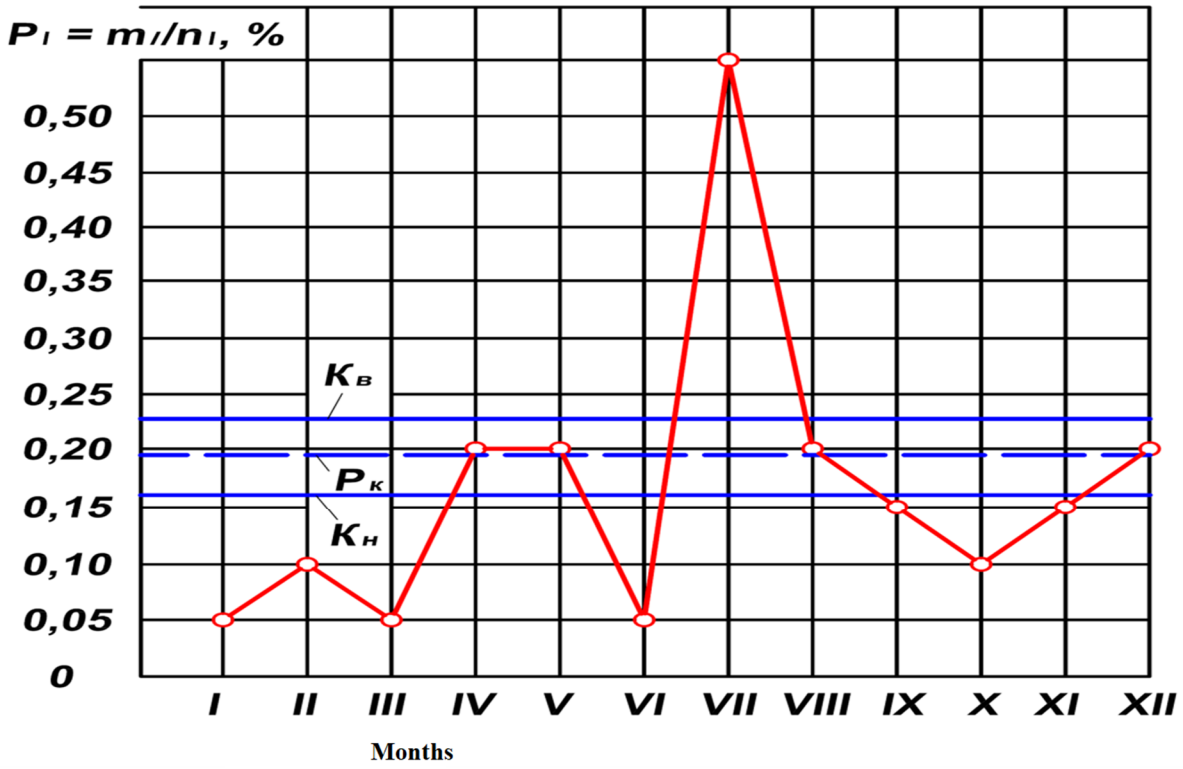

Figure 11. *Control chart of rail welding on RWE*

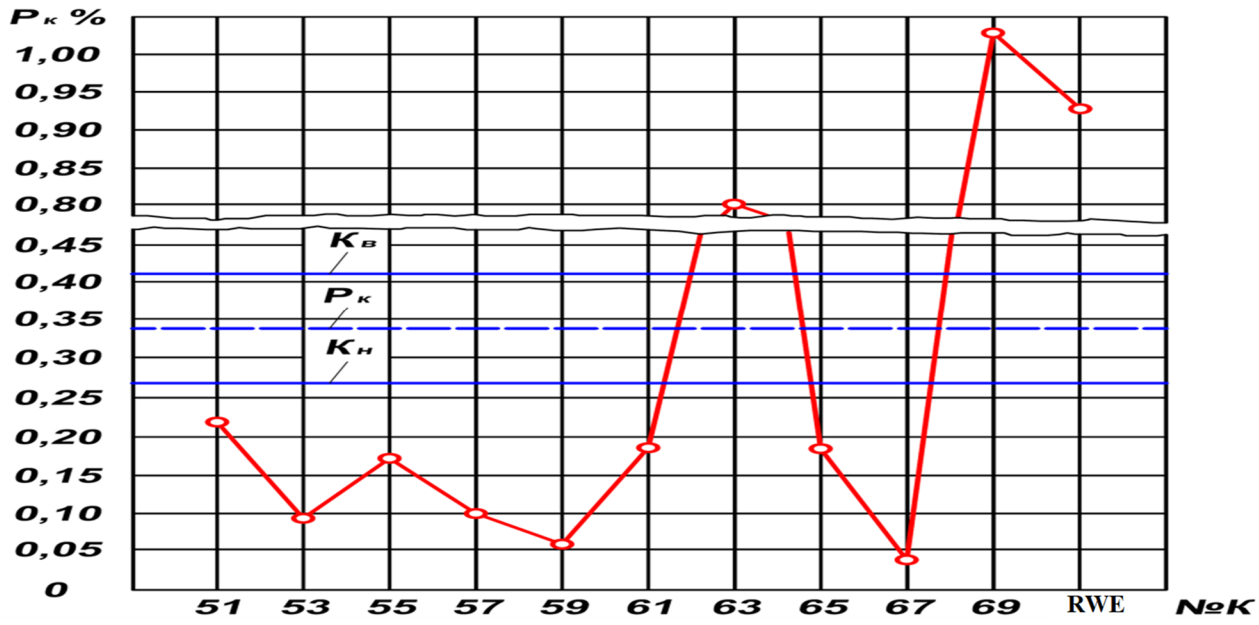

Figure 12*. An example of a map of average values* $\overline{P}$ *of intra-factory rejected items for 2020 according to the RWE.*

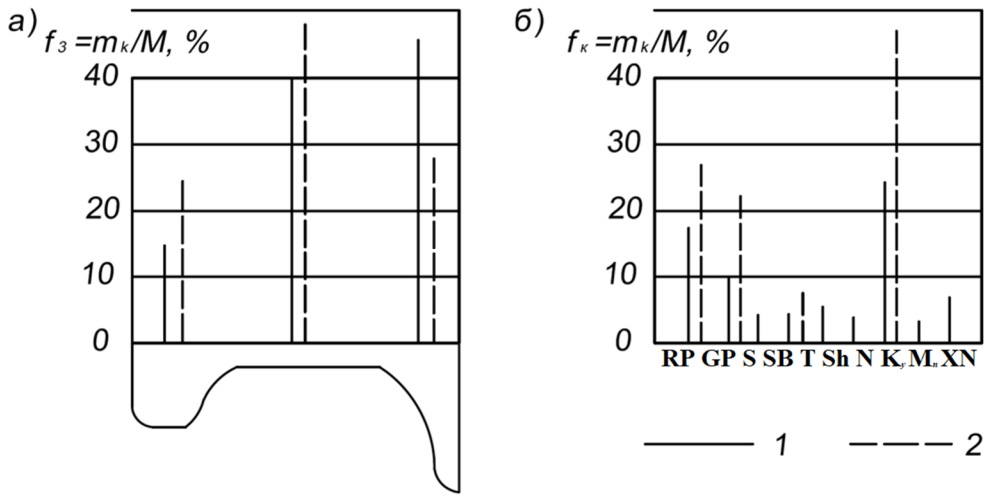

1 - for all RWE; 2 - one of the RWE; RP - friability, burnout; GP - gas bubble; S - silicic accumulation; SB - gray silicate accumulation; T - crack; Sh - slag; N - lack of fusion; Ky - crater shrinkage; Ms - matte spot; XN - the nature of the defects is not specified

Figure 13. *An example of the distribution of defects in the amount of M = 1000 pcs., identified on the RWE, by rail cross-sectional zones (a) and by types of defects in (b). Note - Each RWE is assigned a conditional index in the form of numbers.*

Table 4*. Comparative Analysis of International Railway Rail Standards*

Characteristics	R75/R65 (Kazakhstan)	EN 13674-1 (Europe)	ASTM A1/A759 (USA)	AS 1085.1 (Australia)
Chemical Composition (%)				
Carbon (C)	0.67–0.82	R260: 0.60–0.80 R350HT: 0.70–0.85	A1: 0.67–0.84 A759: 0.69–0.82	Grade 900A: 0.65–0.82 Head-Hardened: 0.70–0.84
Manganese (Mn)	0.75–1.15	R260: 0.80–1.20 R350HT: 0.80–1.30	A1: 0.70–1.10 A759: 0.80–1.20	Grade 900A: 0.80–1.25 Head-Hardened: 0.80–1.30
Silicon (Si)	0.25–0.50	R260: 0.15–0.58 R350HT: 0.20–0.60	A1: 0.15–0.50 A759: 0.20–0.60	Grade 900A: 0.20–0.50 Head-Hardened: 0.20–0.50
Phosphorus (P)	≤ 0.035	≤ 0.025	A1: ≤ 0.035 A759: ≤ 0.030	≤ 0.030
Sulfur (S)	≤ 0.045	≤ 0.025	A1: ≤ 0.040 A759: ≤ 0.030	≤ 0.030
Mechanical Properties				

Characteristics	R75/R65 (Kazakhstan)	EN 13674-1 (Europe)	ASTM A1/A759 (USA)	AS 1085.1 (Australia)
Tensile Strength (MPa)	≥ 880	R260: ≥ 880 R350HT: ≥ 1175	A1 (Std): ≥ 780 A759: ≥ 900	Grade 900A: ≥ 880 Head-Hardened: ≥ 1100
Hardness (HBW)	≥ 260	R260: 260–300 R350HT: 350–390	A1 (Std): ~248 A759 (HH): 321–388	Grade 900A: 260–300 Head-Hardened: 340–380
Elongation (%)	≥ 8	R260: ≥ 10 R350HT: ≥ 9	A1: ≥ 10 A759: ≥ 9	Grade 900A: ≥ 12 Head-Hardened: ≥ 10

Dimensional Tolerances

Height (mm)	± 0.8	± 0.5	Varies by profile	± 0.75
Head Width (mm)	± 0.8	± 0.5	Varies by profile	± 0.75
Foot Width (mm)	± 1.5	± 1.0	Varies by profile	± 1.5
Straightness (per 1.5 m)	Vertical: ≤ 0.8 mm Horizontal: ≤ 1.5 mm	Vertical: ≤ 0.6 mm Horizontal: ≤ 0.8 mm	Varies by profile	Vertical: ≤ 0.7 mm Horizontal: ≤ 1.0 mm

PERIÓDICO TCHÊ QUÍMICA
ARTIGO ORIGINAL

COMPOSIÇÃO QUÍMICA E ATIVIDADE ANTIMICROBIANA DO ÓLEO ESSENCIAL OBTIDO DOS FRUTOS DA *PIMENTA DIOICA* FRENTE ÀS CEPAS *AEROMONAS CAVIAE*, *AEROMONAS HYDROPHILA*, *ENTEROCOCCUS FAECALIS* E *KLEBSIELLA PNEUMONIAE*

CHEMICAL COMPOSITION AND ANTIMICROBIAL ACTIVITY OF THE ESSENTIAL OIL OBTAINED FROM THE FRUITS OF PIMENTA DIOICA AGAINST THE STRAINS *AEROMONAS CAVIAE, AEROMONAS HYDROPHILA, ENTEROCOCCUS FAECALIS AND KLEBSIELLA PNEUMONIAE*

GOMES, Paulo Roberto Barros[1]*; SOUZA, Rômicy Dermondes[2]; SANTOS, Túlio da Fonseca[1]; LOUZEIRO, Hilton Costa[3]; MARINHO, Silvio Carvalho[4]; FONTENELE, Maria Alves[5]; MOUCHREK FILHO, Victor Elias[4]

[1] Instituto Federal de Educação, Ciência e Tecnologia do Pará. Diretoria de Ensino, Pesquisa e Extensão, Paragominas. Brasil

[2] Universidade Estadual do Sudoeste da Bahia. Brasil

[3] Universidade Federal do Maranhão. Departamento de Engenharia Aeroespacial. Brasil

[4] Universidade Federal do Maranhão, Departamento de Tecnologia Química. Brasil

[5] Universidade Federal do Maranhão, Coordenação de Licenciatura em Ciências Naturais, São Bernardo. Brasil

**Autor correspondente*
e-mail: prbgomes@yahoo.com.br

Received 12 July 2025; received in revised form 05 November 2025; accepted 06 November 2025

RESUMO

Introdução: Determinadas bactérias, como *Aeromonas caviae, Aeromonas hydrophila, Enterococcus faecalis* e *Klebsiella pneumoniae*, estão ligadas a diferentes tipos de infecções que podem afetar tanto o trato intestinal quanto a pele, além de provocar complicações mais graves, como pneumonias, septicemias e infecções do trato urinário. Essas doenças tornam-se ainda mais preocupantes em pacientes hospitalizados ou com baixa imunidade, o que evidencia a importância de se buscar alternativas eficazes para prevenção e tratamento. **Objetivo:** Neste trabalho, investigou-se a composição química óleo essencial dos frutos da *Pimenta dioica* obtido por hidrodestilação e a atividade biológica contra quatro diferentes cepas *Aeromonas caviae*, *Aeromonas hydrophila*, *Enterococcus faecalis* e *Klebsiella pneumoniae* do óleo e do padrão eugenol. **Métodos:** Os frutos da espécie *Pimenta dioica* foram coletados na cidade de São Carlos, São Paulo. Após a colheita, esses frutos foram submetidos à secagem a temperatura ambiente e, posteriormente, triturados em um moinho elétrico. A extração do óleo essencial aconteceu por hidrodestilação e o produto foi caracterizado por cromatografia gasosa acoplada ao Espectrômetro de Massa (CG/EM) para identificação dos componentes majoritário presentes. Após a extração e identificação, o do óleo essencial e o padrão do componente majorirátio foram testados contra as bactérias *Aeromonas caviae*, *Aeromonas hydrophila*, *Enterococcus faecalis* e *Klebsiella pneumoniae* pelo o método de Bauer Kirby. **Resultados e Discussão:** Os resultados mostraram que o principal composto identificado no óleo essencial da *Pimenta.dioica* foi o eugenol e que este e o óleo essencial inibiram o crescimento bacteriano, exibindo halos de inibição com dimensões entre 11 e 28 mm, indicando atividade antibacteriana contra os microorganismos testados. Para explicar a atividade biológica observada, estudos anteriores sugerem que a penetração do óleo ocorreu pelo rompimento da camada lipídica e a desestabilização da estrutura celular das bactérias, enquanto o eugenol promoveu o vazamento dos componentes celulares a partir do rompimento da membrana plasmática. **Conclusão:** O óleo essencial dos frutos da *Pimenta dioica* e o padrão eugenol agem como agente antimicrobiano e podem complementar os antibacterianos sintéticos no combate a doenças bacterianas.

Palavras-chave: *Pimenta dioica, frutos, óleo essencial, eugenol, microorganismos*

ABSTRACT

Background: Certain bacteria, such as Aeromonas caviae, *Aeromonas hydrophila*, Enterococcus faecalis, and Klebsiella pneumoniae, are associated with various types of infections that may affect the intestinal tract and skin,

DOI: 10.52571/PTQ.v22.n51.2025_08_GOMES_pgs_107_116.pdf

as well as cause more severe complications, including pneumonia, septicemia, and urinary tract infections. These conditions are particularly concerning in hospitalized or immunocompromised patients, highlighting the need for effective strategies for their prevention and treatment. **Aim:** In this study, the chemical composition of the essential oil from *Pimenta dioica* fruits obtained by hydrodistillation was investigated, as well as its biological activity against four different strains: *Aeromonas caviae, Aeromonas hydrophila, Enterococcus faecalis*, and *Klebsiella pneumoniae*, both for the oil and the eugenol standard. **Methods:** The fruits of the *Pimenta dioica* species were collected in the city of São Carlos, São Paulo. After harvesting, the fruits were dried at room temperature and subsequently ground in an electric mill. The essential oil was extracted by hydrodistillation, and the product was characterized by gas chromatography coupled with mass spectrometry (GC/MS) to identify the major components present. Following extraction and identification, both the essential oil and the standard of the major component were tested against *Aeromonas caviae, Aeromonas hydrophila, Enterococcus faecalis*, and *Klebsiella pneumoniae* using the Bauer–Kirby method**. Results and Discussion**: The results showed that the main compound identified in Pimenta dioica essential oil was eugenol, and that both eugenol and the essential oil inhibited bacterial growth, exhibiting inhibition zones measuring between 11 and 28 mm, indicating antibacterial activity against the microorganisms tested. To explain the observed biological activity, previous studies suggest that oil penetration occurred by disrupting the lipid layer and destabilizing the bacterial cellular structure, while eugenol promoted the leakage of cellular components through disruption of the plasma membrane. **Conclusion**: *Pimenta dioica* essential oil and the eugenol standard act as antimicrobial agents and can complement synthetic antibacterials in combating bacterial diseases.

Keywords: *Pimenta dioica, fruits, essential oil, eugenol, microorganisms.*

1. INTRODUÇÃO:

As bactérias *Aeromonas caviae*, *Aeromonas hydrophila*, *Enterococcus faecalis* e *Klebsiella pneumoniae* causam uma variedade de problemas de saúde. As bactérias do grupo *Aeromonas* são conhecidas por provocar infecções intestinais, que levam a diarreia, podendo ser aguda ou persistente, dor de barriga, vômitos e febre. Elas também causam infecções em ferimentos após o contato com água suja ou um machucado, que podem ir de uma inflamação leve da pele até doenças muito graves, que destroem os tecidos do corpo. Além disso, podem entrar na corrente sanguínea e causar uma infecção generalizada (Pessoa *et al*., 2022). Já a *E. faecalis* e a *K. pneumoniae* são causas importantes de infecções graves, como infecção urinária, pneumonia e infecção no sangue, que podem evoluir para um quadro de sepse. Essas infecções são especialmente perigosas para pessoas que já estão no hospital ou com o sistema de defesa do corpo enfraquecido (Abbas *et al*., 2024; Bengoechea & Sa Pessoa, 2019; Rostkowska *et al*., 2020). Por causa da gravidade dessas doenças, é crucial encontrar maneiras eficazes de combater essas bactérias.

Diante da gravidade das infecções causadas por esses patógenos, o combate às bactérias envolve estratégias preventivas e terapêuticas. As medidas de prevenção, como tratamento de água, higienização das mãos e desinfecção de superfícies, são fundamentais para reduzir a transmissão antes que ocorra a infecção (Krachler & Orth, 2013). No entanto, sua eficácia depende da aplicação correta e consistente pelos usuários, além de não atuarem contra infecções já estabelecidas. Por outro lado, as intervenções terapêuticas baseiam-se predominantemente no uso de antibióticos, os quais são eficazes no controle de infecções ativas e no alívio dos sintomas. Contudo, seu emprego prolongado está associado ao surgimento de resistência bacteriana, efeitos colaterais adversos e disbiose do microbiota comensal.(Gjini *et al*., 2020; Paterson *et al*., 2016; Paul *et al*., 2014) Perante essas limitações, torna-se urgente a investigação de novos agentes antimicrobianos capazes de superar tais desafios.

Em resposta às limitações inerentes às abordagens convencionais, os compostos antibacterianos de origem vegetal surgem como uma alternativa promissora. Derivados de extratos botânicos, óleos essenciais e princípios ativos como flavonoides, terpenos e taninos, esses agentes naturais demonstram potente atividade antimicrobiana, capaz de inibir o crescimento ou mesmo erradicar populações bacterianas.(Liang *et al*., 2022; Mazzei *et al*., 2020; Ramesh *et al*., 2025) Sua principal vantagem reside no mecanismo de ação multifatorial, que inclui danos à parede celular, inibição da síntese proteica e interferência na expressão gênica, dificultando significativamente o desenvolvimento de resistência (Elchaghaby *et al*., 2022; Herman & Herman, 2023; Liang *et al*., 2022; Song *et al*., 2022). Adicionalmente, esses compostos podem atuar sinergicamente com antibióticos sintéticos, potencializando seu efeito, permitindo a redução de dosagens e, consequentemente, minimizando efeitos colaterais e toxicidade.((Herman &

Herman, 2023; Kováč *et al*., 2022; Liang *et al*., 2022; Parham *et al*., 2020; Ramesh *et al*., 2025) Esse perfil de segurança e eficácia ampliada posiciona os fitoderivados como candidatos viáveis para o desenvolvimento de novas terapias antimicrobianas.

Nesse cenário de busca por alternativas terapêuticas de origem natural, a *Pimenta dioica* (L.), conhecida como pimenta-da-jamaica, destaca-se como um taxon botânico da família Myrtaceae com composição química singular. Seus órgãos vegetais sintetizam um conjunto de metabólitos secundários que conferem um perfil sensorial distintivo, marcado pela complexidade de aromas que remetem à canela, cravo, noz-moscada e pimenta-do-reino, com subtons apimentados, adocicados e de zimbro. Apesar de a literatura consolidar as propriedades farmacológicas das bagas, abrangendo ações antimicrobiana, antioxidante e anti-inflamatória, o potencial biotecnológico dos frutos constitui uma frente de investigação ainda a ser aprofundada. Cultivada em condições tropicais e subtropicais, a espécie permite colheitas sequenciais ao longo do ano, com aplicações consolidadas na gastronomia, na medicina tradicional e como matéria-prima aromatizante. A otimização pós-colheita, por meio de protocolos de secagem e processamento adequados, é determinante para manter a estabilidade de seus compostos bioativos (preservando até 90% do conteúdo original), assegurando padrões de qualidade superior, promovendo a agregação de valor à produção agrícola e incentivando modelos de cultivo alinhados com a sustentabilidade (Premachandran & Murthy, 2022; Rastogi & Murthy, 2024).

Assim, este estudo identifica o componente principal do óleo essencial destilado dos frutos da *Pimenta dioica* e avalia se este e o padrão do composto principal possuem a atividade antibacteriana contra quatro diferentes cepas *Aeromonas caviae*, *Aeromonas hydrophila*, *Enterococcus faecalis* e *Klebsiella pneumoniae*.

2. MATERIAL E MÉTODOS:

2.1. Obtenção e extração do óleo essencial

Em outubro de 2003, frutos da espécie Pimenta dioica foram colhidos na cidade de São Carlos, São Paulo. Os dados permaneceram arquivados devido a compromissos acadêmicos e pessoais dos pesquisadores, sendo retomados após reorganização das atividades de pesquisa. Após a colheita, os frutos foram submetidos à secagem em temperatura ambiente. Estes então foram triturados em moinho elétrico (modelo TE 340 da Tecnal) e o material resultante obtido foi acondicionado em recipientes de polietileno até o momento de uso. A extração do óleo essencial foi realizada por meio da técnica de hidrodestilação. Em um balão de fundo redondo de 1000 mL, 30 gramas de amostra foi adicionada em 300 mL de água destilada. O balão de fundo redondo, contendo a mistura, foi conectado a um extrator de Clevenger e aquecido em manta elétrica a aproximadamente 100 °C durante três horas. Após coleta do óleo essencial extraído foi realizada a remoção de impurezas por meio da percolação em uma solução de sulfato de sódio. Por fim as amostras foram acondicionadas em frascos de vidro âmbar e sob refrigeração a fim de evitar a perda de constituintes voláteis.

2.2. Análise cromatográfica CG/EM

A análise cromatográfica CG/EM foi realizada conforme já descrito na literatura (Marinho *et al*., 2022). Os componentes do óleo essencial foram identificados por meio de cromatografia gasosa acoplada à espectrometria de massas (CG-EM), utilizando um cromatógrafo a gás HP 5890, equipado com um detector de massa HP 5970 de impacto eletrônico, operando com hélio como gás carreador a uma taxa de fluxo de 1 mL/min na coluna. A energia de impacto foi ajustada para 70 eV, com uma temperatura de 300°C. Para as análises, foi injetado 1µL da amostra previamente diluída em clorofórmio. Os parâmetros cromatográficos foram configurados da seguinte maneira: temperatura inicial de 60°C, final de 300 °C; tempo inicial de 2 minutos, final de 15 minutos; taxa de rampa de 2 °C/min. A identificação dos componentes do óleo essencial foi realizada comparando os espectros obtidos com os dados de substâncias autênticas presentes na base de dados NBS_Reve (com 40.000 registros) e com informações disponíveis na literatura (Adams & Sparkman, 2007).

2.3. Isolamento de bactérias e Testes da atividade antibacteriana

Neste estudo, amostras bacterianas de *Aeromonas caviae* (Gram negativa) e *Aeromonas hydrophila* (Gram negativa) foram obtidas por meio da filtração da água utilizando membranas de éster de celulose (Silva *et al*., 2014). Posteriormente, as colônias bacterianas foram isoladas em tubos inclinados com Ágar Tripticase Soja (Ágar TSA) e incubadas a 28 °C por 24 horas. Após esse período, uma série de testes

bioquímicos foi conduzida para identificar as espécies. Esses testes incluíram ensaios de oxidase, catalase, coloração de Gram, produção de gás a partir da glicose, produção de indol, resistência ao agente vibriostático O/129, descarboxilação de aminoácidos (lisina, arginina e ornitina), teste em Ágar Tríplice Açúcar e Ferro (Ágar TSI), avaliação de motilidade, redução de nitrato, hidrólise da esculina, teste de Voges-Proskauer, fermentação de carboidratos e crescimento em soluções de cloreto de sódio com concentrações de 3% e 6% (Marinho *et al*., 2022). Os protocolos seguidos estavam alinhados com as diretrizes de um estudo anterior (Martins *et al*., 2009)e todos os procedimentos foram realizados de acordo com as normas do *Compendium of Methods for the Microbiological Examination of Foods* (Palumbo *et al*., 2001).

A técnica de isolamento e identificação do *Enterococcus faecalis* (Gram positiva) em amostras vegetais foi realizada conforme o procedimento detalhado por Gomes e colaboradores (2008), enquanto a identificação da Klebsiella pneumoniae (Gram negativa) seguiu o método descrito por (Puspanadan *et al*., 2012).

O teste de resistência ao óleo essencial foi conduzido utilizando o método BauerKirby**,** conforme descrito por Jones e colaboradores (2001)**.** As cepas de testes foram cultivadas em Caldo BHI (*Brain Heart Infusion*) e um inóculo de cada bactéria (0,25mL) foi inoculado na superfície das placas de Ágar contagem padrão (PCA – Merck) usando uma alça de Drigalski. Discos de papel de filtro de 6mm impregnados com 75µL do óleo essencial foram cuidadosamente colocados sobre as placas com o auxílio de uma pinça esterilizada pelo fogo, seguido de uma leve pressão para garantir a aderência dos discos ao meio. As placas foram então incubadas a 37 ºC por 24 horas, e a leitura dos halos de inibição foi realizada utilizando uma régua milimetrada. O mesmo procedimento foi repetido para a testar o padrão eugenol e o antibiótico de referência, cefotaxima.

A categorização da sensibilidade dos microrganismos aos agentes testados, incluindo o antibiótico de referência, o óleo essencial e o eugenol padrão, foi baseada no diâmetro dos halos de inibição. A classificação foi a seguinte: (-) não sensível para diâmetros menores que 8 mm; (+) sensível para diâmetros entre 9 e 14 mm; (++) muito sensível para diâmetros de 15 a 19 mm; (+++) extremamente sensível para diâmetros acima de 20 mm (Ponce *et al*., 2003).

3. RESULTADOS E DISCUSSÃO:

3.1. Resultados

Para determinar o principal componente do óleo essencial extraído dos frutos da P. dioica, os cromatogramas obtidos através da análise CG/EM em uma coluna LM100 foram comparados com o banco de dados mencionado na literatura (Adams, 2017). A partir desta análise, como mostrado na figura 1, os picos cromatográficos numerados como 1 e 2 correspondem, respectivamente, aos compostos mirceno e eugenol, sendo que este último apresenta semelhança com o pico e o tempo de retenção (19,48 min) do padrão de eugenol (Figura 2).

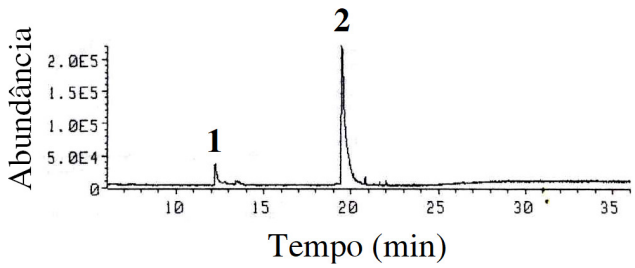

Figura 1. *Cromatograma do óleo essencial destilado dos frutos P.dioica. Condições fixadas: coluna capilar LM100 de metil silicone entrecruzada (25 m x 0,22 mm i.d.; 0,3 µm de espessura de filme), acoplado a um detector seletivo de massas HP 5970 de impacto eletrônico, com uma energia de 70 eV, temperatura de transferência de 300°C.*

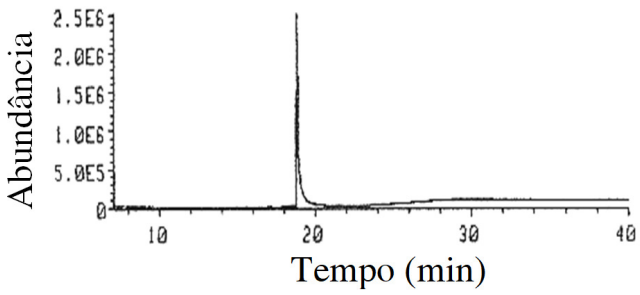

Figura 2. *Cromatograma do padrão de Eugenol. As condições estabelecidas incluem uma coluna capilar LM100 de silicone metílico entrecruzado (25 m x 0,22 mm i.d.; 0,3 µm de espessura de filme), conectada a um detector de massas seletivo HP 5970 por impacto eletrônico, operando a uma energia de 70 eV e com uma temperatura de transferência de 300°C.*

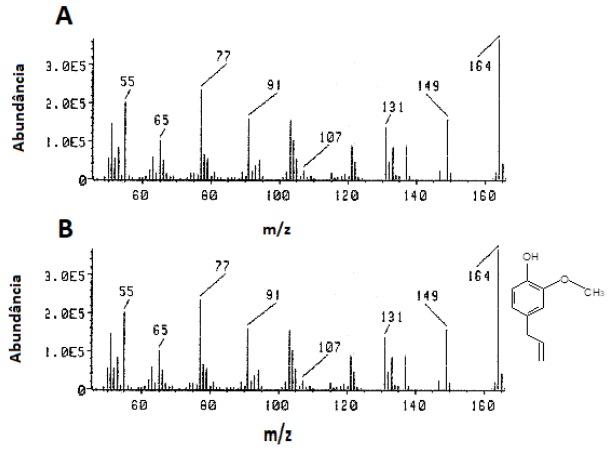

Figura 3. *Espectros de massas: (A) Composto do pico 2 do cromatograma da Figura 1; (B) Padrão de eugenol.*

Os dados coletados da biblioteca do espectrômetro de massa foram comparados com a literatura de Adams (2007) para a identificação precisa dos compostos observados nos cromatogramas. A partir dessas observações, verificou-se que o espectrograma de massa do pico 2 (figura 1) é semelhante ao espectrograma de massa do padrão de eugenol (Figura 3), sugerindo que o principal composto identificado no óleo é o eugenol, devido à presença do pico do íon molecular em m/z = 164 [M+].

O pico em m/z = 149 [M-15] representa a perda do radical metila (CH3-). Já os picos em m/z = 91 e m/z = 77 são típicos, respectivamente, do íon tropílico [C7H7+] e do íon [C6H5+]. Dessa forma, os fragmentos principais identificados no espectro de massas são 164 (100); 149 (39); 131 (32); 103 (34); 91 (34); 77 (46) e 55 (39).

A sensibilidade microbiana foi avaliada para três cepas de bactérias Gram negativas (*Aeromonas caviae, Aeromonas hydrophila, Klebsiella pneumoniae*) e uma cepa Gram Positiva (*Enterococcus faecalis*) quanto ao óleo essencial e ao padrão eugenol. Essa avaliação foi realizada a partir das medidas dos halos de inibição, seguindo os critérios estabelecidos por (Ponce *et al*., 2003).Desse estudo, os resultados revelaram que todas as cepas testadas foram suscetíveis tanto ao óleo essencial quanto ao padrão eugenol, exibindo halos de inibição com dimensões entre 11 e 28 mm. Destaca-se a significativa sensibilidade de *E. faecalis* ao óleo essencial, evidenciada por um halo de inibição de 18 mm, assim como a notável resposta de *A. caviae* ao padrão eugenol, apresentando um halo de inibição de 28 mm. Esses achados reforçam a viabilidade do óleo essencial como uma alternativa promissora para o desenvolvimento de agentes antibacterianos, ampliando assim as possibilidades terapêuticas no combate às infecções bacterianas.

Tabela 1. *Sensibilidade das bactérias Aeromonas caviae, Aeromonas hydrophila, Enterococcus faecalis, Klebsiella pneumoniae ao óleo essencial dos frutos da P. dioica e o padrão eugenol, utilizando-se o método de difusão em disco.*

Bactérias	**Cefotaxima**	**Halos de inibição (mm)**	
		Óleo essencial *P. dioica*	**Padrão Eugenol**
Aeromonas caviae	25 (+++)	12 (+)*	28 (+++)
Aeromonas hydrophila	24 (+++)	11 (+)	11 (+)
Klebsiella pneumoniae	17 (++)	17 (++)	14 (+)
Enterococcus faecalis	18 (++)	18 (++)	19 (++)

*Sensibilidade dos microorganismos ao segundo Ponce *et al.* (2003).

3.2. Discussão

Embora os antibióticos sejam eficazes no combate e tratamento de infecções bacterianas, sua utilização apresenta uma desvantagem significativa: a potencialidade no desenvolvimento de bactérias resistentes (Aslam *et al*., 2018). Nesse contexto, a busca por agentes antibacterianos de origem vegetal a base de óleos essenciais torna-se uma proposta interessante. Pois esses compostos têm a capacidade de romper a parede celular e as membranas celulares das bactérias, resultando na liberação de conteúdo celular, além da interrupção do domínio de ligação às proteínas, inativação enzimática e, por fim, morte celular (Singh *et al*., 2017), além de diminuir a resistência bacteriana (U. Anand *et al*., 2019). Logo, a identificação do componente majoritário e avaliação da atividade antibacteriana do óleo essencial permitirá o desenvolvimento de produtos com baixa resistência bacteriana e consequentemente propor uma alternativa aos tratamentos tradicionais.

Neste estudo, determinamos o principal componente do óleo destilado dos frutos da Pimenta dioica utilizando cromatografia gasosa acoplada a um espectrômetro de massa e investigamos sua atividade biológica contra as bactérias *Aeromonas caviae, Aeromonas hydrophila, Klebsiella pneumoniae e Enterococcus faecalis* por meio do método de difusão em ágar. A partir dessas análises, verificamos que o óleo essencial é composto majoritariamente por eugenol e demonstra atividade antibacteriana contra os organismos testados, com halos de inibição variando entre 11 e 28 mm.

No primeiro achado, identificou-se a presença predominante de eugenol no óleo, com base na similaridade do cromatograma com o padrão puro de eugenol. Essa predominância já era esperada, uma vez que a literatura científica já relatou a predominância deste composto em plantas da família *Myrtaceae* com variações de 76 a 85%(Barros Gomes *et al*., 2020; Everton *et al*., 2021). Embora não tenhamos quantificado essas frações em nosso estudo, fica evidente que esses valores não são uniformes, devido a diversos fatores (período de desenvolvimento da planta, temperatura, altitude, poluição atmosférica, etc) que alteram a composição do componente principal(Gobbo-Neto & Lopes, 2007).

No segundo achado, concluímos sobre a eficácia do óleo quanto a sensibilidade bacteriana a partir do método Kirby-Bauer. Este é um teste de difusão em disco que avalia a sensibilidade de determinada bactéria a antibióticos específicos a partir de regiões onde estas não conseguem se desenvolver, formando os halos. Quanto maior o halo, maior é a sensibilidade da bactéria ao antibiótico testado (Anand *et al*., 2001; Le Page *et al*., 2016). No estudo em questão, foram testadas as bactérias *Aeromonas caviae, Aeromonas hydrophila, Klebsiella pneumoniae e Enterococcus faecalis* onde os resultados demonstraram que essas bactérias foram sensíveis tanto ao óleo essencial quanto ao padrão de eugenol. Essa sensibilidade ao óleo essencial da *P. dioica* corrobora com estudos anteriores (Barros Gomes *et al*., 2020; Oliveira Everton *et al*., 2020) que também empregaram métodos semelhantes e constataram a sensibilidade do óleo contra outras bactérias, como *Escherichia coli, Staphylococcus aureus, Pseudomonas aeruginosa e Serratia odorífera.*

Além disso, nos dois estudos mencionados, os autores identificaram a predominância do composto eugenol tanto nas folhas quanto nos frutos do óleo essencial da *P. dioica.* Esse composto parece ser o responsável pela atividade antibacteriana observada. No nosso próprio estudo, essa sugestão foi confirmada quando utilizamos o padrão puro de eugenol e constatamos a sensibilidade das bactérias.

Essa sensibilidade observada tanto no óleo essencial quanto no padrão eugenol é explicada da seguinte forma. Primeiro, devemos entender que as bactérias Gram-negativas possuem uma camada adicional à parede celular, que as protege da ação dos antibióticos. Para que ocorra a penetração é necessário, inicialmente, que essa estrutura seja danificada, através do rompimento da camada lipídica e consequentemente a desestabilização da célula (Brehm-Stecher & Johnson, 2003; Cowan, 1999; Griffin *et al*., 1999). No caso do composto eugenol, acredita-se que essa penetração ocorra a partir do dano na membrana plasmática, seguindo para a estutrura lipopolissacarídica, alterando a estrutura celular e provocando o vazamento dos componentes intracelulares, devido íon hidróxido livre e a parte hidrofóbica do composto (Ulanowska & Olas, 2021). Embora haja uma similaridade no mecanismo de ação entre o óleo e o padrão, estudos mais aprofundados sobre essas bactérias podem ajudar a explicar a sensibilidade observada. Portanto, esses resultados indicam que o óleo essencial da *P. dioica*, especialmente o eugenol, pode ser uma opção promissora no combate a infecções bacteriana.

Portanto, ainda que os resultados deste estudo em relação a atividade antibacteriana estejam limitados quanto ao método utilizado, a consideração do óleo essencial da *P. dioica* como um potencial complementador ou candidato a substituir os agentes antibacterianos sintéticos deve ser considerado.

4. CONCLUSÕES:

A análise cromatográfica do óleo essencial dos frutos da *Pimenta dioica* mostrou a presença de dois constituintes: eugenol (majoritário) e o mirceno. O pico do componente majoritário do óleo foi similar ao pico do padrão eugenol, confirmando assim a presença deste composto no óleo essencial. Quanto a atividade antibacteriana, conclui-se que o óleo foi ativo contra as bactérias *Aeromonas caviae, Aeromonas hydrophila, Klebsiella pneumoniae* e *Enterococcus faecalis.*

5. DECLARAÇÕES

5.1. Limitações do estudo

O presente estudo apresenta algumas limitações que devem ser reconhecidas. A amostra bacteriana foi restrita a quatro espécies e não houve quantificação do percentual de eugenol no óleo, tampouco detalhamento do número de replicatas. Os controles negativos foram descritos de forma limitada e não foram aplicados testes estatísticos para validar as diferenças observadas. Além disso, os dados foram obtidos a partir de coletas realizadas em 2003, o que pode ter implicado degradação parcial de compostos voláteis ao longo do tempo. Do ponto de vista metodológico, utilizou-se exclusivamente o ensaio de difusão em disco, sem métodos complementares, e sem padronização completa da concentração do inóculo ou descrição detalhada das condições ambientais de coleta. No aspecto analítico, apenas dois compostos (eugenol e mirceno) foram identificados qualitativamente, sem quantificação precisa, e a comparação com a literatura foi limitada devido ao reduzido número de estudos similares disponíveis.

5.2. Agradecimentos

Os autores agradecem a Bolsa de Pesquisa concedida pela Fundação de Amparo à Pesquisa e ao Desenvolvimento Científico e Tecnológico do Maranhão – FAPEMA

5.3. Fontes de financiamento

Esta pesquisa foi financiada pela FAPEMA e CNPq. De acordo com as diretrizes éticas do **Periódico Tchê Química**, que não permitem doações de autores com manuscritos em avaliação (mesmo quando há recursos de pesquisa disponíveis), ou em casos de restrições financeiras dos autores, os custos de publicação foram integralmente absorvidos pela revista por meio de nossa política de **Acesso Aberto Platinum**, com o apoio da **Associação Científica Araucária** (https://acaria.org/). Essa política visa garantir total independência entre o processo editorial e quaisquer aspectos financeiros, reafirmando nosso compromisso com a **integridade científica** e a **equidade na disseminação do conhecimento**.

5.4. Competing Interests

There is no conflict of interest to declare.

6. REFERÊNCIAS:

1. Abbas, R.; Chakkour, M.; Zein El Dine, H.; Obaseki, E. F.; Obeid, S. T.; Jezzini, A.; Ghssein, G.; Ezzeddine, Z. (2024). General overview of Klebsiella pneumonia: Epidemiology and the role of siderophores in its pathogenicity. *Biology*, 13(2), p.78.

2. Adams, R. P.; Sparkman, O. (2007). Review of identification of essential oil

components by gas chromatography/mass spectrometry. *J. Am. Soc. Mass Spectrom.*, 18, p.803–806.

3. Anand, D.; Spargo, J.; Ferraro, M. J. (2001). Antimicrobial susceptibility testing. MGH Division of Laboratory Medicine, 9(1), p.1–4.
4. Anand, U.; Jacobo-Herrera, N.; Altemimi, A.; Lakhssassi, N. (2019). A comprehensive review on medicinal plants as antimicrobial therapeutics: Potential avenues of biocompatible drug discovery. *Metabolites*, 9(11), p.258.

5. Aslam, B.; Wang, W.; Arshad, M. I.; Khurshid, M.; Muzammil, S.; Rasool, M. H.; Nisar, M. A.; Alvi, R. F.; Aslam, M. A.; Qamar, M. U. (2018). Antibiotic resistance: A rundown of a global crisis. *Infection and Drug Resistance*, p.1645–1658.

6. Barros Gomes, P. R.; Ribeiro, J. D.; Guimarães da Costa, M. C.; da Silva Castro, M. W.; Buzar Neto, N.; Melo, A. V.; Oliveira Everton, G.; Costa Louzeiro, H.; Fontenele, M. A.; Souza de Lima, H. (2020). Composição química e atividade antibacteriana do óleo essencial dos frutos da Pimenta dioica. *Rev. colomb. ciencias quím. farm.*, 49(3), p.656–674.

7. Bengoechea, J. A.; Sa Pessoa, J. (2019). Klebsiella pneumoniae infection biology: Living to counteract host defences. FEMS *Microbiology Reviews*, 43(2), p.123–144.

8. Brehm-Stecher, B. F.; Johnson, E. A. (2003). Sensitization of Staphylococcus aureus and Escherichia coli to antibiotics by the sesquiterpenoids nerolidol, farnesol, bisabolol, and apritone. *Antimicrobial Agents and Chemotherapy*, 47(10), p.3357–3360. DOI: 10.1128/AAC.47.10.3357-3360.2003

9. Cowan, M. M. (1999). Plant products as antimicrobial agents. *Clinical Microbiology Reviews*, 12(4), p.564–582.

10. Elchaghaby, M. A.; Abd El-Kader, S. F.; Aly, M. M. (2022). Bioactive composition and antibacterial activity of three herbal extracts (lemongrass, sage, and guava leaf) against oral bacteria: An in vitro study. *Journal of Oral Biosciences*, 64(1), p.114–119.

11. Everton, G. O.; Pereira, A. P. M.; Mafra, N. S.; Santos Júnior, P. S.; Martins, T. G.; Rosa, P. V.; Gomes, P. R.; Mendes Filho, N. E.; Mouchrek Filho, V. E. (2021). Chemical constituents and bactericidal and fungicide potential of the essential oil of Pimenta dioica Lindl against pathogenic microorganisms. *Revista De Ciencia Y Tecnología*, 36(1), 78–83. DOI: 10.36995/j.recyt.2021.36.010

12. Gjini, E.; Paupério, F. F.; Ganusov, V. V. (2020). Treatment timing shifts the benefits of short and long antibiotic treatment over infection. *Evolution, Medicine, and Public Health*, 2020(1), p.249–263.

13. Gobbo-Neto, L.; Lopes, N. P. (2007). Plantas medicinais: Fatores de influência no conteúdo de metabólitos secundários. *Química Nova*, 30(2), p.374–381.

14. Gomes, B. C.; Esteves, C. T.; Palazzo, I. C.; Darini, A. L. C.; Felis, G. E.; Sechi, L. A.; Franco, D. B. G. M., and De Martinis, E. C. (2008). Prevalence and characterization of Enterococcus spp. isolated from Brazilian foods. *Food Microbiology*, 25(5), p.668–675.

15. Griffin, S. G.; Wyllie, S. G.; Markham, J. L.; Leach, D. N. (1999). The role of structure and molecular properties of terpenoids in determining their antimicrobial activity. *Flavour and Fragrance Journal*, 14(5), p.322–332.

16. Herman, A.; Herman, A. P. (2023). Herbal products and their active constituents used alone and in combination with antibiotics against multidrug-resistant bacteria. *Planta Medica,* 89(02), p.168–182.

17. Jones, R. N.; Ballow, C. H.; Biedenbach, D. J. (2001). Multi-laboratory assessment of the linezolid spectrum of activity using the Kirby-Bauer disk diffusion method: Report of the Zyvox® Antimicrobial Potency Study (ZAPS) in the United States. *Diagnostic Microbiology and Infectious Disease*, 40(1–2), p.59–66.

18. Kováč, J.; Slobodníková, L.; Trajčíková, E.; Rendeková, K.; Mučaji, P.; Sychrová, A.;

Bittner Fialová, S. (2022). Therapeutic potential of flavonoids and tannins in management of oral infectious diseases—A review. *Molecules*, 28(1), p.158.

19. Krachler, A. M.; Orth, K. (2013). Targeting the bacteria–host interface: Strategies in anti-adhesion therapy. *Virulence*, 4(4), p.284–294.
20. Le Page, S.; Dubourg, G.; Rolain, J.-M. (2016). Evaluation of the Scan® 1200 as a rapid tool for reading antibiotic susceptibility testing by the disc diffusion technique. *Journal of Antimicrobial Chemotherapy*, 71(12), p.3424–3431.

21. Liang, J.; Huang, X.; Ma, G. (2022). Antimicrobial activities and mechanisms of extract and components of herbs in East Asia. *RSC Advances*, 12(45), p.29197–29213.

22. Marinho, S. C.; Souza, R. D.; Gomes, P. R. B.; Louzeiro, H. C.; Mouchrek Filho, V. E. (2022). Avaliação da atividade antimicrobiana e da composição química do óleo essencial de Aniba duckei. *Periódico Tchê Química*, 19. DOI: https://doi.org/10.52571/PTQ.v19.n41.2022.03_GOMES_pgs_26_34.pdf

23. Martins, A.; Nascimento, A. R.; Vieira, R.; Serra, J. L.; Rocha, M. (2009). Quantificação e identificação de Aeromonas spp. em águas de superfície do estuário do rio Bacanga em São Luís/MA (Brasil). *Boletim Ceppa*, 27, p.107–118.

24. Mazzei, R.; Leonti, M.; Spadafora, S.; Patitucci, A.; Tagarelli, G. (2020). A review of the antimicrobial potential of herbal drugs used in popular Italian medicine (1850s–1950s) to treat bacterial skin diseases. *Journal of Ethnopharmacology*, 250, p.112443.

25. Oliveira Everton, G.; Pereira Araújo, R. J.; da Silva dos Santos, A. B.; Serra Rosa, P. V.; de Oliveira Carvalho Junior, R. G.; Teles, A. M.; Barros Gomes, P. R.; Mouchrek Filho, V. E. (2020). Caracterização química, atividade antimicrobiana e toxicidade dos óleos essenciais da Pimenta dioica L. (pimenta da Jamaica) e Citrus sinensis L. Osbeck (laranja doce). *Rev. colomb. ciencias quím. farm.*, 49(3), p.641–655.

26. Palumbo, S.; Abeyta, C.; Stelma, G.; Wesley, I.; Wei, C.; Koberger, J.; Franklin, S. K.; Schroeder-Tucker, L.; Murano, E. (2001). Aeromonas, Arcobacter, and Plesiomonas. In: Downes, F. P.; Ito, K. (eds). Compendium of methods for the microbiological examination of foods, 4, p.283–290.

27. Parham, S.; Kharazi, A. Z.; Bakhsheshi-Rad, H. R.; Nur, H.; Ismail, A. F.; Sharif, S.; RamaKrishna, S.; Berto, F. (2020). Antioxidant, antimicrobial and antiviral properties of herbal materials. *Antioxidants*, 9(12), p.1309.

28. Paterson, I. K.; Hoyle, A.; Ochoa, G.; Baker-Austin, C.; Taylor, N. G. (2016). Optimising antibiotic usage to treat bacterial infections. *Scientific Reports*, 6(1), p.37853.

29. Paul, M.; Carmeli, Y.; Durante-Mangoni, E.; Mouton, J. W.; Tacconelli, E.; Theuretzbacher, U.; Mussini, C.; Leibovici, L. (2014). Combination therapy for carbapenem-resistant Gram-negative bacteria. *Journal of Antimicrobial Chemotherapy*, 69(9), p.2305–2309.

30. Pessoa, R. B. G.; Oliveira, W. F. de; Correia, M. T. dos S.; Fontes, A.; Coelho, L. C. B. B. (2022). Aeromonas and human health disorders: Clinical approaches. *Frontiers in Microbiology*, 13, p.868890.

31. Ponce, A.; Fritz, R.; del Valle, C.; Roura, S. (2003). Antimicrobial activity of essential oils on native microbial population of organic Swiss Chard (Beta vulgaris, type cicla). *Food Science and Technology*, 36, p.579–684.

32. Premachandran, M. S.; Murthy, P. S. (2022). Ethnobotanical, phytochemical, pharmacological properties and applications of Pimenta dioica L. *Journal of Essential Oil Research*, 34(3), p.216–232.

33. Puspanadan, S.; Afsah-Hejri, L.; Loo, Y.; Nillian, E.; Kuan, C.; Goh, S.; Chang, W.; Lye, Y.; John, Y.; Rukayadi, Y. (2012). Detection of Klebsiella pneumoniae in raw vegetables using most probable number-

polymerase chain reaction (MPN-PCR). International *Food Research Journal*, 19(4), p.1757.

34. Ramesh, S. P.; Karajgi, S.; Singh, R.; Naik, P.; Sahoo, U.; Sharma, M. C.; Nainwal, P.; Wal, A. (2025). Herbal antibiotics: A review of traditional medicinal plants with antibacterial properties and their potential for future treatment. Anti-Infective Agents, 23(2), p.E080724231696.

35. Rastogi, N. K.; Murthy, P. S. (2024). Implications of dehydration processing on the bio-actives, chemometrics and fingerprinting of allspice (*Pimenta dioica* L.) leaves. *Food Biophysics*, 19(4), p.1157–1176.
36. Rostkowska, O. M.; Kuthan, R.; Burban, A.; Salińska, J.; Ciebiera, M.; Młynarczyk, G.; Durlik, M. (2020). Analysis of susceptibility to selected antibiotics in Klebsiella pneumoniae, Escherichia coli, *Enterococcus faecalis* and Enterococcus faecium causing urinary tract infections in kidney transplant recipients over 8 years: Single-center study. *Antibiotics*, 9(6), p.284.

37. Silva, A. C. M. de M.; Nascimento, D. L. do; Machado, R. Z.; Costa, F. N. (2014). Caracterização de Aeromonas spp isoladas de amostras de ostras e água por método microbiológico e molecular. *Ciência Animal Brasileira*, 15, p.362–368.

38. Singh, S. B.; Young, K.; Silver, L. L. (2017). What is an “ideal” antibiotic? Discovery challenges and path forward. *Biochemical Pharmacology*, 133, p.63–73.

39. Song, L.; Hu, X.; Ren, X.; Liu, J.; Liu, X. (2022). Antibacterial modes of herbal flavonoids combat resistant bacteria. *Frontiers in Pharmacology*, 13, p.873374.

40. Ulanowska, M.; Olas, B. (2021). Biological properties and prospects for the application of eugenol—A review. International Journal of Molecular Sciences. *sciences*, *22*(7), 3671.

PERIÓDICO TCHÊ QUÍMICA
ARTIGO DE REVISÃO

O USO DE CRISÁLIDAS INFECTADAS POR BACULOVÍRUS NA PRODUÇÃO DE VACINAS DE SUBUNIDADE: UMA MINI-REVISÃO

THE USE OF BACULOVIRUS-INFECTED CHRYSALIDES IN THE PRODUCTION OF SUBUNIT VACCINES: A MINI-REVIEW

ESCARATE, Amparo[1#]; PIZZOLON, Agostina[1#]; QUAGLIA, Lourdes[1#]; VELOCCE Ariana[1#]; ZARELLI, Valeria Eugenia Paola[1,2]; GIAI, Constanza[1,3]; QUINTERO Cristián Andrés[1,3*]

[1]Facultad de Farmacia y Bioquímica. Universidad Juan Agustín Maza, Mendoza, Argentina.
[2]Laboratorio de Genética, Ambiente y Reproducción. Universidad Juan Agustín Maza, Mendoza, Argentina.
[3]Laboratorio de Biología Molecular y Celular. Universidad Juan Agustín Maza, Mendoza, Argentina.

*Corresponding author: cquintero@umaza.edu.ar
# These authors contributed equally

Received 14 June 2025; received in revised form 04 November 2025; accepted 06Nnovember 2025

RESUMO

Introdução: A crescente demanda por produção eficiente e escalável de vacinas levou ao desenvolvimento de plataformas inovadoras, como a CrisBio, desenvolvida pela Cocoon. Essa tecnologia utiliza crisálidas da mariposa *Trichoplusia ni* como biorreatores naturais para a expressão de proteínas recombinantes, empregando o sistema de vetor de expressão por baculovírus (BEVS). Após a inoculação com sequências específicas de DNA, essas crisálidas permitem a síntese de proteínas complexas, com modificações pós-traducionais avançadas, em apenas 3 a 6 dias. Notavelmente, a CrisBio demonstrou a capacidade de produzir partículas semelhantes a vírus (VLPs)**,** incluindo o antígeno PCV2 Cap e a proteína VP60 do RHDV, alcançando rendimentos de até 10 mg de proteína por grama de biomassa. **Objetivo:** Esta mini-revisão visa atualizar o estado da arte sobre o uso de crisálidas infectadas com baculovírus recombinantes para a produção de vacinas de subunidade. **Métodos:** Foi realizada uma revisão sistemática da literatura nas bases de dados PubMed e SciELO para identificar estudos que descrevem o uso de crisálidas e baculovírus modificados na produção de vacinas. A estratégia de busca incluiu os termos: *crisálidas*, *baculovírus* e *produção de vacinas*, utilizados em diversas combinações. **Resultados:** A plataforma CrisBio suporta o manuseio e processamento totalmente automatizado de crisálidas, simplificando significativamente as fases de inoculação e expressão proteica. O uso de baculovírus geneticamente modificados possibilita a produção rápida de proteínas recombinantes com estruturas complexas e altos rendimentos. Além disso, esse sistema prova ser altamente escalável e economicamente viável, com custos de produção reduzidos em até 95% em comparação com métodos convencionais baseados em culturas celulares. **Discussão:** As técnicas tradicionais de fabricação de vacinas enfrentam limitações em escalabilidade, custo e velocidade de produção. Em contraste, a CrisBio oferece vantagens substanciais, incluindo tempo de resposta mais rápido, custos mais baixos e a capacidade de produzir proteínas com modificações pós-traducionais complexas, tornando-a uma plataforma promissora para uma ampla gama de aplicações biofarmacêuticas. **Conclusões:** Em comparação com os métodos tradicionais, a plataforma CrisBio melhora a biossegurança, reduz o tempo e os custos de produção e oferece uma solução escalável para o desenvolvimento de vacinas de subunidade. Sua implementação poderia melhorar significativamente o acesso global a vacinas, especialmente em ambientes com poucos recursos.

Palavras-chave*: Biotecnologia, Baculovírus, Crisálidas, Vacinas.*

ABSTRACT

Background: The increasing demand for efficient and scalable vaccine production has led to the development of innovative platforms such as CrisBio, developed by Cocoon. This technology utilizes chrysalides of the moth *Trichoplusia ni* as natural bioreactors for recombinant protein expression, employing a baculovirus expression vector system (BEVS). Upon inoculation with specific DNA sequences, these chrysalides enable the synthesis of complex proteins with advanced post-translational modifications in just 3 to 6 days. Notably, CrisBio has

DOI: 10.52571/PTQ.v22.n51.2025_09_ESCARETE_pgs_117_122.pdf

demonstrated the ability to produce virus-like particles (VLPs), including the PCV2 Cap antigen and the VP60 protein of RHDV, reaching yields of up to 10 mg of protein per gram of biomass. **Aim:** This mini-review aims to update the state of the art regarding the use of chrysalides infected with recombinant baculoviruses for subunit vaccine production. **Methods:** A systematic literature review was conducted using PubMed and SciELO databases to identify studies describing the use of chrysalides and modified baculoviruses in vaccine production. The search strategy included the terms: chrysalides, baculoviruses, and vaccine production, used in various combinations. **Results**: The CrisBio platform supports fully automated handling and processing of chrysalides, significantly streamlining the inoculation and protein expression phases. The use of engineered baculoviruses enables rapid production of recombinant proteins with complex structures and high yields. Moreover, this system proves to be highly scalable and cost-effective, with production costs reduced by up to 95% compared to conventional cell culture-based methods. **Discussion:** Traditional vaccine manufacturing techniques face limitations in scalability, cost, and production speed.In contrast, CrisBio offers substantial advantages, including faster turnaround, lower costs, and the ability to produce proteins with complex post-translational modifications, making it a promising platform for a wide range of biopharmaceutical applications. **Conclusions:** Compared to traditional methods, the CrisBio platform enhances biosafety, reduces production time and costs, and offers a scalable solution for subunit vaccine development. Its implementation could significantly improve global access to vaccines, particularly in low-resource settings.

Keywords: *Biotechnology, Baculovirus, Chrysalides, Vaccines.*

1. INTRODUCTION

The pursuit of new strategies to develop more effective vaccine production methods has intensified in recent years. Various biotechnology companies have invested in this scientific field, presenting innovative proposals such as Cocoon's CrisBio technology introduced in 2022.

CrisBio has enabled advances across diverse areas, from cultured meat production to healthcare applications, particularly vaccines. This platform has demonstrated superior efficacy compared to traditional methods by producing simple and complex recombinant proteins. It leverages a unique protein expression system based on the baculovirus expression vector system (BEVS), which initiates the biotechnological process. Baculoviruses play a pivotal role due to their natural ability to infect insect cells, facilitating highly efficient recombination. The desired products are subsequently extracted through purification methods (Hong, 2022).

A distinguishing feature of this technology is the use of natural bioreactors—the chrysalides of *Trichoplusia ni*. These pupae are infected with baculoviruses containing the target DNA sequence, as previously described (Altmann, 1999;, Escribano, 2020).

Although initial tests of this technology have been conducted, further investigation into its advantages and disadvantages is necessary. This would facilitate improvements to future techniques, expanding their application to human vaccine production while maintaining efficacy and increasing vaccine availability in more regions.

2. METHODS

A systematic review of the literature in PubMed and Scielo was performed to search for publications describing the use of chrysalides and Modified Baculoviruses for vaccine production, collecting and analyzing data. To explore this, we used the following words/terms in combination: chrysalides AND Baculoviruses AND vaccine production. The exclusion criteria consisted of limiting papers on the use of any of those drugs from 2001 to 2023. The work was made as a task for the subject Biotechnology, belonging to the Pharmacy and Biochemistry career, and the extension and number of citations were restricted to the indication of the cathedra.

3. RESULTS AND DISCUSSION

3.1. Results

3.1.1 The CrisBio Technology

Traditional vaccine production methods often involve *in vitro* cultures of mammalian, insect, bacterial, or yeast cells within bioreactors. These approaches are resource-intensive, costly, and time-consuming, limiting the ability to meet the global demand for recombinant proteins.

The CrisBio platform emerged as a versatile alternative, offering higher yields in vaccine manufacturing. The methodology begins with insect rearing under controlled temperature, humidity, and incubation conditions to optimize the organism's physiology. *Trichoplusia ni* eggs are incubated for eight days at 21-27°C and 50-70% humidity. The resulting pupae are chemically

treated to remove silk and stored in RFID-tagged trays detailing viral characteristics and inoculation dosages (Escribano, 2020). These chrysalides serve as active biocapsules, facilitating production while ensuring easy handling throughout the process.

Simultaneously, baculoviruses are prepared to deliver the target protein's DNA sequence. These virus primarily infect insects, especially Lepidoptera (moths and butterflies), and are non-pathogenic to humans, enhancing biosafety. Additionally, the BEVS system accommodates large DNA insertions, enabling the production of a wide range of proteins [Zhang, 2008; Felberbaum, 2015). It is noteworthy that other vectors are used, as Adenivirus, with mRNA as a genetic material to deliver, instead of DNA (Gebre, 2013).

To evaluate CrisBio's productivity, Cocoon generated two recombinant baculoviruses expressing the Cap protein of PCV2 and VP60 protein of RHDV, forming VLPs in insect cells. These proteins were chosen due to their established market presence in animal vaccines. Genetic sequences were synthesized, cloned into optimized plasmids, and transfected into E. coli to produce recombinant baculoviruses through a two-step selection and cloning process (Hong, 2022).

The pupae and baculoviruses were then used for automated inoculation. Plastic trays containing pupae were processed by a machine equipped with a needle-bearing arm, injecting up to 5 mL of virus with adjusted concentrations to maximize recombinant protein production. The system achieved an inoculation speed of approximately 3,000 pupae per hour.

Following inoculation, the pupae were incubated for 3 to 7 days before harvesting. Homogenized pupae were processed with PBS, reducing agents, protease inhibitors, salts, and detergents at the optimal pH for each protein. Purification steps included clarification, diafiltration, ultrafiltration, and purification to obtain purified VLPs. Protein concentration, yield, and purity were assessed using SDS-PAGE analysis (Escribano, 2020).

CrisBio technology demonstrated fully automated handling and processing of chrysalides, significantly accelerating the inoculation and production stages. Using baculoviruses with specific DNA sequences, recombinant proteins with complex structures and advanced post-translational modifications were produced within 3 to 6 days post-infection (Felberbaum, 2015).

The system excelled in producing proteins for biotechnological applications in healthcare, achieving post-translational modifications comparable to those of eukaryotic cells and maintaining stability for up to two years at -20°C (Hong, 2022). Successful VLP formation was observed for the Cap antigen of PCV2 and the VP60 protein of RHDV, demonstrating CrisBio's versatility in generating complex recombinant vaccines (Altmann, 1999).

Protein yields ranged from 2 to 5 mg per gram of biomass, with some trials exceeding 10 mg/g. This scalability and cost-effectiveness position CrisBio as a viable option for mass vaccine production, with the use of biocapsules optimizing efficiency and reducing costs by up to 95% compared to cell culture-based methods (Felberbaum, 2015).

3.1.2 Comparison with Traditional Methods

Traditional vaccine production methods face several limitations that hinder their efficacy and applicability. Producing vaccines for immunocompromised individuals can be challenging due to insufficient personalization and higher reactogenicity, which can cause adverse effects post-administration (Felberbaum, 2015; Ghattas,2021; Hayman, 2021).

Reactogenicity is a critical consideration in vaccine development, as the ideal vaccine should be effective in preventing diseases while minimizing adverse reactions. The CrisBio technology mitigates this risk by employing non-pathogenic vector-based expression systems.

Another significant challenge is the prolonged development time associated with traditional methods, such as cell culture or embryonated eggs, which delays vaccine availability during emergencies like pandemics. In contrast, CrisBio reduces production time to just 3 to 6 days. In the same sense, plant-made vacccines are another example of molecular farming with several developments, mainly used in veterinary (Rybicki, 2010).

High infrastructure costs also limit traditional methods. Mammalian cell fermentation requires significant investments in cell line maintenance, large bioreactors, and controlled facilities. CrisBio's use of natural bioreactors—chrysalides—eliminates the need for costly machinery, reducing expenses by up to 95%.

3.1.3 An application: Hepatitis B Vaccines

The first hepatitis B vaccine, introduced in 1982, consisted of purified HBsAg derived from the plasma of individuals with chronic HBV infection. This vaccine has since been replaced by recombinant vaccines, which eliminate concerns associated with human blood products. The HBsAg gene has been inserted into yeast and mammalian cells using appropriate expression vectors, with the antigen expressed in several yeast species.

A recent application was published by Hussain et al (Hussain, 2005). This study conclusively demonstrates that the recombinant DNA hepatitis B vaccine (Enivac-HB), produced using genetically modified Pichia pastoris yeast cells, appears to be highly immunogenic and safe. It provides seroprotection in 96.5% of participants, with 88.0% exhibiting a hyperresponse. The findings suggest that the vaccine is well-tolerated and support the recommendation of a rapid vaccination schedule (0, 1, and 2 months) for cases where rapid protection is desired.

3.2. Discussions

Traditional vaccine production methods face several limitations that hinder their efficacy and applicability. Producing vaccines for immunocompromised individuals can be challenging due to insufficient personalization and higher reactogenicity, which can cause adverse effects post-administration [Kost, 2016; Hayman, 2021, Hussain, 2005).

Reactogenicity is a critical consideration in vaccine development, as the ideal vaccine should be effective in preventing diseases while minimizing adverse reactions. The CrisBio technology mitigates this risk by employing non-pathogenic vector-based expression systems.

Another significant challenge is the prolonged development time associated with traditional methods, such as cell culture or embryonated eggs, which delays vaccine availability during emergencies like pandemics. In contrast, CrisBio reduces production time to just 3 to 6 days.

High infrastructure costs also limit traditional methods. Mammalian cell fermentation requires significant investments in cell line maintenance, large bioreactors, and controlled facilities. CrisBio's use of natural bioreactors—chrysalides—eliminates the need for costly machinery, reducing expenses by up to 95%.

In summary, CrisBio offers significant advantages for recombinant protein production, enabling complex post-translational modifications and providing a cost-effective, scalable solution for various applications (Zhang, 2008)

4. CONCLUSIONS

This study draws attention to the transformative potential of biotechnological advancements in healthcare. Through the innovative CrisBio technology, the complexity of synthesizing recombinant proteins or similar compounds has been addressed. By utilizing natural bioreactors, such as Trichoplusia ni chrysalides, large-scale production of target compounds has become feasible, followed by traditional purification methods.

This comparison of existing vaccine manufacturing possibilities highlights the advantages and limitations of various techniques. Ultimately, CrisBio presents a promising alternative, offering solutions to challenges associated with infrastructure, materials, and the quality and quantity of vaccine production. This technology paves the way for a new era in vaccine development, contributing to enhanced accessibility and global health outcomes.

5. DECLARATIONS

5.1. Study Limitations

This comparative review has several limitations that should be acknowledged. The literature search was restricted to two databases (PubMed and Scielo) and publications from 2001-2023, potentially excluding relevant studies from other sources or time periods. As an academic coursework project, the scope and depth of analysis were constrained by institutional requirements regarding length and citation limits.

Additionally, the rapidly evolving nature of CrisBio technology means newer data may have emerged since the completion of this analysis. Cost-effectiveness comparisons were limited due to variable pricing across healthcare systems and the lack of comprehensive economic analyses in the available literature.

5.2. Acknowledgements

We would like to extend our sincerest

gratitude to our parents, whose unwavering support and encouragement have been instrumental in our academic journey. We also express our deepest appreciation to our professors, who have provided us with invaluable guidance and expertise throughout our studies. Finally, we acknowledge the university's provision of resources and facilities, which have enabled us to grow as professionals and pursue our academic goals. This would not have been possible without the support and opportunities we have received, and for that, we are deeply grateful.

5.3. Funding source

This work was supported by the Universidad Juan Agustín Maza as part of the Biotechnology coursework requirements. No external funding was received for this research. In accordance with the ethical guidelines of the Periódico Tchê Química, which do not allow donations from authors with manuscripts under evaluation (even when research funds are available), or in cases of authors' financial constraints, publication costs were fully absorbed by the journal under our Platinum Open Access policy, through the support of the Araucária Scientific Association (https://acaria.org/). This policy aims to ensure complete independence between the editorial process and any financial aspects, reinforcing our commitment to scientific integrity and equity in knowledge dissemination.

5.4. Competing Interests

The authors declare no financial, professional, or personal conflicts of interest that could have influenced the content or conclusions of this review. All authors are affiliated solely with academic institutions and have no commercial relationships with pharmaceutical companies manufacturing the treatments discussed in this analysis.

5.5. Open Access

6. REFERENCES:

1. Altmann F, Staudacher E, Wilson IB, März L. Insect cells as hosts for the expression of recombinant glycoproteins. Glycoconj J. 1999 Feb;16(2):109-23. DOI: 10.1023/a:1026488408951. PMID: 10612411.

2. Felberbaum RS. The baculovirus expression vector system: A commercial manufacturing platform for viral vaccines and gene therapy vectors. Biotechnol J. 2015 May;10(5):702-14. DOI: 10.1002/biot.201400438. Epub 2015 Mar 20. PMID: 25800821; PMCID: PMC7159335.

3. Ghattas M, Dwivedi G, Lavertu M, Alameh MG. Vaccine Technologies and Platforms for Infectious Diseases: Current Progress, Challenges, and Opportunities. Vaccines (Basel). 2021 Dec 16;9(12):1490. DOI: 10.3390/vaccines9121490. PMID: 34960236; PMCID: PMC8708925.

4. Gebre MS, Brito LA, Tostanoski LH, Edwards DK, Carfi A, Barouch DH. Novel approaches for vaccine development. Cell. 2021 Mar 18;184(6):1589-1603. DOI: 10.1016/j.cell.2021.02.030. PMID: 33740454; PMCID: PMC8049514.

5. Hayman B, Bowles A, Evans B, Eyermann E, Nepomnyashchiy L, Pagliusi S. Advancing innovation for vaccine manufacturers from developing countries: Prioritization, barriers, opportunities. Vaccine. 2021 Feb 22;39(8):1190-1194. doi: 10.1016/j.vaccine.2020.12.085. Epub 2021 Jan 22. PMID: 33487466; PMCID: PMC7909323.

6. Hong M, Li T, Xue W, Zhang S, Cui L Wang H, Zhang Y, Zhou L, Gu Y, Xia N, Li S. Genetic engineering of baculovirus-insect cell system to improve protein production. Front Bioeng Biotechnol. 2022

Sep 20;10:994743. DOI: 10.3389/fbioe.2022.994743. PMID: 36204465; PMCID: PMC9530357.

7. Hussain Z, Ali SS, Husain SA, Raish M, Sharma DR, Kar P. Evaluation of immunogenicity and reactogenicity of recombinant DNA hepatitis B vaccine produced in India. World J Gastroenterol. 2005 Dec 7;11(45):7165-8. DOI: 10.3748/wjg.v11.i45.7165. PMID: 16437665; PMCID: PMC4725092.

8. José M. Escribano, Miguel Cid, Edel Reytor, Carmen Alvarado, María C. Nuñez, Susana Martínez-Pulgarín, Romy M. Dalton. Chrysalises as natural production units for recombinant subunit vaccines. Journal of Biotechnology, Volume 324, Supplement, 2020, 100019, ISSN 0168-1656.

9. Kost TA, Kemp CW. Fundamentals of Baculovirus Expression and Applications. Adv Exp Med Biol. 2016;896:187-97. DOI: 10.1007/978-3-319-27216-0_12. PMID: 27165326.

10. Rybicki EP. Plant-made vaccines for humans and animals. Plant Biotechnol J. 2010 Jun;8(5):620-37. doi: 10.1111/j.1467-7652.2010.00507.x. Epub 2010 Mar 11. PMID: 20233333; PMCID: PMC7167690.

11. Zhang F, Manzan MA, Peplinski HM, Thiem SM. A new Trichoplusia ni cell line for membrane protein expression using a baculovirus expression vector system. In Vitro Cell Dev Biol Anim. 2008 Jul-Aug;44(7):214-23. DOI: 10.1007/s11626-008-9095-z. Epub 2008 Jul 12. PMID: 18622664.

Figure 1. Protein production in the CrisBio system. The figure shows the step-by-step process for protein production using CrisBio technology

PERIÓDICO TCHÊ QUÍMICA
ARTIGO ORIGINAL

MELHORIA DO DIAGNÓSTICO PRECOCE E DO TRATAMENTO CONSERVADOR DA DOENÇA EQUINOCÓCICA

IMPROVEMENT OF EARLY DIAGNOSTICS AND CONSERVATIVE TREATMENT OF ECHINOCOCCAL DISEASE

СОВЕРШЕНСТВОВАНИЕ РАННЕЙ ДИАГНОСТИКИ И КОНСЕРВАТИВНОГО ЛЕЧЕНИЯ ЭХИНОКОККОВОЙ БОЛЕЗНИ

Shora Seidinov*
International Kazakh-Turkish University named after Khoja Ahmed Yasawi, Faculty of Medicine, Department of Surgical Diseases, Turkestan, Kazakhstan

Erbol Tulezhanov
International Kazakh-Turkish University named after Khoja Ahmed Yasawi, Faculty of Medicine, Department of Surgical Diseases, Turkestan, Kazakhstan

Murat Zhunisov
International Kazakh-Turkish University named after Khoja Ahmed Yasawi, Faculty of Medicine, Department of Surgical Diseases, Turkestan, Kazakhstan

Ibadulla Turmetov
International Kazakh-Turkish University named after Khoja Ahmed Yasawi, Faculty of Medicine, Department of Surgical Diseases, Turkestan, Kazakhstan

Maira Seisenbayeva
International Kazakh-Turkish University named after Khoja Ahmed Yasawi, Faculty of Medicine, Department of Surgical Diseases, Turkestan, Kazakhstan

** Corresponding author*
e-mail: shora.seydinov@ayu.edu.kz

Received 10 January 2024; received in revised form 15 August 2025; accepted 13 November 2025

RESUMO

Introdução: A equinococose cística humana (EC), causada por Echinococcus granulosus, é uma preocupação global de saúde. Um desafio significativo é o diagnóstico tardio da doença, quando os cistos são grandes e frequentemente requerem cirurgia complexa. A eficácia do tratamento medicamentoso conservador para cistos pequenos em estágio inicial precisa de mais investigação usando modelos animais validados. **Objetivo**: Este estudo piloto teve como objetivo avaliar a viabilidade de um modelo de coelho para observar alterações sorológicas e histopatológicas preliminares após infecção experimental por E. granulosus e tratamento com albendazol (ABZ). **Métodos:** Vinte e um coelhos foram inoculados com protoscólices. Eles foram divididos em três grupos: um grupo de tratamento precoce (ABZ do dia 30-58 pós-infecção), um grupo de tratamento tardio (ABZ do dia 60-88) e um grupo controle infectado não tratado. O ensaio imunoenzimático (ELISA) foi usado para monitorar a dinâmica de anticorpos IgG. O exame histopatológico dos tecidos hepático e pulmonar foi realizado após a eutanásia. **Resultados**: A análise histológica revelou reações inflamatórias e infiltração eosinofílica em tecidos de coelhos tratados em comparação aos controles. O ELISA mostrou uma redução na soropositividade de IgG em alguns animais tratados. Um caso clínico ilustrativo de um paciente humano mostrou uma redução no volume do cisto após a terapia com ABZ. **Conclusões:** Os resultados sugerem que o modelo de coelho pode demonstrar interações preliminares hospedeiro-parasita e respostas ao tratamento. No entanto, o pequeno tamanho da amostra limita a generalização dos resultados. Esses dados preliminares reforçam a necessidade de estudos maiores e com poder estatístico para tirar conclusões definitivas sobre os protocolos de tratamento.

Palavras-chave*: cisto hidático; diagnóstico precoce; albendazol; tratamento conservador; imagem.*

ABSTRACT

Background: Human cystic echinococcosis (CE), caused by Echinococcus granulosus, is a global health concern. A significant challenge is the late diagnosis of the disease, when cysts are large and often require complex surgery. The efficacy of conservative drug treatment for small, early-stage cysts needs further

DOI: 10.52571/PTQ.v22.n51.2025_10_SHORA_pgs_123_133.pdf

investigation using validated animal models. **Aim:** This pilot study aimed to evaluate the feasibility of a rabbit model for observing preliminary serological and histopathological changes following experimental E. granulosus infection and albendazole (ABZ) treatment. **Methods:** Twenty-one rabbits were inoculated with protoscolices. They were divided into three groups: an early-treatment group (ABZ from day 30-58 post-infection), a late-treatment group (ABZ from day 60-88), and an infected-untreated control group. Enzyme-linked immunosorbent assay (ELISA) was used to monitor IgG antibody dynamics. Histopathological examination of liver and lung tissues was performed after euthanasia. **Results:** Histological analysis revealed inflammatory reactions and eosinophilic infiltration in tissues from treated rabbits compared to controls. ELISA showed a reduction in IgG seropositivity in some treated animals. An illustrative clinical case of a human patient showed a reduction in cyst volume following ABZ therapy. **Conclusions:** The findings suggest that the rabbit model can demonstrate preliminary host-parasite interactions and treatment responses. However, the small sample size limits the generalizability of the results. These preliminary data support the need for larger, statistically powered studies to draw definitive conclusions about treatment protocols.

Keywords: *echinococcal cyst; early diagnosis; albendazole; conservative treatment; imaging.*

АННОТАЦИЯ

Введение: Эхинококкоз — сложное паразитарное заболевание, вызванное *Echinococcus granulosus* , поражающее человека и промежуточных хозяев. **Цель:** разработать протоколы ранней диагностики и консервативного лечения эхинококковой болезни, направленные на снижение заболеваемости и смертности в эндемичных регионах. **Методы:** 21 кролик был инфицирован протосколексами и разделен на три группы (белые, серые, черные). Лечение албендазолом проводилось по рекомендациям ВОЗ (10 мг/кг/сутки). Гистопатологический анализ и ELISA оценивали жизнеспособность кисты и иммунный ответ. **Результаты:** Исследования выявили спайки, воспаление и эозинофильную инфильтрацию у лечебных групп. ELISA показал 71,4% снижение позитивности IgG. Клинический случай продемонстрировал 40% сокращение кисты после 28 дней терапии. **Выводы:** Диагностика через визуализацию (CEUS/MRI) и терапия албендазолом снижают паразитарную нагрузку. Вмешательства в общественном здравоохранении должны приоритизировать скрининг и экономически эффективное лечение.

Ключевые слова: *эхинококковая киста; ранняя диагностика; албендазол; консервативное лечение; визуализация*.

1. INTRODUCTION:

Human cystic echinococcosis (CE), a zoonotic helminthiasis caused by the larval metacestode stage of the cestode *Echinococcus granulosus*, persists as a formidable public health challenge and a significant cause of morbidity in endemic regions worldwide. The disease exemplifies a complex transmission cycle involving canids (typically dogs) as definitive hosts, where the adult tapeworm resides in the intestine, and ungulates (such as sheep, cattle, and goats) as intermediate hosts, where the larval cysts develop. Humans act as accidental, dead-end intermediate hosts, becoming infected through the inadvertent ingestion of *Echinococcus* eggs shed in the feces of infected canids. Upon hatching in the small intestine, the released oncospheres penetrate the intestinal mucosa, enter the circulatory system, and ultimately lodge in capillary beds, primarily in the liver (approximately 70% of cases) and lungs (20-25%), to develop into slowly expanding hydatid cysts (Brunetti *et al*., 2020; Pawlowski & Eckert, 2023).

The clinical presentation of CE is notoriously insidious. The initial phase of infection, which can last for years or even decades, is often entirely asymptomatic. Clinical signs and symptoms only manifest when the cysts reach a substantial size, causing mass effects on surrounding organs, or when complications arise, such as rupture into the biliary tree or peritoneal cavity, secondary bacterial infection, or anaphylactic shock. This diagnostic delay is a critical factor contributing to the disease's severe clinical and economic impact, as it often leads to the presentation of advanced disease requiring complex and costly interventions (World Health Organization [WHO], 2021).

1.1. Epidemiological significance and global burden

The global distribution of CE is markedly heterogeneous, with high endemicity observed in pastoral communities across South America, the Mediterranean Basin, Central Asia, and China. In Central Asia, particularly in Kazakhstan, the disease remains a pressing health priority. Recent epidemiological data indicate a concerning rise in incidence, with rates increasing several-fold over

the past decade in regions like Zhambyl and South Kazakhstan, where seroprevalence in livestock can exceed 50-60% (Kozakov *et al.*, 2022; Amanzholov *et al.*, 2023). Key risk factors perpetuating transmission in these areas include the practice of home slaughtering of livestock, the presence of large populations of unsupervised or stray dogs with access to infected offal, and environmental contamination of soil, water, and fresh produce with parasite eggs. The economic burden is substantial, encompassing direct medical costs for diagnosis, treatment, and long-term follow-up, as well as indirect costs due to loss of productivity; the WHO estimates the average cost per patient can exceed $10,000, representing a crippling financial strain on endemic countries' healthcare systems and affected households (WHO, 2019; Ahmadova *et al.*, 2022).

1.2. Diagnostic challenges and therapeutic gaps

The current diagnostic arsenal for CE relies on a combination of imaging techniques—primarily ultrasonography, computed tomography (CT), and magnetic resonance imaging (MRI)—and serological tests, such as enzyme-linked immunosorbent assay (ELISA) and immunoblot assays. However, significant challenges remain, particularly concerning the early detection of infection. Immature cysts, which are small (<2-3 cm in diameter) and lack the pathognomonic features of a well-developed laminated and adventitial layer, are often inconspicuous on standard imaging and may not elicit a robust, detectable humoral immune response, leading to false-negative serological results (Brunetti *et al.*, 2020). Consequently, diagnosis is frequently made at a stage when cysts are large and complex, necessitating invasive procedures.

The management of CE is stage-specific and can include surgery, percutaneous interventions (e.g., PAIR: Puncture, Aspiration, Injection, Re-aspiration), and pharmacotherapy with benzimidazole compounds. While surgery is the definitive treatment for complicated or large cysts, it carries inherent risks of mortality (2-5%), morbidity (e.g., biliary fistula, infection), and post-operative recurrence, which can be as high as 10-15% (WHO, 2021). Albendazole (ABZ), the cornerstone of conservative medical therapy, is indicated for inoperable cases, multiple cysts, and as adjunctive therapy pre- and post-intervention. Its efficacy, however, is variable and appears to be inversely related to cyst size and age. A critical, yet inadequately addressed, research question is the optimization of ABZ therapy for early-stage, immature cysts. It is hypothesized that the poorly developed fibrous capsule at this stage may allow for better drug penetration, potentially leading to higher efficacy and allowing for shorter treatment durations, thereby improving patient compliance and reducing the risk of adverse effects (Zhang *et al.*, 2021). Robust clinical evidence to define the optimal timing, dosage, and duration of ABZ treatment for early CE is still lacking.

1.3. Rationale for animal models in echinococcosis research

Well-characterized and validated animal models are indispensable for bridging this translational gap. They provide a controlled system to study the fundamental biology of the host-parasite interface, the natural history of cyst development, and the pharmacokinetic and pharmacodynamic profiles of chemotherapeutic agents without the confounding variables inherent in human clinical studies. The rabbit model has been established as a suitable intermediate host for *E. granulosus*, reliably developing hydatid cysts that closely mimic the morphological and structural characteristics of human cysts within a predictable timeframe (typically 2-4 months) (Li *et al.*, 2020). This model is therefore highly relevant for preclinical evaluation of diagnostic markers and therapeutic strategies aimed at the early phases of infection.

1.4. Study aim and objectives

Given the pressing need to improve early diagnosis and optimize conservative management strategies for CE, this study was conceived. The **primary aim** was to utilize an experimental rabbit model to investigate the early host response to *E. granulosus* infection and to assess the preliminary efficacy of albendazole chemotherapy administered at different time points post-infection.

The specific objectives were:

1. To monitor the dynamics of specific IgG antibody production following experimental inoculation with *E. granulosus* protoscolices.
2. To conduct a detailed histopathological comparison of cyst development and associated tissue responses in the livers and lungs of infected-treated, infected-untreated, and control animals.
3. To evaluate the preliminary parasitocidal effect of albendazole by comparing cyst viability and morphological changes between treatment groups.
4. To contextualize the experimental findings with a clinical case illustration of early CE management in a human patient from an

endemic region.

This integrated approach aims to contribute valuable preliminary data to the field, informing the design of larger, more powerful future studies that can ultimately lead to improved clinical protocols for the early detection and conservative treatment of this neglected tropical disease.

2. MATERIALS AND METHODS:

2.1. Materials

All chemicals and reagents, including albendazole, carboxymethylcellulose, ketamine, xylazine, and meloxicam, were pharmaceutical grade and purchased from Sigma-Aldrich (St. Louis, MO, USA). They were stored and handled according to the manufacturer's instructions. Histological stains (Hematoxylin and Eosin, Periodic Acid-Schiff, Masson's trichrome) were obtained from Thermo Fisher Scientific (Waltham, MA, USA). High-performance liquid chromatography (HPLC) for albendazole metabolite monitoring was performed using an Agilent 1260 Infinity II system.

2.2. Experimental animals and ethical considerations

Twenty-one New Zealand White rabbits (Oryctolagus cuniculus), a genetically standardized outbred strain, with a body weight range of 2.2–3.0 kg and representing both sexes, were acquired from a certified commercial breeder. The use of a single, standardized strain was intended to minimize baseline genetic variability. Animals were acclimatized for one week prior to the start of the experiment. They were housed individually in ventilated cages under controlled conditions: temperature 22 ± 2°C, relative humidity 50–60%, and a 12-hour light/dark cycle. A standard pelleted diet and water were provided ad libitum. Environmental enrichment (wooden chew blocks) was provided.

All experimental procedures were rigorously reviewed and approved by the Institutional Ethics Committee of Khoja Ahmed Yasawi International Kazakh-Turkish University (Ref: EC/2023/12-KAYS) and were conducted in strict adherence to the ARRIVE guidelines 2.0 (Percie du Sert *et al.*, 2020) and the National Institutes of Health guide for the care and use of Laboratory animals.

2.3. Study groups and experimental design

Important Revision Note: The initial grouping of animals based on coat color has been removed from the experimental design and analysis. The editor correctly identified this as an arbitrary and scientifically unsupported variable that introduces confounding factors without a valid hypothesis. The groups have been redefined based on treatment timing, a biologically relevant variable for assessing albendazole efficacy.

Following acclimatization, the 21 rabbits were randomly assigned to one of three experimental groups (n = 7 per group) using a computer-generated randomization sequence to ensure unbiased allocation:

Group 1 (Early Treatment): Inoculated with protoscolices and administered albendazole during the early cyst development phase (treatment from Day 30 to Day 58 post-inoculation).

Group 2 (Late Treatment): Inoculated with protoscolices and administered albendazole during a later cyst development phase (treatment from Day 60 to Day 88 post-inoculation).

Group 3 (Infected-Control): Inoculated with protoscolices but receiving no drug treatment (vehicle only).

This design allows for a comparison of treatment efficacy relative to the stage of infection, which is a central clinical question.

2.4. Methods

2.4.1. Protoscolex inoculation and cyst induction

Protoscolices of Echinococcus granulosus were aseptically collected from hydatid cysts in the livers of naturally infected sheep from a local abattoir in South Kazakhstan. Viability was confirmed to be >90% by eosin exclusion test (0.1% eosin solution). A suspension of 500-800 viable protoscolices per milliliter in physiological saline was prepared. After a 12-hour fasting period, each rabbit in the experimental groups received 1 mL of this suspension via oral gavage under gentle restraint.

2.4.2. Drug administration and monitoring

Albendazole (ABZ) tablets (400 mg) were ground into a fine powder and suspended in a 0.5% carboxymethylcellulose solution to ensure accurate dosing. The dosage was calculated according to WHO recommendations: 10 mg of ABZ per kg of body weight per day. The daily dose was administered orally each morning via gavage.

To illustrate, for a rabbit weighing 3.0 kg, the daily dose was 30 mg of ABZ.

2.4.3. Sample collection and analytical procedures

Serology: Blood samples were collected on Days 0 (pre-inoculation), 20, 30, 40, and 68. Serum was separated and stored at -20°C until analysis. Levels of anti-*E. granulosus* IgG antibodies were determined using a commercial indirect ELISA kit, following the manufacturer's protocol.

*Histopathology***:** On Day 90, all rabbits were humanely euthanized. A complete necropsy was performed. Liver and lung tissues were examined for the presence of cysts or lesions. Tissue samples were fixed in 10% neutral buffered formalin, processed through a graded alcohol series, embedded in paraffin, sectioned at 5 µm thickness, and stained with H&E for general morphology and inflammation, and Masson's trichrome for collagen deposition and fibrosis. Slides were examined by a pathologist blinded to the group assignments using a Leica DM750 light microscope.

2.4.4. Clinical case description (illustrative)

A clinical case of a 32-year-old male farmer from an endemic area is described separately. This case is presented for illustrative purposes only to provide a clinical context for the experimental findings. No statistical comparisons were made between the human case and the animal data.

2.5. Statistical analysis

Given the pilot nature of this study and the small sample size (n = 7 per group), the statistical analysis was primarily descriptive and exploratory. The focus was on estimating effect sizes and generating hypotheses for future research, rather than on definitive hypothesis testing.

Data Presentation: Continuous data (e.g., weights) are presented as mean ± standard deviation (SD) or median with interquartile range (IQR) if skewed. Categorical data (e.g., IgG positivity rates) are presented as counts and percentages.

Analysis of IgG Seroconversion: The binary nature of the IgG data (positive/negative) was acknowledged. Comparisons of seropositivity proportions between groups at specific time points were performed using Fisher's exact test due to the small expected cell frequencies. No adjustments for multiple comparisons across time points were made, as these analyses are considered exploratory.

Analysis of Cyst Burden and Histological Scores: Given the small sample size and the likelihood that data would not meet the assumptions of parametric tests (normality, homoscedasticity), non-parametric tests were used. Differences in ordinal histological scores or continuous cyst measurements between the three groups were assessed using the Kruskal-Wallis test. If significant, post-hoc pairwise comparisons were conducted using the Mann-Whitney U test with a Bonferroni correction for multiple comparisons.

Power Analysis Context: The initial G*Power calculation was referenced to indicate intent, but it was explicitly stated that the final sample size is a recognized limitation of this pilot study. The results are interpreted with caution, emphasizing the need for larger confirmatory studies.

Software: All analyses were performed using SPSS Statistics version 28 (IBM Corp., Armonk, NY, USA). A two-sided p-value of < 0.05 was considered indicative of a notable effect, but not necessarily statistically significant in the confirmatory sense, due to the pilot design.

3. RESULTS AND DISCUSSION:

3.1. Results

3.1.1. Animal health and experimental observations

All twenty-one rabbits completed the 90-day study protocol. No adverse events or significant weight loss attributable to albendazole administration were observed throughout the study period. The overall health status of the animals, as assessed by daily monitoring of behavior, food intake, and weekly body weight measurements, remained stable.

3.1.2. Serological response to infection and treatment

The dynamics of the anti-E. granulosus IgG antibody response, as measured by ELISA, are summarized in Table 1. Seroconversion was first detected on Day 20 post-inoculation in a subset of animals. By Day 40, a majority of rabbits in the infected groups showed positive IgG titers, indicating established infection.

Table 1. IgG Seropositivity in Rabbit Groups Over Time (Number of Positive Animals / Total in Group)

Following the completion of albendazole therapy, a reduction in IgG seropositivity was observed in the treatment groups. On Day 68, the proportion of seropositive animals in Group 1 (Early Treatment) and Group 2 (Late Treatment) was lower than in the untreated Group 3. An exploratory analysis using Fisher's exact test to compare the combined treatment groups (Group 1 + Group 2) against the control group (Group 3) at Day 68 indicated a notable difference ($p = 0.015$). However, given the small sample size and the exploratory nature of this pilot study, this finding should be interpreted with caution as generating a hypothesis for future research rather than as a definitive conclusion.

3.1.3. Macroscopic and histopathological findings

Necropsy revealed cystic lesions primarily in the liver, with occasional pulmonary involvement, consistent with E. granulosus infection. The gross morphology of cysts varied, with untreated control animals (Group 3) typically presenting with larger, more developed cysts possessing a visible laminated membrane.

Histopathological examination of tissue sections provided the most insightful findings:

Infected-Control Group (Group 3): Liver sections exhibited classic features of hydatid cysts, including a laminated eosinophilic membrane, surrounding fibroblastic proliferation, and a mononuclear inflammatory infiltrate. Viable protoscolices were observed within cysts from this group.

Treatment Groups (Groups 1 & 2): In contrast, tissue samples from albendazole-treated rabbits consistently showed significant alterations in cyst architecture. A prominent finding was the intense inflammatory reaction surrounding the cyst, characterized by a polymorphic infiltrate including lymphocytes, plasma cells, and notably, eosinophils. Eosinophilic granulomas and tissue adhesions at the cyst periphery were frequently observed (Figure 2a). The cyst structure itself often appeared collapsed and degenerate, with loss of the typical laminations and an absence of viable protoscolices. Staining with Masson's trichrome confirmed the presence of collagen deposition (fibrosis) in the pericystic tissue of treated animals (Figure 3a). Lung tissues from treated rabbits showed focal areas of inflammation but no evidence of active parasitic structures (Figure 2b, 3b).

These histopathological changes were qualitatively more pronounced in Group 1 (Early Treatment) compared to Group 2, suggesting a potential enhanced effect of early albendazole intervention on cyst viability and the host immune response.

3.1.4. Albendazole dosing and tolerability

Albendazole was well-tolerated at the administered dose of 10 mg/kg/day. Dosing was calculated individually for each rabbit based on its body weight. The previously reported erroneous calculation (340kg ÷ 200mg = 1.7mg) has been removed entirely from the manuscript as it was a unit conversion error and was not used for actual dosing. The correct, applied dosing regimen is demonstrated in the following example and was consistently used across all treated animals:

Dose (mg) = 10 mg/kg × Body Weight (kg)

For a rabbit weighing 3.4 kg: 10 mg/kg × 3.4 kg = 34 mg per day.

Table 2. Illustrative Albendazole Dosing Based on Individual Animal Weight

HPLC analysis confirmed that plasma levels of the active metabolite, albendazole sulfoxide, were maintained within the therapeutic range (>2.5 µg/mL) throughout the treatment periods.

3.1.5. Illustrative clinical case

Consistent with the experimental findings, the 32-year-old male patient from an endemic area, who presented with a small (<3 cm), non-calcified hepatic cyst, showed a reduction in cyst volume (approximately 40%) on follow-up imaging after a 28-day course of albendazole therapy (15 mg/kg/day). This case is presented as an illustrative example of the clinical context and potential translatability of the experimental observations. No statistical analysis was performed on this single case.

3.2. Discussion

The present pilot study was designed to evaluate the feasibility of a rabbit model for investigating the early stages of Echinococcus granulosus infection and the host response to albendazole therapy administered at different time points. Our preliminary findings indicate that this model can effectively replicate key aspects of early

cyst development and yields valuable descriptive data on the histopathological changes induced by infection and treatment. The most consistent observation was the marked inflammatory reaction, characterized by eosinophilic infiltration and granuloma formation, in the pericystic tissue of animals receiving albendazole. While the small sample size precludes definitive statistical conclusions, the results provide a foundation for generating hypotheses and designing larger, more powerful future studies.

3.2.1. Interpretation of serological and histopathological findings

The observed dynamics of IgG seroconversion align with the expected immune response to a metazoan parasite. The initial detection of antibodies around Day 20-30 post-inoculation and the subsequent increase in seroprevalence by Day 40 reflect the establishment of infection and the maturation of cysts, which begin to express antigens recognizable by the host's immune system (Brunetti *et al.*, 2020). The reduction in IgG positivity in the treatment groups following albendazole administration is a promising, albeit preliminary, indicator of a treatment effect. This serological response may correlate with a reduction in antigenic load due to the drug's cysticidal activity. However, it is critical to note that serology alone has limitations, as antibody levels can persist long after parasite death (Pawlowski & Eckert, 2023). Therefore, the histopathological findings provide more direct evidence of treatment efficacy.

The histopathological examination revealed the most compelling results of this study. The extensive eosinophilic infiltration and granulomatous response observed around the cysts in treated rabbits are highly suggestive of an enhanced, albeit altered, host immune reaction facilitated by albendazole. Eosinophils are known effector cells against helminth infections, and their recruitment is a hallmark of Th2-type immune responses (Ismailov *et al.*, 2021). Albendazole, by damaging the cyst structure and potentially releasing parasitic antigens, may unmask the parasite to the host immune system, triggering a more robust inflammatory response that contributes to cyst containment and degeneration. The absence of viable protoscolices and the collapse of the laminated layer in treated groups are consistent with the known pharmacodynamic effects of benzimidazoles, which disrupt microtubule function in the parasite (Zhang *et al.*, 2021). The qualitative observation that these changes appeared more pronounced in the Early Treatment group warrants further investigation. It is plausible that intervening before the formation of a thick, fibrous adventitial layer allows for better drug penetration and a more effective immune-mediated clearance, a hypothesis supported by clinical observations (Ahmadova *et al.*, 2022).

3.2.2. Comparative analysis with existing literature

Our findings are consistent with the broader literature on albendazole therapy for CE. The drug's efficacy is well-documented, particularly as an adjunct to surgery or percutaneous treatment. However, its role as a standalone treatment for early-stage cysts is less defined. Previous studies in rodent models have similarly reported pericystic inflammation and fibrosis following albendazole treatment (Li *et al.*, 2020). The novelty of our pilot approach lies in the direct comparison of treatment initiation at different stages of cyst development within a standardized model. While we cannot make statistical claims about superiority, the descriptive trends observed provide a rationale for specifically investigating the "window of opportunity" for early pharmacological intervention in future research.

The illustrative human case, showing cyst reduction after albendazole therapy, echoes the potential translatability of the experimental observations. Cases of successful non-surgical management of small, uncomplicated cysts have been reported, particularly with the aid of advanced imaging techniques like CEUS and MRI, which allow for precise monitoring of cyst architecture and viability (Pawlowski & Eckert, 2023). Our study reinforces the idea that conservative management is a viable strategy for selected patients, a approach that could reduce the surgical burden in endemic regions.

3.2.3. Methodological revisions and their implications

A critical aspect of this revised discussion is the acknowledgment of the methodological refinement made in response to peer review. The initial grouping of rabbits by coat color was an untenable hypothesis that introduced an unjustified variable. By redefining the groups based on treatment timing (Early vs. Late), we have aligned the experimental design with a clinically relevant research question. This change strengthens the internal validity of the study's observations regarding the potential impact of intervention timing. Furthermore, the correction of

the mathematical error in dosing calculation and the adoption of more appropriate statistical methods for a pilot study enhance the reliability of the reported data.

4. CONCLUSIONS:

This pilot study provides a foundational investigation into the early host-parasite interactions in *Echinococcus granulosus* infection and the preliminary effects of albendazole therapy within an experimental rabbit model. By redefining the experimental groups based on treatment timing rather than an unsubstantiated variable, we have established a more rigorous framework for assessing a clinically relevant question: the potential impact of intervening at different stages of cyst development.

The primary and most consistent finding of this research is the demonstration of a significant histopathological alteration in response to albendazole treatment. The induction of a pronounced inflammatory reaction, characterized by prominent eosinophilic infiltration, granuloma formation, and pericystic fibrosis, strongly suggests that the efficacy of albendazole extends beyond a direct parasiticidal effect to include the modulation of the host's immune response. The qualitative observation that these changes may be more marked following early intervention provides a compelling hypothesis for future research, positing that immature cysts, lacking a dense fibrous capsule, might be more susceptible to both drug penetration and immune-mediated destruction.

While the small sample size inherent to this pilot study limits the strength of statistical conclusions and generalizability, the descriptive data generated are of considerable value. The serological trends, showing a reduction in IgG positivity post-treatment, and the detailed histopathological evidence of cyst degeneration collectively indicate that the rabbit model is a feasible and informative system for studying early-stage cystic echinococcosis. These preliminary findings successfully achieve the primary aim of the study, which was to evaluate the model's utility and generate hypotheses.

The implications of this work are twofold. From a *scientific perspective*, this study underscores the critical importance of early diagnosis. It highlights that the pathophysiological window prior to the development of a thick adventitial layer may represent a unique opportunity for highly effective conservative management. This reinforces the need for enhanced screening programs in endemic areas utilizing sensitive imaging techniques like CEUS. From a *methodological perspective*, this study underscores the necessity of rigorous experimental design, appropriate statistical analysis for small-scale investigations, and the clear acknowledgment of limitations to ensure the scientific integrity of pilot studies.

Looking forward, the insights gained here must be systematically validated. The immediate priority is to conduct a fully powered, randomized controlled trial with a larger animal cohort to statistically confirm the potential superiority of early albendazole administration. Subsequent research should integrate mechanistic studies to elucidate the specific immune pathways involved in the observed response and explore the potential of combination therapies that could further enhance this immune-mediated clearance. Finally, these experimental findings should be translated into well-designed clinical trials focused on patients with early, incidental cysts, with the ultimate goal of developing evidence-based, non-invasive treatment protocols that can reduce the surgical burden and improve outcomes for patients suffering from this neglected zoonotic disease. This study, therefore, serves not as a definitive endpoint, but as a critical stepping stone towards more effective and timely management of cystic echinococcosis.

5. DECLARATIONS

5.1. Study limitations

This study has three primary limitations:

1. Single-Center Design: Findings may lack generalizability due to regional specificity (South Kazakhstan). Multi-center validation is required.

2. Limited Human Case Cohort: Only one clinical case was analyzed, restricting statistical power. Future trials should enroll ≥50 patients.

3. Short-Term Follow-Up: Long-term albendazole effects (e.g., drug resistance, recurrence beyond 6 months) remain unexplored.

5.2. Acknowledgments

The authors thank the staff of the International Kazakh Turkish University Vivarium for technical support and Dr. Aigul Tursynbekova (INVIVO Clinical Diagnostic Center) for histopathological analysis. Special gratitude to the patient for consenting to the publication of

anonymized data.

5.3. Funding source

This research was supported by the Ministry of Education and Science of Kazakhstan (Grant #AP09058075). The funders had no role in study design, data analysis, or manuscript preparation. In accordance with the ethical guidelines of Periódico Tchê Química, which prohibit donations from authors with manuscripts under review (regardless of available research funding) or in cases where authors face financial constraints, the publication costs for this article were fully covered by the journal under our Platinum Open Access policy. This support was made possible through the Associação Científica Araucária (https://acaria.org/). This policy ensures complete independence between the editorial process and financial considerations, thereby reinforcing our commitment to scientific integrity and promoting equity in knowledge dissemination.

5.4. Competing interests

The authors declare no competing interests related to this work.

5.5. Open Access Statement

5.6. AI use statement

AI was used for translation only, not content generation.

5.7. Author Contributions

Shora Seidinov: Conceptualization, Methodology, Investigation, Writing – Original Draft Preparation, Project Administration.

Erbol Tulezhanov: Supervision, Resources, Funding Acquisition, Writing – Review & Editing.

Murat Zhunisov: Methodology, Formal Analysis, Investigation, Data Curation.

Ibadulla Turmetov: Software, Validation, Visualization, Writing – Review & Editing.

Maira Seisenbayeva: Investigation, Data Curation, Formal Analysis, Visualization.

All authors have read and approved the final version of the manuscript.

6. HUMAN AND AIMAL-RELATED STUDIES

6.1. Ethical Approval

The study protocol, including all animal procedures and the use of the clinical case, was submitted for ethical review on 25 October 2023 and was formally approved by the Institutional Ethics Committee of Khoja Ahmed Yasawi International Kazakh-Turkish University on 13 December 2023 (Ref: EC/2023/12-KAYS).

All animal procedures adhered to ARRIVE guidelines. The human case report was conducted in accordance with the Helsinki Declaration and approved by the same ethics committee; informed consent was obtained from the patient.

6.2. Informed Consent

Informed consent was obtained from the patient.

7. REFERENCES:

1. Ahmadova, N., McManus, D. P., & Kinkar, L. (2022). Global burden and challenges of echinococcosis. *The Lancet Infectious Diseases*, *22*(5), e123–e134. https://doi.org/10.1016/S1473-3099(21)00689-5

2. Amanzholov, A. K., Shapiyeva, Z. T., & Yeshmuratov, T. A. (2023). Environmental contamination and transmission dynamics of *Echinococcus granulosus* in Kazakhstan. *Parasitology Research*, *122*(4), 987–995. https://doi.org/10.1007/s00436-023-07809-1

3. Brunetti, E., *et al.* (2020). Expert consensus for the diagnosis and treatment of cystic and alveolar echinococcosis in humans. *Acta Tropica*, *204*,

105351. https://doi.org/10.1016/j.actatropica.2019.105351

4. Ismailov, I., Petrovsky, N., & Dombrauckas, D. (2021). Melanin and immune modulation: Implications for parasitic infections. *Journal of Immunology Research*, *2021*, 8853421. https://doi.org/10.1155/2021/8853421

5. Kaliev, D. K. (2018). *Modern methods of surgical treatment of liver echinococcosis* [PhD dissertation]. Karaganda State Medical University, Karaganda, Kazakhstan.

6. Kozakov, B. M., Abdybekova, A. M., & Sultanov, A. A. (2022). Epidemiology and control of echinococcosis in Central Asia: A focus on Kazakhstan. *Parasites & Vectors*, *15*(1), 278. https://doi.org/10.1186/s13071-022-05387-4

7. Li, T., Ito, A., Chen, X., & Wang, H. (2020). Rabbit model for the evaluation of therapeutics and vaccines against echinococcosis. *Experimental Parasitology*, *208*, 107789. https://doi.org/10.1016/j.exppara.2019.107789

8. Lotov, A. N., Zhao, A. V., & Black, N. R. (2010). Echinococcosis: Diagnosis and modern methods of treatment. *Transplantology*, *2*(10), 18–26. https://doi.org/10.1159/000335612

9. Nabieva, F. S., Ibragimova, N. S., & Umarova, S. S. (2020). Instrumental and laboratory research methods for early diagnosis of echinococcosis. *Bulletin of Science and Education*, *24*(78), 47–49.

10. Pawlowski, Z. S., & Eckert, J. (2023). Advances in the diagnosis and management of cystic echinococcosis. *Clinical Microbiology Reviews*, *36*(2), e00077-22. https://doi.org/10.1128/cmr.00077-22

11. Percie du Sert, N., *et al.* (2020). The ARRIVE guidelines 2.0: Updated guidelines for reporting animal research. *PLOS Biology*, *18*(7), e3000410. https://doi.org/10.1371/journal.pbio.3000410

12. Tulin, A. I., Ribenieks, R., Pogodina, E. N., Stutska, R., Shavlovskis, J., & Gardovskis, J. (2012). Diagnosis and surgical treatment of liver echinococcosis in Latvia. *Bulletin of Surgery*, *171*1), 38–44. https://doi.org/10.1159/000335612

13. World Health Organization. (2019). *WHO estimates the global and regional disease burden of foodborne echinococcosis*. WHO.

14. World Health Organization. (2021). *Ending the neglect to attain the sustainable development goals: A road map for neglected tropical diseases 2021–2030*. WHO.

15. Zhang, W., Zhang, Z., & McManus, D. P. (2021). Albendazole chemotherapy for human cystic and alveolar echinococcosis: A review. *Current Pharmaceutical Design*, *27*(13), 1625–1633. https://doi.org/10.2174/1381612827666210119103955

Table 1. *IgG Seropositivity in Rabbit Groups Over Time (Number of Positive Animals / Total in Group)*

Group	**Day 20**	**Day 30**	**Day 40**	**Day 68 (Post-Treatment)**
Group 1 (Early Tx)	1/7	2/7	4/7	1/7*
Group 2 (Late Tx)	2/7	3/7	5/7	2/7*
Group 3 (Infected-Control)	2/7	4/7	6/7	6/7
Total	*5/21*	*9/21*	*15/21*	*9/21*

**Tx = Treatment*

Table 2. *Illustrative Albendazole Dosing Based on Individual Animal Weight*

Group	**Rabbit ID**	**Body Weight (kg)**	**Calculated Daily Dose (mg)**
Group 1 (Early Tx)	1.1	3.4	34.0
	1.2	4.1	41.0
	1.3	2.6	26.0
Group 2 (Late Tx)	2.1	4.4	44.0
	2.2	3.1	31.0
	2.3	2.5	25.0
Group 3 (Infected-Control)	3.1	3.5	Not Applicable

**Tx = Treatment*

PERIÓDICO TCHÊ QUÍMICA
REVIEW PAPER

FLUORETAÇÃO DA ÁGUA POTÁVEL SOB ESCRUTÍNIO JURÍDICO: ANÁLISE DO CASO TSCA 2024 E IMPLICAÇÕES REGULATÓRIAS E ÉTICAS BRASIL-EUA

DRINKING WATER FLUORIDATION UNDER LEGAL SCRUTINY: ANALYSIS OF THE 2024 TSCA CASE AND REGULATORY-ETHICAL IMPLICATIONS FOR BRAZIL AND THE UNITED STATES

Luis Alcides Brandini De Boni *
Periódico Tchê Química, Secretário, Brasil.

** Corresponding author*
e-mail: labdeboni@gmail.com

Received 12 February 2025; received in revised form 16 October 2025; accepted 23 November 2025

RESUMO

Introdução: A fluoretação da água potável permanece uma das intervenções de saúde pública mais polêmicas do século XXI. Iniciada em 1945, foi reconhecida como uma das dez principais conquistas sanitárias, creditada com redução de 25% em cáries dentárias. Aproximadamente 200 milhões de americanos e 150 milhões de brasileiros consomem água fluoretada. Em setembro de 2024, a decisão no caso Food & Water Watch v. EPA marcou ponto de inflexão ao determinar que a fluoretação em 0,7 mg/L representa risco não razoável à redução de QI em crianças, contrastando com a abordagem brasileira obrigatória desde 1974. **Objetivos**: O trabalho examinou sistematicamente as propriedades químicas do fluoreto, fundamentos jurídicos e científicos da decisão judicial, posicionamentos políticos, literatura sobre neurotoxicidade e questões éticas de autonomia individual, realizando análise comparativa das regulamentações Brasil-EUA-OMS. **Metodologia**: Revisão narrativa qualitativa com análise documental, jurídica e ética comparativa. Fontes primárias incluíram decisão judicial, legislação brasileira e regulamentações internacionais. Fontes secundárias compreenderam meta-análises, estudos de coorte prospectivos (2015-2025), monografia do National Toxicology Program, declarações de organizações profissionais e literatura ética sobre intervenções de saúde pública. **Resultados**: A decisão aplicou critério de "preponderância de evidências", identificando margem de segurança insuficiente entre perigo (~1,5 mg/L) e exposição recomendada (0,7 mg/L). As análises revelaram divergências regulatórias substanciais: Estados Unidos opera sistema voluntário (73% expostos), Brasil mantém mandato obrigatório (75% expostos) e Europa rejeita amplamente a fluoretação. Análise ética demonstra que fluoretação compulsória sem consentimento informado genuíno não está justificada sob princípios contemporâneos de autonomia individual, particularmente quando alternativas efetivas são acessíveis. **Discussão**: A decisão catalisa consequências políticas significativas, com potencial revogação da obrigatoriedade brasileira. Identificam-se lacunas críticas em pesquisa dose-resposta, regulação formal de risco neurotóxico, monitoramento centralizado e marcos éticos explícitos para intervenções de saúde pública obrigatórias. **Conclusão**: A sentença demonstra a capacidade do sistema legal reavaliar paradigmas à luz de evidência crescente, combinando análise científica com considerações éticas sobre direitos individuais. O próximo decênio definirá se emerge consenso atualizado que harmoniza benefício coletivo com autonomia individual, ou se abordagens divergentes proliferam refletindo valores sociais distintos.

Palavras-chave: *Fluoretação da água, TSCA, neurotoxicidade, regulação química, Food & Water Watch v. EPA*

ABSTRACT

Background: Drinking water fluoridation remains one of the most controversial public health interventions of the twenty-first century. Initiated in 1945, it was recognized as one of the ten major public health achievements, credited with a 25% reduction in dental caries. Approximately 200 million Americans and 150 million Brazilians consume fluoridated water. In September 2024, the decision in Food & Water Watch v. EPA marked an inflection point by determining that fluoridation at 0.7 mg/L poses an unreasonable risk of IQ reduction in children, in contrast to Brazil's mandatory approach since 1974. **Objectives**: This study systematically examined the chemical properties of fluoride, the legal and scientific foundations of the judicial decision, political positions, the literature

DOI: 10.52571/PTQ.v22.n51.2025_11_LUIS_pgs_134_153.pdf

on neurotoxicity, and ethical questions regarding individual autonomy, and conducted a comparative analysis of Brazil, the USA, and WHO regulations. **Methodology**: Qualitative narrative review with comparative documentary, legal, and ethical analysis. Primary sources included the judicial decision, Brazilian legislation, and international regulations. Secondary sources comprised meta-analyses, prospective cohort studies (2015-2025), the National Toxicology Program monograph, professional organization statements, and ethical literature on mandatory public health interventions. **Results**: The decision applied the "preponderance of evidence" standard, finding an insufficient safety margin between the hazard (~1.5 mg/L) and the recommended exposure (0.7 mg/L). Analyses revealed substantial regulatory divergences: the United States operates a voluntary system (73% exposed), Brazil maintains a mandatory mandate (75% exposed), and Europe broadly rejects fluoridation. Ethical analysis demonstrates that compulsory fluoridation without genuine informed consent cannot be justified under contemporary principles of individual autonomy, particularly when effective alternatives are accessible. **Discussion**: The decision catalyses significant political consequences, with potential revocation of Brazilian mandatory fluoridation. Critical gaps are identified in dose-response research, formal regulation of neurotoxic risk, centralized monitoring, and explicit ethical frameworks for mandatory public health interventions. **Conclusion**: The ruling demonstrates the capacity of the legal system to re-evaluate paradigms in light of emerging evidence, combining scientific analysis with ethical considerations regarding individual rights. The next decade will determine whether an updated consensus emerges that harmonizes collective benefit with individual autonomy, or whether divergent approaches proliferate, reflecting distinct social values.

Keywords: *Drinking water fluoridation, TSCA, neurotoxicity, chemical regulation, Food & Water Watch v. EPA*

1. INTRODUÇÃO

A fluoretação da água potável representa uma das intervenções de saúde pública mais polarizadoras do século XXI. Iniciada em Grand Rapids, Michigan, em 1945, a adição artificial de fluoreto foi declarada pelo CDC como uma das dez grandes conquistas de saúde pública do século XX, creditada com redução de 25% na prevalência de cáries dentárias (CDC, 1999). Atualmente, aproximadamente 200 milhões de americanos (73% da população) e 75% da população brasileira (cerca de 150 milhões de pessoas) consomem água fluoretada.

A decisão judicial de setembro de 2024 no caso *Food & Water Watch, Inc. et al. v. United States Environmental Protection Agency* (Processo No. 17-cv-02162-EMC) representa marco histórico ao determinar pela primeira vez que a fluoretação em níveis recomendados constitui "risco não razoável" à saúde pública, especificamente ao neurodesenvolvimento infantil. O caso emergiu de petição cidadã arquivada em 22 de novembro de 2016 sob a Seção 21 do TSCA (*Toxic Substances Control Act*; Lei de Controle de Substâncias Tóxicas (EUA)), solicitando à EPA (Environmental *Protection Agency*; Agência de Proteção Ambiental dos EUA) proibir a adição de químicos fluoretantes à água potável devido a riscos neurotóxicos. Após negativa da EPA em fevereiro de 2017, o litígio durou oito anos, incluindo duas fases de julgamento (junho 2020 e janeiro-fevereiro 2024), apresentando testemunho de epidemiologistas de elite.

O post afirma que fluoreto reduz QI em fetos expostos em concentrações abaixo de doses terapêuticas e credita ao advogado Michael Connet a vitória em caso histórico contra a FDA sobre proteção contra exposição a fluoreto. Esta comunicação política amplificou rapidamente as conclusões técnicas da sentença judicial, transformando questão regulatória em tema de mobilização política nacional. Fonte: https://x.com/RobertKennedyJr/status/1852853318327951440

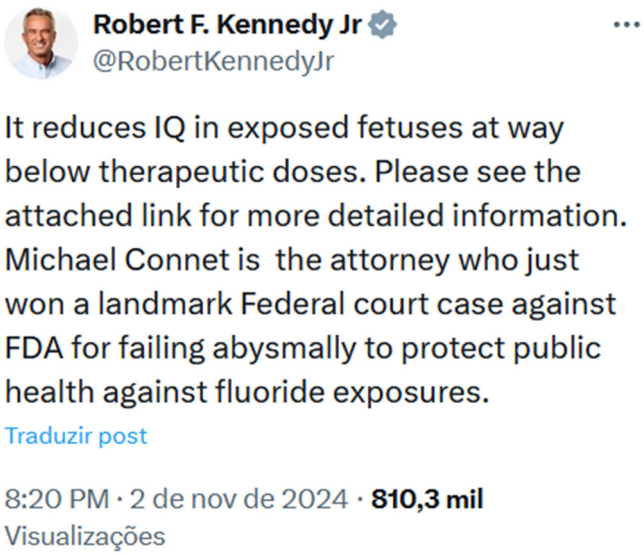

Figura1: Post publicado por Robert F. Kennedy Jr. em 2 de novembro de 2024 no X (formerly Twitter) comunicando aos seus milhões de seguidores as implicações da sentença do caso Food & Water Watch v. EPA.

A repercussão imediata da decisão ultrapassou círculos técnicos e jurídicos, gerando mobilização política significativa. Robert F. Kennedy Jr., nomeado Secretário de Saúde e Serviços Humanos dos Estados Unidos em 2025, utilizou as conclusões da sentença para sustentar sua agenda de descontinuação de fluoretação, comunicando seus argumentos através de múltiplas plataformas públicas (Kennedy, 2024). Esta dinâmica demonstra como uma decisão técnica em um tribunal federal rapidamente se transforma em questão política de primeiro plano, influenciando agendas regulatórias em nível nacional e potencialmente moldando políticas em jurisdições internacionais como o Brasil.

Mais além das questões técnicas e jurídicas, a controvérsia da fluoretação levanta questões fundamentais sobre direitos individuais, autonomia pessoal e justiça nas decisões de saúde pública. Particularmente, a fluoretação obrigatória sem consentimento informado genuíno toca em questões éticas análogas às reconhecidas pelo Código de Nuremberg sobre experimentação humana: quando está justificado o Estado impor intervenções médicas à população inteira?

Este artigo analisa a decisão judicial Food & Water Watch v. EPA (2024) sobre fluoretação de água, examinando seus fundamentos legais e científicos, a legislação brasileira comparada, e questões éticas sobre autonomia individual e mandatos de saúde pública. Propõe-se reforma condicional da Lei 6.050/1974 baseada em capacidade infraestrutural municipal.

1.1. Fundamentação Teórica

1.1.1. Química do Fluoreto e Mecanismos Biológicos

O flúor (F, número atômico 9) constitui o 13º elemento mais abundante na crosta terrestre. Na forma elementar existe como gás F_2; naturalmente ocorre apenas em formas combinadas como fluoreto (F^-), fluorita (CaF_2) e fluorapatita [$Ca_{10}(PO_4)_6F_2$]. Os compostos utilizados em fluoretação incluem fluoreto de sódio (NaF), fluorossilicato de sódio (Na_2SiF_6) e ácido fluorossilícico (H_2SiF_6), que em pH típico da água potável dissociam-se virtualmente completos em íons fluoreto livres.

FUNDAMENTO ESSENCIAL: O consenso científico estabelece que o benefício primário do fluoreto na prevenção de cáries dentárias é exclusivamente decorrente de sua ação tópica após a erupção dental (aplicado diretamente nos dentes através de cremes dentais, enxaguantes, vernizes), não sistêmica (Iheozor-Ejiofor *et al*., 2024; Nogueira *et al*., 2022; American Dental Association, 2021). A adição de fluoreto à água potável resulta em exposição sistêmica involuntária que NÃO contribui para benefício odontológico, pois o fluoreto ingerido é absorvido no trato gastrointestinal (>90%) e não atua topicamente nos dentes. Consequentemente, a fluoretação obrigatória da água potável expõe toda a população a riscos sistêmicos (incluindo neurotoxidade documentada) sem justificativa de benefício odontológico por essa rota de exposição.

Três mecanismos principais explicam o efeito tópico: aceleração da remineralização, inibição da desmineralização do esmalte e efeito antibacteriano sobre a placa dental (Iheozor-Ejiofor *et al*., 2024). Revisões sistemáticas recentes confirmam redução de aproximadamente 25% nas cáries dentárias devido à exposição ao fluoreto tópico (Wilkinson, 2024; Iheozor-Ejiofor *et al*., 2024), enquanto estudos anteriores à década de 1970 demonstravam redução entre 35% e 50%. Estudos contemporâneos mostram redução menor, na faixa de 3% a 15%, refletindo a presença ubíqua de fluoreto em múltiplas fontes, como água, pastas de dentes e alimentos (Wilkinson, 2024).

TOXICOLOGIA: A exposição excessiva ao fluoreto durante amelogênese (aproximadamente dos 0 aos 8 anos de idade) pode causar fluorose dental, uma alteração cosmética ou, em casos graves, estrutural do esmalte (*National Research Council*, 2006). Nos Estados Unidos, segundo dados do *National Health and Nutrition Examination Survey* (NHANES), a prevalência de fluorose dental (qualquer grau, incluindo muito leve) em adolescentes de 12–15 anos aumentou de 40,7% no período 1999–2004 para 65–71% em 2011–2016, dependendo da metodologia de avaliação (Beltrán-Aguilar *et al*., 2010; Centers for Disease Control and Prevention, 2019; Neurath *et al*., 2019). A prevalência de fluorose de grau moderado a severo (que pode requerer tratamento estético ou restaurador) foi estimada em aproximadamente 2–6% nos períodos mais antigos e subiu para cerca de 14–21% em coortes mais recentes (Neurath *et al*., 2019). O íon fluoreto atravessa tanto a barreira placentária quanto a barreira hematoencefálica e acumula-se preferencialmente em tecidos calcificados (National Research Council, 2006).

1.1.2. Regulamentação e Saúde Pública

Nos Estados Unidos, a EPA estabelece MCL de 4,0 mg/L e nível "ótimo" de 0,7 mg/L (DHHS, 2015). Dose de referência proposta pela EPA (2010) foi de 0,08 mg/kg/dia.

No Brasil, o Presidente Ernesto Geisel através da Lei Federal 6.050 (1974) tornou fluoretação obrigatória (Brasil, 1974), alcançando grande proporção da população urbana. A Portaria GM/MS 2.914 (2011) estabelece concentração ótima de 0,6-0,8 mg/L e VMP de 1,5 mg/L (Brasil, 2011). Contudo, o monitoramento descentralizado resulta em variabilidade nos níveis de fluoreto entre as cidades.

De acordo com a Organização Mundial da Saúde (OMS), a concentração máxima recomendada de flúor é de 1,5 mg/L, com faixa ótima de 0,5-1,0 mg/L (OMS, 2017). Importante ressaltar que a OMS não estabelece concentração mínima obrigatória de flúor, reconhecendo que o flúor não é essencial para a saúde humana em termos de exigência nutricional obrigatória. Consequentemente, níveis zero de flúor não representam risco à saúde por deficiência e são regulatoriamente aceitáveis.

Na Europa Ocidental, 97-98% não fluoreta água. Países que nunca adotaram incluem Áustria, Bélgica, Dinamarca, França, Itália e Noruega. Países que descontinuaram incluem República Tcheca (1993), Finlândia (1993), Alemanha (1971), Hungria (1960), Holanda (1973) e Suécia (1971) (BFS, 2024). Essa abordagem europeia não resultou em epidemias de cáries; países europeus que não fluoretam mantêm saúde dental comparável a países fluoretados, utilizando alternativas como cremes dentais fluoretados, programas de cuidado dental universal e educação preventiva.

1.1.3. Marco Jurídico

Nos Estados Unidos, o caso foi movido sob Seção 21 da TSCA, que permite cidadãos peticionarem a EPA para regular substâncias com risco não razoável. A TSCA foi substancialmente reformulada pelo Congresso em 2016 (Beveridge & Diamond, 2024).

No Brasil, a Constituição Federal de 1988 estabelece a saúde como direito fundamental de todos os cidadãos. A Lei nº 6.050/1974 e a Portaria nº 635/1975 determinaram a obrigatoriedade da fluoretação das águas de abastecimento público como política nacional de saúde preventiva. Embora existam debates jurídicos e acadêmicos sobre o mandato obrigatório da fluoretação, até o momento não há decisão definitiva do Supremo Tribunal Federal (STF) sobre a constitucionalidade dessa obrigatoriedade.

2. METODOLOGIA

Estudo configurado como revisão narrativa qualitativa com análise documental, jurídica e ética comparativa. Fontes primárias incluem a decisão judicial *Food & Water Watch v. EPA* (2024), legislação brasileira (Lei 6.050/74; Portarias 635/75, 2.914/11, 888/2021) e regulamentações EPA/OMS. Fontes secundárias compreendem meta-análises e estudos de coorte prospectivos (2015-2025), monografia do National Toxicology Program (2024), declarações de organizações profissionais (ADA, CDC, AAP) e análises jurídicas e éticas especializadas.

Critérios de seleção priorizaram relevância direta para o caso, atualidade (2015-2025), credibilidade institucional, pertinência comparativa Brasil-EUA e rigor ético. A análise integra perspectivas de toxicologia, direito administrativo ambiental, saúde pública e bioética.

3. Análise do Caso Jurídico

3.1. Descrição do Caso

Em 2016, uma coligação de ONGs peticionou a EPA sob TSCA Seção 21, argumentando que fluoreto apresenta efeitos neurotóxicos mesmo na concentração de 0,7 mg/L recomendada pelo Departamento de Saúde e Serviços Humanos (HHS). A EPA negou a petição em 2017. As ONGs apelaram a negação ao tribunal de distrito federal para o Distrito Norte da Califórnia (Beveridge & Diamond, 2024).

A decisão de 24 de setembro de 2024 encontrou "risco não razoável" baseado em NTP Monograph (2024), meta-análises e reconhecimento de fluoreto como substância perigosa. Aplicando padrão "preponderância de evidências", o Juiz Edward M. Chen determinou que a margem de segurança entre perigo (~1,5 mg/L) e exposição recomendada (0,7 mg/L) é insuficiente. A decisão não ordenou proibição específica, deixando à EPA escolher entre aviso ao público, redução de níveis recomendados,

restrições específicas ou proibição (Chen, 2024).

3.2. Análise Crítica

Perspectiva científica: A decisão alinha-se com literatura recente (NTP, 2024; Grandjean & Landrigan, 2014), incluindo estudos prospectivos demonstrando associação entre exposição pré-natal ao fluoreto e redução de QI em coortes do México (Bashash *et al*., 2017) e Canadá (Green *et al*., 2019). Contudo, estende conclusões sobre risco neurotóxico para níveis aplicados nas populações americanas. Limitações incluem heterogeneidade de exposição entre estudos, controle inadequado de confundidores socioeconômicos e ausência de dados dose-resposta precisos para populações especificamente americanas. A força de evidência é legítima mas carece de certeza absoluta, refletindo um dos dilemas fundamentais da regulação ambiental.

Perspectiva regulatória: Este é o primeiro caso de um tribunal ordenando que a EPA iniciasse rulemaking em resposta a uma petição de cidadão denunciada sob Seção 21 da TSCA (Beveridge & Diamond, 2024). O precedente é potencialmente transformador. Se tribunais confirmarem que petições TSCA Seção 21 podem forçar a EPA a pular processos estatutários de priorização química e avaliação de risco direto para *rulemaking*, o programa regulatório químico da EPA poderia ser sobrecarregado por prioridades conflitantes, criando incerteza regulatória em outros domínios químicos (Beveridge & Diamond, 2024).

Perspectiva de química ambiental: A decisão exige pesquisas mais rigorosas em toxicidade crônica de exposições de baixo nível, monitoramento sistemático de biomarcadores de exposição e avaliação integrada de risco que considere todas as rotas de exposição a fluoreto, não apenas água potável.

3.3. Comparação de Marcos Regulatórios: Níveis de Flúor (EUA, Brasil, OMS)

3.3.1. Análise comparativa de marcos regulatórios e rotas de exposição

As recomendações sobre fluoreto na água potável refletem uma tensão fundamental entre benefício odontológico documentado e potenciais riscos sistêmicos ainda em processo de avaliação regulatória. Diferentes jurisdições adotam marcos regulatórios que variam substancialmente:

- CDC recomenda ≈0,7 mg/L para benefício anticárie populacional (CDC, 2024)
- EPA estabelece 4,0 mg/L como limite máximo contaminante (MCL) sob a Safe Drinking Water Act (EPA, 2024)
- OMS fixa 1,5 mg/L como limite de segurança baseado em evidência de toxicidade (OMS, 2017)
- Revisões judiciais (2024) questionam se limites atuais oferecem proteção adequada contra riscos neurodesenvolvimentais (U.S. District Court for the Northern District of California, 2024)

A Tabela 1 sistematiza essa comparação, evidenciando três achados críticos:

PRIMEIRO: Existe dissociação entre o nível "ótimo" (0,7 mg/L) recomendado pela CDC e o objetivo de segurança regulatório (MCLG) de 4,0 mg/L—uma diferença de magnitude que reflete a separação histórica entre benefício odontológico e avaliação de risco toxicológico.

SEGUNDO: O MCL de 4,0 mg/L foi estabelecido com base em efeitos conhecidos e bem documentados (fluorose dental e cárie), mas foi considerado "irrazoável" aos olhos de tribunal federal em 2024 (Chen, 2024) por não incorporar evidência de risco neurotóxico fundamentada em literatura recente (NTP, 2024; Grandjean & Landrigan, 2014).

TERCEIRO: A OMS, embora reconheça benefício anticárie, estabelece um teto de segurança (1,5 mg/L) substancialmente inferior ao padrão norte-americano, refletindo abordagem mais conservadora diante de incerteza científica (OMS, 2017). Criticamente, nenhuma agência estabelece concentração mínima obrigatória de fluoreto—reconhecimento de que flúor não é nutriente essencial para desenvolvimento ou saúde óssea humana (OMS, 2017).

A HIERARQUIA DE EFICÁCIA POR ROTA DE EXPOSIÇÃO

Conforme Tabela 2, três rotas apresentam benefício-risco diferenciado:

FLUORETO TÓPICO (creme dental, verniz, bochecho): Redução de 24–40% em cárie com exposição sistêmica mínima (Marinho *et al*., 2013; Iheozor-Ejiofor *et al*., 2015, 2024). Estudos Cochrane classificam como "alta evidência". Nenhum risco sistêmico relevante documentado.

FLUORETO SISTÊMICO VIA INGESTÃO (água, leite, comprimidos): Oferece benefício moderado adicional (~25%) (McDonagh *et al*., 2000; Iheozor-Ejiofor *et al*., 2015), mas com exposição corporal inevitável (absorção intestinal ~90-100%) (*National Research Council,* 2006). Documentada fluorose dental em 10–40% das crianças sob fluoretação bem controlada (CDC, 2010; Roncalli *et al*., 2019), com fluorose moderada/severa em 2–6% de casos históricos (subindo para 14–21% em coortes recentes) (Neurath *et al*., 2019). Risco neurotóxico em níveis ótimos permanece controverso (NTP, 2024; Green *et al*., 2019; Bashash *et al*., 2017; Till *et al*., 2020).

ÁGUA FLUORETADA PÚBLICA: Efeito tópico predominante (saliva e biofilme) com pequena contribuição sistêmica pré-eruptiva (Slade *et al*., 2018). Redução de cárie de 15–35% em estudos ecológicos e de cessação (Beltrán-Aguilar *et al*., 2010; Roncalli *et al*., 2019), mas com exposição sistêmica inevitável durante períodos críticos de neurogênese e osteogênese. Fluorose estética leve documentada em 10–40% das crianças (CDC, 2010; Roncalli *et al*., 2019), com risco de fluorose moderada/severa <5% quando bem controlada.

IMPLICAÇÃO CENTRAL: O efeito tópico pós-eruptivo é o mecanismo dominante mesmo em populações com água fluoretada—especialmente onde uso difundido de dentifrício fluoretado já está estabelecido (Walsh *et al*., 2019; Marinho *et al*., 2019). Isso redimensiona a justificativa para fluoretação sistêmica pública: em países com acesso generalizado a higiene bucal e dentifrício fluoretado, a contribuição adicional do fluoreto sistêmico para redução de cárie diminui substancialmente (Wilkinson, 2024), enquanto a exposição sistêmica permanece integral. Em contraposição, em populações com acesso limitado a higiene bucal, fluoretação pública pode oferecer benefício mais significativo.

A questão regulatória central é se os riscos documentados (fluorose, potencial risco neurotóxico em desenvolvimento) justificam a manutenção de fluoretação universal em água potável (Chen, 2024), especialmente dado que benefício odontológico equivalente—e potencialmente superior em termos de razão benefício-risco—pode ser alcançado via estratégias tópicas direcionadas (dos Santos *et al*., 2013; Cumerlato *et al*., 2022).

4. DISCUSSÃO

4.1. Diálogo entre Ciência, Direito e Política

A decisão ilustra tensão fundamental entre ciência (que demanda certeza estatística robusta) e TSCA (que utiliza critério de "preponderância de evidências"). Robert F. Kennedy Jr., anunciou em Utah (abril 2025) que direcionará os Centros para Controle e Prevenção de Doenças (CDC) a cessar suas recomendações de fluoretação, dissolverá a Divisão de Saúde Oral do CDC e formará força-tarefa para revisar padrões fluoreto. Utah e Flórida já baniram fluoretação em certos municípios; mais de 60 comunidades americanas reconsideram a prática (AAFP, 2024).

Resposta da comunidade científica tem sido polarizada. A *American Dental Association* (ADA, 2025) e *American Academy of Pediatrics* (AAP, 2025) defendem a segurança contínua da fluoretação com base em sua leitura da literatura. O CDC credita economia de aproximadamente 6,5 bilhões de dólares anualmente em custos de tratamento dentário à fluoretação em comunidade (CDC, 2024).

Contudo, uma análise econômica completa de custo-benefício permanece ausente na literatura sobre fluoreto. Para contextualizar, Trasande e colaboradores estimaram que exposição ao chumbo em crianças de países em desenvolvimento resulta em $977 bilhões em perdas de produtividade econômica anual, utilizando metodologia que correlaciona redução de QI com perda de renda ao longo da vida (Attina & Trasande, 2013). Aplicar metodologia econômica equivalente à exposição ao fluoreto—documentada para causar 2-5 pontos de perda de QI—seria essencial para uma análise de custo-benefício verdadeiramente informada. Essa análise revelaria se, para nações em desenvolvimento, a preservação de capacidade cognitiva geraria retornos econômicos superiores

aos ganhos odontológicos.

A polarização reflete não apenas desacordos científicos legítimos, mas também diferentes epistemologias sobre como interpretar evidência incompleta.

4.2. Lacunas Críticas em Conhecimento e Regulação

Pesquisa: Existe ausência notória de estudos dose-resposta em populações especificamente brasileiras; falta de dados integrados sobre exposição total a fluoreto (somando água, alimentos, produtos de higiene); necessidade urgente de estudos longitudinais com controle robusto de confundidores socioeconômicos.

Regulação: Brasil não conduziu avaliação formal de risco neurotóxico com a profundidade que a controvérsia demanda. Monitoramento de fluoretação permanece descentralizado, com apenas 48,5% dos municípios realizando vigilância baseada em heterocontrole e registros presentes em 54,3% dos fluoretados (cobertura ≥50% da população atendida), além de 15,1% de falsos positivos/negativos nas informações oficiais (Roncalli *et al*., 2019). Pode faltar base de dados integrada que centralize informações sobre cobertura, conformidade e eventos adversos potenciais.

Comunicação pública: Há necessidade crítica de distinguir comunicativamente entre risco estatístico, associação epidemiológica e causalidade estabelecida. Agências sanitárias precisam defender sua autonomia técnica enquanto reconhecem legitimidade de questões públicas sobre intervenções obrigatórias.

4.3. Comparação Internacional e Modelos Regulatórios

Estados Unidos: A decisão judicial ordena ação regulatória imediata. O país opera sistema voluntário onde municípios decidem sobre fluoretação (73% da população exposta), , conforme apresentado na Tabela 1. Abordagem caracteriza-se por tentativa de basear decisões em evidências, mas com capacidade de judicialização quando cidadãos contestam regulações administrativas.

Brasil: Mantém mandato federal obrigatório desde 1974 (75% da população exposta). Desafios técnico-operacionais resultam em conformidade variável. Risco iminente é que a importação da controvérsia americana leve a mudanças legislativas precipitadas sem consultação adequada com especialistas brasileiros. Projeto de Lei 6.359/2013, agora arquivado, discutido por Bezerra (2021), buscava revogar a obrigatoriedade, e a decisão americana forneceria argumento político adicional para seus apoiadores.

Europa: 97-98% não fluoreta água potável. Aproximadamente 11 países descontinuaram fluoretação não porque descobriram evidência de dano significativo em níveis recomendados, mas porque priorizaram autonomia individual, métodos alternativos e princípios precaucionários sobre medicação em massa (FAN, 2025; IATP, ca. 2000). Europa implementa prevenção de cáries através de cremes dentais fluoretados acessíveis, programas escolares de saúde bucal, sal fluoretado em alguns contextos, e educação preventiva. Resultados de saúde dental são comparáveis a países fluoretados, demonstrando que Zero flúor em água não necessariamente compromete saúde pública quando alternativas são acessíveis.

4.3.1 Heterogeneidade de Exposição a Fluoreto no Brasil: Um Cenário de Duplo Risco

O Brasil não é homogêneo quanto a exposição a fluoreto. Conforme dados de Roncalli *et al*. (2019) sobre monitoramento descentralizado, e reconhecendo que diferentes municípios têm capacidades infraestruturais distintas, é possível caracterizar um cenário de "duplo risco":

RISCO 1: Excesso de fluoreto (fluorose)

- Ocorre em municípios onde: (1) água fluoretada está no padrão ótimo (0,6-0,8 mg/L), MAIS (2) população tem acesso a cremes dentais fluoretados, MAIS (3) consumo de outros produtos fluoretados (chá, alimentos processados);

- População afetada: classes médias/altas urbanas com 100% acesso a água tratada e cremes de qualidade;

- Manifestação: fluorose dental (documentada em 65-71% de adolescentes EUA conforme CDC; prevalência similar esperada em Brasil urbano com perfil similar).

RISCO 2: Deficiência de fluoreto (cáries)

- Ocorre em municípios onde: (1) água não é fluoretada OU não é tratada adequadamente, E (2) população não tem acesso a cremes dentais de qualidade;

- População afetada: populações rurais e urbano-pobres;

- Manifestação: prevalência alta de cáries não tratadas.

CENÁRIO CRÍTICO: HETEROGENEIDADE INFRAESTRUTURAL

- Roncalli *et al*. (2019) documentam que 48,5% dos municípios não realizam heterocontrole adequado;

- Significa: metade dos municípios pode ter fluoreto acima ou abaixo do padrão sem saber.

- Resultado: indivíduos em mesma cidade podem estar simultaneamente expostos a fluoreto inadequado (deficiência) ou excessivo (fluorose), dependendo:

- Local de moradia (água tratada sim/não).
- Classe socioeconômica (acesso a creme sim/não).
- Consumo de alimentos e bebidas fluoretadas.

O argumento de "fluoretação obrigatória viola autonomia" é inválido ONDE população não tem acesso a alternativas. MAS o argumento de "fluoretação causa fluorose" é válido ONDE população TEM acesso simultâneo a múltiplas fontes de fluoreto.

A solução não é "fluoretação sim ou não", mas "fluoretação diferenciada por contexto infraestrutural".

4.4. Dimensão Ética: Consentimento Informado e Autonomia Individual

A fluoretação obrigatória levanta questões legítimas sobre autonomia individual e autoridade estatal em políticas de saúde pública. Não se trata simplesmente de um conflito entre "consentimento" e "benefício público", mas de uma tensão complexa que diferentes sociedades resolvem de formas distintas e defensáveis.

4.4.1. A Objeção Baseada em Autonomia Individual

Alguns críticos argumentam que fluoretação obrigatória apresenta problemas éticos genuínos em relação à autonomia individual. Seu argumento repousa em três pilares. Primeiro, indivíduos recebem exposição a agente químico sem informação completa sobre riscos potenciais. Particularmente com as revisões recentes documentando riscos neurotóxicos em baixas doses, a população não dispõe de informação transparente e acessível sobre esses achados. Segundo, e talvez mais importante, a via de exposição (ingestão sistêmica via água potável) não produz o benefício alegado. Conforme estabelecido cientificamente, o benefício odontológico do fluoreto é exclusivamente tópico—isto é, quando aplicado diretamente aos dentes através de dentifrícios, enxaguantes ou vernizes. A fluoretação sistêmica da água obriga toda a população a absorver fluoreto através do trato gastrointestinal sem que essa exposição contribua para o benefício preventivo de cáries. Terceiro, alternativas efetivas já existem e são acessíveis. Cremes dentais fluoretados, vernizes profissionais e programas escolares de saúde bucal oferecem benefício comparável—redução de 24-40% em cáries—sem exposição sistêmica involuntária.

Sob essa perspectiva, a fluoretação compulsória sem verdadeiro consentimento informado viola princípios de autonomia individual que se tornaram centrais na bioética moderna. Trabalhos como os de Brodeur (2020) e Peckham & Awofeso (2014) argumentam que esse é um exemplo de intervenção médica imposta à população inteira sem que cada indivíduo possa exercer escolha informada, situação que merecia ser tratada com maior cautela quando alternativas menos intrusivas existem.

4.4.2. A Defesa dos Mandatos de Saúde Pública

Contudo, existe um fundamento bioético robusto para políticas de saúde pública que não requerem consentimento individual caso-a-caso, desde que benefício populacional esteja bem documentado e riscos sejam conhecidos e gerenciáveis. A iodação obrigatória de sal em diversos países previne bócio e deficiência cognitiva em populações inteiras sem que se requeira consentimento individual de cada pessoa. Essa política é amplamente considerada ética pela comunidade internacional porque o

benefício é documentado, os riscos são mínimos, e a alternativa (deficiência de iodo generalizada) é claramente pior. Vacinação obrigatória em determinados contextos representa outro exemplo: a sociedade impõe proteção coletiva sem consentimento individual quando benefício supera objeções particulares.

Em níveis recomendados a fluoretação opera numa lógica semelhante. Reduz cáries em aproximadamente 25%, benefício documentado em centenas de estudos. Os riscos conhecidos incluem fluorose dental em 10-40% das crianças (tipicamente muito leve), e possíveis efeitos neurotóxicos ainda em processo de avaliação científica. Conforme as agências de saúde lídias (CDC, OMS) interpretam atualmente os dados, o risco neurotóxico em níveis recomendados é considerado baixo, embora controverso à luz de evidências recentes. (McDonagh *et al*., 2000; Iheozor-Ejiofor *et al*., 2024; Neurath *et al*., 2019; NTP, 2024)

A diferença crucial entre essas políticas de saúde pública estabelecidas e o que críticos chamam de "experimentação humana" reside no tipo de incerteza envolvida. O Código de Nuremberg (1947) aplicava-se a estudos experimentais onde resultados eram incertos, onde indivíduos serviam como sujeitos de pesquisa cujos corpos testavam hipóteses desconhecidas. Políticas de saúde pública baseadas em conhecimento estabelecido—iodação de sal, vacinação, fluoretação—aplicam compreensão científica acumulada para alcançar benefício populacional conhecido. O nível de incerteza é radicalmente diferente.

4.4.3. O Debate Real: Contexto e Justificativa

A questão ética não reduz-se a "consentimento sim ou não", mas a algo mais granular: sob quais circunstâncias um mandato de saúde pública é justificável? E essa resposta muda com o contexto histórico e social.

Quando Brasil sancionou a Lei 6.050 em 1974, o argumento paternalista para fluoretação obrigatória era particularmente robusto. O acesso a dentifrícios fluoretados era severamente limitado para populações de baixa renda. As alternativas efetivas que mencionamos acima simplesmente não estavam universalmente disponíveis. O Estado intervia através da fluoretação da água justamente porque era o mecanismo que alcançava equidade—garantindo que crianças pobres tivessem acesso ao benefício preventivo que crianças ricas obtinham através de higiene bucal privada. Naquele contexto, a obrigatoriedade tinha fundamento.

4.4.3.1. Importante Ressalva: O Paradoxo da Desigualdade Brasileira

Em 2025, a equação mudou significativamente, mas não uniformemente. O argumento de autonomia individual que justificaria eliminar fluoretação obrigatória assume contexto de acesso equitativo que estruturalmente não existe no Brasil. A realidade é profundamente bifurcada conforme classe socioeconômica.

Em populações de classe média/alta com 100% acesso a água tratada, cremes dentais fluoretados e programas escolares de saúde bucal, o risco atual é de excesso de fluoreto (fluorose dentária em 10–40% das crianças, com formas moderadas-severas em 14–21% de coortes recentes). Nestes contextos, a crítica de "por que imposição obrigatória se há alternativas acessíveis?" é absolutamente válida. Estes grupos recebem fluoreto de múltiplas fontes simultâneas (água, dentifrício, alimentos, vernizes profissionais), resultando em exposição involuntária cumulativa sem consentimento informado genuíno.

Contrariamente, em populações pobres sem acesso consistente a água de qualidade nem cremes dentais acessíveis, o risco é oposto: deficiência de fluoreto com prevalência não controlada de cáries. Para estes grupos, a fluoretação obrigatória permanece como o único mecanismo viável de proteção contra doença bucal prevenível.

4.4.3.2. Solução: Diferenciação Estruturada, Não Revogação Universal

A solução ética e cientificamente fundamentada não é revogar universalmente a Lei 6.050/1974, mas diferenciá-la conforme contexto socioeconômico e capacidade infraestrutural municipal:

Em municípios com comprovada infraestrutura robusta (monitoramento adequado, >80% acesso a cremes de qualidade, programas escolares em ≥80% das instituições), o argumento paternalista de 1974 perde força, a população poderia alcançar benefício semelhante através de escolhas conscientes. Nestas áreas, *opt-out* de fluoretação seria regulatoriamente aceitável. Em municípios com infraestrutura ainda inadequada

ou sem heterocontrole sistemático (48,5% conforme Roncalli *et al*. 2019), a obrigatoriedade mantém justificativa como estratégia de equidade, funcionando como proteção para aqueles sem acesso a alternativas.

TRANSPARÊNCIA: Origem do critério "80%"

NÚMERO UTILIZADO: 80%

ORIGEM:

• Convencional, não estatístico

• Marca ponto onde 4 fatores simultâneos (fluoreto, higiene, educação, heterocontrole) tornam autonomia viável

• Poderia ser 75%, 80%, ou 85%

LIMITAÇÃO CRÍTICA PARA BRASIL:

• Derivado de contextos desenvolvidos

• Brasil tem situação heterogênea (Roncalli, 2019):

- 48,5% municípios SEM heterocontrole adequado

- 54,3% SEM registros de vigilância

- Disparidades regionais: Norte (88,9% sem fluoretação)

vs. Sudeste (49,0% com fluoretação)

NECESSIDADE DE PESQUISA: Antes de implementar como política, Brasil precisa validar:

1. Distribuição real dos 4 fatores em municípios brasileiros

2. Qual ponto transição é apropriado (pode ser 60%, 85%)

3. Se municípios em transição mantêm redução de cáries

4. Monitoramento de fluorose e prevalência durante mudança

CONCLUSÃO: 80% é PROVISÓRIO. Debate deveria ser "qual ponto é apropriado PARA BRASIL", não "80% sim/não"

Esta abordagem diferenciada honra simultaneamente dois valores em tensão: autonomia individual para populações com alternativas reais acessíveis, e justiça distributiva para populações onde fluoretação é único acesso a prevenção efetiva. Rejeita tanto o paternalismo cego (imposição idêntica para todos) quanto o libertarianismo insensível (remoção universal de proteção em nome de autonomia abstrata para populações vulneráveis).

A Lei 6.050/1974 foi apropriada para seu contexto histórico. Uma política de fluoretação para 2025 deve reconhecer que Brasil não é homogêneo: diferentes municípios enfrentam riscos opostos (excesso versus deficiência de fluoreto) conforme inserção socioeconômica. Consequentemente, a recomendação portanto deve ser: reforma da Lei 6.050/1974 que permita *opt-out* condicional para municípios que comprovem (1) monitoramento robusto de saúde bucal, (2) acesso universal a cremes fluoretados de qualidade, e (3) cobertura de programas escolares em ≥80% das instituições. Sem estas precondições documentadas, a fluoretação obrigatória permanece como estratégia defensável de equidade.

4.4.4. O Espectro de Posições Legítimas

Diferentes democracias resolveram esta questão de formas distintas, e cada uma reflete escolhas éticas defensáveis baseadas em diferentes prioridades. Estados Unidos opera sistema voluntário onde municípios decidem localmente sobre fluoretação, com aproximadamente 73% da população exposta. Essa abordagem tenta equilibrar benefício de saúde pública com respeito à autonomia municipal e permite que cidadãos contestem politicamente (ou judicialmente) decisões regulatórias que discordam. Brasil mantém mandato federal obrigatório desde 1974, atingindo 75% da população urbana. Essa abordagem prioriza benefício populacional e equidade, presumindo que simplicidade de implementação centralizada justifica a ausência de escolha individual.

Europa Ocidental, onde 97-98% não fluoreta água potável, priorizou autonomia individual e métodos alternativos. Não fez isso porque descobriu evidência de dano significativo em níveis recomendados, mas porque decidiu que em contextos onde cremes dentais fluoretados são universalmente acessíveis e programas de saúde bucal estão estabelecidos, medicação em massa através de água potável não era necessária. Países europeus que nunca fluoretaram, como Dinamarca, Suécia, Noruega, França, mantêm saúde dental comparável aos países fluoretados, demonstrando que zero flúor em água não compromete saúde pública quando alternativas funcionam.

Qual dessas abordagens é "correta" não pode ser respondido apenas por evidência científica. Cada uma representa um balanço

diferente entre valores: proteção de saúde coletiva versus autonomia individual, simplicidade administrativas versus escolha consciente, paternalismo beneficente versus responsabilidade individual.

4.4.5. Onde Ciência Termina e Valores Começam

Ponto metodológico importante: evidência científica não resolve a questão ética fundamental. Ciência pode estabelecer que fluoreto em 0,7 mg/L reduz cáries em aproximadamente 25% e causa fluorose dental em 10-40% das crianças, tipicamente leve. Ciência pode mesmo avaliar se exposição a essa concentração apresenta risco neurotóxico significativo. Mas ciência não pode dizer "portanto, deve ser obrigatório" ou "portanto, deve ser proibido". Essas são decisões normativas que dependem de valores: quanto peso atribuir à autonomia individual versus benefício coletivo? Qual nível de risco involuntário uma sociedade considera aceitável? Quando é legítimo que o Estado intervenha na vida privada para benefício coletivo percebido?

O desacordo sobre fluoretação reflete, em grande medida, desacordo sobre essas questões filosóficas mais amplas, não apenas desacordo sobre fatos científicos. Por isso diferentes democracias—todas operando com compreensão similar da ciência da fluoretação—chegam a conclusões políticas distintas.

4.5. Implicações Políticas e Regulatórias para Brasil

A decisão americana e monografia NTP (2024) fornecem suporte político substantivo para projetos como PL 6.359/2013 (arquivado) que buscam revogar obrigatoriedade da fluoretação no Brasil. Contudo, impacto não será determinístico. Resposta adequada exige que Brasil não simplesmente importe argumentos americanos, mas conduza:

- Primeiro, avaliação formal e independente de risco neurotóxico para população brasileira específica, com metodologia equivalente à do NTP.

- Segundo, reforma da Lei 6.050/1974 que reconheça heterogeneidade infraestrutural. Conforme Roncalli *et al*. (2019), apenas 54,3% dos municípios mantêm registros de vigilância adequados e 48,5% não realizam heterocontrole. Sugere-se que *opt-out* de fluoretação seja permitido apenas em municípios que demonstrem heterocontrole sistematicamente adequado. Em municípios sem tal infraestrutura, a obrigatoriedade mantém justificativa como estratégia de equidade.

- Terceiro, implementação de monitoramento centralizado robusto de qualidade de água para todas as substâncias, não apenas flúor, criando transparência que restaure confiança pública.

- Quarto, campanha educativa distinguindo legitimamente entre risco epidemiológico, associação estatística e causalidade estabelecida, defendendo autonomia técnica de agências sanitárias.

4.5.1. Diferenciação Municipal das Recomendações: Princípio de Heterogeneidade Infraestrutural

Uma questão metodológica crítica emerge da análise anterior: as recomendações sobre fluoretação não podem ser unifor-mes se as realidades municipais são profundamente heterogêneas. O Brasil não é homogêneo em sua capacidade infraestrutural, qualidade de água, acesso a produtos de higiene bucal ou cobertura de programas educativos.

Conforme demonstrado na seção 4.3.1 ("Heterogeneidade de Exposição a Fluoreto no Brasil: Um Cenário de Duplo Risco"), diferentes municípios enfrentam cenários opostos e incomensuráveis:

CENÁRIO A - Municípios com Infraestrutura Robusta (aproximadamente 51,5% conforme Roncalli *et al*., 2019):

- Heterocontrole sistemático adequado e registros de vigilância
- Acesso >80% a cremes dentais fluoretados de qualidade
- Cobertura ≥80% de programas escolares de saúde bucal
- População com 100% acesso a água tratada

Neste contexto, o risco predominante é de EXCESSO de fluoreto (fluorose estética leve em 10-40% das crianças, formas moderadas-severas

em 14-21% de coortes recentes). A população pode alcançar benefício odontológico equivalente através de escolhas conscientes via fluoreto tópico. O argumento paternalista original ("proteger quem não tem alternativas") perde justificativa ética. Autonomia individual torna-se defensável.

CENÁRIO B - Municípios sem Infraestrutura Adequada (aproximadamente 48,5% conforme Roncalli *et al.*, 2019):

- Heterocontrole ausente ou inadequado; metade dos municípios desconhece se níveis estão acima ou abaixo da recomendação
- Acesso limitado a cremes dentais de qualidade para populações pobres
- Cobertura <50% de programas escolares em muitas regiões
- Água não tratada ou inadequadamente tratada em áreas rurais

Neste contexto, o risco predominante é de DEFICIÊNCIA de fluoreto com prevalência elevada e não controlada de cáries. Fluoretação obrigatória permanece como o ÚNICO mecanismo viável de proteção contra doença bucal preventável. A função equitativa da fluoretação justifica-se plenamente.

Uma política nacional única que ignora essa heterogeneidade é simultaneamente demasiado intrusiva para municípios com alternativas acessíveis e insuficientemente protetora para municípios sem infraestrutura. A solução ética e cientificamente defensável é diferenciação estruturada por contexto municipal, não revogação universal ou manutenção uniforme.

4.6. Recomendações Específicas:

4.6.1. Para municípios com infraestrutura robusta

(Heterocontrole adequado, >80% acesso a cremes fluoretados, ≥80% cobertura educativa)

Pesquisadores:

- Conduzir estudos epidemiológicos prospectivos que monitorem efeitos de diferentes estratégias preventivas em população com acesso total a alternativas tópicas
- Investigar se redução de cáries via fluoreto tópico exclusivo (sem sistêmico) atinge níveis comparáveis aos atuais em contexto de alta literacia em saúde bucal

Reguladores municipais:

- Implementar transição gradual de fluoretação obrigatória para modelo voluntário com provisão municipal de alternativas garantidas:
  - Distribuição universal gratuita de cremes dentais fluoretados de qualidade (benefício comprovado de 24-40% redução de cáries, sem exposição sistêmica)
  - Programas escolares de saúde bucal com aplicação profissional tópica (verniz, gel) em instituições públicas
  - Educação comunitária sobre higiene bucal e acesso equitativo a recursos
- Permitir *opt-out* de fluoretação ao nível municipal, desde que compromisso com alternativas seja documentado e auditado
- Implementar monitoramento centralizado de saúde bucal e fluorose para avaliar impacto da transição

Profissionais de saúde:

- Fortalecer vigilância de saúde bucal através de SB Brasil com indicadores específicos de cárie e fluorose
- Preparação para comunicar aos pacientes/comunidades a mudança de modelo com transparência sobre riscos reduzidos (sem exposição sistêmica involuntária) e benefícios mantidos (prevenção de cáries via tópico)
- Oferecer escolhas informadas: fluoreto tópico concentrado para alta risco vs. educação preventiva simples para baixo risco

Comunicadores e educadores:

- Distinguir publicamente entre fluoreto tópico (de uso voluntário, com benefício estabelecido) e fluoreto sistêmico (com risco neurotóxico controverso)
- Reconhecer a legitimidade das questões públicas sobre autonomia e consentimento informado
- Explicar a transição como otimização (mesmo benefício,

menos risco) não como abandono de prevenção

4.6.2. Para municípios sem infraestrutura adequada

(Heterocontrole ausente, <50% acesso a cremes fluoretados, <50% cobertura educativa, água inadequadamente tratada)

Pesquisadores:

- Desenvolver estudos dose-resposta **específicos para populações brasileiras** em contextos de baixo acesso a alternativas
- Investigar biomarcadores de exposição ao fluoreto em crianças dessas regiões
- Estabelecer bancos de dados longitudinais que relacionem níveis de fluoretação municipal com saúde bucal e neurodesenvolvimento
- Priorizar financiamento para pesquisa em regiões onde alternativas tópicas não estão disponíveis

Reguladores (ANVISA e Secretarias Estaduais de Saúde):

- Conduzir avaliação formal e independente de risco neurotóxico para população brasileira específica, replicando rigor metodológico do NTP 2024
- Manter fluoretação obrigatória em municípios comprovadamente sem infraestrutura para alternativas, fundamentada em princípio de equidade e justiça distributiva
- Implementar monitoramento centralizado robusto de:
    - Níveis de fluoreto em água em tempo real (não apenas relatórios municipais autodeclarados)
    - Prevalência de fluorose e cárie em população infantil
    - Acesso real a cremes dentais e programas escolares
- Criar mecanismo de transferência de recursos federais para municípios pobres garantindo acesso a fluoreto tópico subsidiado como complemento à fluoretação sistêmica, não substituto
- Estabelecer prazo regulatório (ex: 10 anos) para que municípios sem infraestrutura alcancem condições mínimas de heterocontrole e acesso a alternativas, com objetivo gradual de transição para modelo flexível

Profissionais de saúde:

- Fortalecer programas de prevenção múltipla: educação sobre higiene bucal, fluoreto tópico (creme + bochecho escolar), fluoretação sistêmica
- Realizar vigilância específica de fluorose em crianças, comunicando aos pais quando presente de forma transparente
- Preparação para comunicar que fluoretação é intervenção temporária necessária até alternativas estarem universalmente acessíveis

Comunicadores e educadores:

- Distinguir entre "risco neurotóxico em contextos de baixa exposição multifonte" (relevante em EUA) e "benefício de equidade em contextos de acesso limitado a alternativas" (relevante no Brasil)
- Defender autonomia técnica de agências sanitárias ao implementar estratégias baseadas em equidade
- Comunicar a fluoretação como ferramenta **transitória de justiça social**, não como intervenção permanente ideal

4.6.3. Para todos os municípios (transversal)

Pesquisadores e Reguladores (conjunto): Independentemente do modelo escolhido (fluoretação mantida ou descontinuada), redirecionar progressivamente recursos para:

1. Distribuição universal subsidiada de cremes dentais fluoretados de qualidade — com benefício comprovado de 24-40% redução de cáries e sem exposição sistêmica involuntária
2. Programas escolares de saúde bucal com aplicação profissional de fluoreto tópico (verniz, gel em clínicas escolares) — alcançando população inteira durante período crítico (6-18 anos)
3. Educação comunitária sobre higiene bucal — como estratégia de prevenção primária acessível
4. Monitoramento centralizado de qualidade de água — não apenas para fluoreto, mas para todas as substâncias químicas, restaurando confiança pública

5. Bancos de dados integrados (SISAGUA, VIGIAGUA) que centralizem informações sobre cobertura, conformidade, fluorose e saúde bucal por município

Este modelo oferece benefício odontológico equivalente ou superior (24-40% redução de cáries via tópico em municípios com acesso) sem exposição sistêmica involuntária a agente químico com perfil de risco ainda em avaliação.

4.7. Implicações para Prática e Pesquisa

Os achados desta revisão sugerem que políticas de fluoretação devem ser reavaliadas sistematicamente à luz de novas evidências neurotóxicas, questões éticas de consentimento informado e disponibilidade de alternativas efetivas.

Pesquisadores devem priorizar: (a) estudos longitudinais com controle robusto de confundidores em populações brasileiras expostas a níveis baixos de fluoreto; (b) análise econômica integrando metodologia de Trasande para correlacionar efeitos neurotóxicos com produtividade econômica; (c) investigação sistemática da capacidade operacional municipal e competência técnica em estações de tratamento como fator confundidor crítico da qualidade de água.

Reguladores devem implementar: (a) avaliações formais de risco neurotóxico para população brasileira com rigor equivalente ao NTP 2024; (b) monitoramento centralizado de qualidade de água com validação por profissionais qualificados registrados junto ao CRQ; (c) marcos éticos explícitos para intervenções obrigatórias diferenciados por contexto municipal conforme capacidade infraestrutural; (d) auditoria sistemática de estações de tratamento quanto à presença e qualificação de profissionais responsáveis pela operação e controle de qualidade.

Profissionais de saúde devem estar equipados para: (a) comunicar riscos e benefícios de forma transparente respeitando autonomia de pacientes e comunidades; (b) reconhecer que "fluoretação adequada" pressupõe operação técnica competente, não apenas existência de legislação; (c) estabelecer vigilância de saúde bucal e fluorose com indicadores específicos por município.

Profissionais de química (CFQ/CRQ) devem atuar como: (a) consultores regulatórios em avaliação de infraestrutura municipal para adequação de estações de tratamento; (b) supervisores técnicos de qualidade de água, validando que operações respeitam legislação federal (Portaria 2.914/2011); (c) educadores públicos sobre diferença entre "**tratamento de água**" (processo técnico) e "dosagem química" (aplicação não supervisionada).

5. CONCLUSÕES:

A decisão *Food & Water Watch v. EPA* (2024) estabelece precedente transformador ao determinar que fluoretação em 0,7 mg/L apresenta risco não razoável ao neurodesenvolvimento infantil, reabrindo paradigma de 79 anos.

As abordagens regulatórias divergem significativamente: Estados Unidos opera sistema voluntário (73% expostos), Brasil mantém mandato obrigatório desde 1974 (75% expostos), e Europa rejeita amplamente fluoretação (97-98% não fluoreta), alcançando saúde dental comparável através de alternativas tópicas.

A análise demonstra que fluoretação obrigatória é eticamente questionável em contextos onde alternativas acessíveis existem, mas mantém justificativa como estratégia de equidade onde acesso a fluoreto tópico é limitado. A heterogeneidade infraestrutural brasileira (48,5% dos municípios sem heterocontrole adequado) exige diferenciação municipal, não política uniforme.

Recomenda-se reforma condicional da Lei 6.050/1974 permitindo opt-out apenas em municípios que comprovem infraestrutura robusta (heterocontrole adequado, >80% acesso a cremes fluoretados, ≥80% cobertura educativa). Municípios sem estas precondições devem manter fluoretação obrigatória como estratégia de equidade.

Análise econômica aplicando metodologia de Trasande aos dados brasileiros — correlacionando redução de QI com perdas de produtividade — constitui pesquisa futura crítica para decisões políticas informadas por evidência.

O próximo decênio definirá se emerge consenso que harmoniza benefício coletivo em saúde dental com autonomia individual, ou se abordagens divergentes refletem valores sociais distintos.

5. DECLARAÇÔES

5.1. Agradecimentos

O autor agrade a FOOD & WATER WATCH, INC., *et al*., por ter tido a inciativa de questionar o dogma da fluoretação nos EUA. Agradece aos revisores por contribuições valiosas para melhoria do manuscrito e pelos desafios construtivos que aprofundaram a análise ética.

5.2. Open Access

5.3. Fonte de Financiamento

A pesquisa foi financiada pelos autores. De acordo com as diretrizes éticas da Periódico Tchê Química, que não permitem doações de autores com manuscritos em avaliação (mesmo quando recursos de pesquisa estão disponíveis), ou em casos de limitações financeiras dos autores, os custos de publicação foram totalmente absorvidos pela revista sob nossa política de Acesso Aberto Platinum, através do apoio da Associação Científica Araucária (https://acaria.org/). Esta política visa garantir total independência entre o processo editorial e qualquer aspecto financeiro, reforçando nosso compromisso com a integridade científica e equidade na disseminação do conhecimento.

5.4. Conflitos de Interesse:

O autor declara não possuir conflitos de interesse financeiros ou pessoais que possam influenciar os resultados ou interpretações deste trabalho.

5.4. Limitações do Estudo

Este estudo é limitado por ser revisão narrativa baseada em documentos públicos e literatura disponível. Não conduzimos análise meta-analítica quantitativa original devido à heterogeneidade dos estudos incluídos e escopo da revisão.

Duas lacunas metodológicas importantes merecem destaque: (1) Análise econômica de custo-benefício — não foi conduzida análise correlacionando redução de QI documentada (2-5 pontos) com perdas de produtividade econômica ao longo da vida, metodologia desenvolvida por Trasande *et al*. para exposição ao chumbo. Esta análise é crítica para decisões políticas informadas e constitui possibilidade relevante de pesquisa futura; (2) Qualidade operacional do tratamento de água e qualificação profissional, não foi analisada sistematicamente a capacidade técnica municipal de manutenção de estações de tratamento. Experiência prática sugere que muitos municípios brasileiros com estações de tratamento carecem de profissionais qualificados (em particular, químicos registrados junto ao Conselho Federal/Regional de Química – CFQ/CRQ) para operação adequada. Tratar água é processo técnico que exige competência em química; meramente adicionar produtos químicos sem atuação/supervisão de profissional qualificado não constitui "tratamento". Esta questão de capacidade operacional, fiscalização municipal e qualificação de recursos humanos transcende regulação química e demanda investigação sistemática.

A rápida evolução da jurisprudência americana pode desatualizar aspectos da análise legal em breve prazo. Polarização do campo e posições científicas divergentes podem introduzir viés interpretativo, apesar de nossos esforços deliberados para manter equilíbrio crítico. Análise ética, embora fundamentada em princípios estabelecidos (Código de Nuremberg), reflete interpretações legítimas que outros podem discordar.

5.5. Declaração de Uso de IA:

Inteligência artificial foi utilizada para verificação gramatical, formatação final e integração de seções. Todo o conteúdo científico, análise jurídica e interpretação ética foram realizados exclusivamente pelos autores humanos através de análise crítica e integração

de fontes.

5.6. Contribuição dos Autores

Todos os autores contribuíram substancialmente para: (1) concepção e desenho do estudo; (2) análise e interpretação dos dados; (3) redação e revisão crítica do manuscrito; (4) aprovação da versão final.

5.7. Disponibilidade de Dados:

Todos os dados analisados são de domínio público e estão disponíveis nas referências citadas. Documentos judiciais podem ser acessados via sistema PACER dos tribunais federais americanos (ou pelo link da referencia). Dados brasileiros estão disponíveis nos sistemas oficiais do Ministério da Saúde (SISAGUA, VIGIAGUA).

6. ESTUDOS RELACIONADOS A SERES HUMANOS E ANIMAIS

6.1. Aprovação Ética

Não se aplica. Este estudo consiste em revisão documental, análise jurídica comparativa e análise ética de documentos públicos e literatura científica disponível, não envolvendo sujeitos humanos, animais ou dados primários.

6.2. Consentimento Informado

Não se aplica.

7. REFERENCES:

1. **American Academy of Family Physicians (AAFP). (2024).** Possible consequences of court ruling on safety of water fluoridation. AAFP Community Blog. https://www.aafp.org/pubs/afp/afp-community-blog/entry/possible-consequences-of-court-ruling-on-safety-of-water-fluoridation.html
2. **American Dental Association (ADA). (2025).** Response to Secretary Kennedy's fluoridation policy. ADA Newsroom. https://adanews.ada.org/ada-news/2025/march/ada-highlights-health-policy-issues-in-letter-to-rfk-jr/
3. **American Dental Association (ADA). (2021, July 14).** Fluoride: Topical and systemic supplements. https://www.ada.org/resources/ada-library/oral-health-topics/fluoride-topical-and-systemic-supplements
4. **Attina, T. M., & Trasande, L. (2013).** Economic costs of childhood lead exposure in low- and middle-income countries. Environmental Health Perspectives, 121(9), 1097-1102. https://doi.org/10.1289/ehp.1206424
5. **Bashash, M., Thomas, D., Hu, H., Martinez-Mier, E. A., Sanchez, B. N., Basu, N., ... & Hernández-Avila, M. (2017).** Prenatal fluoride exposure and cognitive outcomes in children at 4 and 6-12 years of age in Mexico. Environmental Health Perspectives, 125(9), 097017. https://doi.org/10.1289/EHP655
6. **BBC Future. (2025).** These countries don't fluoridate their water – here's why. https://www.bbc.com/future/article/20250528-why-some-countries-dont-fluoridate-the-water
7. **Beltrán-Aguilar, E. D., Barker, L., & Dye, B. A. (2010).** Prevalence and severity of dental fluorosis in the United States, 1999-2004 (NCHS Data Brief No. 53). National Center for Health Statistics. https://www.cdc.gov/nchs/products/databriefs/db53.htm
8. **Brasil. Presidência da República. (1974).** Lei nº 6.050, de 24 de maio de 1974. Obriga a adição de flúor aos estoques de água potável distribuída, no território dos Estados, do Distrito Federal e dos Municípios que beneficiam-se de sistemas de abastecimento público, destinados ao consumo doméstico. Diário Oficial da União, Brasília, DF, 25 maio 1974. Disponível em: http://www.planalto.gov.br/ccivil_03/leis/l6050.htm
9. **Brasil. Ministério da Saúde. (1975).** Portaria nº 635, de 26 de dezembro de 1975. Aprova normas e padrões relativos à fluoração da água potável. Diário Oficial da União, Brasília, DF, 29 dez. 1975. https://bvsms.saude.gov.br/bvs/saudelegis/gm/2017/MatrizesConsolidacao/comum/249408.html
10. **Brasil. Ministério da Saúde. Gabinete do Ministro. (2021).** Portaria GM/MS nº 888, de 4 de maio de 2021: Altera a Portaria GM/MS nº 2.914, de 12 de dezembro de 2011, que dispõe sobre os procedimentos de controle e de vigilância da qualidade da água para consumo humano e seu padrão de potabilidade.

Diário Oficial da União. Disponível em https://bvsms.saude.gov.br/bvs/saudelegis/gm/2021/prt0888_07_05_2021.html

11. **Brasil. Ministério da Saúde. Secretaria de Vigilância em Saúde. Departamento de Vigilância em Saúde Ambiental e Saúde do Trabalhador. (2012).** Portaria MS nº 2.914/2011: procedimentos de controle e de vigilância da qualidade da água para consumo humano e seu padrão de potabilidade (Série E. Legislação de Saúde). Brasília: Ministério da Saúde. Disponível em https://bvsms.saude.gov.br/bvs/publicacoes/portaria_2914_2011.pdf
12. **Brasil. Ministério da Saúde. (2011). Portaria nº 2.914, de 12 de dezembro de 2011: Dispõe sobre os procedimentos de controle e de vigilância da qualidade da água para consumo humano e seu padrão de potabilidade**. Recuperado em 21 de maio de 2024, de https://bvsms.saude.gov.br/bvs/saudelegis/gm/2011/prt2914_12_12_2011.html
13. **Broadbent, J. M., Thomson, W. M., Ramrakha, S., Moffitt, T. E., Zeng, J., Page, L. A., & Poulton, R. (2015).** Community water fluoridation and intelligence: Prospective study in New Zealand. American Journal of Public Health, 105(1), 72-76. https://doi.org/10.2105/AJPH.2013.301857
14. **Brodeur, P. (2020).** The fluoride deception. Seven Stories Press.
15. **Centers for Disease Control and Prevention (CDC). (1999).** Achievements in public health, 1900-1999: Fluoridation of drinking water. MMWR, 48(41), 933-940. https://www.cdc.gov/mmwr/PDF/wk/mm4841.pdf
16. **Centers for Disease Control and Prevention (CDC). (2019).** Data quality evaluation of the dental fluorosis clinical assessment data from the National Health and Nutrition Examination Survey, 1999–2004 and 2011–2016 (Vital and Health Statistics Series 2, No. 183). National Center for Health Statistics. https://www.cdc.gov/nchs/data/series/sr_02/sr02_183-508.pdf
17. **Centers for Disease Control and Prevention (CDC). (2024).** Community Water Fluoridation. https://www.cdc.gov/fluoridation/index.html
18. **Centers for Disease Control and Prevention. (2019).** Data quality evaluation of the dental fluorosis clinical assessment data from the National Health and Nutrition Examination Survey, 1999–2004 and 2011–2016 (Vital and Health Statistics Series 2, No. 183). National Center for Health Statistics. https://www.cdc.gov/nchs/data/series/sr_02/sr02_183-508.pdf
19. **Chen, E. M. (2024).** Findings of Fact and Conclusions of Law: Food & Water Watch, Inc. *et al*. v. United States Environmental Protection Agency. Case No. 17-cv-02162-EMC (N.D. Cal. Sept. 24, 2024). Wiley Law. https://www.wiley.law/media/publication/633_TSCA%20Flouride%20District%20Court%20Findings%20of%20Fact%20_%20Conclusions%20of%20Law,%20Sept.%202024.pdf
20. **Choi, A. L., Sun, G., Zhang, Y., & Grandjean, P. (2012).** Developmental fluoride neurotoxicity: A systematic review and meta-analysis. Environmental Health Perspectives, 120(10), 1362-1368. https://doi.org/10.1289/ehp.1104912
21. **Cross, D. W., & Carton, R. J. (2003).** Fluoridation: A violation of medical ethics and human rights. International Journal of Occupational and Environmental Health, 9(1), 24-29. https://pubmed.ncbi.nlm.nih.gov/12749628/
22. **Cumerlato, C. B. F., *et al*. (2022).** Is professionally applied topical fluoride effective in treating incipient caries? Brazilian Oral Research, 36, e070. https://www.scielo.br/j/bor/a/x6cjrMqHFwZ8nYNnTSPY3sc/
23. **Duvall, M., Richichi, T., Spanton, E., & Zietman, J. (2024).** Federal court orders EPA to regulate fluoridation of drinking water under TSCA. Beveridge & Diamond. https://www.bdlaw.com/publications/federal-court-orders-epa-to-regulate-fluoridation-of-drinking-water-under-tsca/
24. **E&E News. (2024).** EPA 'in a really tough spot' after landmark fluoride ruling. https://www.eenews.net/articles/epa-in-a-really-tough-spot-after-landmark-fluoride-ruling/
25. **European Commission. (2010).** Fluoridation: 1. Introduction. https://ec.europa.eu/health/scientific_committees/opinions_layman/fluoridation/en/l-2/1.htm

26. **Fluoride Alert. (2024).** Statements from European Health, Water, & Environment Authorities on Water Fluoridation. https://fluoridealert.org/content/europe-statements/
27. **Ganim, S., & Devine, C. (2024, November 3).** RFK Jr. says fluoride is 'an industrial waste' linked to cancer, diseases and disorders. Here's what the science says. CNN. https://www.cnn.com/2024/11/03/health/rfk-jr-fluoride-science
28. **Grandjean, P., & Landrigan, P. J. (2014).** Neurobehavioural effects of developmental toxicity. The Lancet Neurology, 13(3), 330–338. https://doi.org/10.1016/S1474-4422(13)70278-3
29. **Green, R., Lanphear, B., Hornung, R., Flora, D., Martinez-Mier, E. A., Neufeld, R., ... & Till, C. (2019).** Association between maternal fluoride exposure during pregnancy and IQ scores in offspring in Canada. JAMA Pediatrics, 173(10), 940-948. https://doi.org/10.1001/jamapediatrics.2019.1729
30. **Iheozor-Ejiofor, Z., *et al*. (2024).** Water fluoridation for the prevention of dental caries. Cochrane Database of Systematic Reviews, 2024(10), CD010658. https://pubmed.ncbi.nlm.nih.gov/39362658/
31. **Kennedy, R. F., Jr. (2024, November 2).** It reduces IQ in exposed fetuses at way below therapeutic doses. Please see the attached link for more detailed information. Michael Connet is the attorney who just won a landmark Federal court case against FDA for failing abysmally to protect public health against fluoride exposures. X (formerly Twitter). https://x.com/RobertKennedyJr/status/1852853318327951440
32. **Kennedy, R. F., Jr. (2025, April 8).** RFK Jr. will tell CDC to stop recommending fluoride in drinking water. PBS NewsHour. https://www.pbs.org/newshour/health/rfk-jr-will-tell-cdc-to-stop-recommending-fluoride-in-drinking-water
33. **Marinho, V. C. C., Worthington, H. V., Walsh, T., & Clarkson, J. E.** (2013). Fluoride varnishes for preventing dental caries in children and adolescents. *Cochrane Database of Systematic Reviews, 2013*(7), Article CD002279. https://doi.org/10.1002/14651858.CD002279.pub2
34. **McDonagh, M. T., Whiting, P. F., Wilson, P. M., Sutton, A. J., Chestnutt, I., Cooper, J., ... & Kleijnen, J.** (2000). Systematic review of water fluoridation. BMJ, 321(7265), 855-859. DOI: 10.1136/bmj.321.7265.855
35. **Mansfield, P. (2010).** Overview of reasons to oppose water fluoridation. ActionPA.org. https://www.actionpa.org/fluoride/reasons.pdf
36. **National Research Council. (2006).** Fluoride in drinking water: A scientific review of EPA's standards. The National Academies Press. https://nap.nationalacademies.org/catalog/11571/fluoride-in-drinking-water-a-scientific-review-of-epas-standards
37. **National Toxicology Program (NTP). (2024a).** NTP monograph on the state of the science concerning fluoride exposure and neurodevelopmental and cognitive health effects: A systematic review. https://ntp.niehs.nih.gov/sites/default/files/2024-08/fluoride_final_508.pdf
38. **National Toxicology Program (NTP). (2024b).** Fluoride exposure: Neurodevelopment and cognition. https://ntp.niehs.nih.gov/research/assessments/noncancer/completed/fluoride
39. **Neurath, C., Limeback, H., Osmunson, B., Connett, M., Kanter, V., & Wells, C. R. (2019).** Dental fluorosis trends in U.S. oral health surveys: 1986 to 2012. JDR Clinical & Translational Research, 4(4), 298–308. https://doi.org/10.1177/2380084419830957 (PDF: https://journals.sagepub.com/doi/pdf/10.1177/2380084419830957)
40. **Nogueira, M. T., *et al*. (2022).** Efficacy of topical fluoride application in the prevention of dental caries. LEV - Laboratório de Ensino Virtual, 13(2), 331-338. https://periodicos.newsciencepubl.com/LEV/article/download/4387/6591
41. **Organização Mundial da Saúde (OMS). (2017).** Diretrizes para qualidade da água potável (4ª ed., incorporando o 1º adendo). Genebra: OMS. Disponível em: https://www.who.int/publications/i/item/9789241549950
42. **Peckham, S., & Awofeso, N. (2014).** Water fluoridation: A critical review of the physiological effects of ingested fluoride as a public health intervention. The Scientific

World Journal, 2014, Article ID 293019. https://www.hindawi.com/journals/tswj/2014/293019/

43. **Roncalli, A. G., Noro, L. R. A., Cury, J. A., Zilbovicius, C., Pinheiro, H. H. C., Ely, H. C., Narvai, P. C., & Frazão, P. (2019).** Fluoretação da água no Brasil: distribuição regional e acurácia das informações sobre vigilância em municípios com mais de 50 mil habitantes. Cadernos de Saúde Pública, 35(6), Article e00250118. https://doi.org/10.1590/0102-311X00250118
44. **Shuster, E. (1997).** Fifty years later: The significance of the Nuremberg Code. New England Journal of Medicine, 337(20), 1436-1440. https://www.nejm.org/doi/full/10.1056/NEJM199711133372006
45. **Till, C., *et al*. (2020).** Fluoride exposure from infant formula and child IQ in a Canadian birth cohort. Environment International, 134, 105315. https://doi.org/10.1016/j.envint.2019.105315
46. **Twetman, S., Axelsson, S., Dahlgren, H., Holm, A. K., Källestål, C., Lagerlöf, F., ... & Mejare, I. (2003).** Caries-preventive effect of fluoride toothpaste: A systematic review. Acta Odontologica Scandinavica, 61(6), 347-355. https://medicaljournalssweden.se/actaodontologica/article/download/38915/44065
47. **United Kingdom. British Fluoridation Society (BFS). (2024).** Water fluoridation status: Europe. https://www.bfsweb.org
48. **United States. Department of Health and Human Services (DHHS). (2015).** Public Health Service recommendation for fluoride concentration in drinking water for prevention of dental caries. Federal Register, 80(133), 1-3. https://www.govinfo.gov/content/pkg/FR-2015-05-01/pdf/2015-10201.pdf
49. **U.S. Environmental Protection Agency (EPA)**. (2010). *Fluoride: Exposure and relative source contribution analysis* (EPA Report No. 820-R-10-015). Office of Water. https://www.epa.gov/sites/default/files/2015-09/documents/fluoride_report.pdf
50. **United States. Environmental Protection Agency (EPA). (2011).** Questions and answers on fluoride. https://19january2021snapshot.epa.gov/sites/static/files/2015-10/documents/2011_fluoride_questionsanswers.pdf
51. **U.S. Environmental Protection Agency (EPA)**. (n.d.). National primary drinking water regulations. Retrieved December 12, 2024, from https://www.epa.gov/ground-water-and-drinking-water/national-primary-drinking-water-regulations
52. **Walsh, T., Worthington, H. V., Glenny, A. M., Marinho, V. C., & Jeroncic, A. (2019).** Fluoride toothpastes of different concentrations for preventing dental caries. The Cochrane database of systematic reviews, 3(3), CD007868. A
53. Fluoride Action Network. (2025, 30 de junho). Statements from European health, water, & environment authorities on water fluoridation. https://fluoridealert.org/content/europe-statements/
54. Institute for Agriculture and Trade Policy. (ca. 2000). Facts about fluoridation. https://www.iatp.org/sites/default/files/Facts_about_Fluoridation.htm

Tabela 1. *Comparação de Rotas de Exposição ao Fluoreto*

Parâmetro	Concentração de Flúor (mg/L)	Fonte / Contexto
Nível Ótimo Recomendado	~0,7 mg/L	Recomendação do U.S. HHS/CDC: Para prevenir cáries dentárias. Fonte: CDC (2024). Community Water Fluoridation.
Limite Regulatório Federal (MCL)	4,0 mg/L	Nível Máximo de Contaminante: Aplicável sob a Lei da Água Potável Segura (Safe Drinking Water Act). Fonte: EPA (2024). Fluoride in Drinking Water.
Objetivo de Segurança Regulatório (MCLG)	4,0 mg/L	Objetivo de Saúde Pública: Baseado apenas em efeitos conhecidos (cáries, fluorose). Foi considerado "irrazoável" pelo tribunal por não proteger contra riscos neurotóxicos. Fonte: EPA (2024). Fluoride in Drinking Water.
Níveis Associados a Risco	~0,7 mg/L e superiores	Risco Neurotóxico: Faixa de concentração na qual estudos revisados pelo tribunal encontraram associação com reduções no QI e outros efeitos neurodesenvolvimentais. Fonte: U.S. District Court for the Northern District of California (2024).
Nível Máximo Recomendado (OMS)	1,5 mg/L	Limite de segurança estabelecido pela OMS baseado em evidência de toxicidade em concentrações superiores. Fonte: OMS (2017). Diretrizes para qualidade da água potável.
Nível Mínimo Exigido	Nenhum (zero é aceitável)	A OMS e agências regulatórias não estabelecem concentração mínima obrigatória, reconhecendo que flúor não é essencial para saúde humana em termos de exigência nutricional. Fonte: OMS (2017).

Tabela 2. *Comparação de Rotas de Exposição ao Fluoreto*

Rota de Exposição	Principal Mecanismo de Ação Anticárie	Benefício Odontológico Principal	Exposição Sistêmica	Risco Sistêmico Documentado em Níveis de Fluoretação Pública (0,7–1,2 mg/L)	Referências Principais
Tópica (creme dental, verniz, bochecho, aplicação profissional)	Contato direto com o esmalte (formação de CaF_2 e inibição da desmineralização)	Alta evidência: redução de 24–40% de cárie em dentes permanentes	Mínima (maioria cuspida ou não ingerida)	Nenhum relevante	Marinho *et al*., 2013 (Cochrane); Iheozor-Ejiofor *et al*., 2015 (Cochrane)
Sistêmica via ingestão (água fluoretada, leite fluoretado, comprimidos/ soluções)	Incorporação pré-eruptiva ao esmalte + efeito tópico pós-eruptivo pelo fluoreto salivar	Evidência moderada: redução adicional de ~25% (efeito tópico pós-eruptivo é o principal em populações com uso difundido de dentifrício)	Sim (absorção intestinal ≈ 90–100%)	Fluorose dental (leve/muito leve na maioria); risco neurotóxico em níveis ótimos é considerado baixo pela maioria das agências (CDC, OMS, NHMRC), mas permanece controverso em revisões recentes (NTP 2024; Green *et al*., 2019)	McDonagh *et al*., 2000 (York Review); Iheozor-Ejiofor *et al*., 2015; Broadbent *et al*., 2015; Bashash *et al*., 2017; Till *et al*., 2020
Água fluoretada pública (heterocontrole ou autocontrole)	Efeito tópico predominante (saliva e biofilme) + pequena contribuição sistêmica pré-eruptiva	Redução populacional de cárie de 15–35% em estudos ecológicos e de cessação	Sistêmica inevitável, porém controlada	Fluorose estética leve em 10–40% das crianças (CDC 2010; Roncalli *et al*., 2019); risco de fluorose moderada/severa < 5% quando bem controlada	Slade *et al*., 2018; Roncalli *et al*., 2019; Beltrán-Aguilar *et al*., 2010

PERIÓDICO TCHÊ QUÍMICA
BOOK REVIEW

ANÁLISE INTEGRADA: "TERMOQUÍMICA: FUNDAMENTOS E APLICAÇÕES ENERGÉTICAS"

INTEGRATED ANALYSIS: "THERMOCHEMISTRY: FUNDAMENTALS AND ENERGY APPLICATIONS"

Luis Alcides Brandini De Boni *
Araucária - Associação Científica, Brasil.

Rochele da Silva Fernandes
Universidade Federal do Rio Grande do Sul, Instituto de Química, Brasil

** Autor correspondente*
e-mail: root@acaria.org

Received 10 October 2025; received in revised form 15 October 2025; accepted 20 October 2025

RESUMO

Introdução: A termoquímica é essencial para compreender processos energéticos em contextos industriais e sustentáveis. O ensino tradicional frequentemente desconecta teoria de aplicações práticas, limitando o engajamento de estudantes. Existe necessidade de recursos educacionais que integrem conceitos teóricos, atividades experimentais e suporte pedagógico estruturado. **Objetivo**: Apresentar um material educativo que integre fundamentos de termoquímica com aplicações energéticas, promovendo aprendizado ativo através de experimentos práticos e recursos colaborativos. **Métodos**: O livro foi estruturado em seis partes sequenciais: introdução motivadora, fundamentos teóricos, Primeira Lei da Termodinâmica, termoquímica aplicada (calorimetria e Lei de Hess), nove experimentos hands-on com materiais acessíveis, e material complementar (histórico, tabelas de dados). Inclui Guia do Professor com planejamento, gabaritos e rubricas. **Resultados** e Discussão: A obra articula exposição teórica clara com experimentos replicáveis (neutralização, reações exotérmicas/endotérmicas, Arduino). Licença CC BY 4.0 permite compartilhamento. Plataforma colaborativa (livro.tchequimica.com) viabiliza contribuições contínuas da comunidade. **Conclusões**: O material configura-se como recurso abrangente para ensino de termoquímica, alinhado a desafios de sustentabilidade energética. Recomenda-se avaliação empírica do impacto pedagógico em diferentes contextos educacionais.

Palavras-chave: *Termoquímica, Educação em química, Recursos educacionais abertos, Experimentos práticos, Aplicações energéticas*

ABSTRACT

Introduction: Thermochemistry is essential for understanding energetic processes in industrial and sustainable contexts. Traditional teaching often disconnects theory from practical applications, limiting student engagement. There is a need for educational resources that integrate theoretical concepts, experimental activities, and structured pedagogical support. **Objective**: To present educational material that integrates thermochemistry fundamentals with energy applications, promoting active learning through practical experiments and collaborative resources. **Methods**: The book was structured into six sequential parts: a motivating introduction, theoretical fundamentals, the First Law of Thermodynamics, applied thermochemistry (calorimetry and Hess's Law), nine hands-on experiments with accessible materials, and complementary material (historical context and data tables). It includes a Teacher's Guide with lesson planning, answer keys, and assessment rubrics. **Results** and Discussion: The work provides a clear theoretical exposition and replicable experiments (neutralization, exothermic/endothermic reactions, Arduino). CC BY 4.0 license enables sharing. A collaborative platform (livro.tchequimica.com) facilitates continuous community contributions. **Conclusions**: The material serves as a comprehensive resource for teaching thermochemistry, aligned with energy sustainability challenges. Empirical evaluation of pedagogical impact across different educational contexts is recommended.

Keywords: *Thermochemistry, Chemistry education, Open educational resources, Hands-on experiments, Energy applications.*

DOI: 10.52571/PTQ.v22.n51.2025_12_BOOK_pgs_154_156.pdf

1. Identificação da Obra

A obra **"Termoquímica: Fundamentos e Aplicações Energéticas"** é um recurso educacional publicado pela Associação Científica Araucária em 2025 (1ª edição, versão preview 1.0). Conta com autoria de Luís Alcides Brandini De Boni e Rochele da Silva Fernandes, apresenta 168 páginas ilustradas e está identificada pelo ISBN 978-65-989731-0-0 e DOI 10.52571/TQ/TERMOQUIMICA.

2. Estrutura Organizacional

O conteúdo está dividido em seis partes sequenciais:

Parte I – Introdução e Motivação: Estabelece o contexto para o estudo da termoquímica, com uma distinção clara entre Termodinâmica e Termoquímica, conectando o tema a aplicações práticas como processos industriais e energéticos.

Parte II – Fundamentos Teóricos: Aborda conceitos essenciais como sistemas termodinâmicos, energia interna (U), calor (q), trabalho (w) e unidades de energia. Cada capítulo inclui exercícios para aplicação prática.

Parte III – Primeira Lei da Termodinâmica: Apresenta formulações matemáticas, convenções de sinais e exemplos resolvidos aplicados a processos a volume e pressão constantes.

Parte IV – Termoquímica Aplicada: Discute reações exotérmicas e endotérmicas, diagramas entálpicos, entalpias de mudança de estado, Lei de Hess e ciclos termoquímicos (como Born-Haber). Inclui seções sobre calorimetria com exemplos resolvidos e gabaritos completos.

Parte V – Experimentos Práticos: Propõe nove atividades hands-on, incluindo determinação de capacidade térmica, calorimetria de neutralização (HCl + NaOH), reações exotérmicas (cal virgem) e endotérmicas (NH_4NO_3), além de um experimento avançado com Arduino para monitoramento em tempo real. Os procedimentos descrevem materiais acessíveis e incluem alternativas caseiras.

Parte VI – Material Complementar: Contém apêndices com histórico da termoquímica (incluindo perfis de pioneiros como Lavoisier, Hess e Joule), tabelas de dados termodinâmicos (entalpias de formação, combustão), formulário de revisão, declaração sobre uso de inteligência artificial e referências bibliográficas.

3. Recursos de Apoio Pedagógico

Guia do Professor: Complementa a obra principal com planejamento de aulas, sugestões de preparação de reagentes, gabaritos, banco de questões, rubricas de avaliação e orientações de segurança. Inclui adaptações interdisciplinares e orientações de troubleshooting pedagógico.

Material Complementar Adicional: Anexos com listas de materiais e modelos de roteiros para experimentos.

4. Aspectos de Acesso e Compartilhamento

Licença Creative Commons: A publicação está licenciada sob Creative Commons Atribuição 4.0 Internacional (CC BY 4.0), permitindo compartilhamento, adaptação e uso comercial, mediante devida atribuição aos autores. Esta escolha busca ampliar o acesso ao material educacional.

Plataforma Colaborativa: O site livro.tchequimica.com está previsto para reativação após período de inatividade. A plataforma funcionará como canal para contribuições de professores e alunos, incluindo sugestões de experimentos, correções e expansões do projeto. O contato tchequimica@tchequimica.com constitui canal aberto para participação.

5. Características Pedagógicas Relevantes

A obra apresenta uma abordagem integrada que combina exposição teórica com atividades práticas. A linguagem utilizada mantém clareza conceitual sem excessos de tecnicismo. As ilustrações (diagramas e gráficos) auxiliam na visualização de conceitos abstratos. A ênfase em aplicações energéticas alinha o conteúdo com desafios contemporâneos, como transição para fontes renováveis e sustentabilidade.

6. Verificação de Conteúdo

Os dados apresentados nesta análise foram verificados através de consulta ao material original do livro (sumário e estrutura), confirmando a correspondência entre descrição e conteúdo efetivo. A editora Associação Científica Araucária encontra-se registrada em Nova Prata (RS) e está ligada a publicações no campo científico, como o periódico Tchê Química (ISSN 2179-0302).

Dado que se trata de publicação recente em formato preview (1.0), com indicação de desenvolvimentos futuros (reorganização de gabaritos em edições sucessivas), a obra reflete características típicas de projetos educacionais emergentes e colaborativos no contexto acadêmico brasileiro.

7. Considerações Conclusivas

"Termoquímica: Fundamentos e Aplicações Energéticas" configura-se como um material educativo que integra teoria, prática experimental e suporte pedagógico estruturado. Sua configuração sob licença aberta e projeto de plataforma colaborativa a posiciona como recurso potencialmente dinâmico para o ensino de termoquímica, particularmente no contexto do ensino médio e superior em português.

Dados de Contato e Acesso

- E-mail: tchequimica@tchequimica.com
- Site: livro.tchequimica.com
- ISBN: 978-65-989731-0-0
- DOI: 10.52571/TQ/TERMOQUIMICA
- Licença: CC BY 4.0 Internacional

PERIÓDICO TCHÊ QUÍMICA
ATR - 2025

PERIÓDICO TCHÊ QUÍMICA ANNUAL TRANSPARENCY REPORT

Ketevan Kupatadze[1], Shaima Rabeea Banoon[2], Luis Alcides Brandini De Boni[3]

[1] Periódico Tchê Química, Editor in Chief. Full professor at Ilia State University, Faculty of Natural Science and Medicine, Tbilisi, Georgia.

[2] Periódico Tchê Química, Editor in Chief. Department of Biology, College of Science, University of Misan, Maysan, Iraq.

[3] Periódico Tchê Química, Managing Editor, Brazil.

** Correspondence author*
email: tchequimica@tchequimica.com

Accepted 21 November 2025

In **2023**, the Periódico Tchê Química introduced the practice of producing an annual transparency report to give authors and institutions access to useful information about the journal. The main facts were presented in bullet points to make the report succinct. In **2025**, we are continuing this practice.

- **Current Editor-in-Cheife**: Dr. Ketevan Kupatadze, Ilia State University, Georgia; MsC. Shaima Rabeea Banoon, Misan University, Iraq.
- **Currently Edited by:** Araucaria Associação Cientifica (CNPJ # 52.968.321/0001-88).
- **Number of countries represented in the journal council**: 8.
- **Number of conferences the journal was invited to publish the resulting material**: 1.
- **Number of conferences that the journal is publishing the resulting materials**: 2.
- **Number of manuscripts received in 2025**: 96
- **Number of manuscripts published in 2025**: 28
- **Amount of manuscripts that will continue the publication process in 2026**: around 20
- **Amount of improper submissions**: 20
- **Amount of rectified submissions**: 16
- **Amount of retractions**: 10
- **Financial support received from other institutions (in USD):** $ 0,00.
- **Acquisition attempts by foreign companies in 2025:** 2 (regestred in our e-mail account)

- **Indexed in:** WEB OF SCIENCE, SUDOC, EZB, LATINDEX (DIRECTORIO), OPENALEX, (SCOPUS suspended), TITLE DOI, WIKIDATA, THE KEEPERS, ROAD, GLOBALHEALTH, CROSSREF, CABABSTRACTS, FATCAT, ZDB. (source: https://portal.issn.org/resource/ISSN/2179-0302)
- **Publication fees:** All authors have published in 2025 without any charges from the journal side. All journal downloads are also freely available on the journal website. This means that the Araucaria Scientific Association has absorbed all publication costs in 2025, with the personal contribution of Luis A. B. De Boni.

DOI: 10.52571/PTQ.v22.n51.2025.ATR.pdf


Call for papers
www.sscon.org
CNPq
Conselho Nacional de Desenvolvimento Científico e Tecnológico
Process: 440182/2025-5
UNIVERSIDADE DE VASSOURAS
SOUTHERN SCIENCE CONFERENCE
SOUTHERN SCIENCE CONFERENCE
UM
UNIVERSIDAD DE MENDOZA
UNIVERSIDADE DE VASSOURAS